(NASA-CR-145369-Vol-2) STUDY OF FUEL SYSTEMS FOR LH2-FUELED SUBSONIC TRANSPORT AIRCRAFT, VOLUME 2 Final Report, Sep. 1976 - Dec. 1977 (Lockheed-California Co., Burbank.) 256 p HC A16/MF A01 CSCL 21C G3/05

N78-31086

Unclas
29147

-145369

FINAL REPORT— Volume II

STUDY OF FUEL SYSTEMS FOR LH2-FUELED SUBSONIC TRANSPORT AIRCRAFT

by
G. D. Brewer
R. E. Morris
G. W. Davis
E. F. Versaw
G. R. Cunnington, Jr.
J. C. Riple
C. F. Baerst
G. Garmong

July, 1978
Prepared under Contract NAS 1-14614

for

NASA

Langley Research Center
National Aeronautics and Space Administration

by

Lockheed — California Company
Burbank, California

supported by

Lockheed Missiles and Space Company, Inc.
AiResearch Divisions of the Garrett Corporation
Rockatdyne Division of Rockwell International

PRECEDING PAGES BLANK NOT FILMED

FOREWORD

This is the final report of a study made under Contract NAS 1-141614 for NASA-Langley Research Center, Hampton, Virginia. Mr. Robert D. Witcofski of the Aeronautical Systems Division at NASA-Langley Research Center was technical monitor for the study. The report presents results of work performed during the 14 month period, October 1976 through November 1977. Volume I contains Sections 1 through 6; Volume II contains Sections 7 through 10, and Appendixes A through G.

The Lockheed-California Company was the prime contractor to NASA and the work was performed in the Commercial Advanced Design Division at Burbank, California. In addition, important segments of the work which required special expertise were subcontracted to the following organizations. The individuals named were principal contributors.

<u>LOCKHEED-CALIFORNIA COMPANY</u>

G. Daniel Brewer, Study Manager

Robert E. Morris, Project Engineer

George Davis, Structures

Edward Versaw, Fuel Systems

Roger Jensen, Weights

Roy Adamson, Propulsion

Dalen Horning, DOC Analysis

<u>LOCKHEED MISSILES AND SPACE COMPANY, INC.</u>

George Cunnington, Jr., Tank Insulation

Richard Parmley, Tank Insulation

Jorgen Skogh, Tank Stress Analysis

Richard Cima, Heat Transfer Analysis

<u>AIRESEARCH DIVISION OF THE GARRETT CORP.</u>

James C. Riple, Engine Pump and Fuel Control System

Carl F. Baerst, LH_2 Engine Design

ROCKETDYNE DIVISION OF ROCKWELL INTERNATIONAL

Greg Garmong, Engine Fuel Supply System

William R. Bissell, Boost Pump

Ron Tobin, Fuel Feed Lines

TABLE OF CONTENTS

TABLE OF CONTENTS (Continued)

TABLE OF CONTENTS (Continued)

TABLE OF CONTENTS (Continued)

TABLE OF CONTENTS (Continued)

LIST OF FIGURES

LIST OF FIGURES (Continued)

LIST OF FIGURES (Continued)

LIST OF FIGURES (Continued)

LIST OF FIGURES (Continued)

LIST OF FIGURES (Continued)

LIST OF FIGURES (Continued)

LIST OF FIGURES (Continued)

LIST OF FIGURES (Continued)

LIST OF FIGURES (Continued)

LIST OF TABLES

LIST OF TABLES (Continued)

LIST OF TABLES (Continued)

LIST OF TABLES (Continued)

LIST OF TABLES (Continued)

7. FUEL CONTAINMENT SYSTEM

As used herein, the term fuel containment system refers to two basic subsystems; the fuel tank structure and its associated supporting structural components, and the tank cryogenic insulation system. Both integral and nonintegral fuel tanks were evaluated. An integral tank is defined as one which provides the aircraft structure in the tank area to carry fuselage structural loads as well as providing for fuel containment. A nonintegral tank is mounted within a conventional airframe and serves only as a fuel containment vessel.

The methodology used in the selection of a preferred design of fuel containment system was to apply a consistent set of criteria to a three-step process, varying only in extent of analysis, proceeding from concept screening, to evaluation of preferred candidates, to selection of a final configuration. This process is shown diagrammatically in Figure 82 using the insulation system as an example.

In order to focus design and analysis attention on constructive aspects, the aft tank of the aircraft was selected and used as the model for evaluation of candidate structure and insulation concepts. After a preferred aft tank design was established, the forward tank was sized and weighed using the same design concepts for both structure and insulation based on spot analysis as deemed necessary to account for local differences.

The procedures and results of the investigation of tank insulation systems are presented in 7.1. Information relative to the tank structure is presented in 7.2.

7.1 Tank Insulation

A total of 15 candidate tank insulation concepts were evaluated in the initial screening operation to find the two most promising for use with integral-type tanks and the two most promising for nonintegral tanks. The 15 candidates included both active (inert gas purged and dynamically pumped vacuum systems) and passive concepts. A closed cell polymeric foam insulation, applied to the external surfaces of an integral tank was used as the baseline system for comparative evaluation purposes.

The four preferred insulation systems (two for integral and two for nonintegral tanks) were subjected to a more rigorous analysis, leading finally to selection of one concept to be incorporated in the design of the subject LH_2-fueled transport aircraft.

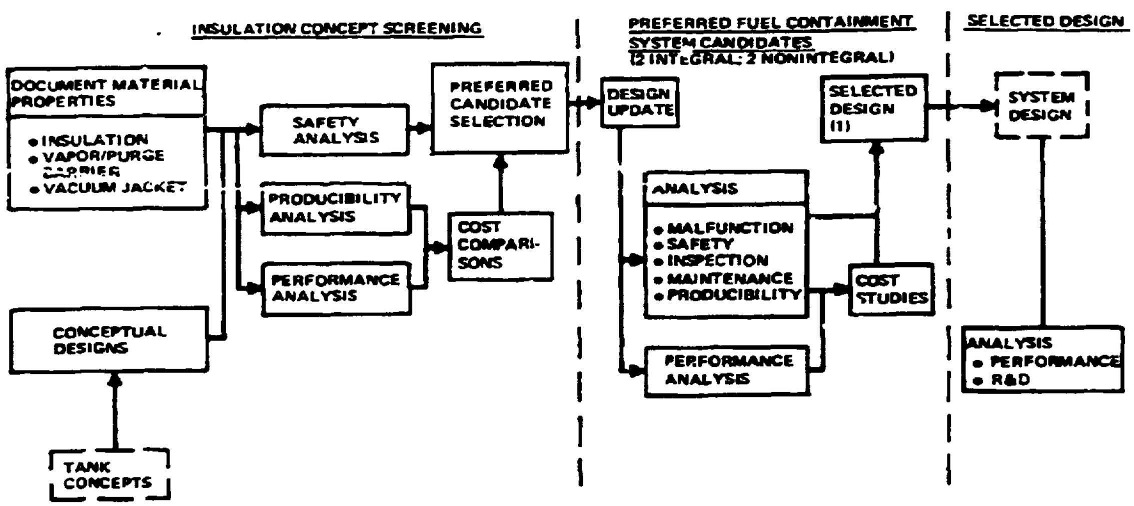

Figure 82. Tank insulation analysis procedure.

The procedures employed in each step of this selection process, and the results which were obtained, are discussed in the following paragraphs.

In the initial phase of the program, a preliminary study was made of the benefits which could be derived by using active cooling to reduce fuel tank boiloff and eliminate venting in-flight and on the ground. The active systems considered were:

- Refrigeration of the liquid using a closed cycle mechanical refrigerator.
- A thermodynamic vent system incorporating a vapor-cooled shield within the insulation and a Joule-Thompson (J-T) expansion device.
- An intermediate N_2-cooled shield within the insulation, using either vaporization of liquid or a cooled gas.

For all of these systems the weights associated with the refrigeration devices, shields, and plumbing lines exceeded the weight of fuel saved by a minimum of 1000 kg (2200 lb) per tank for an insulation system having an equivalent (unassisted by external cooling) liquid-wetted wall heat flux of 31.5 W/m^2 (10 Btu/hr ft^2).

In addition to the weight penalty associated with active cooling, the normal aircraft operational and maintenance procedures are more complex and the dispatch reliability is decreased. Also, aircraft and terminal vent systems would have to be provided to accommodate tank venting in the event of cooling system malfunction.

Because of these operational disadvantages, and because the weight estimates far exceeded the fuel saving benefits, no further study was made to optimize any concept.

7.1.1 Design requirements and evaluation criteria. - Selection of the insulation system for a commercial transport aircraft LH_2 fuel tank is constrained by the requirements of minimum operating costs and the achievement of a very high level of safety throughout the aircraft lifetime. In order to realize cost goals, the system must combine lightweight construction with low heat transfer characteristics which are consistent with in-flight tank pressurization requirements; have a high reliability, low maintenance, long life cycle; and have development and fabrication cost commensurate with commercial aircraft practices. Safety considerations must include freedom, not only from loss of life or aircraft during a flight or ground operation incident, but also failures potentially dangerous to maintenance operations. Design requirements and safety, performance, and operational criteria were established for the fuel containment system of the aircraft.

The aft tank configuration was used for the screening and preferred systems studies to focus the analysis effort to the maximum degree. Prior aerospace research and development results and commercial experience with cryogenic storage vessels were used to evaluate potential problem areas and to assess the applicability of each insulation concept.

The general criteria used in evaluation and ranking of the insulation concepts were:

- Safety - No single or probable combination of failures shall lead to loss of life or aircraft. Assessment of failure modes and their overall impact was consistent with current or anticipated safety practices applicable to commercial aircraft in 1990-1995 and to storage and handling of liquid hydrogen. Modes of failure considered were: accidental penetration of exterior surfaces, air or GH_2 leakage into insulation or aircraft, cryopumping of O_2 in organic materials, malfunction of purge or vacuum system and associated control components, toxicity of products in event of an external fire.

- Performance - Minimization of aircraft DOC. DOC was evaluated as a function of system inert weights (including accessories associated with purge/vacuum concepts); fuel vaporized to maintain tank pressure as well as nonrecoverable fuel loss (vent) weights; system volume; and maintenance requirements (inspection/repair/replacement).

- Producibility - Each system must be designed so it can be fabricated, assembled, inspected and maintained consistent with aircraft practices.

Cost estimates were based on production of 350 ship sets plus 20 percent spares. If costs were competitive, the concept which provided the aircraft with the lowest energy consumption was selected.

7.1.2 Candidate insulation concepts. - Insulation systems for aircraft LH_2 fuel tanks serve the following basic purposes:

- To reduce the heat rates to the tanks to a level consistent with minimizing direct operating costs.
- To prevent the buildup of parasitic weight on the aircraft in flight due to condensation or freezing of atmospheric constituents, e.g., water vapor.

Since all atmospheric gases will freeze at LH_2 temperature, air in the insulation system must either be evacuated by active pumping and/or passive cryopumping, or a non condensible gas such as helium or hydrogen must be substituted in the insulation. Consequently, integrity of the vapor barrier is a critical item in the design of external insulation systems. The insulation thickness on all candidate systems must be sized, as a minimum to keep the external sealed surface above the dew point (the insulation surface for an external application or the tank surface for an internal insulation).

Fifteen insulation system concepts, shown in Table 30, were selected for analysis. Table 31 shows the status of development work on cryogenic insulation systems which is applicable to the candidate concepts. Thermal performance test data from these programs were used in the analysis of the systems for the subject aircraft use.

Plumbing schematics for the active systems, i.e., those requiring either vacuum pumps or purging, are shown in Figures 83 through 85. The plumbing schematic for concept 1, Figure 83, shows the automatic controls used to maintain the correct helium pressure during aircraft ascent and descent so as to prevent structural failure of the purge jacket. Dual N_2/He purge system controls for concept 2 are shown in Figure 84. The differential pressure measurement across the inner purge barrier controls the helium pressure; the nitrogen pressure control is referenced to ambient pressure. The 10^{-4} Torr pressure requirement for concept 9 requires a turbomolecular pump and fore pump in addition to the blowers as shown in Figure 85. Concepts 10, 11, and 12 do not require complex turbomolecular and fore pumps because of the more modest vacuum pressures used in those concepts. Their plumbing schematics are shown in Figure 86. In all concepts the pumping systems operate only when the specified vacuum pressures are exceeded.

	PURGED		CRYOPUMPED		GH_2-FILLE[D]
	1	2	3 OR 3M	4	5
CONCEPT	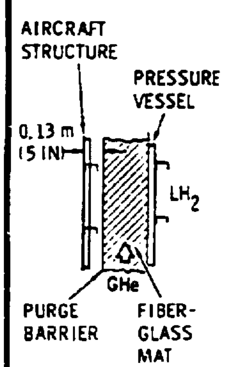	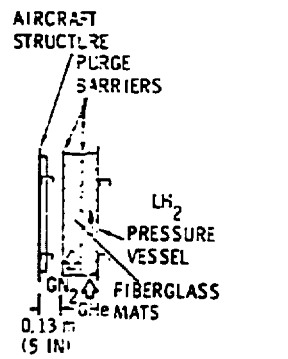	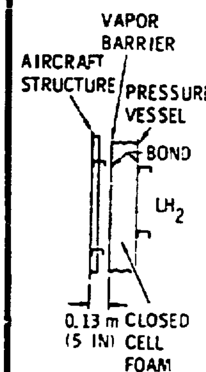	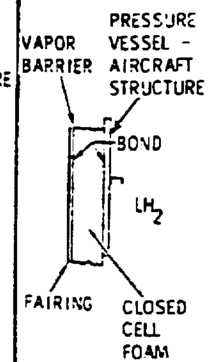	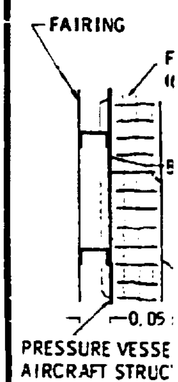
INSULATION TYPE	He PURGE 1.4×10^4 N/m^2 (2 PSI) GAGE PRESSURE	PURGE GAS / GAGE PRESSURE: He 2.8×10^4 N/m^2 (4 PSI); N_2 1.4×10^4 N/m^2 (2 PSI). INTERMEDIATE PURGE BARRIER TEMPERATURE > 83°K (150°R)	CRYOPUMPED AIR-FILLED FOAM; AMBIENT PRESSURE LOAD ON THE FOAM	CRYOPUMPED AIR-FILLED FOAM; AMBIENT PRESSURE LOAD ON FOAM	GH_2-FILLED AT T[...] PRESSURE
PRESSURE VESSEL CONSTRUCTION INTEGRAL (I) NONINTEGRAL (N)	N	N	N	I	I
MATERIALS	• FIBERGLASS MAT 16 kg/m^3 (1 lb/ft^3) • PURGE BARRIER EPOXY/GLASS/TEFLON COMPOSITE 0.69 kg/m^2 (0.14 lb/ft^2)	• FIBERGLASS MATS 16 kg/m^3 (1 lb/ft^3) • PURGE BARRIERS EPOXY/GLASS/TEFLON COMPOSITE 0.69 kg/m^2 (0.14 lb/ft^2)	• CLOSED-CELL POLYURETHANE FOAM 35 kg/m^3 (2.2 lb/ft^3) • VAPOR BARRIER • (3) USES PLASTIC FILM (3M) USES MAAMF 0.673 kg/m^2 • (0.138 lb/ft^2 • POLYURETHANE ADHESIVE (0.15 kg/m^2 (0.03 lb/ft^2 PER BOND LINE	• CLOSED-CELL POLYURETHANE FOAM 35 kg/m^3 (2.2 lb/ft^3) • MAAMF VAPOR BARRIER 0.673 kg/m^2 (0.138 lb/ft^2) • POLYURETHANE ADHESIVE 0.15 kg/m^2 (0.03 lb/ft^2) PER BOND LINE	• CLOSED CELL POLYURETHA[...] FOAM WITH 3[...] GLASS FIBER REINFORCEM[...] 83 kg/m^3 (5.2[...] • POLYURETHAN[...] GLASS LH_2 SE[...] 0.88 kg/m^2 (0.[...] • POLYURETHANE ADHES[...] 0.15 kg/m^2 (0.03 lb/ft^2) P[ER] BOND LINE
OPERATION	PURGE AIR TO 1%; MAINTAIN POSITIVE PRESSURE IN SERVICE; VENT DURING ASCENT; REPLENISH DURING DESCENT; LOAD He AFTER EACH FLIGHT	SAME AS SYSTEM 1 FOR BOTH PURGE GASES	PASSIVE	PASSIVE	PASSIVE

FOLDOUT FRAME

GH_2-FILLED	AIR-FILLED / GH_2-FILLED	GH_2-FILLED		
5	6	7	8	9
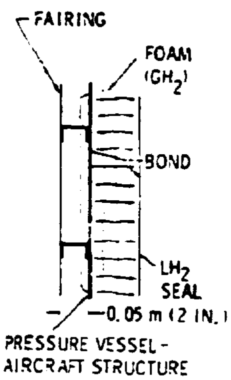	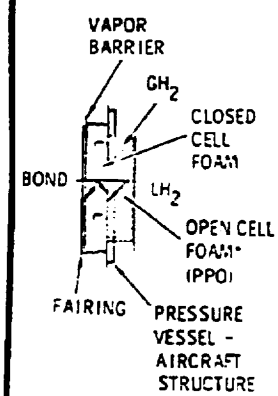	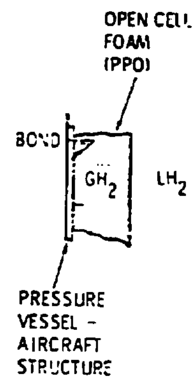	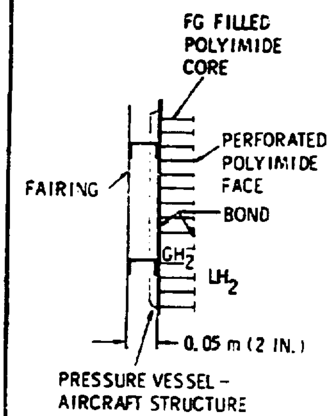	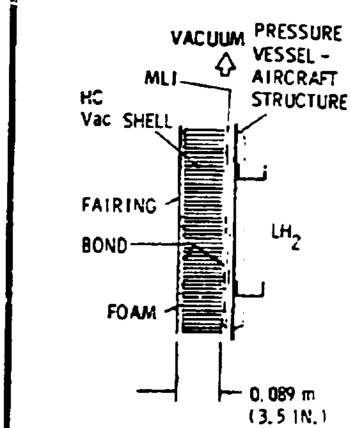
GH_2-FILLED AT TANK PRE[illegible]E	CLOSED FOAM - AIR-FILLED OPEN FOAM - GH_2-FILLED AT TANK PRESSURE TANK TEMPERATURE > 97K (175°R)	GH_2-FILLED AT TANK PRESSURE	GH_2-FILLED AT TANK PRESSURE	HONEYCOMB AND MLI EVACUATED TO $<10^{-5}$ TORR; NO LOAD ON MLI; AMBIENT PRESSURE LOAD ON JACKET
1	1	1	1	1
• CLOSED CELL POLYURETHANE FOAM WITH 3-D GLASS FIBER REINFORCEMENT 83 kg/m^3 (5.2 lb/ft^3) • POLYURETHANE/GLASS LH2 SEAL 0.88 kg/m^2 (0.18 lb/ft^2) • POLYURETHANE ADHESIVE 0.15 kg/m^2 (0.03 lb/ft^2) PER BOND LINE	• CLOSED CELL POLYURETHANE FOAM 35 kg/m^3 (2.2 lb/ft^3) • PPO OPEN-CELL FOAM* 40 kg/m^3 (2.5 lb/ft^3) • MAAMF VAPOR BARRIER 0.673 kg/m^2 (0.138 lb/ft^2) • POLYURETHANE ADHESIVE 0.15 kg/m^2 (0.03 lb/ft^2) PER BOND LINE	• PPO OPEN-CELL FOAM* 40 kg/m^3 (2.5 lb/ft^3) • POLYURETHANE ADHESIVE 0.15 kg/m^2 (0.03 lb/ft^2) PER BOND LINE	• POLYIMIDE HONEYCOMB CORE, 3/8-IN. CELL, FILLED WITH F.G. BATTING 40 kg/m^3 (2.5 lb/ft^3) • PERFORATED POLYIMIDE FACE SHEET 3.5×10^{-2} kg/m^2 (7.3×10^{-3} lb/ft^2) • POLYURETHANE ADHESIVE 0.15 kg/m2 (0.03 lb/ft^2) PER BOND LINE	• ALUMINUM HONEYCOMB CORE 50 kg/m^3 (3.1 lb/ft^3) • ALUMINUM FACE SHEETS, EACH 1.36 kg/m^2 (0.28 lb/ft^2) • EPOXY ADHESIVE 3.7×10^{-2} kg/m^2 (7.5×10^{-3} lb/ft^2) PER BOND LINE • DAM/DARON NET MLI UNIT WEIGHT PER LAYER DAM: 8.8×10^{-3} kg/m^2 (1.8×10^{-3} lb/ft^2) DACRON: 11.7×10^{-3} kg/m^2) (2.4×10^{-3} lb/ft^2)
PASSIVE	PASSIVE *THE MAXIMUM THICKNESS PPO FOAM CAN BE MADE IS ~0.1 m (4 IN.) DUE TO THE DRAWING PROCESS. BEYOND THIS THICKNESS, MULTIPLE LAYERS HAVE TO BE BONDED TOGETHER.	PASSIVE	PASSIVE	EVACUATE HONEYCOMB AND MLI; MAINTAIN VACUUM IN SERVICE (PUMPS OPERATE ONLY WHEN 10^{-5} TORR IS EXCEEDED)

2 FOLDOUT FRAME

TABLE 30. - TANK INSULATION SYSTEM CONCEPTS

		CRYOPUMPED (MULTIPLE SEAL)	AIR-FILLED/CRYOPUMPED (DOUBLE-SEAL)	GN_2 PURGE/CRYOPUMPED
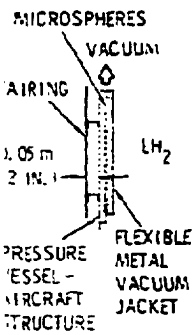	12 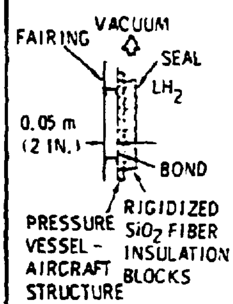	13 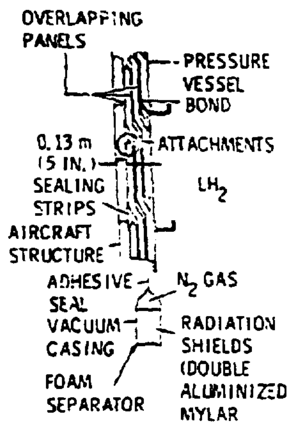	14 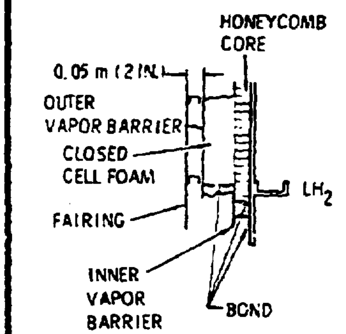	15 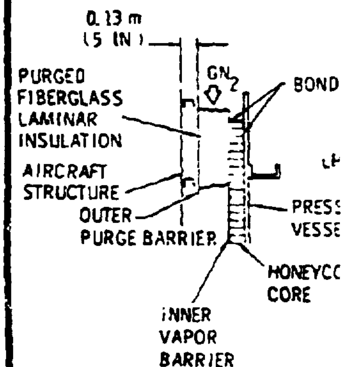
MICROSPHERES VACUATED TO 10^{-2} TORR; TANK PRESSURE LOAD ON MICROSPHERES	RIGIDIZED SiO_2 FIBER EVACUATED TO $<10^{-1}$ TORR; TANK PRESSURE LOAD ON FIBER BLOCKS	CRYOPUMPED N_2 IN PANELS; AMBIENT PRESSURE LOAD ON THE INSULATION	AIR IN HONEYCOMB CRYOPUMPED; CLOSED-CELL FOAM AIR-FILLED; INNER VAPOR BARRIER TEMPERATURE >97°K(>175°R)	AIR IN HONEYCOMB CRYOPUMPED; N_2 PURGE IN BATTING AT 1.4×10^4 N (2 PSI) GAGE PRESSURE; INNER VAPO BARRIER TEMPERATURE >83°K(>150°I
I	I	N	I	N
ALUMINUM HONEYCOMB CORE AND FACE SHEETS • MICROSPHERES 69 kg/m^3 (4.3 lb/ft^3) 321 S.S. FLEX • LINER 1.0 kg/m^2 (0.21 lb/ft^2)	• SiO_2 RIGIDIZED FIBER BLOCKS 112 kg/m^3 (7 lb/ft^3) • INVAR LINER 0.97 kg/m^2 (0.20 lb/ft^2) • POLYURETHANE ADHESIVE 0.15 kg/m^2 (0.03 lb/ft^2) PER BOND LINE	SEALED PANEL CONSISTS OF: • 6 DAM SHIELDS • 12 FOAM SPACERS • 2 MAAM CASINGS 0.55 kg/m^2 (0.113 lb/ft^2) PER PANEL • MAAM SEALING STRIP, EACH 8.5×10^{-2} kg/m^2 (1.7×10^{-2} lb/ft^2) • POLYURETHANE ADHESIVE 0.15 kg/m^2 (0.03 lb/ft^2)	• 3/8-IN. CELL MYLAR HONEYCOMB 34 kg/m^3 (2.1 lb/ft^3) • MAAM INNER VAPOR BARRIER 8.5×10^{-2} kg/m^2 (1.7×10^{-2} lb/ft^2) • POLYURETHANE CLOSED-CELL FOAM 35 kg/m^3 (2.2 lb/ft^3) • MAAMF OUTER VAPOR BARRIER 0.673 kg/m^2 (0.138 lb/ft^2) • POLYURETHANE ADHESIVE 0.15 kg/m^2 (0.03 lb/ft^2) PER BOND LINE	• 3/8-IN. CELL MYLAR HONEYCOMB 34 kg/m^3 (2.1 lb/ft^3) • MAAM INNER VAPOR BARRIER 8.5×10^{-2} kg/m^2 (1.7×10^{-2} lb/ft^2) • FIBERGLASS LAMINAR BATTING 16 kg/m^3 (1 lb/ft^3) • PURGE BARRIER EPOXY/GLASS/TEF COMPOSITE 0.69 kg/m^2 (0.14 lb/ft^2) • POLYURETHANE ADHESIVE 0.15 kg/ (0.03 lb/ft^2)
EVACUATE MICRO-SPHERES; MAINTAIN VACUUM IN SERVICE (PUMPS OPERATE ONLY WHEN 10^{-2} TORR IS EXCEEDED)	EVACUATE SiO_2 BLOCKS; MAINTAIN VACUUM IN SERVICE (PUMPS OPERATE ONLY WHEN 10^{-1} TORR IS EXCEEDED)	PASSIVE	PASSIVE	PURGE AIR TO <1%; MAINTAIN POSI N_2 PRESSURE IN SERVICE; VENT DUR ASCENT; REPLENISH DURING DESCEN LOAD N_2 AFTER EACH FLIGHT

3 FOLDOUT FRA...

TABLE 31. - STATUS OF DEVELOPMENT APPLICABLE TO THE INSULATION SYSTEM CONCEPTS

Insulation System Concept	Applicable Development: Reusable System Design?	Applicable Development: Demonstrated on:	Applicable Development: Comments
1. He Purged	Yes (Space Shuttle Application Technology)	NAS 8-27419, 2.2 m (7.2 ft) tank	Purge jacket is epoxy glass, Teflon coated. Insulation is multilayers. 100 Space Shuttle flight cycles demonstrated with LH_2.
2. He/N_2 Double Purge	No (Orbital Application Technology)	NAS 3-4199, 2.1 m (6.9 ft) tank	Used helium purged fiberglass substrate, nitrogen filled multilayers. Simulated one ground hold, launch, orbit flight cycle with LH_2. Thickness of He to N_2 layers must be controlled accurately to prevent N_2 liquefaction.
3. External Polyurethane Foam Non-integral Tank 4. External Polyurethane Integral Tank	No (Apollo Flight Program)	Saturn S-II Stage, 10 m (33 ft) dia.	Polyurethane foam sprayed on, machined, covered with polyurethane sealer. Conductivity rises with time due to displacement of blowing gas with air. Flight demonstrated.
5. Internal Polyurethane Foam	No (Apollo Flight Program)	Saturn S-IVB Stage 6.7 m (22 ft) dia.	Glass fiber reinforced foam tiles, individually bonded, fiberglass polyurethane resin liquid barrier (GH_2 filled); 135 thermal cycles.

PRECEDING PAGE BLANK NOT FILMED

TABLE 31. - Continued.

Candidate Insulation System	Applicable Development: Reusable System Design?	Demonstrated on:	Comments
6. PPO Internal Foam/ Poly-urethane External Foam	-	This combination has not been demonstrated. See comments on Systems 3 and 7.	
7. PPO Internal Open Cell Foam	Yes (Space Shuttle Technology)	NAS 9-10960, 1.75 m (5.8 ft) tank	Individual tiles bonded to wall. Conductivity higher than GH_2, varies with orientation. 100 Space Shuttle flight cycles demonstrated with LH_2.
8. Honeycomb Gas Layer Barrier	Yes (SST Methane Tank Technology; Space Shuttle Technology)	NAS 3-12425 NAS 8-25974	GH_2 filled insulation.
9. Rigid Vacuum Shell	Yes (Space Shuttle System Technology)	NAS 3-14369, 2.6 m (8.7 ft) dia. Tank	Aluminum honeycomb rigid vacuum shell with aluminum face sheets. Shell collapsed after cycling 29 times due to peeling of inner face sheet. External face sheet should be made vacuum seal to prevent this. Problems making system vacuum tight to 10^{-5} torr. The presence of the closed cell foam, as indicated in Table 30, would create difficulty in maintaining the prescribed level of vacuum due to outgassing.

TABLE 31. - Continued.

Candidate Insulation System	Applicable Development: Reusable System Design?	Demonstrated on:	Comments
10. Microspheres with External Flexible Metal Jacket	Yes (Space Tug System Technology)	NAS 3-17817 1.2 m (3.9 ft) dia. Tank	Stainless steel jacket, 0.008 cm (0.003 in.) thick, has demonstrated vacuum integrity to 10^{-6} Torr. None of 23.2 m (76 ft) of resistance seam welds leaked. Test program demonstrated 13 flight cycles using LN_2 with no change in thermal performance. Microspheres have been loaded compressively in a flat plate 100 times with no change in thermal performance.
11. Microspheres with Internal Liner	Yes (LH_2 aircraft application technology)	This design modification to System 10 has not been demonstrated.	
12. Silica insulation with Internal Liner	Yes (Space Shuttle high temperature insulation)	Properties of insulation have been determined. Liner has not been demonstrated.	
13. Self-evacuating Shingles	No (Orbital Application Technology)	NAS 3-6289, 0.8 m (2.5 ft) calorimeter tank.	Leaktight shingles were not obtained; sealing strips opened upon thermal cycling. This system did not perform as designed; requires further development.

TABLE 31. - Concluded.

Candidate Insulation System	Applicable Development		
	Reusable System Design?	Demonstrated on:	Comments
14. Self-evacuating Honeycomb/ Foam		This combination has not been demonstrated. See comments on Systems 3 and 15.	
15. Self-evacuating Honeycomb/ N_2 Purge.	No (Orbital Application Technology)	NAS 8-11747 0.8 m (2.5 ft) calorimeter tank.	Conductivity of honeycomb degraded with number of LH_2 cycles (up to 14) as gas permeated the honeycomb. Had problems with nitrogen purge gas liquefying in the multilayers (Honeycomb sublayer should have been thicker).

7.1.3 Concept screening procedure. - In the concept screening, each insulation concept was analyzed with regard to safety, performance, producibility and operational requirements. These analyses considered the following aspects:

Safety

- Malfunction
- Leak detection
- Flammability and toxicity
- Inspectability

Performance

- Heat input to fuel (evaporated and vented)
- Weight and volume
- DOC

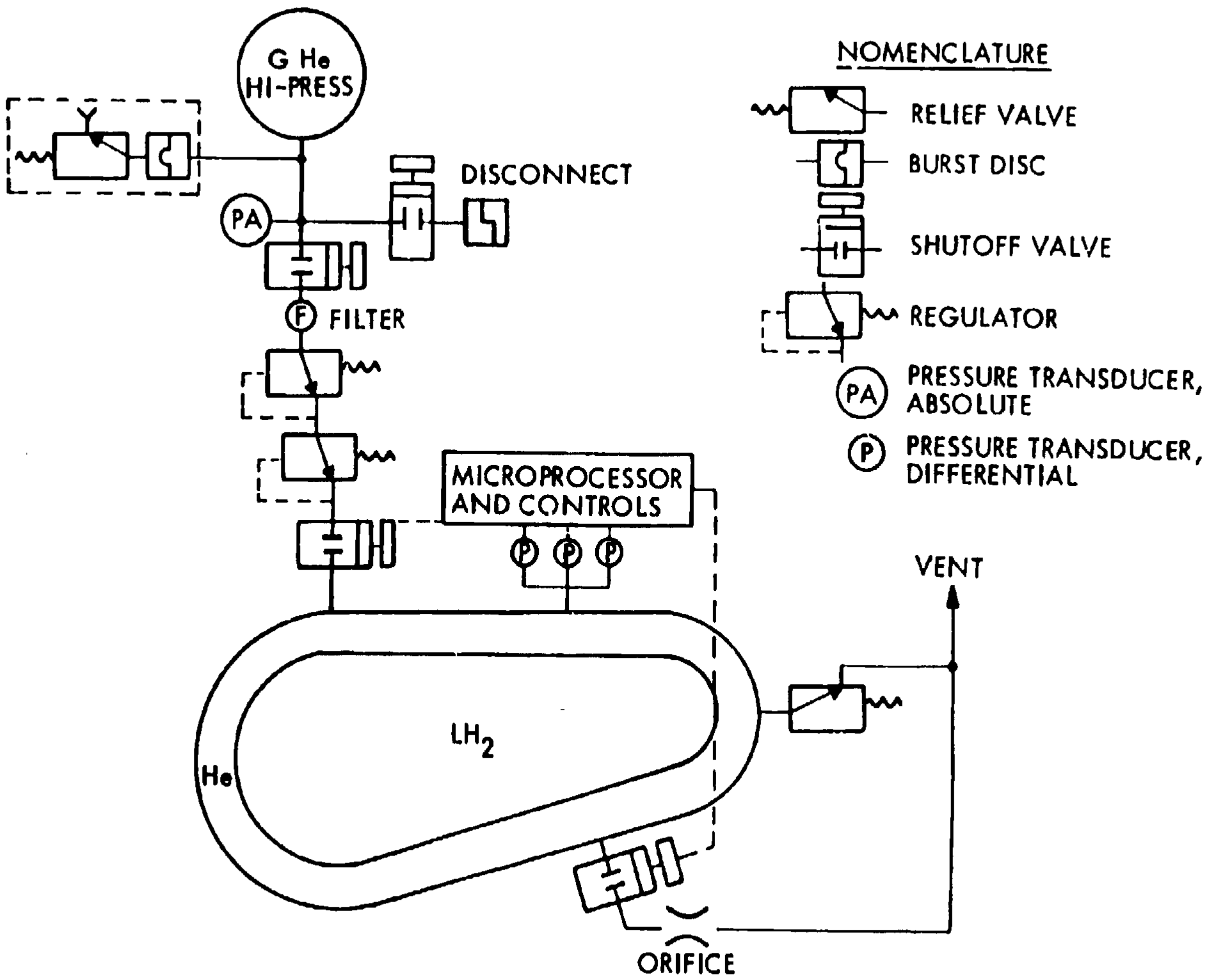

Figure 83. - Plumbing schematic for concept 1.

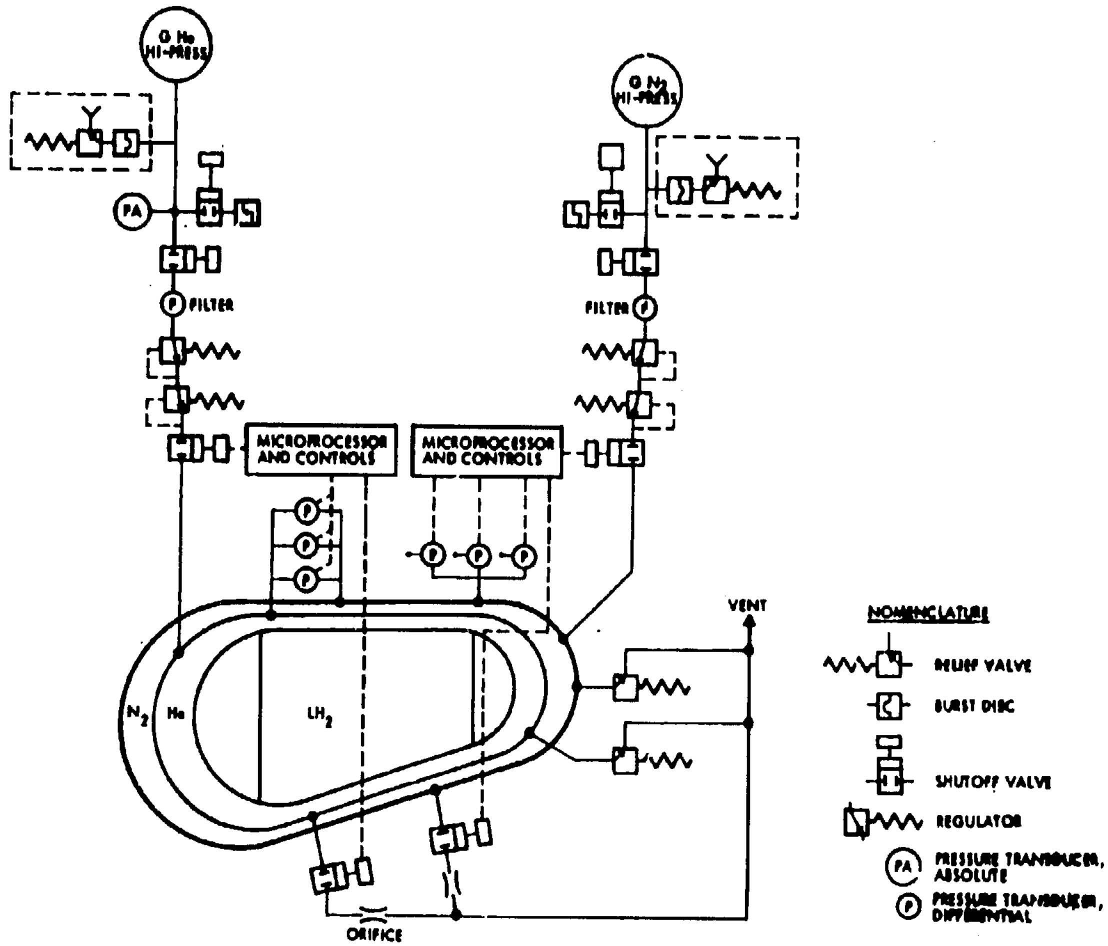

Figure 84. - Plumbing schematic for concept 2.

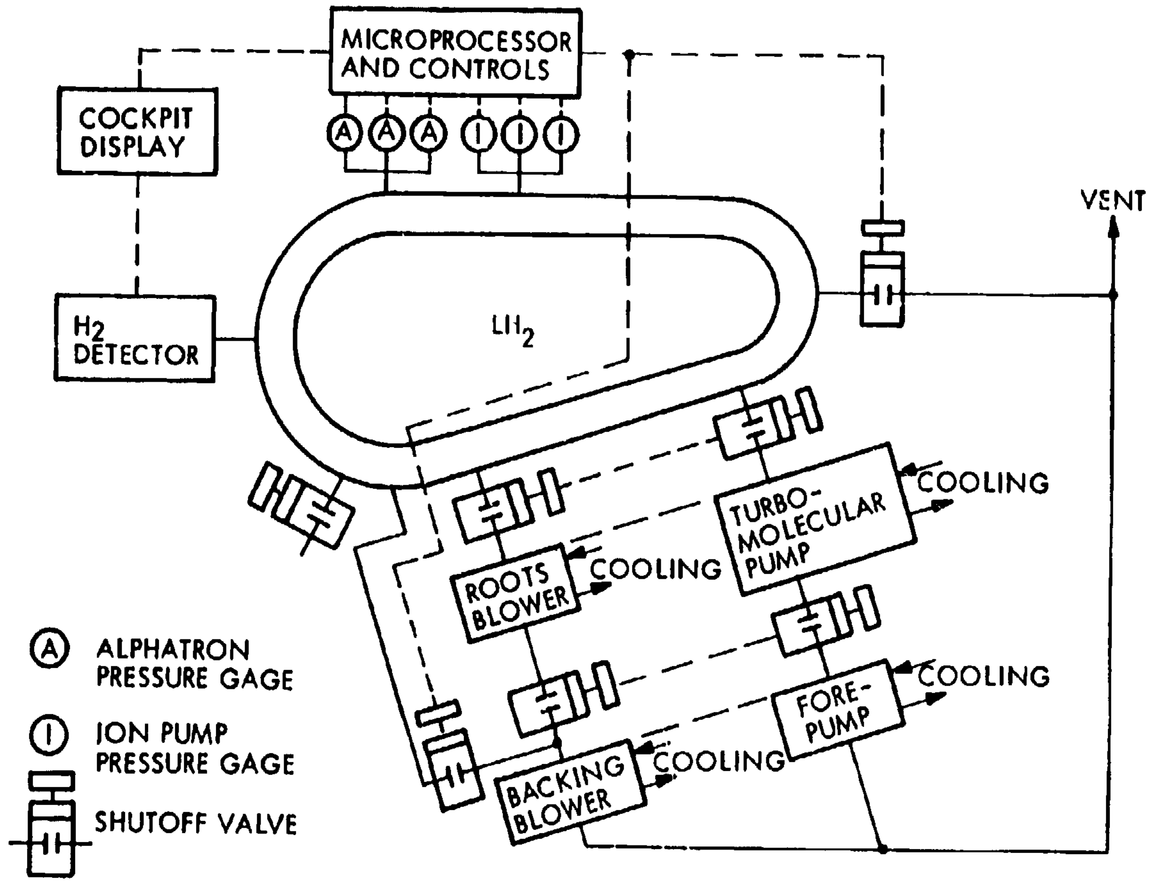

Figure 85. - Plumbing schematic for concept 9.

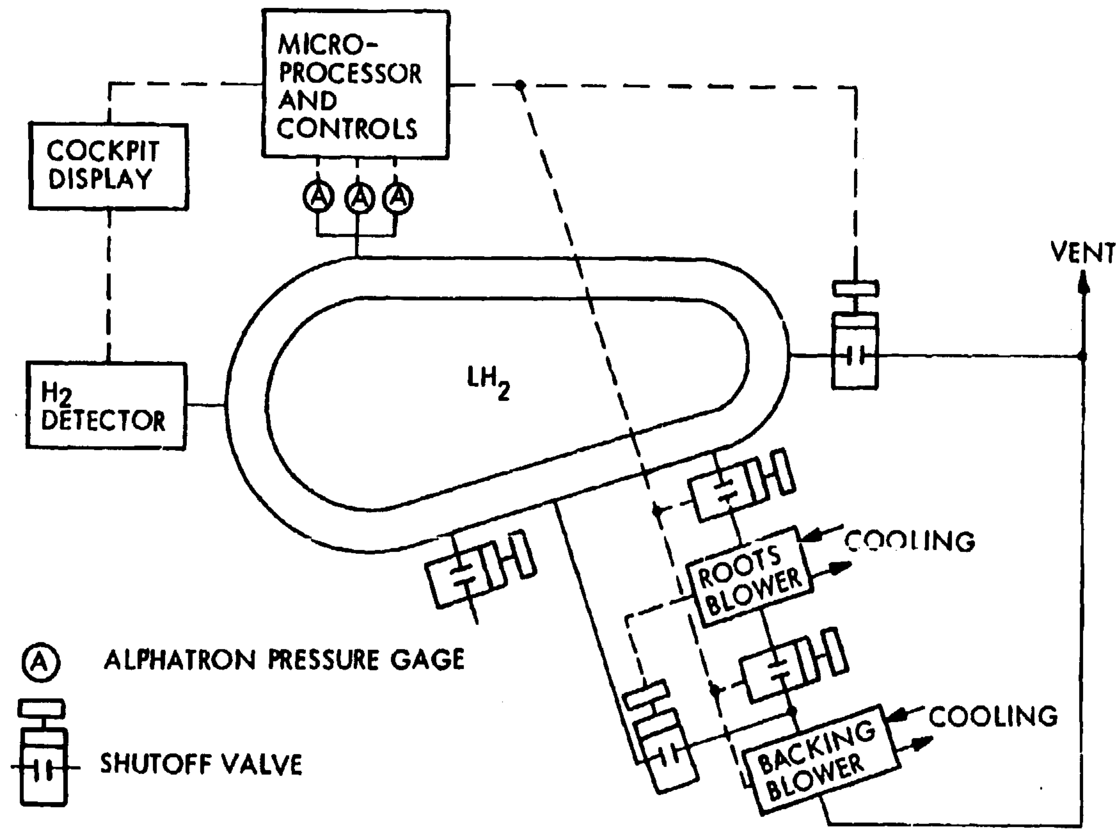

Figure 86. - Plumbing schematic for concepts 10, 11, and 12.

Producibility

- Approach
- Development and Manufacturing Requirements

Operations

- Inspection, Maintenance, and Operational Requirements
- Life Expectancy

Results of these studies were then compared to rank each concept so that the four most promising could be selected for more detailed study.

7.1.3.1 Safety analysis: The safety analysis considered four major aspects. These were evaluated against the criteria shown in Table 32 and a numerical weighting factor assigned to each. The parameters considered under the malfunction testing included the type of failure (e.g., vacuum jacket leakage), the condition resulting from this failure, its effect on flight operation and aircraft safety, and protective measures that could be provided to overcome or minimize the failure effect. The problem of GH_2 leakage from the tank was examined in terms of the ability to detect leakage into the insulation, and into the airframe interior in the case of a nonintegral tank. A second aspect of the safety analysis considered the potential for removal of hydrogen or inerting of the system during aircraft operation, as well as when it is necessary to enter the fuel tank for inspection or repair. Flammability of the materials used in the system, and the possible toxic products resulting from combustion of a material were included in the third category of the safety analysis. The final aspect was how the system design affects the capability to inspect for tank wall or vapor barrier leakage.

For purposes of comparison, numerical ranking factors were assigned to each individual parameter. A value of four signifies maximum importance with smaller values indicating considerations of lesser impact on aircraft and passenger safety. The ranking scale was selected to give an acceptable value of resolution for comparison between concepts and was consistent with the level of analysis in this screening operation.

7.1.3.2 Performance analysis: The procedure followed in developing performance data for each system in the concept screening phase was to compute the amount of fuel evaporated during flight and ground segments as a function of insulation thickness. From the weight of fuel required to fly the design mission, plus allowance for necessary reserves, the required fuel load (the weight of liquid + evaporated fuel) and subsequent tank volumes were computed. Fuel containment system dry weight and fuselage length requirements were then calculated. These parameters, together with total fuel and ground vent loss weights, were then used to calculate DOC as a function of insulation thickness. Optimum thickness was selected as that corresponding to the minimum DOC, as obtained graphically from the DOC versus insulation thickness results.

TABLE 32. - SAFETY RANKING CRITERIA

Criteria	Ranking Weight*	
Malfunction		
Barriers		
• Permeability and leakage	4 (mixing of H_2 and air)	For Each Consideration
	4 (LO_2)	
• ΔP and flow direction	2 (H_2)	
	2 (Air)	
• Effect of thermal cycles	3	
• Resistance to accidental penetration	4	
Active systems	3	
Leak detection and control		
Time	1	
Sensitivity	1	
Safe removal in service	3	
Safe removal for tank inspection	1	
Flammability and toxicity	2	
Inspectability		
Tank	1	
Barrier	1	

*4 = Maximum importance:

Total of 44 = Maximum safety

7.1.3.2.1 Fuel tank geometry: As stated earlier, the aft tank of the aircraft was used as a basis for both the screening and preferred candidate analysis phases. The general configuration of the tank and its geometric relationships which were assumed for preliminary analysis purposes are illustrated in Figure 87. Solutions to the relationships between required volume and insulation thickness and the tank length and forward diameter parameters are represented in Figures 88 and 89. These graphical relationships were used in the iterative process of tank sizing as a function of insulation system heat transfer characteristics and the corresponding thickness of the candidate insulation system.

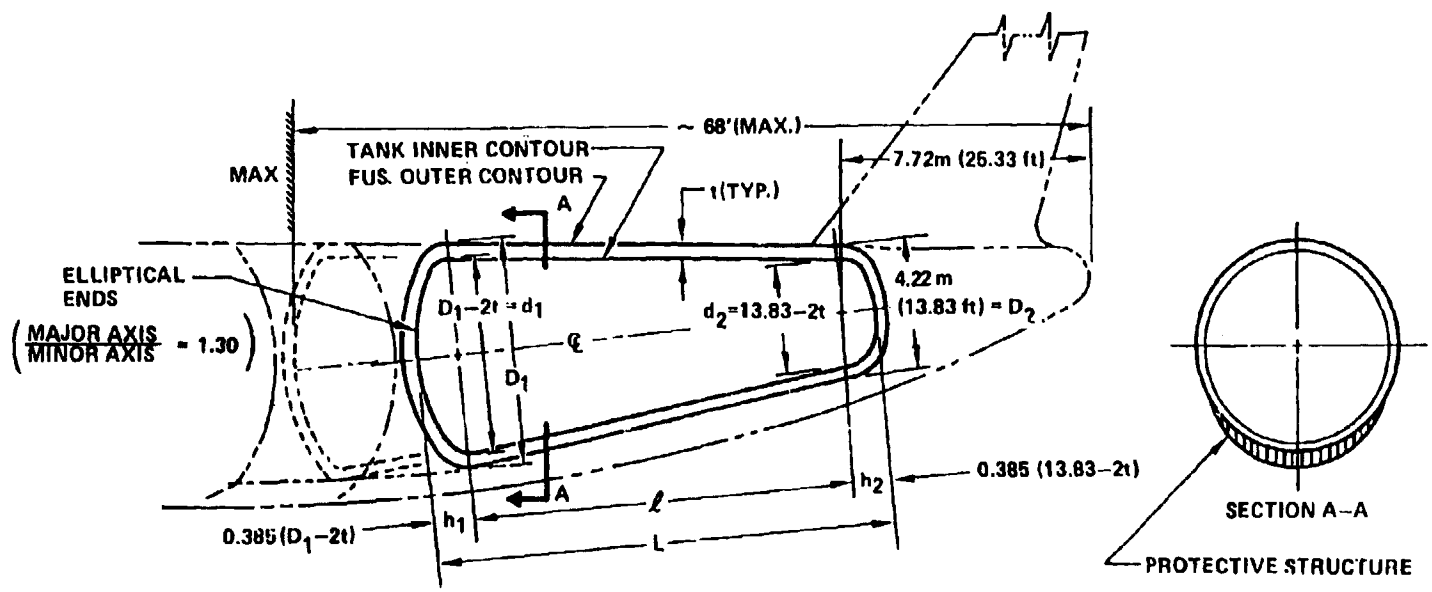

Figure 87. – General configuration of aft tank.

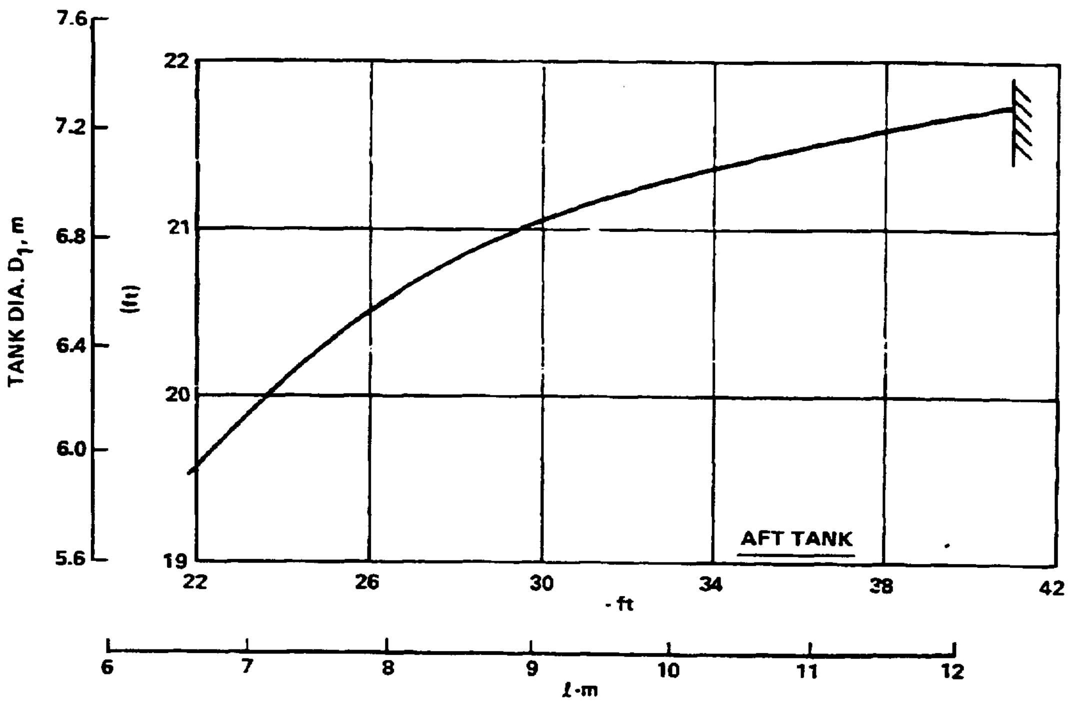

Figure 88. – Tank diameter D_1 vs tank length ℓ.

7.1.3.2.2 Thermal analysis: The thermal model used in the concept screening phase was developed as a closed form type of solution which considers the heat transfer in both liquid and vapor phases present in the tank as a function of liquid fraction, vapor and liquid-wetted wall heat fluxes, exterior temperature, and tank wall and insulation thermal properties. Net heat input to the liquid (and vapor generation) is a function of heat transfer across the liquid wetted portion of the tank wall, the liquid/vapor interface, along the tank wall from the ullage to liquid region, and radiation from the ullage portion of the tank wall to the liquid. The model is illustrated in Figure 90. Derivation of the model for wall and vapor heat transfer to the liquid is presented in Appendix C.

Vent [illegible] are calculated for a constant vent pressure of 145 kPa (21 psia). The differential equation includes variable thermodynamic properties for the liquid and vapor as well as for the insulation and tank wall. Radiation heat input to the liquid surface was computed as a function of average ullage region wall temperature for each of three areas corresponding to equal area times view factor products. Interior tank wall and liquid surfaces were assumed to be grey and to have absorptances of 0.3 and 1.0, respectively.

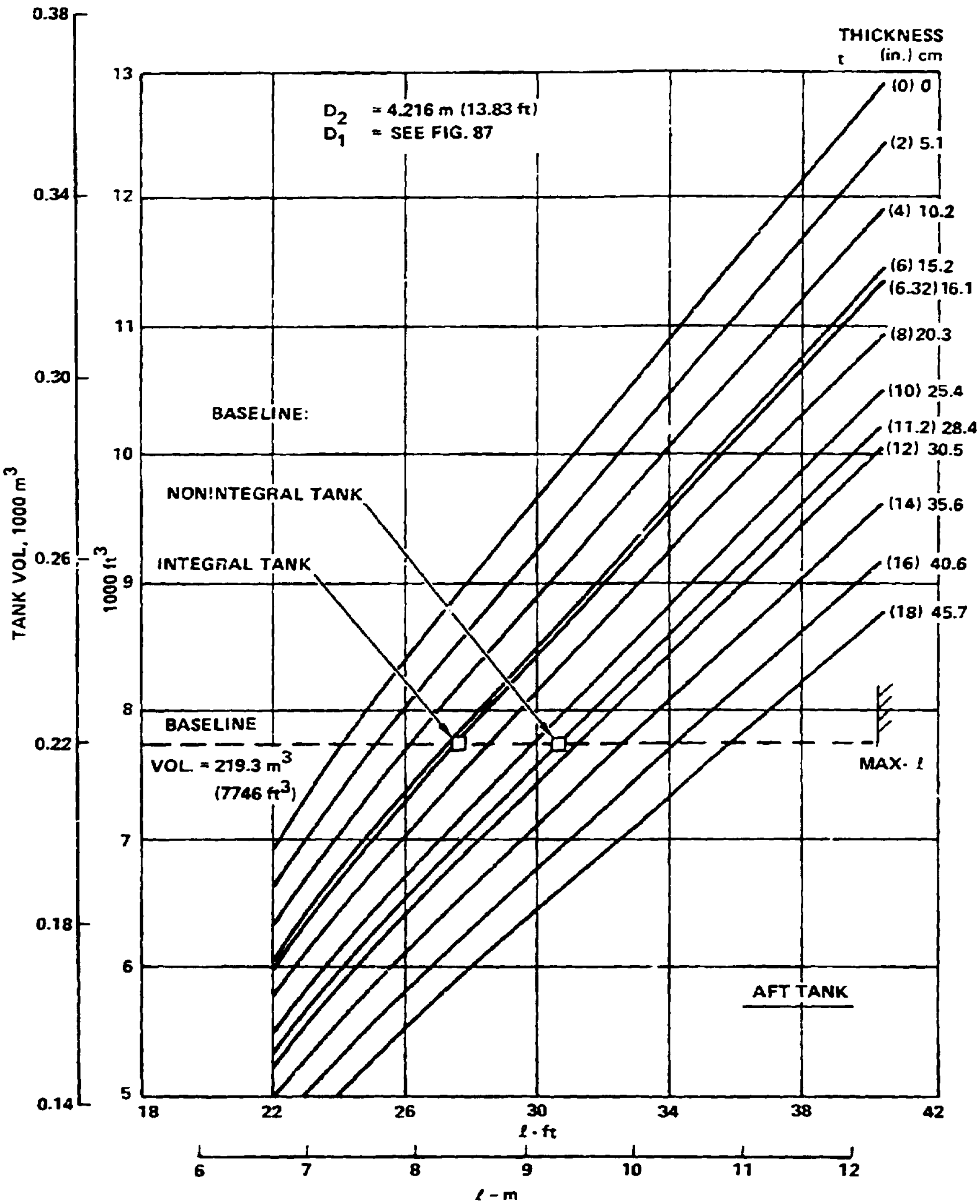

Figure 89. - Tank length ℓ vs volume and thickness.

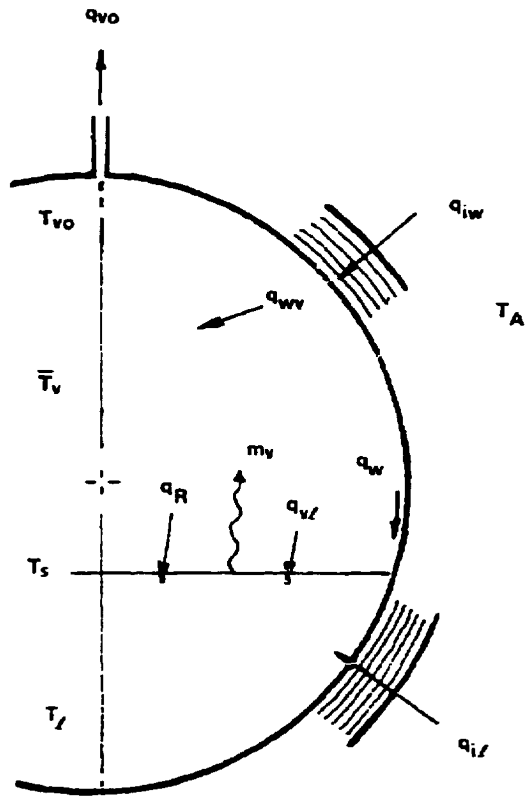

Figure 90. – Thermal model used for concept screening.

The major uncertainty in the thermal analysis, which also applied to the preferred candidate analysis, was the definition of the vapor-wall Nusselt number. This parameter governs the wall temperature distribution opposite the vapor and the subsequent mean vapor temperature. A thorough search of the literature did not reveal a satisfactory correlation for a non-isothermal wall exposed to a non-isothermal fluid for low Prandtl numbers (i.e., H_2 vapor). Consequently, initial studies were conducted varying the Nusselt number from a conduction dominate situation (Rayleigh Number < 6×10^3) to a turbulent boundary layer condition (RA $\geq 10^8$). Change of this parameter resulted in a very significant variation in vapor-wetted wall temperature distributions. As an example, the temperature of the top of the tank for a 50 percent uilage condition showed a variation from 185°K to 28°K as the Nusselt number was varied by a factor of 400 (going from a condition of highly stratified vapor to a turbulent boundary layer). The heat rate to the liquid decreased as the Nusselt number was increased to approximately 10 times the conduction limit. Further increase in Nu resulted in an increase in liquid heat rate. The initial decrease is due to lower conduction heat transfer along the tank wall, a smaller vapor-liquid temperature difference and a decrease of radiation from the vapor space wall to the liquid. This is the result of the enhanced heat transfer between the tank wall and the vapor which reduces the total heat into the liquid because of the removal of a greater fraction as sensible heat of the vapor, i.e., higher vapor exit temperature. Table 33 illustrates the influence of vapor-wall Nusselt number on mass of fuel vented for a 50 percent liquid level with a liquid-wetted wall heat flux of 97.7 W/m (31 Btu/hr ft^2).

The experimental data found in the literature which could be used for correlation of the vapor-wall Nusselt number were very limited. Schalla (Reference 8) reported the results of heat transfer testing on a small diameter (1.27 m (50-in)) liquid hydrogen tank. His vapor-wetted tank wall temperature data were used to correlate Nusselt number using the screening model. For the test tank, the best correlation of predicted and measured temperatures as a function of liquid level was obtained for a Nusselt number of approximately 17 which corresponds to a laminar condition. This comparison is

TABLE 33. - EFFECT OF VAPOR NUSSELT NUMBER ON HEAT INPUT TO LIQUID

[50% LIQUID LEVEL, q_w = 97.7 W/m^2 (31 Btu/hr/ft^2)]

N_u	Conduction	2X Conduction	4X Conduction	40X Conduction	110X Conduction
Average Wall °K Temperature (°R)	153 (276)	123 (221)	96 (173)	46 (83)	33 (59)
Vapor Exit °K Temperature (°R)	33.3 (60)	38.3 (69)	42.2 (76)	38.9 (70)	32.2 (58)
Ratio of Mass Vented*	1.0	0.926	0.878	0.939	1.080
Ratio of Vent Gas Sensible Heat*	1.0	1.287	1.505	1.366	1.059
Heat into Tank W (Btu/hr)	884 (3017	896 (3059)	910 (3107)	919 (3139)	938 (3202)
Heat removed by vented GH_2 W (Btu/hr)	219 (747)	281 (959)	326 (113)	295 (1007)	216 (736)

*Compared to Nusselt No. corresponding to highly stratified gas.

shown in Figure 91 where tank top surface temperature is plotted as a function of Nusselt number for various liquid levels. The dashed line represents the best fit of the experimental data corrected for a 290°K outer surface temperature. Computed and measured liquid heat rates are compared in Figure 92 as a function of liquid fraction. Because of this reasonable correlation with the experimental data a Nusselt number of 17 was employed to generate tank wall temperature distributions and liquid heat rates for the concept screening phase.

Computation of design mission fuel loss for four insulation thicknesses for each concept was performed using the following procedure. Initial tank sizing to determine heat transfer area was based upon the liquid heat input for a 90 percent full tank under cruise conditions. This tank size was used to compute fuel losses for seven segments of a 24-hour period having fuel withdrawal increments, ambient temperatues, and times as shown in Table 34. An initial tank pressure of 145 kPa (21 psia) and a minimum allowable pressure of 124 kPa (18 psia) was assumed for the mission. At low heat rates it may be necessary to vaporize some fuel to maintain the minimum pressure level in the tank. By successive iterations the tank size and fuel loss converged to give the correct tank dimensions for the design mission fuel requirement. Transient conditions were accounted for by computation of the time constant for each insulation using a stepwise ambient temperature change from ground to cruise and proportioning the cruise and ground segment (5 and 7) into two ambient temperature conditions. This resulted in a gross approximation of heat storage within the system.

7.1.3.2.3 Thermal properties: The temperature dependent properties required for the thermal analysis of the concepts, and the sources from which the data were obtained, are as follows:

- <u>Hydrogen</u> - Liquid and vapor phases
  - Density
  - Compressibility
  - Vapor pressure
  - Thermal conductivity
  - Specific heat
  - Latent heat of vaporization
  - Viscosity
  - Sonic velocity

  Properties data were taken from Reference 9.

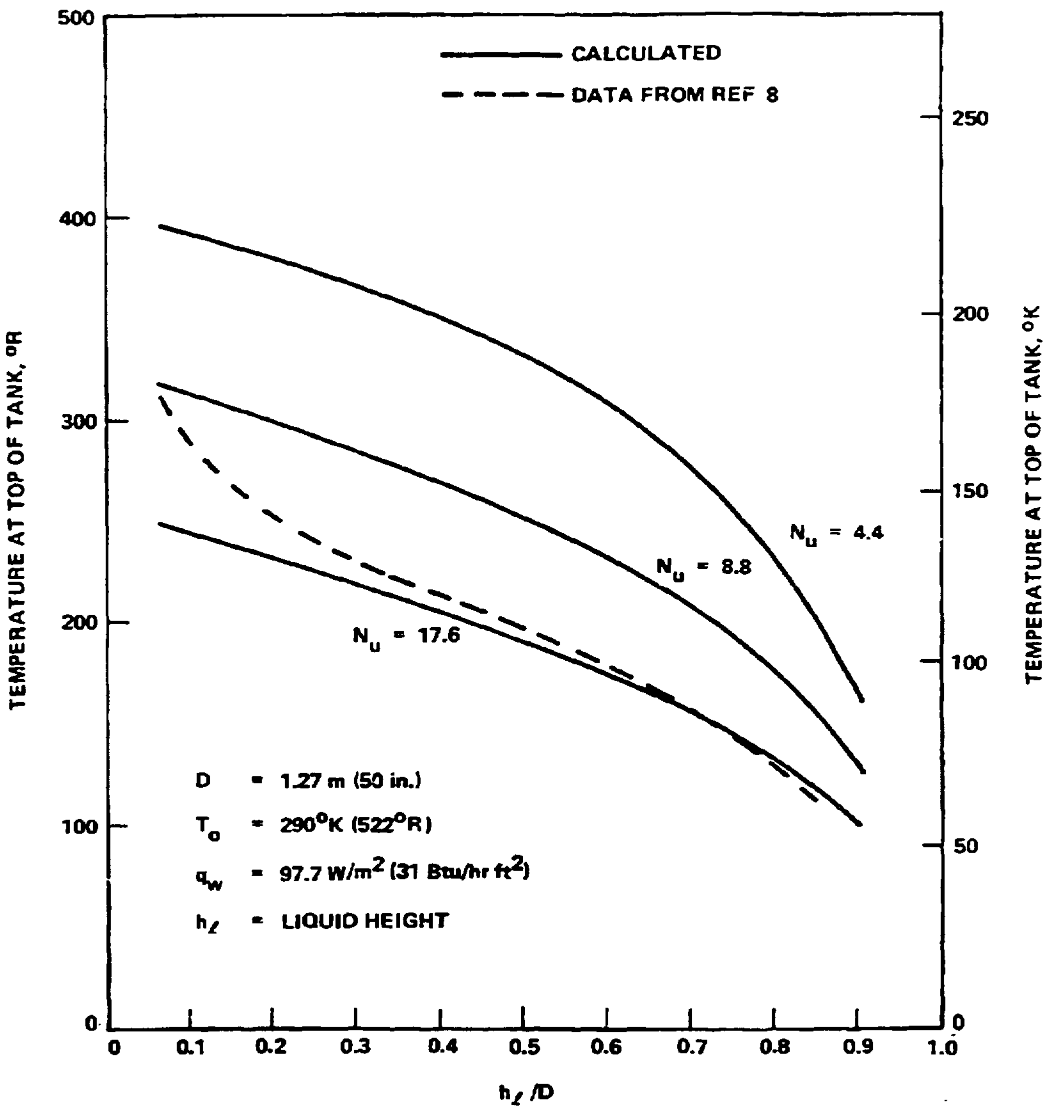

Figure 91. - Correlation of tank top surface temperature with Nusselt number for various liquid levels.

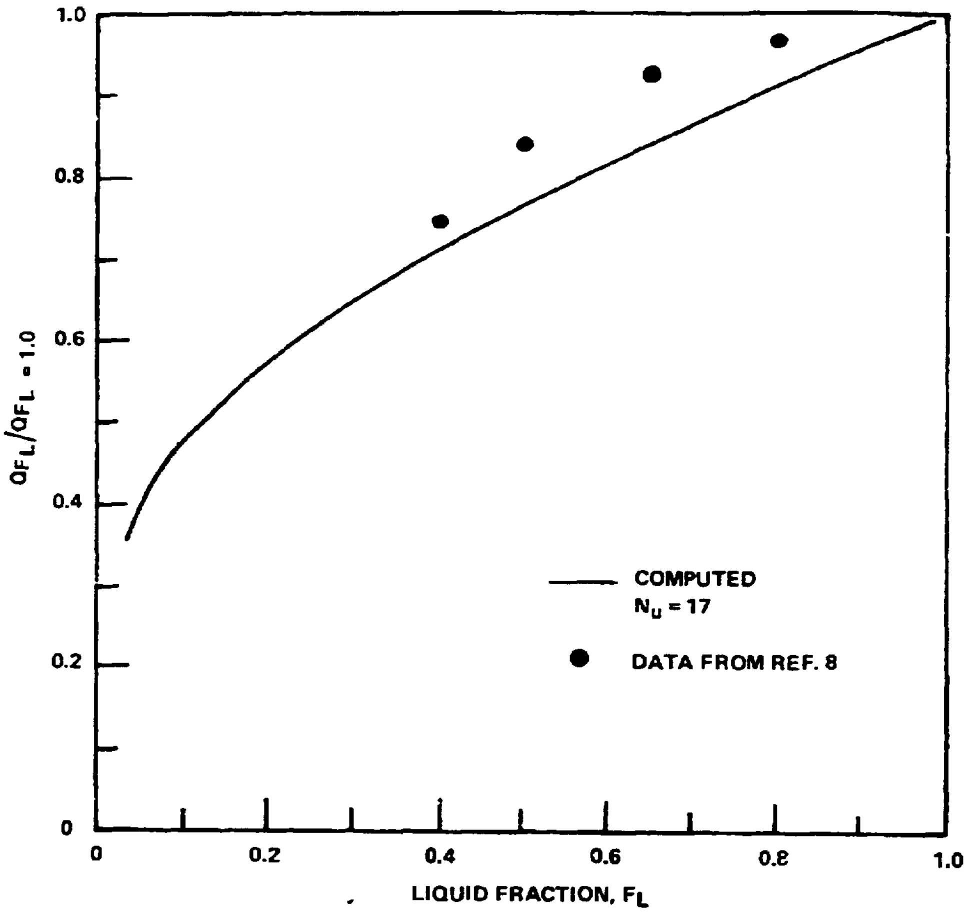

Figure 92. - Comparison of measured and computed liquid heat rate ratio as a function of tank liquid fraction.

- Tank and Fuselage - Aluminum - 2219 alloy for tank and 2024 alloy for fuselage
  - Density (Reference 10)
  - Thermal conductivity (Reference 11)
  - Specific heat (Reference 10)
- Insulations - Where available, data were taken from the literature for the specific material. In cases where data were not available, the properties were estimated using those of similar materials.

TABLE 34. - MISSION FUEL SCHEDULE - AFT TANK

Segment	Time (hr)		Fuel Withdrawal		Ambient Temperature	
	Segment	Total	kg	lb	°K	°R
1. Ground, After Fueling, Engines Off (a)	0.283	0.283	0	0	290	522
2. Taxi	0.233	0.516	35.4	78	290	522
3. Takeoff	0.0817	0.598	221	487	290	522
4. Climb	0.743	1.341	1,086	2,394	290	522
5. Cruise	10.273	11.614	10,466	23,073	222	400
6. Descent-Land	0.383	11.997	178	393	222	400
7. Ground	12.003	24.000	(b)		290	522

(a) APU Fuel not Included

(b) Approximately 1134 kg (2500 lb) of fuel remain in aft tank at start of assumed out-of-service period.

- Density
- Thermal conductivity
- Specific heat

Sources of property values used for each concept are given in Table 35. For the external foam, LI900, and microspheres, the data shown in Figure 93 were used for thermal conductivity values. In the case of polyurethane a composite of the data for densities from 27 to 35 kg/m^3 was used to derive an effective thermal conductivity. Only a single data point at ambient temperature was available for the Rohacell foam. As it falls on the curve for PVC foam, Figure 93, these data were used to represent the temperature dependent conductivity of Rohacell. Because of the long aircraft lifetime and the capability of hydrogen to permeate such materials, the thermal conductivity of the internal polyurethane foam in system 5 was considered as a GH_2 filled foam for this analysis. For the two purged systems, numbers 1 and 2, thermal conductivities were taken to be those of the specific purge gas, assuming the contribution of the low density glass batt material to heat transport was insignificant. (Reference 10)

TABLE 35. - DATA SOURCES FOR PROPERTIES OF INSULATION CONCEPTS

Concept Number	Material	Property and Data Source
1.	He-filled fiberglass	Thermal conductivity and specific heat; Ref. 10
2.	He and N_2-filled fiberglass	Same as No. 1
3., 4.	Rohacell foam	Thermal conductivity; see Fig. 93, extrapolated using PVC data. Specific heat; Ref. 12 for polyurethane
5.	Internal Polyurethane foam, 3D reinforced	Density and thermal conductivity for GH_2 filled condition; Ref. 5-9. Specific heat from ratio of foam and glass reinforcement Refs. 10 and 12
6.	Internal PPO plus external Polyurethane foam	Density and thermal conductivity; PPO, Ref. 5-10; Polyurethane - see Fig. 93. Specific heat; PPO assumed same as Polyurethane - Ref. 12
7.	Internal PPO foam	See No. 6
8.	Internal gas-filled honeycomb	Density and thermal conductivity; Ref. 14 and 15. Specific heat; extrapolated using ratios of constituents and Ref. 12
9.	Polyurethane foam	See Fig. 93, 32 kg/m^3. Specific heat; Ref. 12
10., 11.	Microspheres	Density and thermal conductivity; Ref. 16. Specific heat; Ref. 10
12.	LI-900	Density, thermal conductivity and specific heat; Ref. 17
13.	Self-evacuation shingles	Density and thermal conductivity, Ref. 18. Specific heat, estimate using ratio of constituents, Refs. 10 and 12.

TABLE 35. - CONCLUDED.

Concept Number	Material	Property and Data Source
14.	Self-evacuated honeycomb plus Polyurethane foam	Density and thermal conductivity: Polyurethane foam - see Fig. 93, 32 kg/m^3; honeycomb, Ref. 19. Specific heat estimated using ratios of components; Refs. 10 and 12
15.	Self-evacuated honeycomb plus GN_2 purged fiberglass	See No's. 2 and 14

- Purge Barrier/Vapor Barrier/Vacuum Jacket - Two types of vapor barriers were considered for use with closed cell form insulations to prevent infusion of air or hydrogen. One was a simple plastic sheet such as mylar or Kevlar. The other was a multilayer sandwich called MAAMF, which consists of the following:

Layer	Material Description
1	0.5 mil Mylar, Type A
2	Adhesive
3	0.5 mil Aluminum Series 1100.0 Foil
4	Adhesive
5	0.5 to 1.5 mil Aluminum Series 1100.0 Foil
6	Adhesive
7	0.5 mil Mylar, Type A
8	Dacron or Glass Net Fabric

The total thickness is 5 to 6 mils and it weighs 0.225 kg/m^2 (0.046 lb/ft^2).

Thermal conductivity of the vapor barriers and the thin (5 mil) stainless steel vacuum jacket was not considered because the thermal resistances introduced by these components is negligible. Thermal conductance of the honeycomb composite rigid vacuum shell was computed using both composite and aluminum core conductance data from Reference 22, together with overall thermal resistance data of References 23 and 24 to account for the resistance of the adhesive bonded core-to-face sheet interfaces.

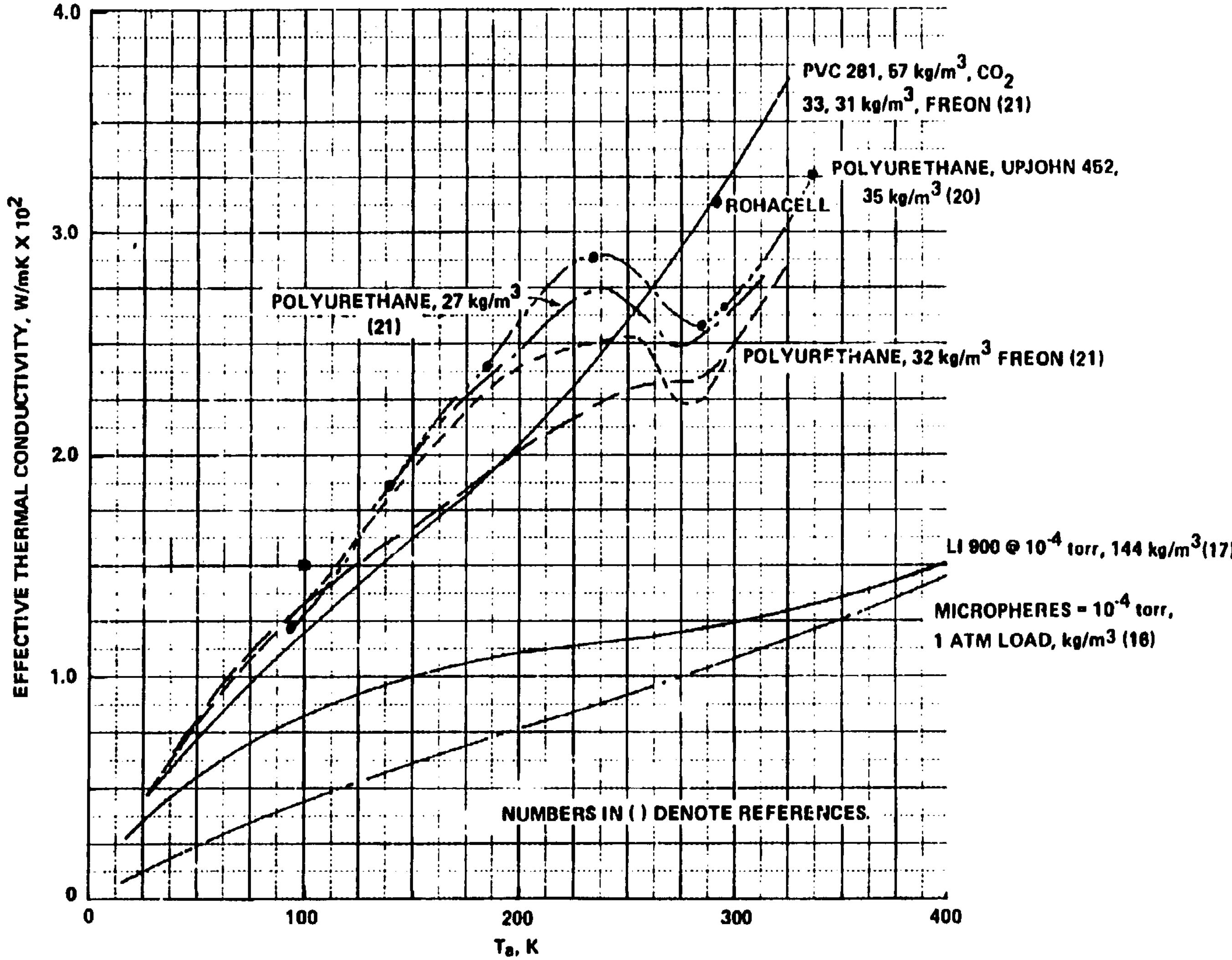

Figure 93. - Thermal conductivity of foams, rigidized silica and microsphere insulations.

Specific heat data were used in the transient program for evaluation of the preferred candidates. For the stainless steel vacuum jacket data were taken from Reference 10. Vapor and purge barrier specific heats were calculated from the specific heats of the constituents of each material weighted by the mass fraction of each in the total composite.

7.1.3.3 Producibility analysis: A preliminary producibility analysis was made for each concept to identify development items, potential fabrication and assembly procedures, and specialized manufacturing inspection requirements. These analyses were made to obtain an order of magnitude estimate of development and production costs which could be translated into DOC increments.

7.1.3.4 Operations analysis: The operations analysis was conducted to define projected maintenance and inspection requirements. Items requiring service were identified and frequencies of inspection and servicing were postulated. These analyses were conducted at the lowest level which would provide a relative comparison between systems.

7.1.4 Screening results. - The 15 candidate fuel tank insulation concepts were subjected to the screening analysis. They represented 12 basic types, 3 of which had 2 variations each. The objective was to provide a basis on which recommendations could be made for two concepts to be evaluated as preferred candidates for use with integral tanks and two for use with non-integral tank designs.

7.1.4.1 Safety: As outlined in 7.1.3.1, the safety analysis was a four-step process. First, a malfunction analysis was performed to determine if any of the systems had failure modes that were dangerous to life on aircraft. The details of the malfunction analysis are given in Appendix E. Second, requirements for hydrogen detectors were established. Third, an assessment of flammability and toxicity was made. Fourth, the ability to perform inspections of barriers and tank structure was evaluated.

The results of the evaluation of each concept with regard to the safety criteria (Table 32) are presented in Table 36. Under each specific criterion, the concepts are ranked in order of decreasing merit. Numerical ranking weights were assigned at each level within a category, based upon the maximum value which corresponds to the importance of the specific consideration. For example, in the category of permeability to gases to allow mixing of air and H_2, concept 4 was assigned a value 4, concept 2 a value of 3 and concept 5 a value of 1. The summation of the category ranking values was then converted to a scale of 0 to 100 to yield a relative ranking of all systems. The resulting composite ranking is presented in Table 37.

TABLE 36. - RANKING OF CANDIDATE INSULATION SYSTEMS BASED ON SAFETY CRITERIA

Criteria	Ranking Weight	Concept Ranking (Safest to Least safe)
Permeability of Barriers to Gases to Allow Mixing of Air and H_2	[illegible]	3M*,9,10,11,12 (2 Barriers, Both Metal); [illegible] (2 Barriers, One Metal); [illegible] (2 Barriers, One Metal); [illegible] (One Metal Barrier)
Permeability of Barriers to Gases to Allow Cryopumping in Organic Material	[illegible]	[illegible] (Gas Flow Outward) [illegible] (Min Organics) 3M Metal Barrier; [illegible] (No Cryopumping); [illegible] (Potential [illegible] Organics)
Potential Rate of H_2 Leakage Based on Pressure Drop Across Barrier	[illegible]	1,2 (ΔP ≈ [illegible]); 4 (ΔP ≈ [illegible]); [illegible] (ΔP = [illegible])
Potential Rate of Air Leakage into the Insulation Based on Pressure Drop and Flow Direction Across Barrier	[illegible]	5,7,8 (Gas Flow Outward); 1,2,15 (ΔP ≈ [illegible]); [illegible] (ΔP ≈ [illegible]); [illegible] (ΔP = [illegible])
Potential Barrier Leakage due to 4400 Thermal Cycles	[illegible]	1,2,9 (Barrier Moves Independent of Tank), 15 (Barrier Seal not Required), 10 (Barrier Seal Designed to Flex Elastically), 11,12 (Barrier Seal not flexed, 69 MPa (10 000 psi Stress in Liner well within Elastic Limits); 3M (Metal Barrier may Buckle during Thermal Cycling), 5 (Liquid Seal may Chip during Cycling), 14,15 (Honeycomb Seal is Cold Worked during Cycling); 3,4,6,8,13 (Organic Seal is not as Resistant to Thermal Cycle Induced Leaks at Lower Temperatures as Metals)
Resistance to Accidental Penetration of External Surface	[illegible]	5,7,8,11,12 (Tank or [illegible]); [illegible] (Vapor Barrier); 10 (Thin Metal Barrier); 13 (Plastic Film Barrier)
Reaction Time to Detect H_2 Leakage	[illegible]	9,10,11,12 (Positive ΔP, Leak into Vacuum); 5,7,8 (Positive ΔP, Detectors Outside Tank); 2,15 (Positive ΔP, 1 Barrier, Detectors in N_2 Layer); 1 (Positive ΔP, 1 Barrier, Detectors Outside Tank); 3,4,13 (Negative ΔP, 1 Barrier, Detectors Outside Tank); 14 (Negative ΔP, 2 Barriers, Detectors Outside Tank)
Sensitivity of Leak Detection Method	[illegible]	[illegible],10,11,12 Low Pressure Detection; [illegible] ΔP [illegible]; 13,14,15 Detection
Capability to Remove Leaking H_2 Safely in Service	[illegible]	9,10,11,12 (Pump) 1,2,15 (Purge); 4,5,6,7,8,13,14 (Nonactive)
Tank Inspectability	[illegible]	5,7,8,11,12 (Ext. Insp.); 1,2,3,4,6 (Int. Insp) 10,13,14,15; 9 (Tank Surface not Visible)
Secondary Barrier Inspectability	[illegible]	[illegible],4,6,9,15 (Ext. Insp.); 5,7,8,11,12 (Int. Insp.); [illegible] (One Barrier can't be Inspected)
Malfunction of Active Systems	[illegible]	3,4,5,6,7,8,13,14,15 (Passive); 1,10,11,12 (Active); 2,9 (Active More Complex)
Ease of GH_2 Removal from Tank for Internal Inspection	[illegible]	1,2,3,4,9,10,11,12,13 14,15 (Metal); 6,7,8 (Open Cell); 5 (Closed Cell)
Flammability and Toxicity of Materials in Case of Fire	[illegible]	10,11,12 (Min Organics); 1,2,9,15 (Mod Organics); 5,7,8 (Inside Tank); 3,4,5,13,14, (Most Organic Ext. to Tank)

*3M designates use of a metal vapor barrier ([illegible]) with concept 3.

LEGEND

Criteria: [X] ← Ranking Weight

Concept Ranking:
Safest
↓
Least safe

ORIGINAL PAGE IS
OF POOR QUALITY

ORIGINAL PAGE IS
OF POOR QUALITY

TABLE 37. - SUMMARY OF SAFETY RANKING

Concept	Ranking Score[a]
11, 12	89
10	84
9	80
7, 8	78
3, 4[b]	77
2	75
1	74
5	73
15	70
14	56
6	54
3, 4[c]	49
13	42

[a] 100 = maximum possible
[b] MAAMF is used as vapor barrier
[c] Plastic film is used as vapor barrier

Insulation Concept Number/Type

1. GHe Purged FG
2. GHe-GN_2 Purged FG
3. Ext. Foam, Nonintegral
4. Ext. Foam, Integral
5. Internal PU Foam
6. Int. PPO, Ext. PU Foams
7. Int PPO Foam
8. Int. Perf HC
9. Rigid Vac Shell
10. Ext. Microspheres
11. Int. Microspheres
12. Int. LI 900
13. Self-Evac. Shingles
14. HC/Foam
15. HC/GN_2 Purged FG

Considering safety alone, concepts 2, 3, 9, and 10 would be the choices for the nonintegral tank design, and concepts 4, 7, 11, and 12 the choices for the integral design.

7.1.4.2 Performance: Results of the thermal performance studies are tabulated in Table 38 for each system. The values presented are those for the insulation thickness giving the minimum DOC as determined graphically from a plot of DOC versus insulation thickness. Weight and volume statements were then recalculated for the thickness corresponding to minimum DOC. Ranking of the concepts based upon DOC is shown in Table 39. The table also shows fuel weight and fuel volume fractions as dimensionless parameters normalized to the values calculated for the baseline system, concept no. 4.

The values of DOC are based upon consideration of both flight and ground fuel losses. A comparison between DOC calculated in this manner and that calculated for flight loss only is given in Table 40. The only impact consideration of flight boiloff alone has on the ranking is that nos. 6 and 9 change positions, no. 6 ranking higher than no. 9.

On the basis of DOC, concepts 4, 14, 11, and 12 remain as logical choices for the integral tank design and concepts 13, 10, 3, and 15 for the nonintegral tank.

7.1.4.3 Producibility and operational: A preliminary producibility analysis was made for each candidate system to identify development items, potential fabrication and assembly procedures, and inspection requirements following or during fabrication as shown in Table F-1 of Appendix F. All systems appear feasible to fabricate although a much more detailed analysis is required, particularly around tank penetrations. From the data in the Appendix, cost differences were developed between the 15 insulation candidates for the development and manufacture of the insulation systems. When the difference in costs is expressed as a percent of direct operating cost per seat nautical mile, it varies up to only 0.2 percent between 14 of the systems. For the other system, no. 9, the percentage increased up to 0.4 percent over the lowest cost system. These cost differences have a minor impact on a selection of a candidate insulation system. For example, a development cost of 10×10^6 dollars spread over 350 aircraft having a 14-year lifetime and operated 350 days per year represents a DOC increment of 1.6×10^{-4}¢/S km (3×10^{-4}¢/S n.mi.). Thus, a 0.4 percent range in these costs is insignificant to DOC. No DOC figures were calculated for production costs in the concept screening phase because of the scope of the analysis that would be required to obtain valid data for the many systems involved.

Estimates for inspection, maintenance and operational requirements of the systems are shown in Table F-2, Appendix F. From these requirements, the magnitude of direct operating costs was estimated assuming a labor cost of $25 per man hour. The estimates vary from 0.000 27 to 0.000 05 ¢/S km (0.0005 to 0.0001 ¢/S n.mi.).

TABLE 38. - CONCEPT SCREENING PERFORMANCE ANALYSIS SUMMARY

Concept Number	1	2	3	4	5	6	7	8	9	10	11	12	13	14	15
Insulation	Fg/CH4 purge	Fg/CH4-GN$_2$ purge	Rohacell Foam Ext.	Rohacell Foam Ext.	PU Foam Int	Int PPO/ Ext PU Foam	Int PPO Foam	Perf HC	Rigid Vac Shell(g)	Micro-sphere Ext Vac	Micro-sphere Int Vac	11-900 Int. Vac	Full-Ext. Shingles	HC/Foam	HC-GN$_2$ Purge
Tank Type	N I(a)	N I	N I	I	I	I	I	I	I	N I	I	I	N I	I	N I
FCS Weight kg (lb)	13 279 (29 275)	12 891 (28 420)	10 134 (22 343)	7 839 (17 283)	11 576 (25 521)	9 505 (20 955)	10 676 (23 536)	11 296 (24 899)	10 225 (22 542)	10 225 (22 542)	8849 (19 509)	9537 (21 025)	8594 (18 947)	8046 (17 739)	11 759 (25 925)
FCS Thickness cm (in.)	33.83 (13.32)	25.2 (9.92)	22.38 (8.81)	10.54 (4.15)	13.11 (5.16)	14.15 (5.57)	20.98 (8.26)	17.17 (6.76)	15.09 (5.93)	20.02 (7.88)	10.67 (4.21)	9.88 (3.89)	15.75 (6.20)	10.87 (4.28)	24.45 (9.64)
Fuel Vaporized Flight (b) kg (lb)	1615 (3560)	1093 (2404)	889 (1960)	916 (2020)	4559 (10 050)	1625 (3583)	3384 (7460)	4117 (9078)	372 (820)	260 (574)	523 (1153)	1021 (2250)	314 (694)	865 (1906)	464 (1024)
Fuel Vaporized Ground (c) kg (lb)	1737 (3830)	1852 (4080)	1613 (3556)	1733 (3820)	5094 (11 230)	3373 (7435)	4491 (9900)	4017 (8855)	191 (420)	1016 (2240)	761 (1678)	1249 (2750)	805 (1775)	1229 (2710)	1017 (2242)
DOC(d)	2.0063	1.9340	1.8818	1.8269	1.9961	1.8866	1.9857	1.9526	1.8575	1.8635	1.82686	1.8538	1.8322	1.8528	1.8861
Fuel Weight Fraction (W_{FCS}/W_{FUEL})(e)	0.475	0.461	0.353	0.280	0.414	0.340	0.382	0.382	0.406	0.356	0.317	0.341	0.322	0.288	0.421
Fuel Volume Fraction (V_{FUEL}/V_{FCS})(f)	0.569	0.645	0.607	0.719	0.449	0.701	0.616	0.639	0.696	0.714	0.761	0.731	0.726	0.733	0.667

(a) N I = nonintegral, I = integral
(b) Includes pressurant gas
(c) Includes tank cooldown for fueling
(d) Fuel vented on ground included
(e) W_{fuel} = mission fuel weight, 61 610 lb
(f) V_{fuel} = mission fuel volume
(g) HC vac-jacket carries aircraft loads

TABLE 39. - DOC, WEIGHT, AND VOLUME SUMMARY FOR CONCEPT SCREENING

	CONCEPT NUMBER														
	$\boxed{4}$ C	14	$\boxed{11}$	13	$\boxed{12}$	$\boxed{10}$ D	9 B	3 A	6	15	2	$\boxed{8}$	$\boxed{7}$	5	1
$\frac{DOC}{DOC_4}$	1.000	1.000	1.001	1.003	1.014	1.020	1.022	1.030	1.033	1.038	1.059	1.069	1.087	1.093	1.097
$\frac{W'_f}{W'_{f4}}$	1.000	1.029	1.132	1.150	1.218	1.307	1.450	1.296	1.214	1.504	1.646	1.364	1.364	1.479	1.696
$\frac{V'_f}{V'_{f4}}$	1.000	0.992	1.003	0.982	0.989	0.966	0.942	0.907	0.949	0.903	0.873	0.865	0.831	0.878	0.770

DOC_4 = 1.8269 ¢/S. n.mi.

W'_{f4} = 0.280 where $W'_f = W_{FCS}/W_{FUEL}$

V'_{f4} = 0.739 where $V'_f = V_{FUEL}/V_{FCS}$

$\square$ INTEGRAL, ◯ NONINTEGRAL } ACCEPTABLE ON BASIS OF SAFETY

TABLE 40. - IMPACT OF GROUND BOILOFF (RECOVERED) ON DOC

Insulation Concept Number/Type	DOC ¢/S km (¢/S n.mi.)	
	Ground Boiloff Not Included	Ground Boiloff Included
1. GHe Purged FG	1.0745 (1.9399)	1.0822 (2.0043)
2. $GHe-GN_2$ Purged FG	1.0366 (1.9197)	1.0448 (1.9349)
3. Ext. Foam, Nonintegral	1.0083 (1.8674)	1.0161 (1.8818)
4. Ext. Foam, Integral	0.9787 (1.8126)	0.9864 (1.8269)
5. Internal PU Foam	1.0551 (1.9540)	1.0778 (1.9961)
6. Int. PPO, Ext. PU Foams	1.0036 (1.8587)	1.0187 (1.8866)
7. Int. PPO Foam	1.0522 (1.9486)	1.0722 (1.9857)
8. Int. Perf. HC	1.0403 (1.9267)	1.0542 (1.9524)
9. Rigid Vac Shell	1.0075 (1.8659)	1.0084 (1.8675)
10. Ext. Microspheres	1.0017 (1.8551)	1.0062 (1.8635)
11. Int. Microspheres	0.9839 (1.8221)	0.9873 (1.8284)
12. Int. LI 900	0.9950 (1.8428)	1.0006 (1.8531)
13. Self-Evac. Shingles	0.9857 (1.8255)	0.9893 (1.8322)
14. HC/Foam	0.9803 (1.8156)	1.0004 (1.8528)
15. HC/GN_2 Purged FG	1.0193 (1.8877)	1.0238 (1.8961)

As in the case of evaluating differences in production cost, these differences are too small to be meaningful in influencing selection of a preferred concept.

There are not sufficient data for any of the insulation systems to quantitatively predict their useful life for an aircraft flying 350 times a year for 14 years (4900 thermal cycles). However, based on the limited test data available and characteristics inherent in their design, a qualitative ranking was made as shown in Table F-3 of Appendix F. The concepts were ranked as 1, 2 or 3 with 1 having the longest projected life system. Concepts 1, 2, 6, 7, 8, 10, 11, and 12 are ranked the highest with 3, 4, 5, 9, 14, and 15 falling into the middle category. It must be emphasized that insufficient information is available at this time to make more than a very tentative judgement of this criterion.

7.1.5 Selection of preferred candidates. - The selection of the concepts to be evaluated as preferred candidates was made primarily on the basis of rankings from the safety and performance results. Analysis of producibility and operations did not yield any quantitative information which would influence the selection. At this stage of development all concepts appear to be feasible in these regards and qualitative estimates of DOC increments due to differences in producibility and operations aspects do not result in any large percentage variations between concepts.

Initially, four candidates for each tank concept (integral and nonintegral) were selected on the basis of DOC. Candidates numbers 4, 14, 11, and 12 were selected for the integral tank. For the nonintegral design, numbers 13, 10, 3 and 15 were selected. These were then compared with a ranking of safety criteria to arrive at the final candidates for each tank concept. Candidates 13, 14, and 15 were eliminated on the basis of poor safety rankings and the fact that satisfactory performance has never been demonstrated in prior development programs. For example, an airtight seal has never been maintained on concept 13 and a leaktight honeycomb construction could not be achieved for multiple cyclic exposure with concept 14. Candidate 15 was also eliminated on the basis of the consideration of failure of previous development efforts to demonstrate satisfactory leaktight construction techniques with honeycomb substrates for cryogenic tanks.

Recommendation of the five remaining concepts was made to NASA. As a result of discussions, Lockheed and NASA mutually agreed to include concepts 3 and 4 with the substitution of modified versions of 9 and 11 for nonintegral and integral tanks respectively. Concept 9 was substituted for 10 in order to include the hard vacuum system in the final evaluation. Further, concept 11 was modified to place the insulation exterior to the tank. The external vacuum jacket was protected with a composite formed by an exterior aerodynamic fairing and a flexible foam layer between the fairing and the jacket. The disadvantages of the original design for concept 11 were (1) the use of honeycomb for the fuel tank structure, (2) making the 5-mil stainless steel liner LH_2 leakproof, (3) fabrication difficulties, and (4) the reduction of allowable stresses in the tank structure due to the warm tank. It was felt that the new concept presented a more reasonable approach and would minimize operational and production problems.

In summary, the concepts approved for the preferred candidates analysis phase were:

- Candidate A (concept 3): Nonintegral tank - external foam.
- Candidate B (modified concept 9): Nonintegral tank - hard shell vacuum jacket.

- Candidate C (concept 4): Integral tank - external foam.

- Candidate D (modified concept 11): Integral tank - external microspheres.

Descriptions of these systems are given in 7.1.6.

7.1.6 Analysis of preferred candidates. - Parametric thermal analysis studies were conducted to develop fuel loss and required tank volume as a function of insulation thickness for each candidate. These data were then translated into DOC for design optimization.

Two different methods of thermodynamic analysis were used for the concept screening and preferred candidate phases of the program. As described in 5.1.2.3, for concept screening a closed form steady-state solution was used to compute heat inputs as a function of tank liquid fraction. These inputs were modified by a heat storage term applied in a stepwise manner to give a pseudo-transient result which followed a seven-segment mission profile for exterior temperature and fuel fraction.

Analysis of the preferred candidates was done in a manner to represent a true transient condition using a finite difference program which followed the specified design mission using inputs of Mach number, altitude, and rate of fuel usage in steps of 5-minute time intervals. In addition to the normal flight mode, a subroutine was included to simulate the effects of severe flight turbulence by assuming complete liquid disorientation and wetting of the inner tank wall, so that the liquid, vapor and inner tank wall reach an equilibrium temperature. The stratification process then resumes following this simulation of a severe, short-term flight disturbance.

7.1.6.1 Description of candidates: The four insulation candidates, selected with NASA concurrence, are:

- Candidate A - Nonintegral fuel tank with an exterior rigit closed-cell foam insulation system using the MAAMF vapor barrier concept.

- Candidate B - Nonintegral fuel tank with a hard shell vacuum jacket; 1.27 cm (0.5 inch) of rigid closed-cell foam located at tank wall to prevent air liquefication in event of external leakage into vacuum space; aluminized Mylar bonded to interior surface of jacket and exterior surface of foam to reduce radiation heat transfer.

- Candidate C - Integral fuel tank with rigid closed cell foam primary insulation; open-cell flexible foam exterior to primary insulation vapor barrier (MAAMF concept) to accommodate dimensional changes and support exterior fairing.

- Candidate D - Integral fuel tank with external evacuated microsphere insulation having flexible metal vacuum jacket; open-cell flexible foam located exterior to flexible vacuum jacket to support fairing.

Cross-sectional views of the four systems are shown in Figures 94 through 97 with the appropriate fixed dimensional properties and component specific weights and densities.

7.1.6.2 Thermal analysis of preferred candidates: The model used for thermal evaluation of the four preferred insulation system candidates was a transient computer program, THERM. The THERM Thermal Analyzer Program, described in Appendix D, solves transient heat flow problems by use of a forward finite-difference algorithm for solving an analogous resistance-conductance (R-C) electrical network. It is structured to allow maximum flexibility in describing energy transport phenomena unique to a specific application. This program computes the tank pressure and vapor vent rates (including vapor required for pressurization) as well as the transient temperature distributions in the tank walls, in the insulation systems, and in the liquid and vapor components. The model uses the design mission fuel flow schedule (Appendix A), and the environment temperatures during flight are from Standard Atmosphere Tables (Reference 25). The program models both integral and nonintegral tanks. Thermal conductivities and specific heats of the tank wall, insulation system materials, and the hydrogen liquid and vapor are specified as a function of temperature throughout the model.

In the thermal model, the liquid and vapor volumes are divided into 9 and 10 horizontal layers, respectively, as shown in Figure 98. The liquid/vapor interface is at the saturation temperature, T_S, corresponding to the tank pressure. Located opposite each liquid and vapor node are a tank wall node, three insulation nodes, and two outer structure nodes for the aircraft fuselage or exterior fairing.

The liquid volume consists of eight nodes of increasing thickness down from the surface in the temperature stratified layer of the upper LH_2 region. The ninth and bottom liquid node corresponds to the uniform bulk liquid temperature, T_B, layer at the bottom of a stratified tank that experiences some degree of bottom heating. The transient stratification analytical model of Reference 26 is used in this program. It was modified to account for the changes in the liquid level that occur during the simulated flight mission.

The vapor volume consists of 10 horizontal layers in which conduction, convection, mass flow and radiation effects between the nodes and their surroundings are modeled. The mass, volume, temperature and pressure of the vapor are computed from liquid/ullage coupling models that consider the thermodynamics of the two modes of tank pressurization and venting. One mode is represented by a closed tank, self-pressurization model; while the second mode is represented by a constant pressure, continuous tank venting model.

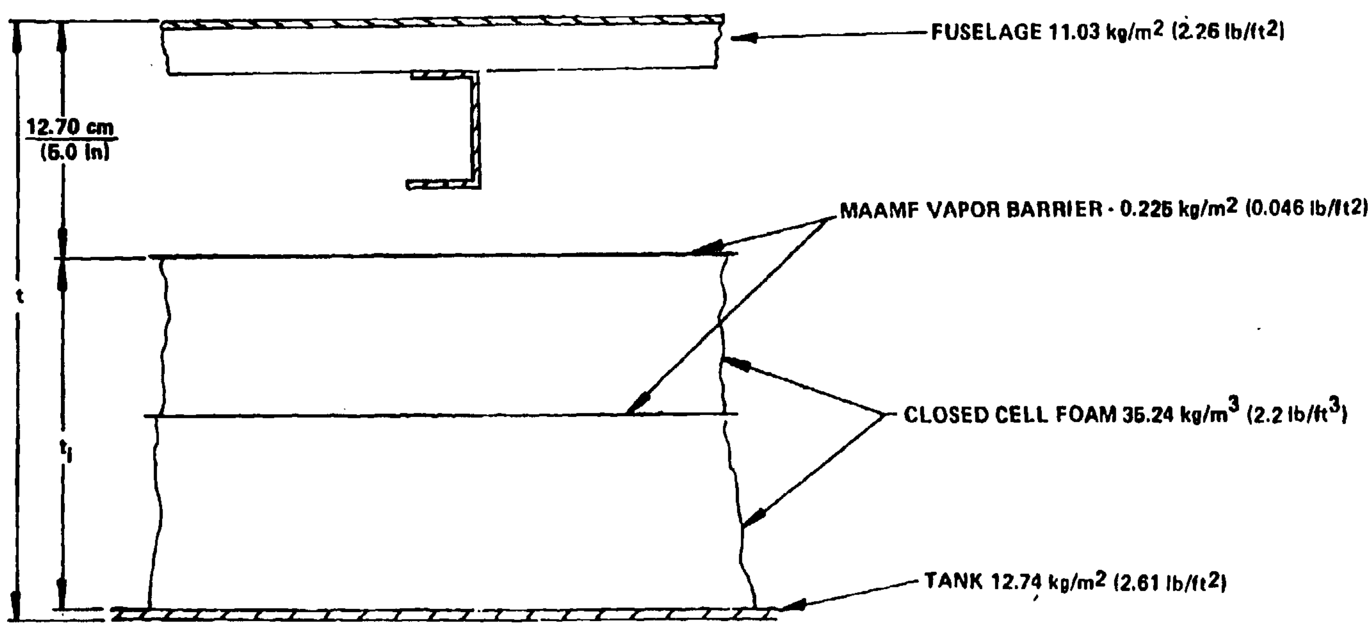

Figure 94. Candidate A, nonintegral tank - external foam.

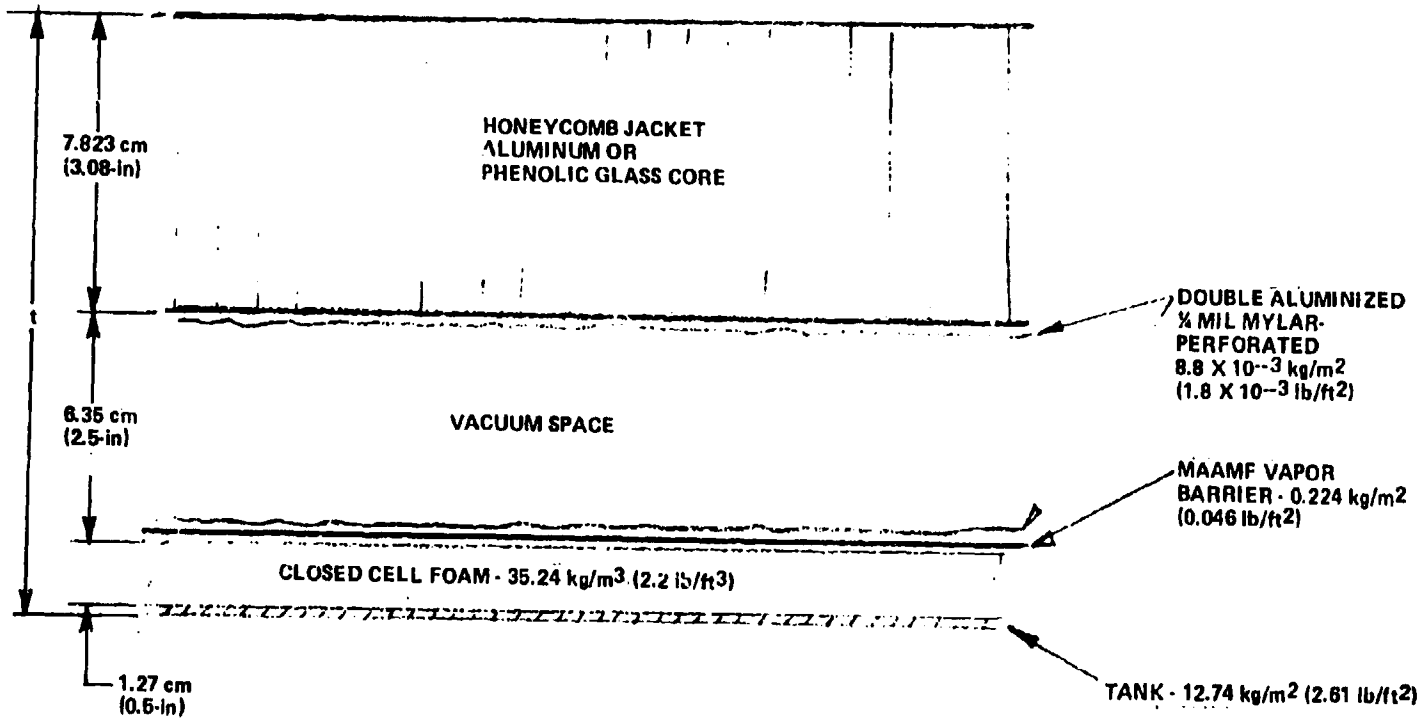

Figure 95. - Candidate B, nonintegral tank - hard shell vacuum.

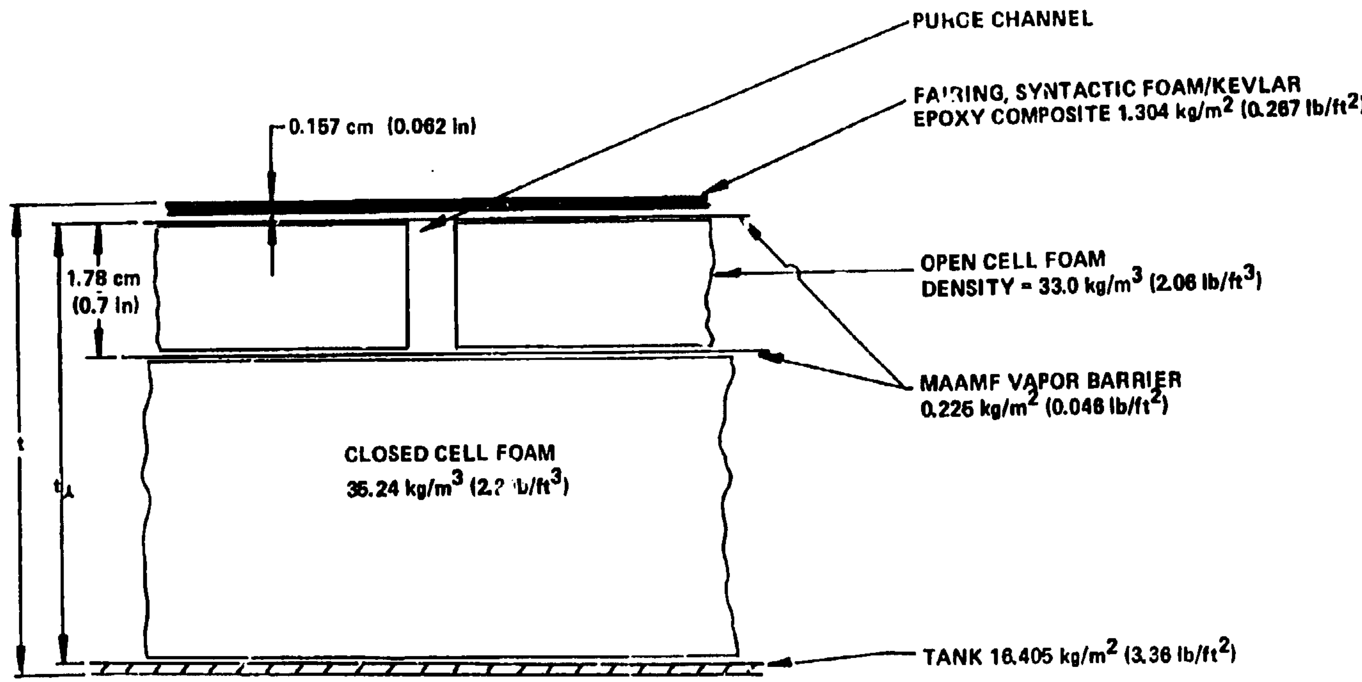

Figure 96. - Candidate C, integral tank - external foam.

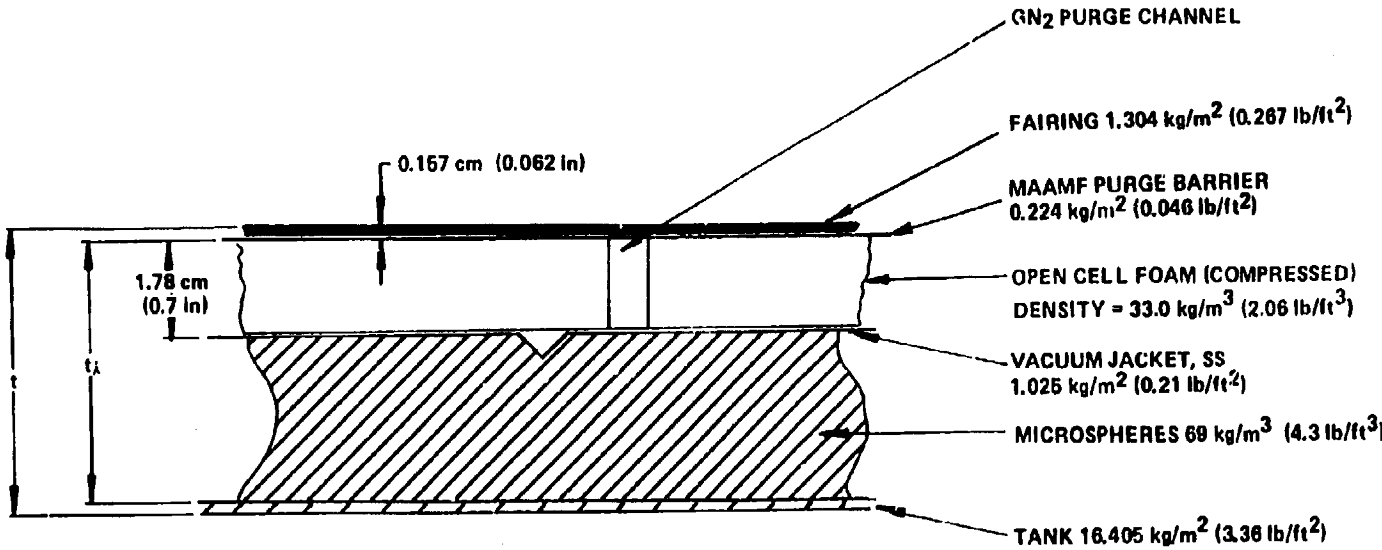

Figure 97. - Candidate D, integral tank - external microspheres

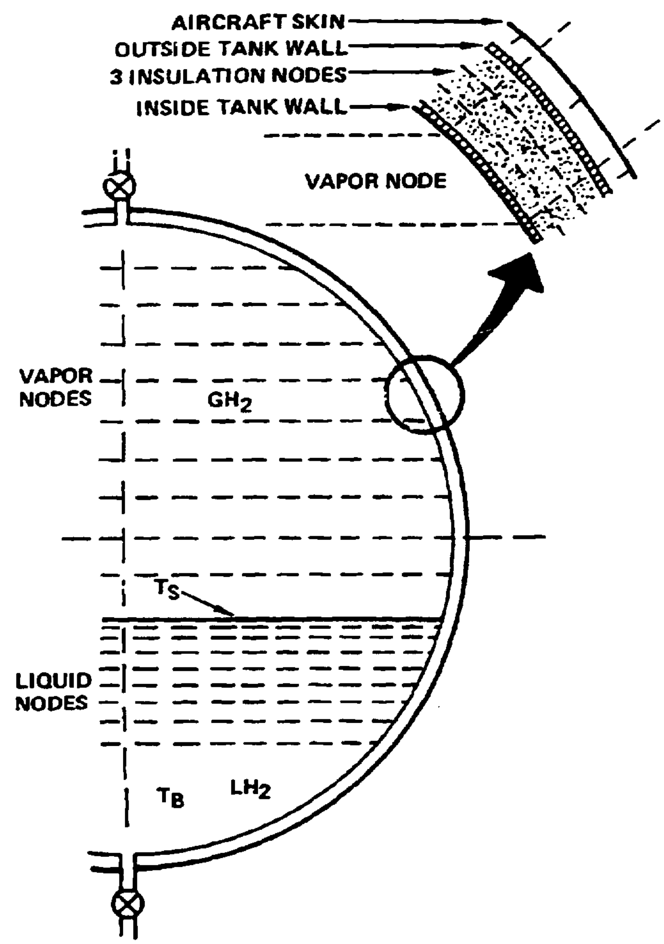

Figure 98. - Tank insulation and vent model for analysis of preferred candidates.

This program has the ability to switch between the two tank pressurization and venting modes depending upon the tank heat input, LH_2 fill level, liquid hydrogen withdrawal rates, etc. In this program a severe flight disturbance that would completely mix the stratified liquid, the vapor, and wet the tank walls, can also be simulated. Following this instantaneous event, the liquid restratifies and the tank self-pressurizes and/or vents.

In operation of the program an initial estimate is made of required tank volume for a given insulation thickness, based upon the results of the concept screening analysis. Using the output data from the first computer run an iterative procedure is then used to obtain convergence of volume in terms of mass of liquid evaporated. Basic output of the program is node temperatures, liquid and vapor mass and volume fractions, vented and evaporated masses and ullage pressure in 5-minute time steps.

The major output parameters of the thermal analysis which were used to evaluate the concepts are:

- Fuel evaporated and fuel vented during flight
- Fuel evaporated during ground hold and filling
- Fuel tank ullage pressure during flight
- Temperature distributions of tank wall, insulation and outer structure
- Vent rate during filling

Additional analyses were conducted to assess the benefit in terms of fuel loss of operating at higher tank pressures, 207 kg (30 psia) and 276 kPa (40 psia). These were done for candidate C only. Also, the effects of air and hydrogen leakage into the vacuum spaces of candidates B and D were examined in limited depth.

7.1.6.2.1 Fuel losses: The fuel losses associated with the filling, flight, and ground hold portions of the aircraft mission were computed for each candidate. Insulation thickness was the variable for candidates A, C, and D. Five different values were examined. Since geometry is fixed for candidate B, losses were computed for the nominal vacuum space pressure of 1×10^{-4} Torr, and for values an order of magnitude above and below (10^{-3} and 10^{-5} Torr). In addition, an emergency condition of 760 Torr, corresponding to loss of vacuum was also calculated. The loss terms are fuel evaporated during flight (vented plus amount required for tank pressurization), fuel vented during flight, and fuel vented during fill and ground hold.

Fuel losses as a function of insulation thickness are shown in Figures 99 through 101 for candidates A, C, and D, respectively. Table 41 presents fuel loss data calculated at each insulation thickness. Overall system thickness, (t), is defined as the distance from the interior of the tank wall to the exterior of the fuselage. Primary and total insulation thicknesses are denoted by t_{ip} and t_i, respectively. Vacuum influence on fuel loss for candidate B is also given in the table. Comparing the rigid, closed cell foam candidates, A and C, it is seen that equal thicknesses of insulation give nearly equal fuel loss data. This is as anticipated because the primary insulations are identical and the secondary foam wrap for C has a thermal conductivity close to that of the primary material. On the basis of system thickness, t, however, C is much more effective from a volume standpoint.

A comparison between candidates C and D shows that the latter is a more thermally efficient concept. Although the microspheres have nearly twice the bulk density of the rigid foam (69 versus 35 kg/m^3), for an equal weight insulation the microsphere concept, D, shows appreciably lower fuel losses. As an example, with 5.08 cm of rigid foam for C, the flight and ground losses are 537 and 780 kg, respectively (per tank). For D at 2.54 cm thickness of microspheres (equal weight of insulation), the flight and ground losses are 397 and 621 kg, respectively. This corresponds to a 279 kg saving for non-recoverable losses and a 317 kg reduction in recoverable loss (for 2 tanks). Candidate D is also slightly more effective on a volume basis because of the superior thermal conductivity of the microspheres.

Candidate B shows the minimum in fuel loss, even for vacuum space pressures as high as 10^{-3} Torr. For flight conditions, little difference in fuel loss is observed with pressure changes from 10^{-5} to 10^{-3} torr. This provides a comfortable design margin for the vacuum system. Ground loss is, of course, affected significantly as all heat input goes to vented mass rather than pressurization.

For the case of the honeycomb and annulus at atmospheric pressure of air (simulating a catastrophic vacuum failure), the evaporation rate at altitude is 107 kg/hr (235 lb/hr) with a vent rate of 77 kg/hr (170 lb/hr). This vent rate is less than that required for fueling so no limitations are placed on the vent system design. Also, the 1.27 cm of rigid closed cell foam with the MAAMF barrier prevents liquefaction of air in the event of vacuum failure. Solidification of water vapor would of course occur at a rapid rate at the lower altitudes.

A nonmetallic honeycomb core (Hexcel - 3/8 in. cells HRP phenolic-glass, having the same specific weight and thickness as the aluminum core) was also investigated for candidate B. Under normal operating conditions (vacuum of 10^{-4} Torr) the fuel loss parameters are essentially independent

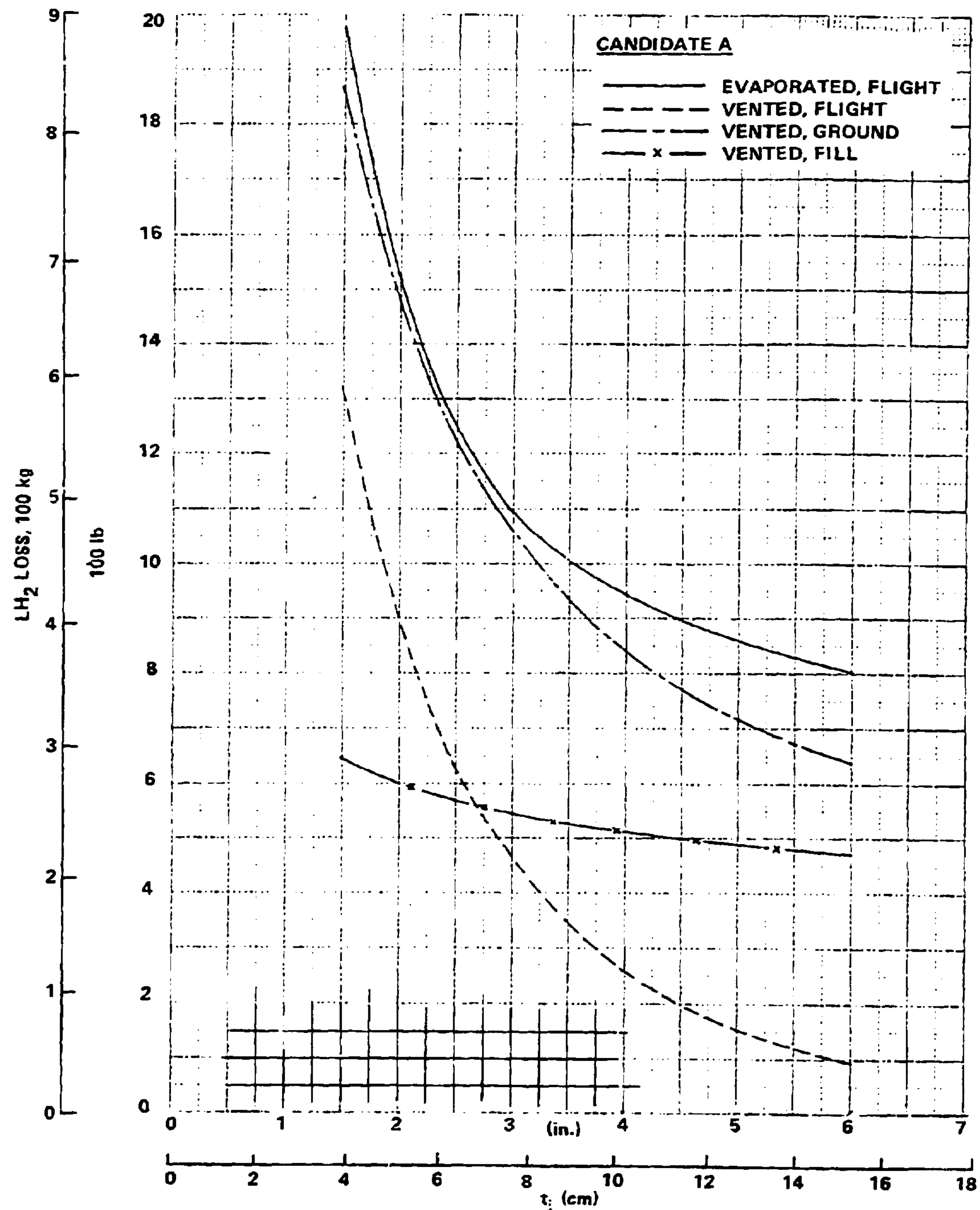

Figure 99. - Fuel losses as a function of insulation thickness for candidate A, aft tank.

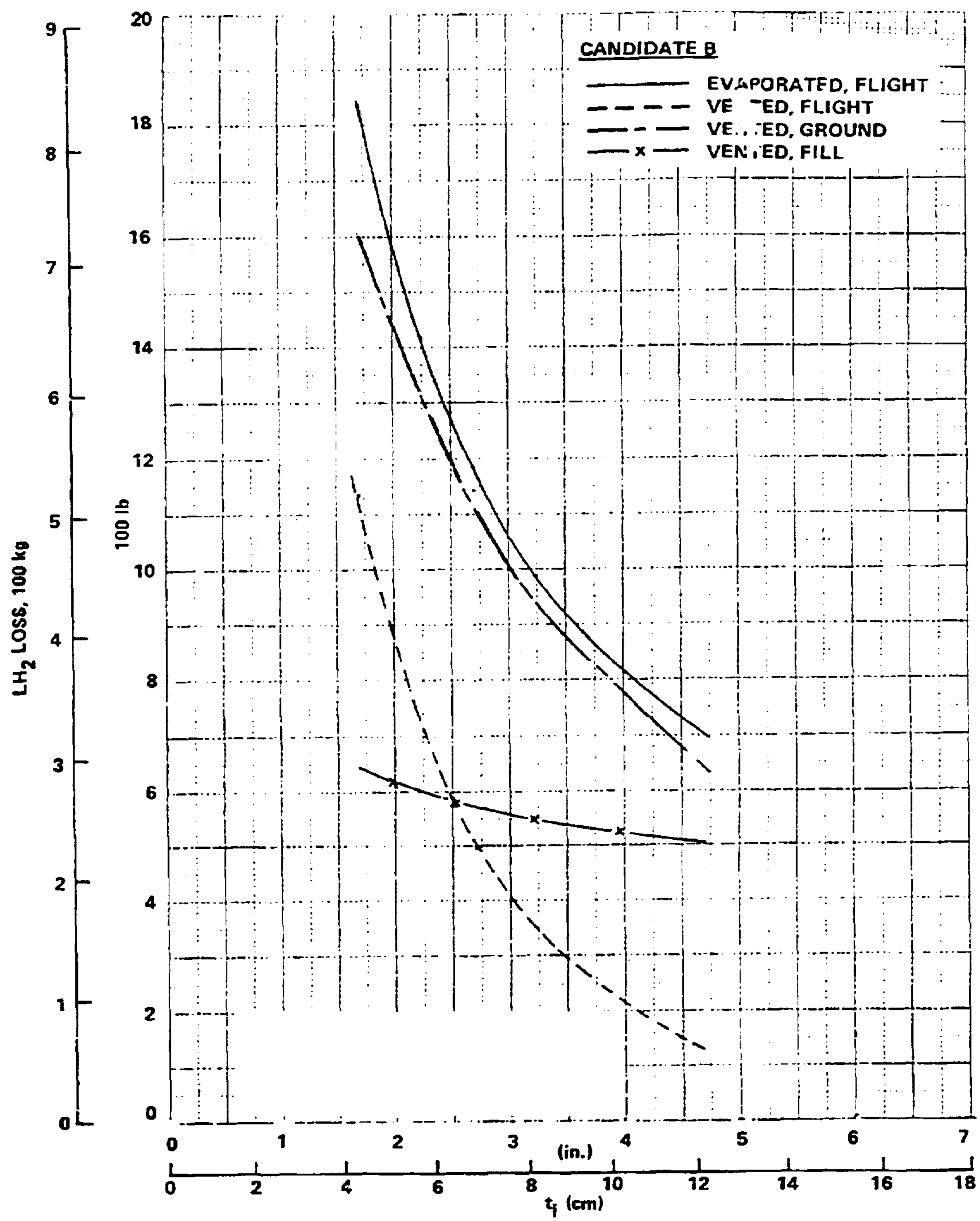

Figure 100. - Fuel losses as a function of insulation thickness (primary and open cell foam) for candidate C, aft tank.

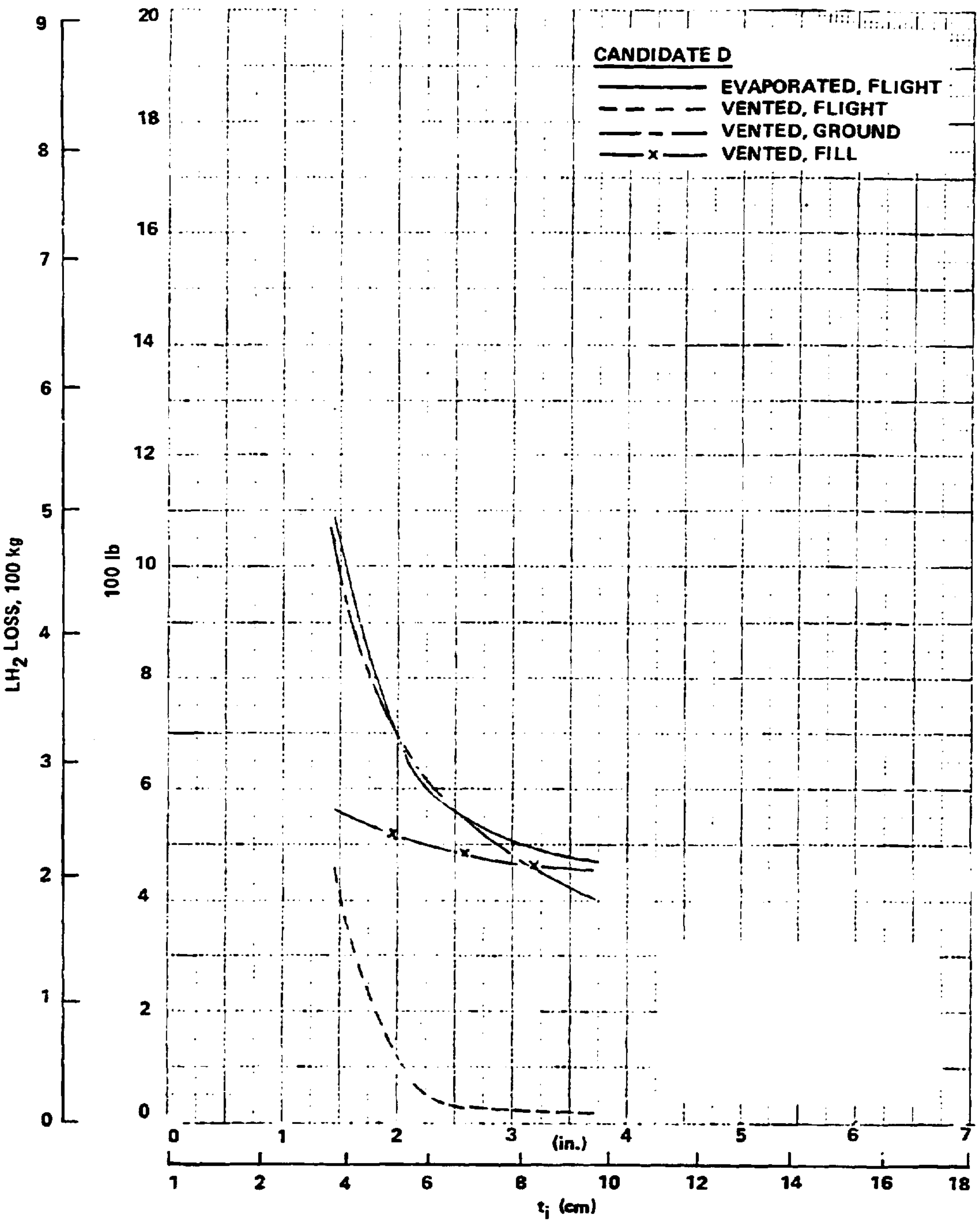

Figure 101. - Fuel losses as a function of insulation thickness (microspheres and open cell foam) for candidate D, aft tank.

TABLE 41. -- SUMMARY OF THICKNESS PARAMETERS AND FUEL LOSSES FOR THE FOUR PREFERRED CANDIDATE INSULATION SYSTEMS (AFT TANK ONLY)

		Candidate Insulation System																	
		A					B			C					D				
Insulation (Type Tank)		Rigid Closed Cell Foam (Nonintegral Tank)					Hard Shell Vacuum (Nonintegral Tank)			Rigid Closed Cell Foam + Flex Foam (Integral Tank)					Microspheres with Flex Foam (Integral Tank)				
$t_{lp}^{(a)}$	cm	3.81	5.08	7.62	10.16	15.24	15.24[a]	15.24[a]	15.24[a]	2.54	3.81	5.08	7.62	10.16	1.91	2.54	3.81	5.08	7.62
	(in)	(1.50)	(2.00)	(3.00)	(4.00)	(6.00)		(6.00)		(1.00)	(1.50)	(2.00)	(3.00)	(4.00)	(0.75)	(1.00)	(1.50)	(2.00)	(3.00)
$t_1^{(b)}$	cm	3.81	5.08	7.62	10.16	15.24				4.32	5.59	6.86	9.40	11.94	3.68	4.32	5.59	6.86	9.90
	(in)	(1.50)	(2.00)	(3.00)	(4.00)	(6.00)				(1.70)	(2.20)	(2.70)	(3.70)	(4.70)	(1.45)	(1.70)	(2.20)	(2.70)	(3.70)
$t^{(c)}$	cm	17.20	18.47	21.01	23.55	28.63	15.24	15.24	15.24	5.11	6.38	7.65	10.19	12.73	4.45	5.08	6.35	7.62	10.16
	(in)	(6.77)	(7.27)	(8.27)	(9.27)	(11.27)		(6.00)		(2.01)	(2.51)	(3.01)	(4.01)	(5.01)	(2.01)	(2.51)	(3.01)	(4.01)	(5.01)
$HEF^{(d)}$	kg	897	691	495	429	365	219	222	242	831	653	537	396	318	495	397	278	242	214
	lb	(1978)	(1524)	(1092)	(945)	(805)	(483)	(489)	(534)	(1832)	(1439)	(1184)	(872)	(702)	(1092)	(876)	(613)	(534)	(472)
$HVF^{(e)}$	kg	596	407	211	117	43	9	10	13	515	335	228	119	59	209	117	27	11	9
	lb	(1313)	(897)	(465)	(257)	(94)	(19)	(21)	(29)	(1135)	(739)	(502)	(262)	(129)	(460)	(259)	(60)	(25)	(20)
$HVC^{(f)}$	kg	1139	948	728	616	503	328	362	480	1017	878	780	619	515	723	621	512	457	369
	lb	(2510)	(2090)	(1605)	(1357)	(1110)	(724)	(798)	(1059)	(2241)	(1936)	(1719)	(1365)	(1135)	(1594)	(1370)	(1129)	(1007)	(816)
Vacuum, Torr		N/A					10^{-5}	10^{-4}	10^{-3}	N/A					10^{-1}				

NOTES:
(a) Thickness, primary insulation: i.e.; rigid closed cell foam or microspheres.
(b) Thickness, total insulation: i.e.; rigid closed cell foam plus flexible open cell foam.
(c) Total thickness, insulation plus structure plus fairing, i.e., from inside surface of fuel containment system to external surface of aircraft.
(d) Total weight of fuel evaporated during flight.
(e) Fuel weight vented during flight.
(f) Total fuel weight vented on ground (recoverable); sum of fill plus ground hold.
(g) 1.27 cm (0.5 in) closed cell rigid foam with MAAHF vapor barrier, plus 2-layers double-aluminized 1/4 mil mylar, 6.35 cm (2.5 in.) clearance, 7.62 cm (3 in.) aluminum honeycomb.

of core conductance as the vacuum space provides the controlling thermal resistance. Results of the system thermal analysis comparing candidate B with aluminum versus composite honeycomb core are:

		Core Type	
		Aluminum	Phenolic/FG
Fuel Evaporated - Flight	kg	444	443
	(lb)	(978)	(976)
Fuel Vented - Flight	kg	19	18
	(lb)	(42)	(40)
Fuel Vented - Ground	kg	724	715
	(lb)	(1596)	(1576)

Under the emergency condition of atmospheric pressure of air in the vacuum space, the evaporation rate with the composite honeycomb core under cruise conditions is 78 kg/hr (172 lb/hr) and under ground conditions is 109 kg/hr (240 lb/hr). Although the lower thermal conductance core reduces fuel losses in this condition, the loss rates in either case do not present an unsafe flight condition. The vent system is designed for the larger vent gas mass flows experienced during filling, and the quantities of fuel lost in flight do not significantly reduce flight duration capability.

7.1.6.2.2 Tank pressure control: A minimum design tank pressure during flight was input into the computer program. For purposes of this analysis a minimum pressure of 110 kPa (16 psia) was arbitrarily assumed. (Note that a minimum pressure of 124 kPa (18 psia) was later selected as a system design value.) If at any time tank pressure falls to this value a subroutine is called, and it computes the additional amount of fuel which must be vaporized to maintain this level of pressure. This additional quantity of vaporized fuel is added to that resulting from heat transfer to the liquid.

For candidate B at vacuums of 1×10^{-5} and 1×10^{-4} Torr, additional fuel vaporization was required at the end of cruise to maintain the minimum pressure level. Without this additional vaporization, tank pressure falls below the minimum value for vacuums of 1×10^{-4} and 1×10^{-5} torr, as shown in Figure 102.

No additional vapor generation was required for the insulation thicknesses investigated for candidate A and C. Vapor generation was required for candidate D at the largest value of insulation thickness; however, this case was not viable because its DOC was not the minimum value for the candidate.

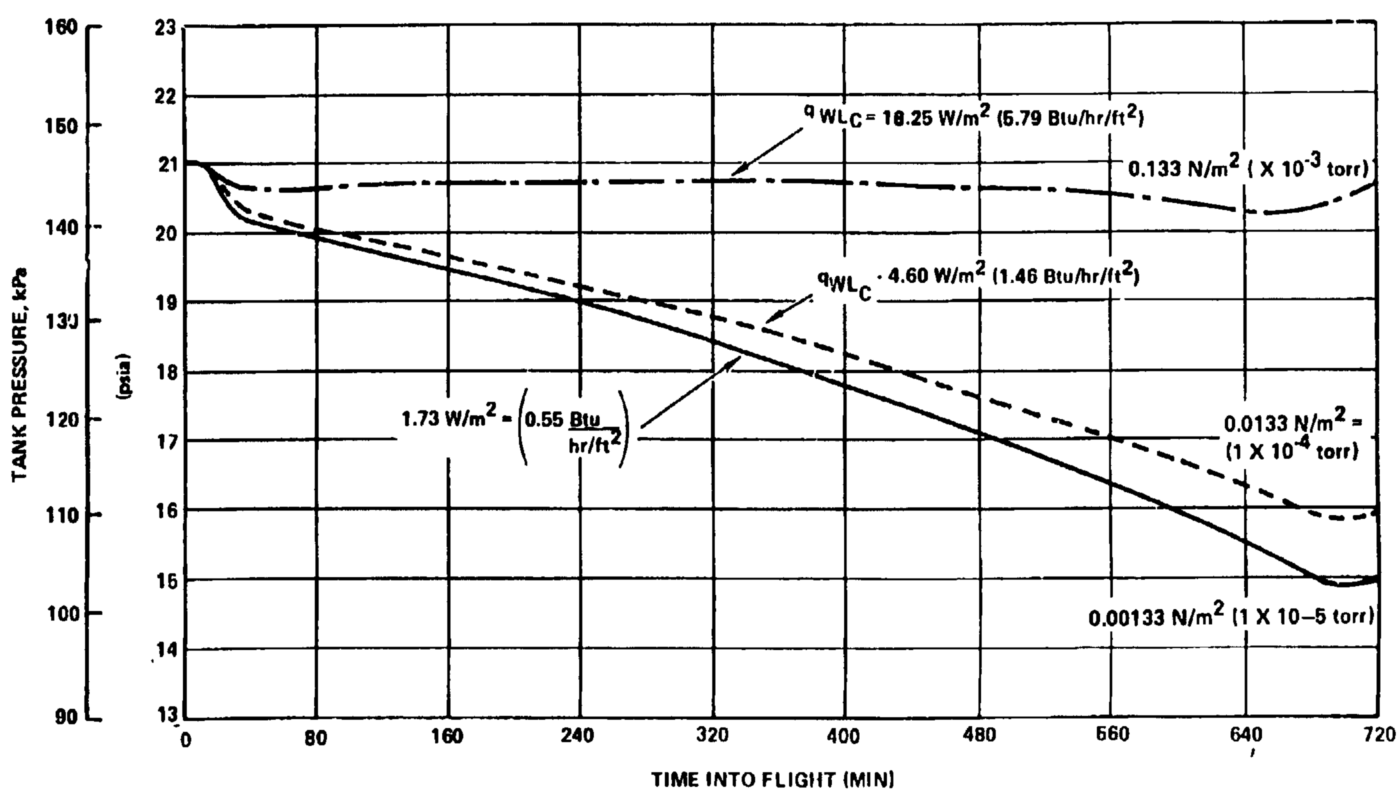

Figure 102. - Tank pressure during flight as a function of vacuum level, candidate B - aluminum core HC.

Using the thickness of insulation consistent with minimum DOC, analysis of the tank pressure variation as a function of time of flight during the mission showed that both candidates A and C vented excess boiloff continuously. The result of the calculation for candidate D is plotted in Figure 103 No venting is required during a period extending from 15 minutes after takeoff until landing.

7.1.6.2.3 Tank pressure level: A separate analysis was performed to determine the effect of higher tank pressures on venting losses. By increasing the tank venting pressure above the 145 kPa (21 psia) value the amount of fuel vented during filling and flight can be reduced by using the sensible heat capacity of the liquid. For example, as the tank is filled with liquid saturated at 138 kPa (20 psia), a relatively large temperature difference exists between the liquid surface and the bulk of the liquid. For a 276 kPa (40 psia) vent pressure setting, this temperature difference is 2.09°K (3.76°R) as compared to a difference of 0.17°K (0.3°R) for a 145 kPa (21 psia) vent pressure. The results of an analysis, performed using candidate C as a basis, shows liquid temperatures as a function of time for three pressure levels in Figure 104. The variation of ullage pressure during flight as a function of vent pressure is shown in Figure 105. Venting occurs only during the initial 15-minute period for both 276 kPa (40 psia) and 207 kPa (30 psia) vent pressure. For the 276 kPa (40 psia) condition, the ground vent loss is reduced approximately 23 percent from that for the normal vent pressure setting of 145 kPa (21 psia). Increasing vent pressure to 207 kPa (30 psia) does not result in a reduction in ground loss.

During filling, the fuel evaporated is 33 kg (73 lb) for the 276 kPa (40 psia) case and 34 kg (75 lb) for a 207 kPa (30 psia) vent pressure. Fuel evaporated and fuel vented during flight are 317 kg (698 lb) and 13.6 kg (30 lb), respectively, for a 276 kPa (40 psia) vent pressure. Similarly, for a 207 kPa (30 psia) vent pressure, these weights are 311 kg (686 lb) and 15.4 kg (34 lb). These compare with 538 kg (1186 lb) and 227 kg (500 lb) for the 145 kPa (21 psia) vent pressure condition as shown in Figure 100. The higher vapor density in the 276 kPa (40 psia) case accounts for the slight increase in fuel loss over that of the 207 kPa (30 psia) condition.

The effect of design pressure level on tank structural weight and overall conclusions regarding a recommended pressure for the aircraft application are presented in 7.2.5.3.

7.1.6.2.4 Liquid stratification: The degree of liquid stratification in the tank during flight is small for all candidates. As shown by Figures 106 and 107, the temperature differences between the liquid at the surface and at the bottom of the tank is less than 0.22°K (0.40°R). During filling, stratification is shown to occur because in the analytical model subcooled liquid is introduced at the bottom of the tank. However, within 100 minutes after start of filling the stratification has essentially disappeared. Figure 106 is representative of the candidate having the highest heat flux, and Figure 107 illustrates a lower heat flux candidate. Because of the essentially uniform liquid temperature during flight, there is little possibility of a sudden pressure reduction by mixing of the liquid as the result of a sudden maneuver or turbulence.

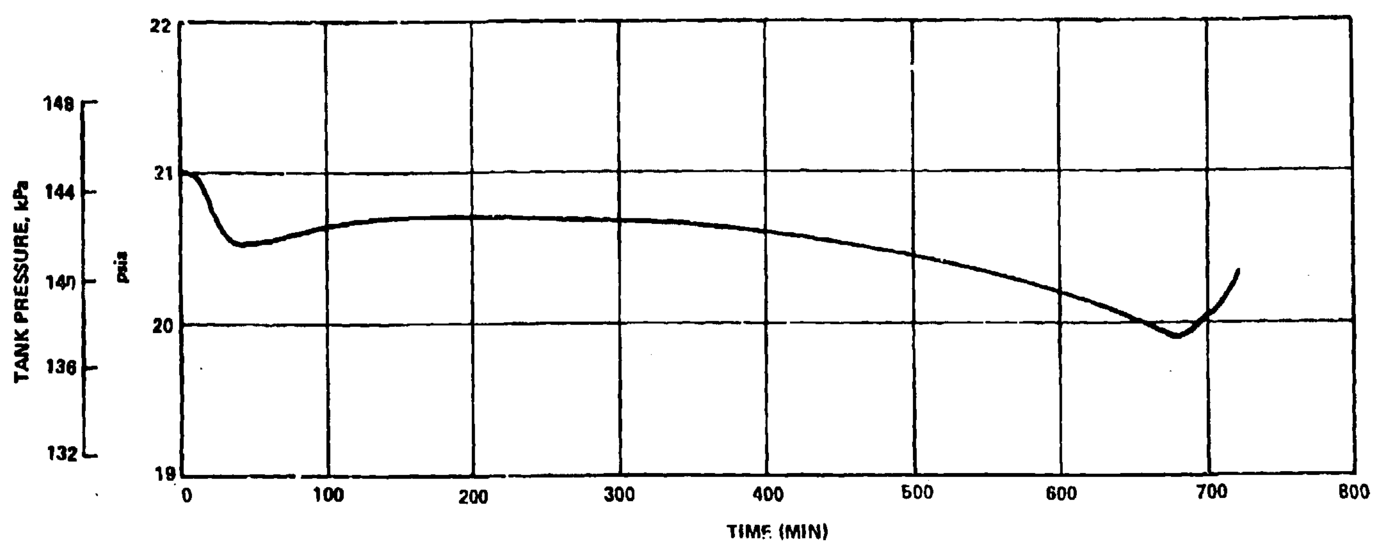

Figure 103. - Tank pressure variation during flight for candidate D.

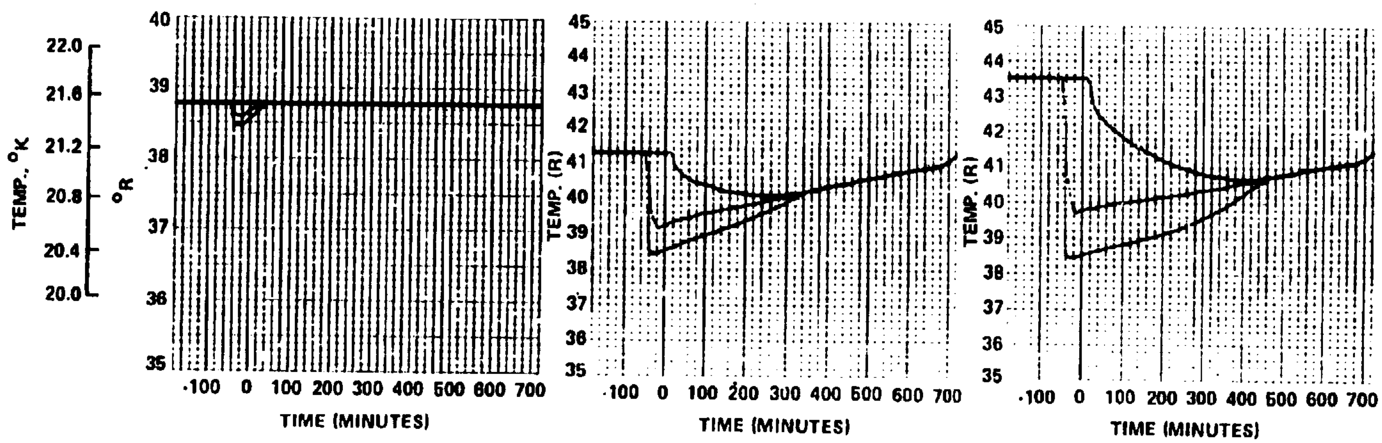

a) 144.8 kPa (21 psia)   b) 206.8 kPa (30 psia)   c) 275.8 kPa (40 psia)

Figure 104. - Liquid temperature differences for three vent pressure settings for candidate C.

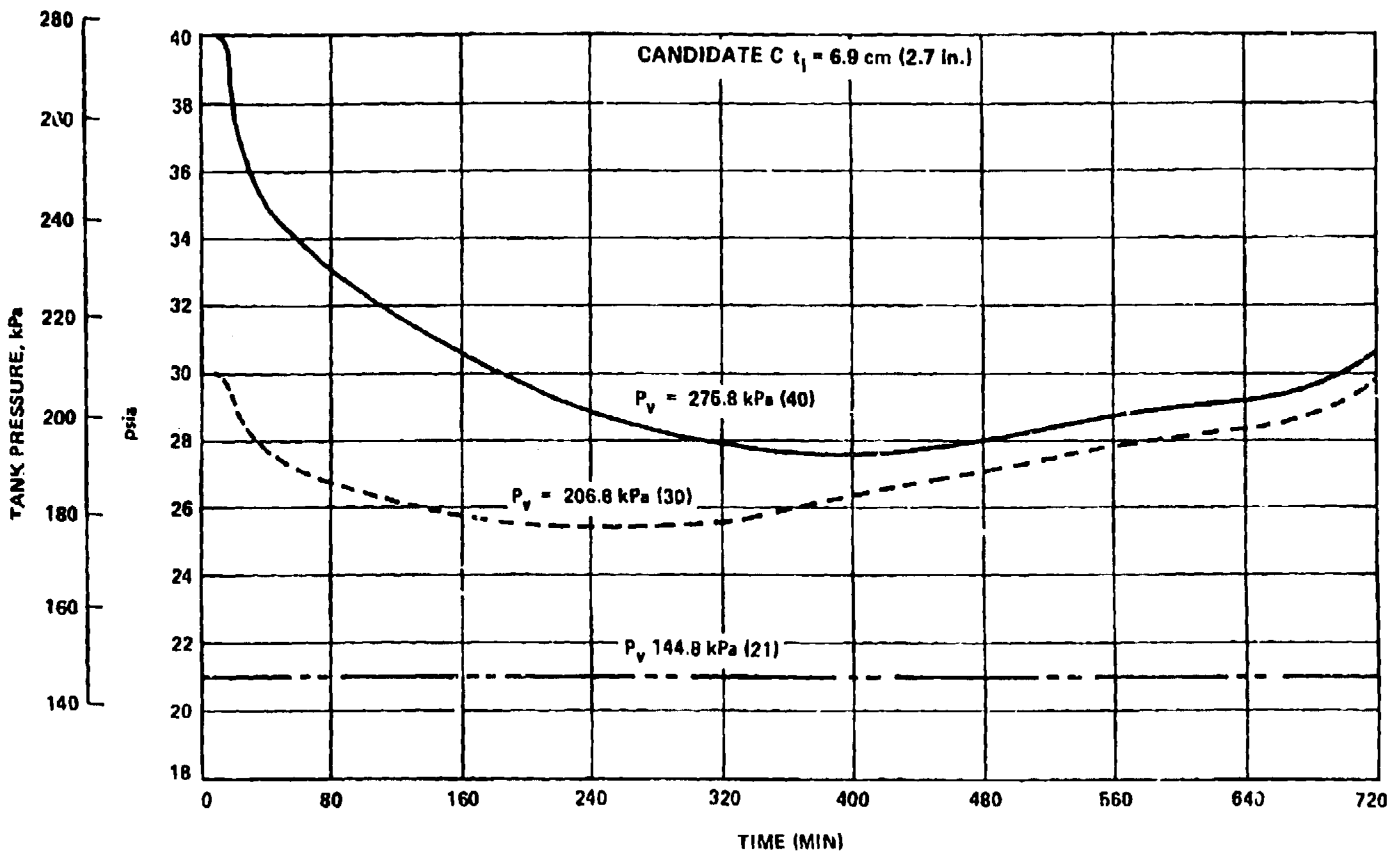

Figure 105. - Tank pressure variation during flight for vent pressure settings of 21, 30 and 40 psia.

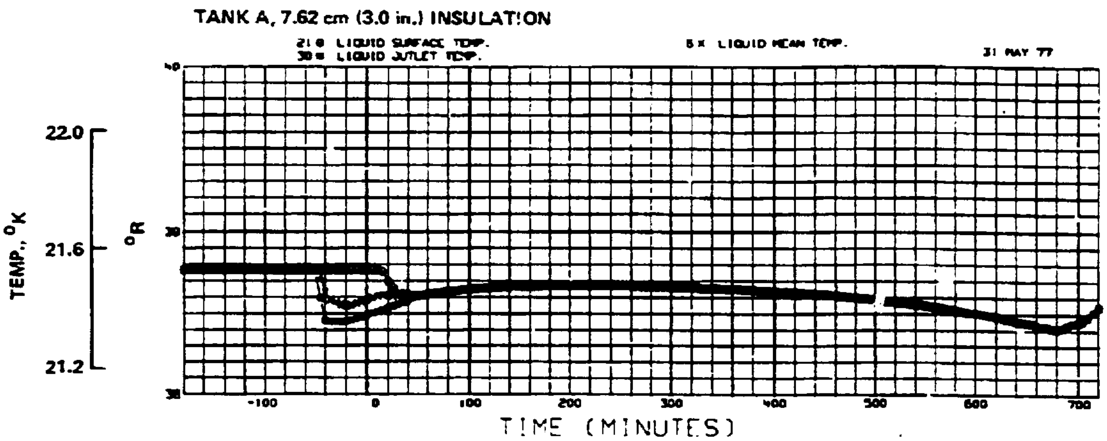

Figure 106. - Liquid temperature differences as a function of flight time for candidate A.

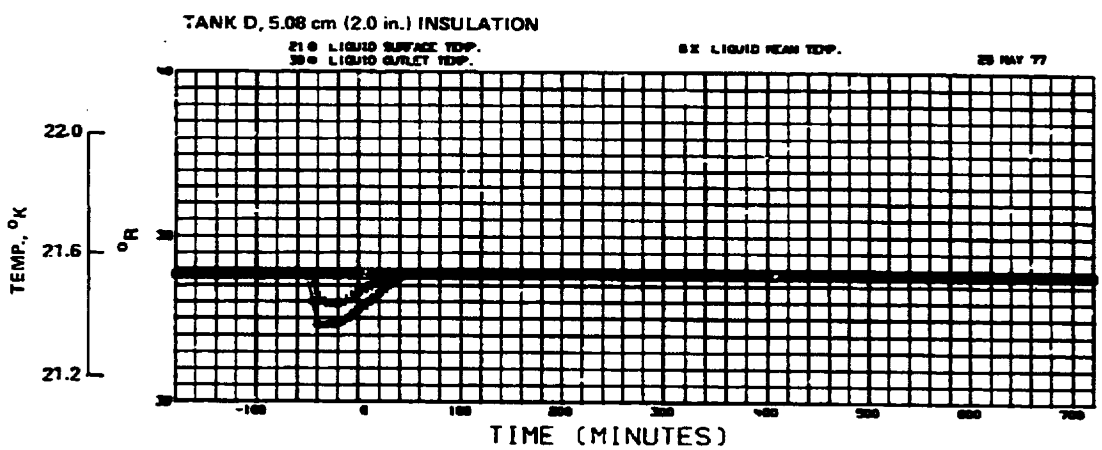

Figure 107. - Liquid temperature differences as a function of flight time for candidate D.

7.1.6.2.5 FCS temperature distributions: Computed temperature distributions for the tank wall, insulation, vapor barrier and exterior structure are shown in Figures 108 through 113 for the four candidates. For candidate B, temperatures are presented for the normal operating condition and for the case where the vacuum space is filled with air for both aluminum and nonmetallic honeycomb cores (Figures 109 through 111). The nodal temperature data are plotted as a function of a dimensionless distance parameter relative to the circumference of the tank wall, ℓ/c. The top of the tank is represented by $\ell/c = 0$ and the bottom by $\ell/c = 1.0$. Distributions are shown for liquid fractions of 0.90, 0.50 and 0.15, with 0.50 corresponding to cruise ambient conditions and 0.90 and 0.15 at ground ambient.

The most severe temperature gradients occur in the area of the liquid-vapor interface at the tank wall and inner insulation nodes. The maximum gradients at these locations are given in Table 42. The maximum gradient in the tank wall occurs at the liquid vapor interface, and it decreases with decreasing wall heat flux. Also, the gradient increases with decreasing liquid level because of the higher tank wall temperatures as the ullage volume increases. Gradients shown in the insulation are for the midplane location of the primary insulation. The exterior vapor barrier location of Table 42 denotes the purge barrier for candidate D and the foam insulation vapor barrier for the other candidates.

7.1.6.2.6 Emergency conditions: The effects of both GH_2 and air leakage into the vacuum space of candidates B and D were evaluated from the standpoint of heat rate to the liquid and vapor barrier (or vacuum jacket temperature for D). A summary of these results is given in Table 43.

For candidate B the vapor barrier temperature remains significantly above the oxygen liquefaction temperature, 109°K (196°R), for the conditions of air leakage into the vacuum space. The maximum liquid heat rates for a full tank will not result in vent rates in excess of the vent system capacity. This calculated heat rate corresponds to an evaporation rate of 347 kg/hr 765 lb/hr). If a failure occurred at the midpoint of cruise, the evaporation rate of 243 kg/hr (535 lb/hr) would require approximately 1500 kg (3300 lb) of reserve fuel to continue the planned flight. It appears that neither failure mechanism would jeopardize the aircraft safety.

A similar conclusion is made for candidate D. Vent rates are lower than for B (even assuming the open cell foam is permeated by GH_2 through the metal vacuum jacket provided for the microspheres). For the condition of GH_2 leakage into the microspheres, the consequences of a double failure with subsequent air leakage into the open cell foam was not considered because of the GN_2 purge system. The air leakage condition was based upon the assumption that the 5-mil stainless steel vacuum jacket has a small leak. The data shown in this case are based upon a small localized leak which was felt to be representative of that which might occur in a welded jacket seam during prolonged service. For these purposes the leakage rate was postulated to be

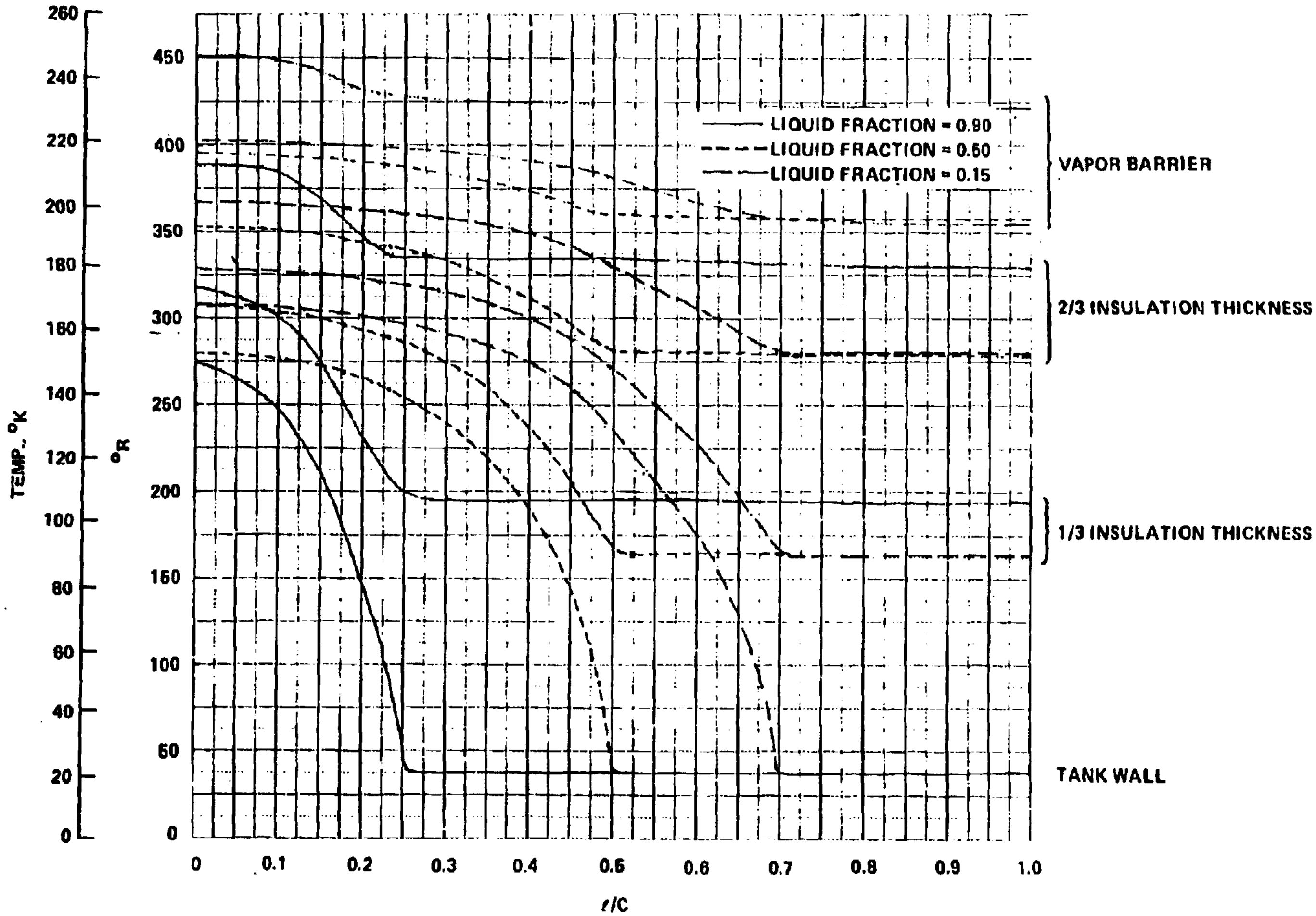

Figure 108. – Candidate A circumferential temperature distributions for liquid fractions of 0.90, 0.50 and 0.15.

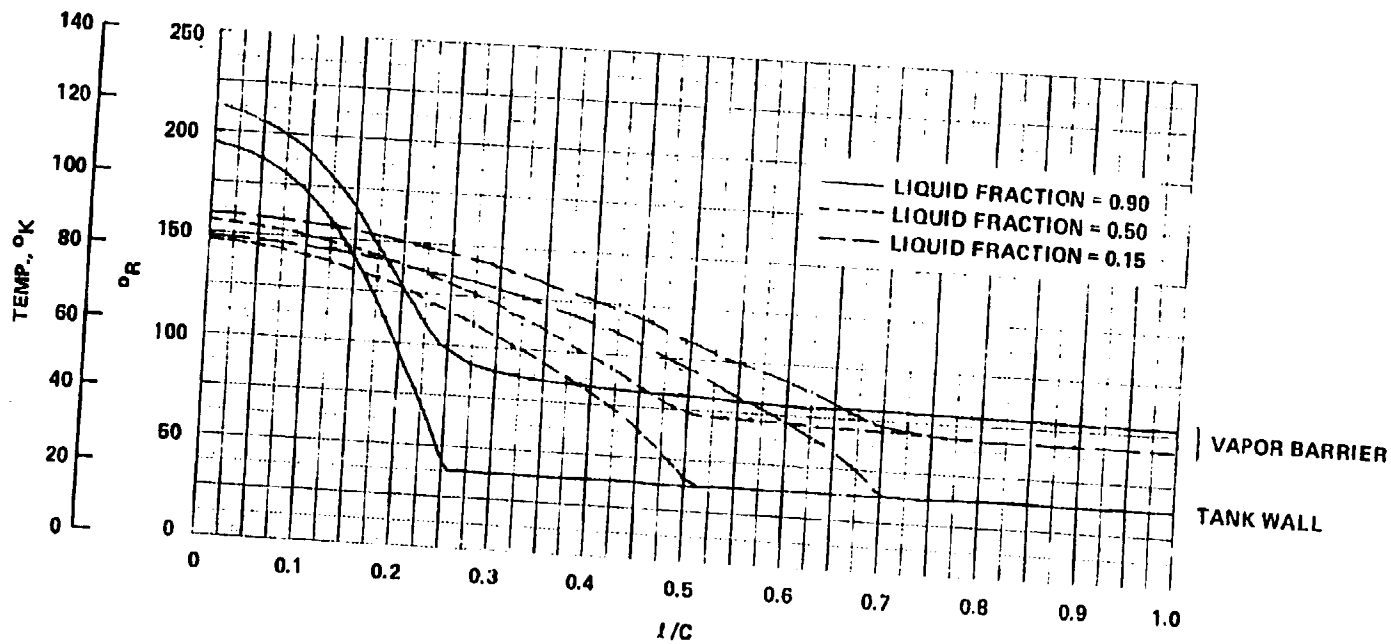

Figure 109. - Candidate B, aluminum core, circumferential temperature distributions in tank wall and vapor barrier for liquid fractions of 0.90, 0.50 and 0.15, vacuum = 1 x 10^{-4} Torr.

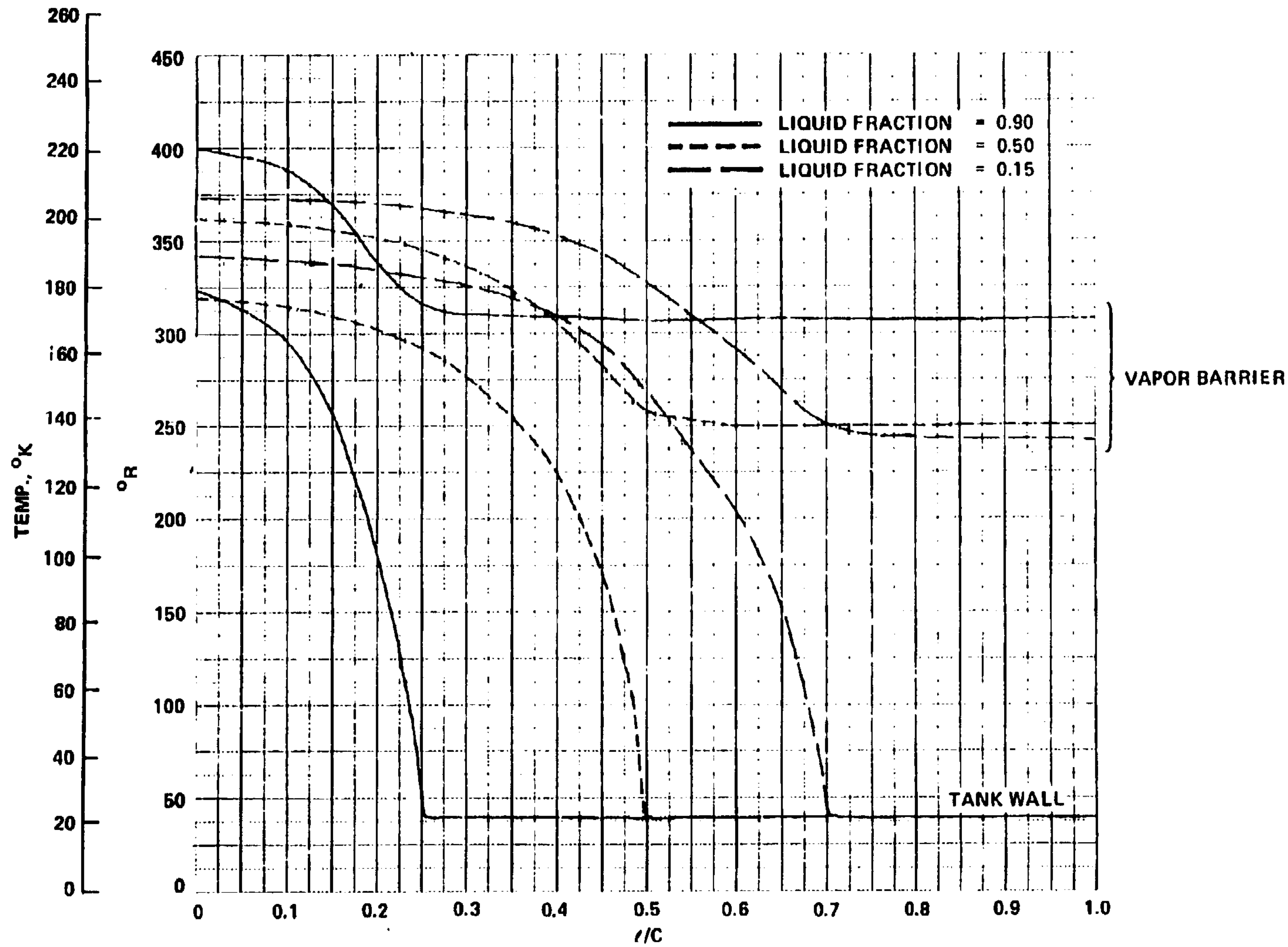

Figure 110. - Candidate B, aluminum core, circumferential temperature distributions in tank wall and vapor barrier for liquid fractions of 0.90, 0.50 and 0.15 with vacuum space at atmospheric pressure.

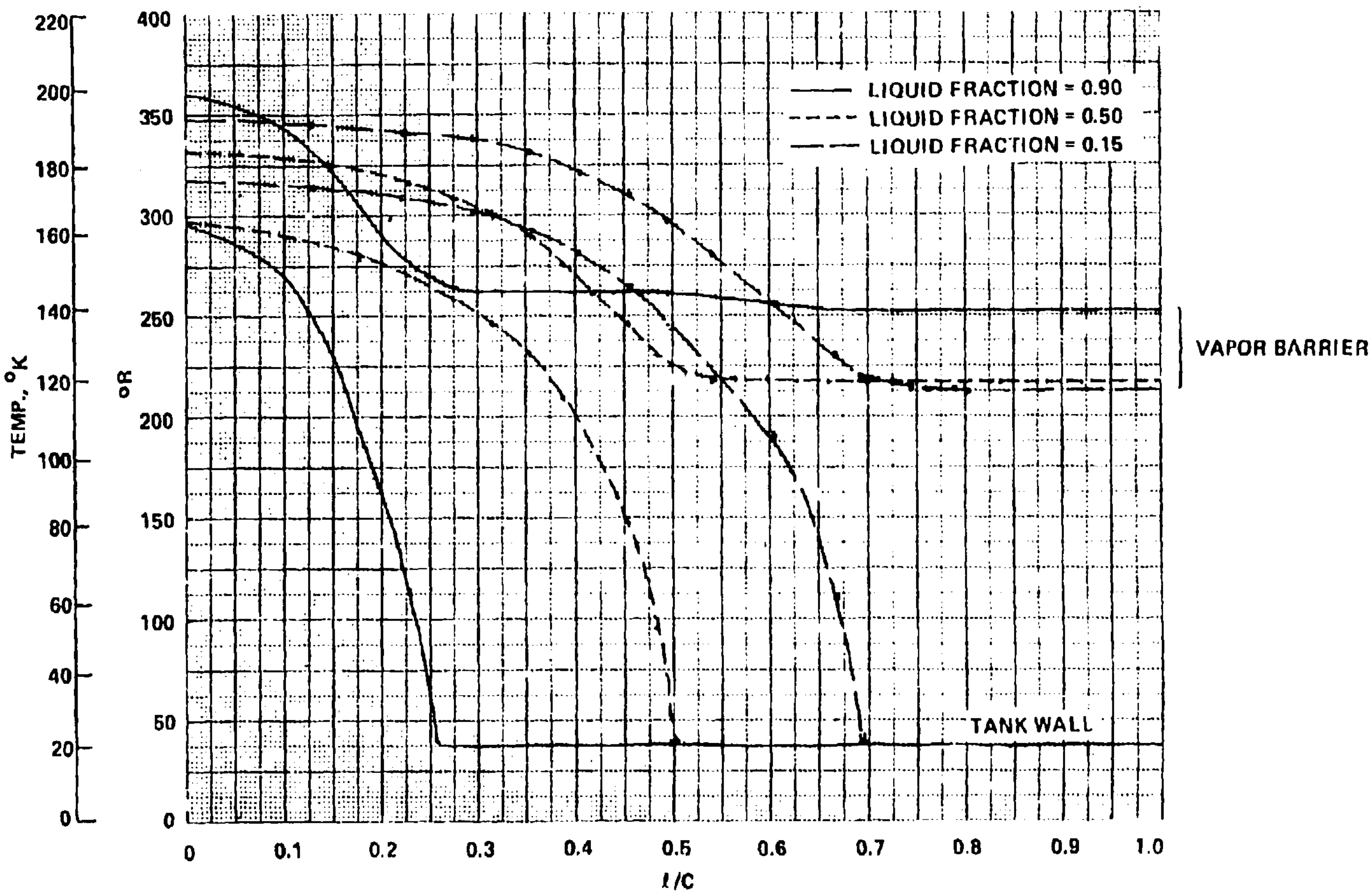

Figure 111. - Candidate B, composite core, circumferential temperature distributions in tank wall and vapor barrier for liquid fractions of 0.90, 0.50 and 0.15 with vacuum space at atmospheric pressure.

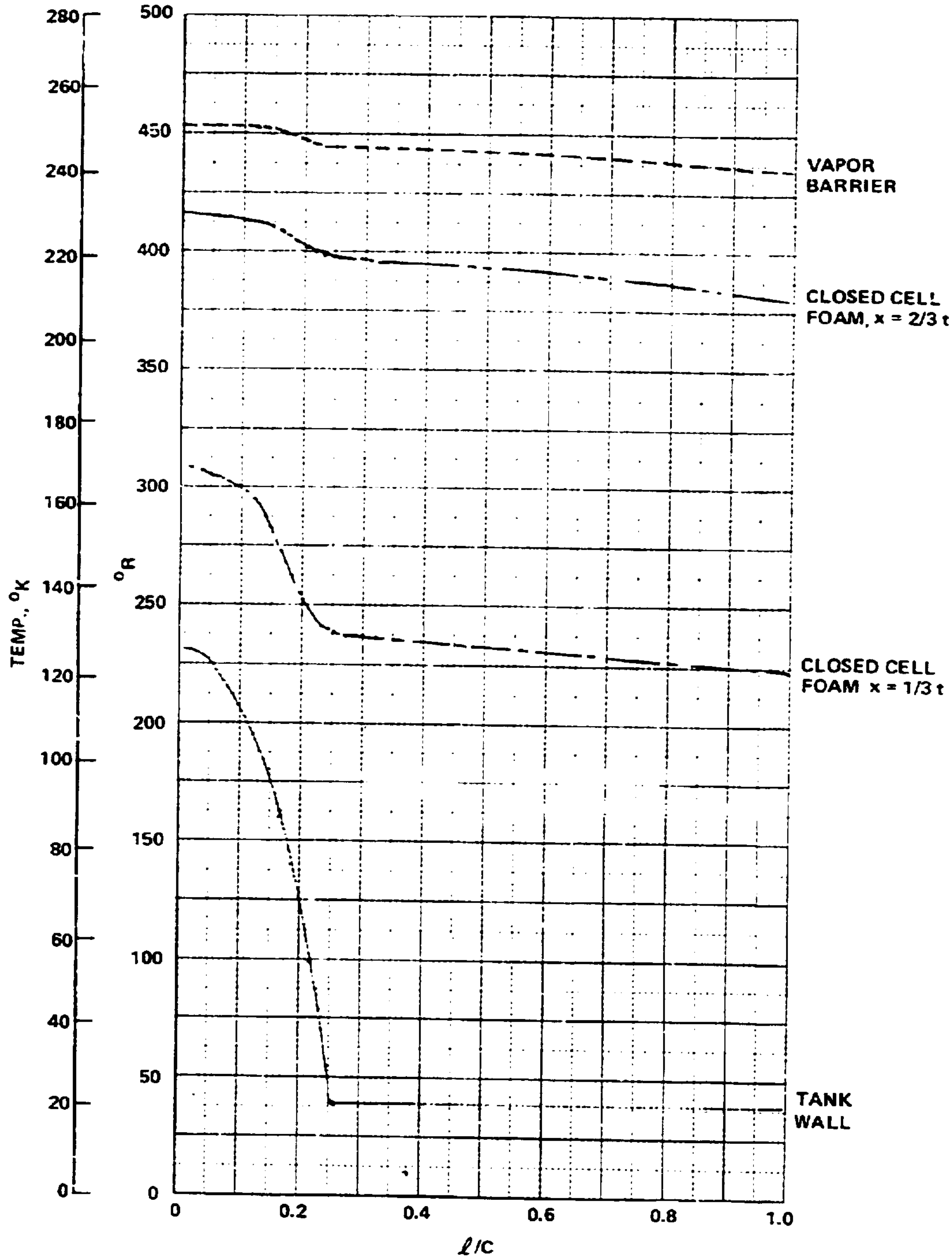

Figure 112. – Candidate C circumferential temperature distributions for liquid fraction = 0.90.

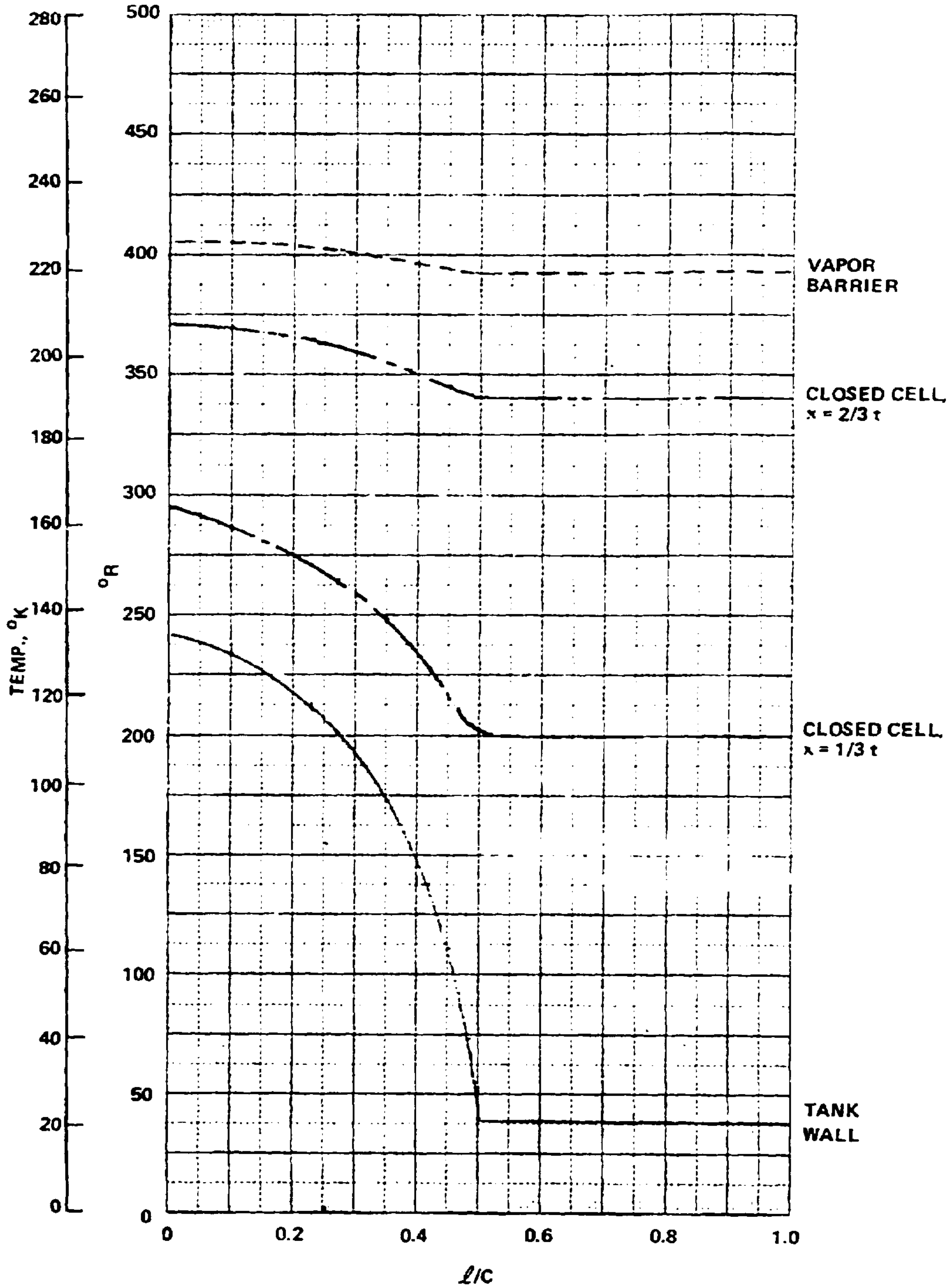

Figure 112. - Continued.

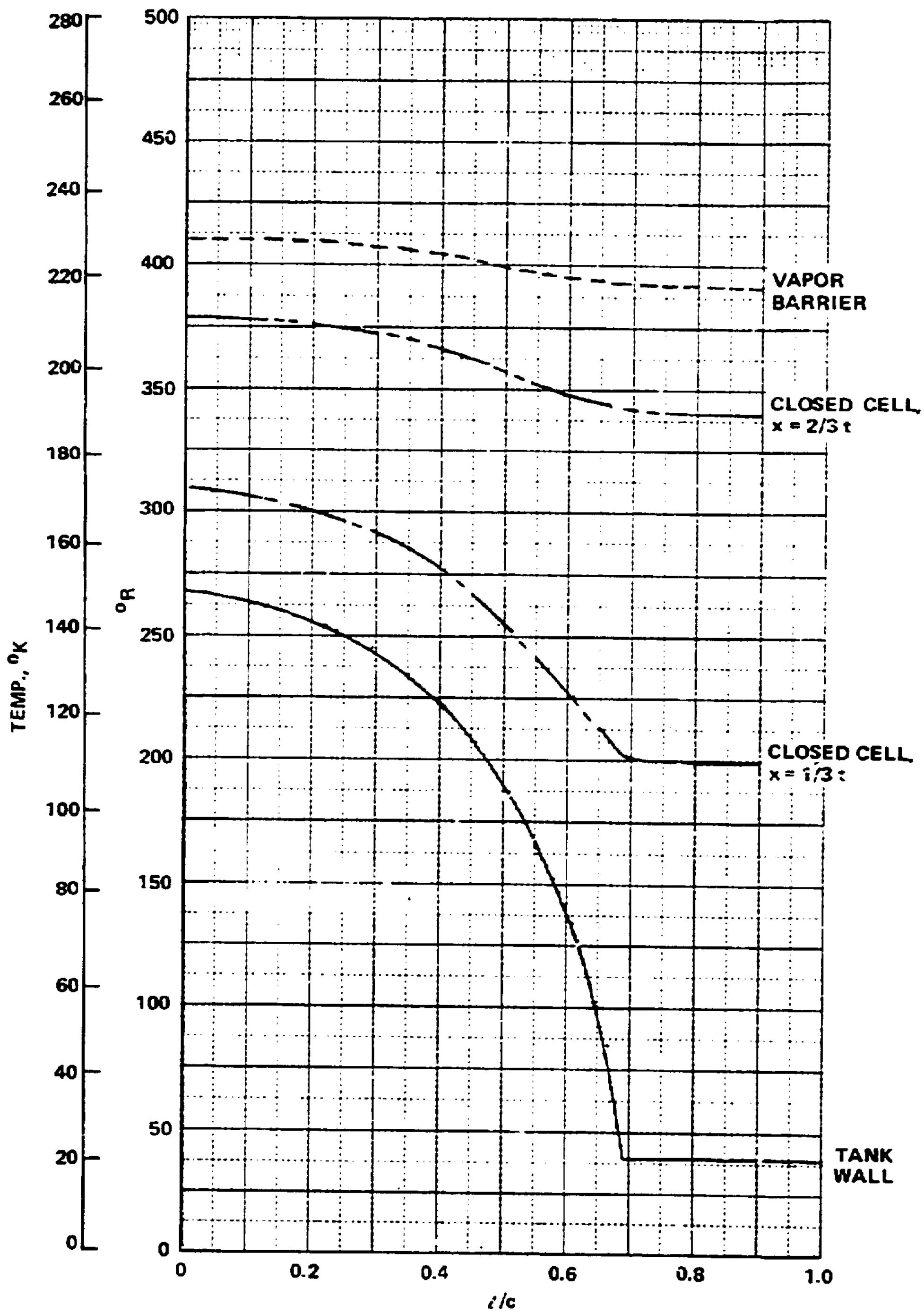

Figure 112. - Concluded.

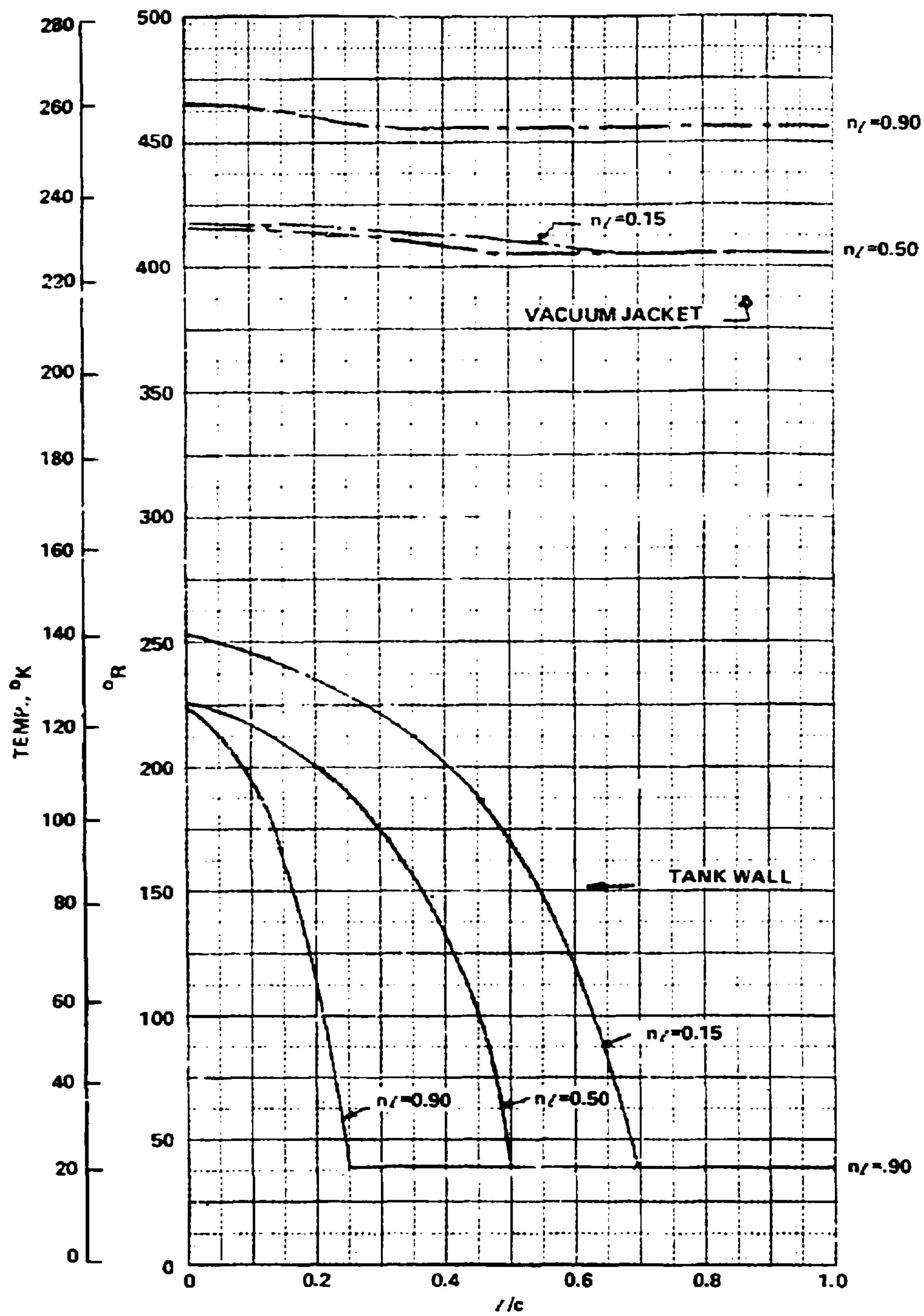

Figure 113. - Candidate D, circumferential temperature distributions for tank wall and vacuum jacket.

TABLE 42. - MAXIMUM COMPUTED CIRCUMFERENTIAL TEMPERATURE GRADIENTS IN TANK WALL AND INSULATION SYSTEM FOR NORMAL OPERATING CONDITIONS

Candidate No.	Liquid Fraction	Maximum Gradient at Location °K/m(°F/in.)					
		Tank Wall		Insulation (Mid thickness)		Exterior Vapor Barrier	
A	0.90	157	(7.2)	37	(1.7)	4	(0.2)
	0.50	339	(15.5)	74	(3.4)	20	(0.9)
	0.15	464	(21.2)	112	(5.1)	33	(1.5)
B	0.90	68	(3.1)	39	(1.8)	33	(1.5)
	0.50	74	(3.4)	44	(2.0)	35	(1.6)
	0.15	116	(5.3)	63	(2.9)	46	(2.1)
C	0.90	125	(5.7)	31	(1.4)	7	(0.3)
	0.50	282	(12.9)	55	(2.5)	22	(1.0)
	0.15	381	(17.4)	90	(4.1)	33	(1.5)
D	0.90	98	(4.5)	17	(0.8)[a]	4	(0.2)
	0.50	232	(10.6)	22	(1.0)[a]	4	(0.2)
	0.15	313	(14.3)	28	(1.3)[a]	4	(0.2)

(a) Microspheres are a packed bed type of insulation and do not transmit tensile loads.

equivalent to that from a 0.32 cm (1/8-inch) diameter orifice. With the vacuum pumps operating the insulation annulus pressure can be maintained at 1 Torr under these conditions (compared to the design pressure of 0.1 Torr). Even assuming the entire microsphere volume is filled with air, the wall heat input due to cryopumping is negligible compared to that through the insulation at the higher pressure.

A second consideration for the vacuum system of candidate D is to assume a catastrophic failure of the vacuum enclosure, such as might be experienced by penetration of the aircraft wall by a foreign object. The flow of air into the vacuum space might not be limited by the jacket, and condensation of air products would occur at a high rate.

TABLE 43. - EFFECTS OF GH_2 AND AIR LEAKAGE INTO EVACUATED INSULATION CANDIDATES

	Candidate B	Candidate C
GH_2 Leakage		
q_w Cruise -W/m^2 (Btu/hr ft^2)	150.3 (47.7)	109.4 (34.7)
q_w Ground -W/m^2 (Btu/hr ft^2)[a]	210.2 (66.7)	137.1, 160.7[b] (43.5), (51.0)[b]
T_{VB} Cruise °K (°R)	167 (300)	112 (201)
T_{VB} Ground °K (°R)[a]	206 (371)	134 (242)
T_F Ground °K (°F)[a]	--	260 (468)
Air Leakage		
q_w Cruise -W/m^2 (Btu/hr ft^2)	79.1, 60.2[c] (25.1), (19.1)[c]	42.2 (13.4)
q_w Ground -W/m^2 (Btu/hr ft^2)[a]	126.1, 84.2[c] (40.0), (26.7)[c]	57.4 (18.2)
T_{VB} Cruise °K (°R)	118, 109[c] (213), (196)[c]	--
T_{VB} Ground °K (°R)[a]	150, 127[c] (270), (228)[c]	--
T_F Ground °K (°R)[a]	277 (498)	279 (502)

(a) $T_{ambient}$ = 289°K (520°R)

(b) GH_2 Leakage into microspheres and open cell foam

q_w = Wetted Wall Heat Flux, T_{VB} = temperature of Vapor Barrier or Vacuum Jacket (no. D)

T_F = Exterior Temperature of Fairing or Vacuum Jacket

(c) Glass/phenolic core

The rate of condensation and solidification is a complex function of heat and mass transport within the porous insulation and its accurate representation is beyond the scope of this program. The microsphere insulation gas flow conductance for GN_2 at atmospheric pressure and 293°K is 5×10^{-4} (gm/sec cm^2) (cm/Torr) so the insulation limits the lateral mass transfer from the opening in the jacket. Also, the void volume for microspheres is on the order of 35 percent so the thermal conductivity of the liquid or solidified layer would be reduced over that of nitrogen in either phase.

During use the jacket is under a mechanical compressive load of approximately 3.5 kPa (0.5 psi) resulting from the compression of the open cell foam by the aircraft exterior skin. This load will keep the microspheres in a densely packed configuration, and they will not flow out of an opening in the jacket other than in the immediate area of puncture. Another consideration is that condensed and solidified air may plug the area adjacent to the opening and further restrict flow of air into the microsphere annulus so it could not cryopump a significant distance from the opening. Because of the very small pores interconnecting each interparticle void, liquid air will be constrained from flowing freely throughout the annulus. With increasing time increments the liquid air will solidify.

Because of the uncertainties associated with the above assumptions and the complexity of a rigorous analysis, an upper limit for LH_2 boiloff was calculated for a worst-case condition resulting from a catastrophic failure. This assumes that air flow is not restricted by the insulation and that air can flow freely to the entire tank surface. It is emphasized that this worst case condition is not considered realistic in that it is highly improbable that air could penetrate to all areas around the tank.

The void volume of the insulation space (solid fraction of microspheres is 0.65) is 2.36 m^3 (83.3 ft^3). Assuming a solid nitrogen density of 962 kg/m^3 (60 lb/ft^3), 2270 kg (5000 lb) of solid air could form in this annular volume. A wall heat rate during condensation was assumed to be 3150 W/m^2 (1000 Btu/hr ft^2) which results in a time of 12 minutes to fill the volume. Including the heat of fusion this corresponds to a mean heat rate, 3546 W/m^2 (1125 Btu/hr ft^2). After 12 minutes, in this worst case situation, the microsphere space is filled and further condensation would occur in the outer covering of open-cell foam. However, the thermal resistance of the solid nitrogen layer will limit tank wall heat rate. For a jacket temperature corresponding to the freezing point of nitrogen and a solid nitrogen thermal conductivity of 0.29 W/m °K (0.17 Btu/hr ft °F) the tank wall heat flux is reduced to 353 W/m^2 (112 Btu/hr ft^2).

The conductivity of the solid layer would actually be less than the above value due to the inclusion of the microspheres (evacuated inner volume) in the layer, but as this value is not known, the higher figure was used for the worst-case estimate.

For a full fuel tank, the boiloff during the initial 12-minute period would be 1145 kg (2525 lb). After this period the boiloff rate would be

558 kg/hr (1230 lb/hr). This maximum fuel loss rate would probably require the addition of an emergency vent.

A major rip or puncture in the vacuum jacket of candidate D is thus seen to represent no critical safety hazard to the aircraft. It will, of course, be cause for the pilot to seek an emergency landing, exactly as he would in the event of a similar puncture of the fuselage of a conventionally fueled aircraft.

A critical sequence in the situation postulated will occur after the aircraft has landed, when the tank is being emptied for repair. As the LH_2 is removed from the tank, the solid air will warm, liquefy, and then boil. Unless special procedures are followed, the cryopumped air can expand so rapidly large areas of the vacuum jacket may be blown off. Proper handling can obviate this situation.

7.1.6.3 Direct operating cost: On the basis of the required tank volumes derived from the thermal analysis procedures for each insulation type and thickness, estimates of weights of all components were made to determine dry weight of the fuel containment system. The following components were included in the dry weight statements for each system:

- Tank shell, integral or nonintegral design
- Tank supports and internal baffle
- Insulation material
- Vapor barriers, where applicable
- Purge barrier, where applicable
- Vacuum jacket, where applicable
- Fuselage structure, nonintegral tank
- Fairing, integral tank
- Vacuum pumps and controls, where applicable
- Purge gas storage and controls, where applicable

This total dry weight combined with design mission fuel weight, weight of fuel evaporated in flight, weight of fuel vented on the ground, and the fuselage length associated with the tank volume were then input into the DOC equation. This was repeated for each insulation thickness, and the values of DOC were plotted against the insulation thickness to graphically determine the thickness associated with the minimum in DOC for a particular system. The form of the DOC eqation which was used in analysis of the fuel containment system is shown in 3.4.

For each DOC calculation in this analysis of the four preferred candidates, the dry fuel containment system weight and fuel loss weights were computed on the basis of the aft tank only, and the results were then multiplied by a factor of 2 to provide a reasonable approximation of total aircraft system weights for application to the DOC equation.

Using the data from Table 41 for system sizing, DOC was calculated as a function of total FCS thickness (t). By plotting DOC versus t, a minimum value of DOC was obtained with a corresponding FCS thickness for candidates A, C, and D; Figure 114. These selected thicknesses were, respectively, 20.32 cm (8.00 in.), 9.14 cm (3.60 in.), and 6.12 cm (2.41 in.). Since candidate B has a fixed geometry, it therefore has a singular value of DOC for the selected vacuum pressure of 10^{-4} Torr.

The characteristics of each of the four candidate insulation systems, using the thicknesses of A, C, and D so chosen, were individually entered into the ASSET computer program for aircraft optimization, along with representation of the preferred tank structural concepts, the LH_2-fueled engine, and the other components of the LH_2 fuel system previously described. The results of this investigation, which provided the basis for selecting a final insulation system concept, are presented in 7.3.

7.2 Tank Structure

An investigation to determine a preferred concept for the fuel tank structural design proceeded in parallel with that of the insulation study. This section presents results of that structural investigation. Design criteria and loads are established, structural concepts for both integral and nonintegral type tanks are described, and the results of the analyses are presented. In addition, the results of parametric studies are reported which determined (1) a preferred shape for the fuel tank dome ends, (2) the effect on economics of specifying a reduced design life for the tank structure, (3) the effect of designing for different pressure levels, and (4) the viability of using a pressure-stabilized structure. An analysis of tank suspension methods for both the integral and the nonintegral tanks was performed.

7.2.1 <u>Structural design criteria and loads</u>. - The structural design criteria and loads defined in this section were developed to provide (1) the basis for the evaluation of the candidate tank configurations and (2) a level of structural safety equivalent to current transports for assessing structural mass trends resulting from application of these criteria.

In general, the criteria are based on the structural requirements of the Federal Aviation Agency, FAR 25 with specific criteria being the same as that used for the L-1011 aircraft. This section presents the following criteria: basic airplane performance data (airplane mass, design speeds, maneuver envelope, etc.), design pressure, emergency landing, thermal stress, combined loads, fatigue and fail-safe. In addition, the design loads are presented for four flight conditions.

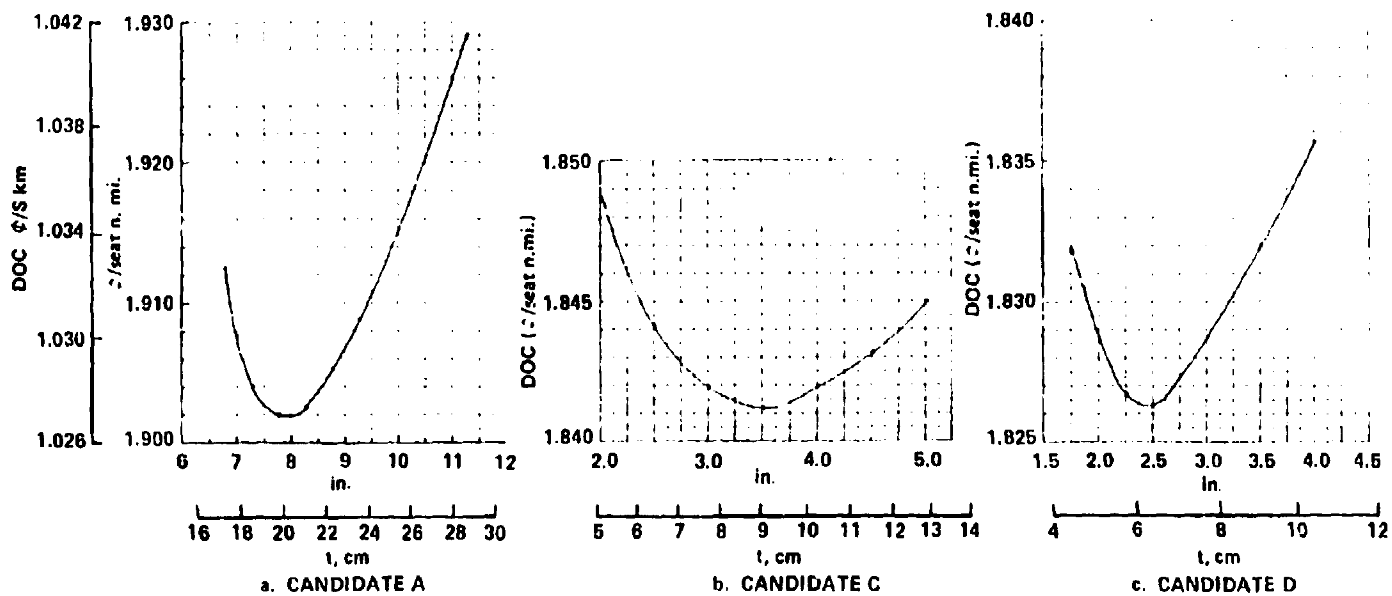

NOTE:
DOC VALUES ARE BASED
ON PRELIMINARY SYSTEM
WEIGHT ESTIMATES.

Figure 114. - Change in DOC with overall fuel containment system thickness (t).

7.2.1.1 Airplane weight and inertia data: The loads are based on the design weights shown in Table 44 which were taken from Reference 1 for use as preliminary values. The inertia distribution data has been estimated based on these weights and the basic geometry and layout of the configuration. Forward c.g. limit was assumed to be 20 percent MAC. Structural reserve fuel is 7 percent of total fuel, the same criterion as used on the L-1011.

7.2.1.2 Design speeds: The design speed-altitude variation is presented in Figure 115. It is the same as the L-1011 airplane. This figure shows the variation of cruise speed, dive speed and maneuver speed with altitude.

Design cruising speed, V_C, is the maximum speed at which encounter of high-intensity nonstorm turbulence (U_{de} = 15.2 m/s (50 fps)) must be considered.

Design dive speed, V_D, is established so that the probability of inadvertently exceeding dive speed is extremely remote even while operating at maximum operating speed.

Design maneuvering speed, V_A, is determined from the aircraft stall characteristics. It is very near to the minimum speed at which the design limit load factor can be attained.

7.2.1.3 Maneuver envelope: The maneuver envelope is a function of weight and altitude. At low speed, the attainable load factor is limited by weight and maximum lift. At speeds above V_A, the allowable maneuver load factor is defined by FAR Part 25.

The envelope shown in Figure 116 corresponds to the altitude at which the constant M_C line intersects the constant V_C line (M_C = 0.9, V_C = 375 KCAS). Other points of interest are defined by the intersection of the constant M_D line and the constant V_D line (M_D = 0.95, V_D = 224 m/s (435 KCAS), h = 6645 m (21 800 ft)), the point where V_C is a maximum (V_C = 193 m/s (375 KCAS) = 189 m/s (368 KEAS), h = 3048 (10 000 ft)) and sea level where V_D is a maximum (V_D = 224 m/s (435 KCAS) = 224 m/s (435 KEAS)).

7.2.1.4 Design loads: Five flight conditions were investigated for static strength of the fuselage aftbody:

(1) A PLA (positive low angle of attack) condition at 6645 m (21 800 ft) of 2.5 g's and a download on the horizontal tail of 45 359 kg (100 000 lb) (Figure 117).

(2) An abrupt pitching maneuver at sea level of 1.0 g with a download on the horizontal tail of 58 967 kg (130 000 lb), included on Figure 117.

(3) A vertical gust condition at 3048 m (10 000 ft) was found to be not critical

TABLE 44. — INITIAL VALUES, DESIGN WEIGHT SUMMARY

Condition	Weight kg	Weight lbm.
Maximum Take off Gross Weight	181 000	400 000
Landing Gross Weight	172 000	380 000
Operating Weight Empty	108 000	238 000
Structural Reserve Fuel	2 200	5 000
Maximum Weight with Structural Reserve Fuel	168 000	370 000
Minimum Flying Weight	110 000	243 000

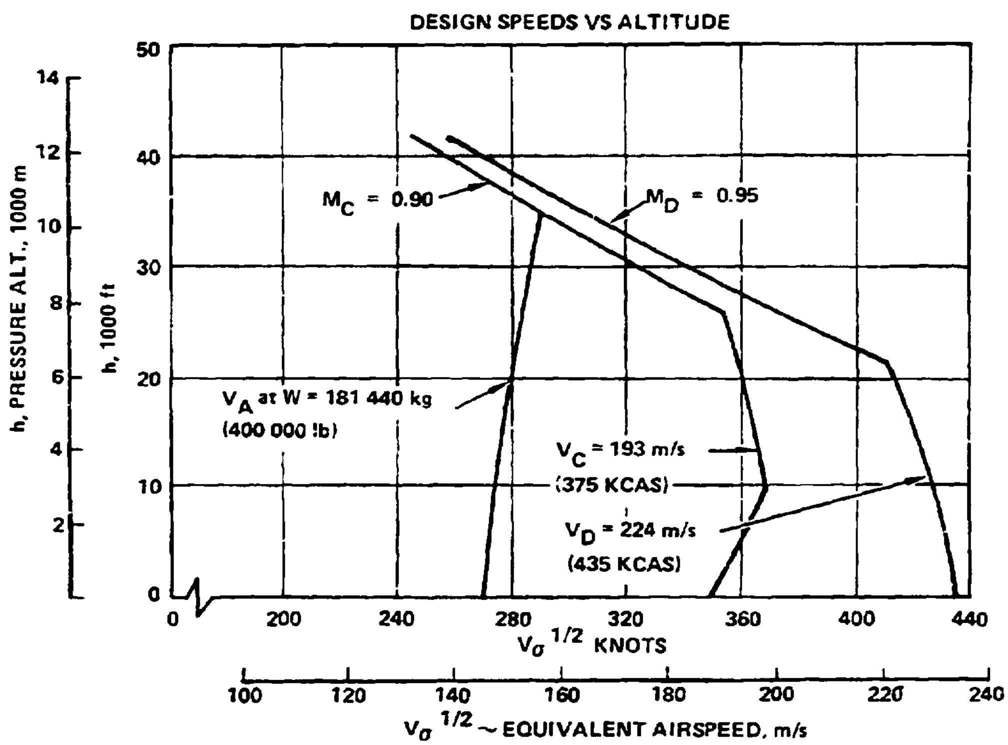

Figure 115. — Design speeds vs altitude.

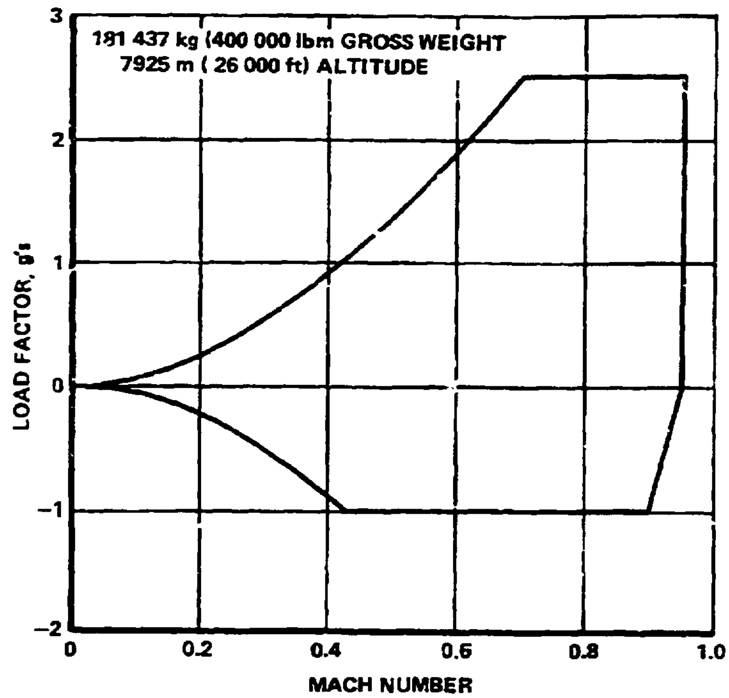

Figure 116 - Maneuver envelope - 181 437 kg (400 000 lb) gross weight, 7925 m (26 000 ft) altitude.

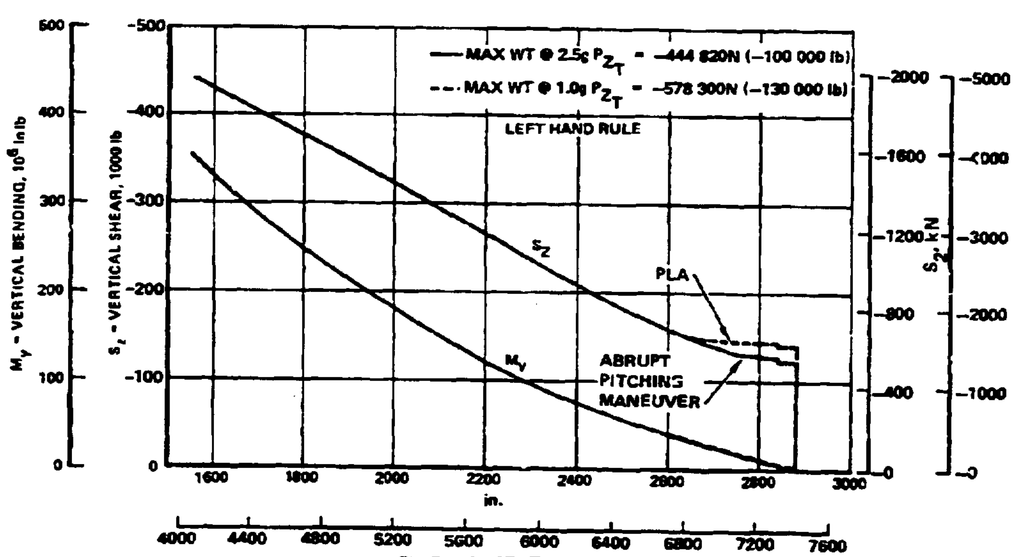

Figure 117 - LH_2 subsonic transport fuselage aftbody limit loads, PLA and abrupt pitching maneuver conditions.

C-2

(4) A negative maneuver condition of -1.0 g with an upload on the horizontal tail of 7257 kg (16 000 lb) (Figure 118).

In addition to the above limit load conditions, a cruise condition was investigated in support of a fatigue evaluation. The condition selected was 1.0 g at start of cruise with a down load on the horizontal tail of 22 680 kg (50 000 lb) (Figure 119).

7.2.1.5 Tank design pressures: LH_2 tanks for the baseline aircraft were designed to operate at a nominal pressure of 14.5 kPa (21 psia). Factors required for cabin pressure (FAR 25) are assumed applicable to the LH_2 tank design and the maximum cruise altitude is assumed to be 11 600 m (38 000 ft).

$$p = 14.5 \text{ kPa } (21.0 \text{ psia})$$

The differential pressure (Δp) acting on the LH_2 tanks is

$$\Delta p = p - p_{at}$$

$$p_{at} = \text{atmospheric pressure}$$

The differential pressure was multiplied by a factor of 1.1 to account for relief valve tolerance and inertia effects, to provide an operating pressure.

$$p_{op} = 1.1 \Delta p$$

- Differential Pressure for Combination with Limit Loads - A limit pressure, equivalent to the operating pressure, is combined with the limit loads due to maneuver or gusts.

$$p_{limit} = p_{op}$$

- Differential Pressure for Combination with Ultimate Loads - An ultimate pressure that corresponds to the operating pressure multiplied by 1.50, was defined for combining with the ultimate loads due to maneuver or gusts.

$$p_{ult} = 1.50 \times p_{op}$$

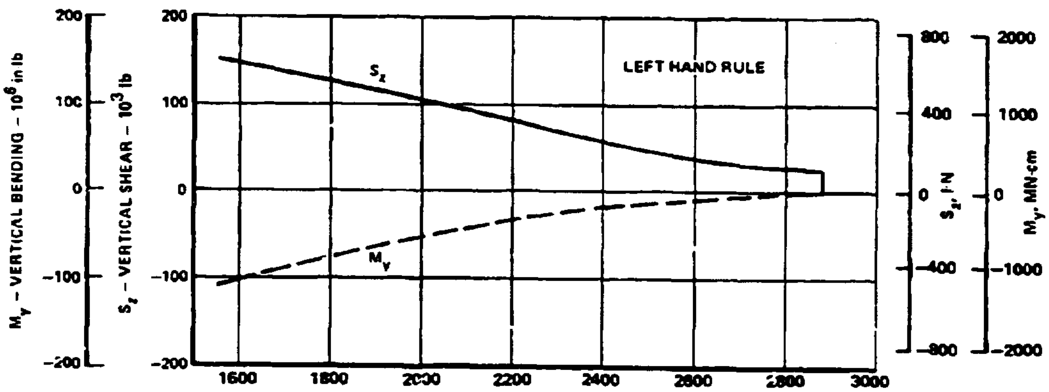

Figure 118. - LH_2 subsonic transport fuselage aftbody limit loads (-1.0 g max, P_{z_T} = 71 170 N (16 000 lb).

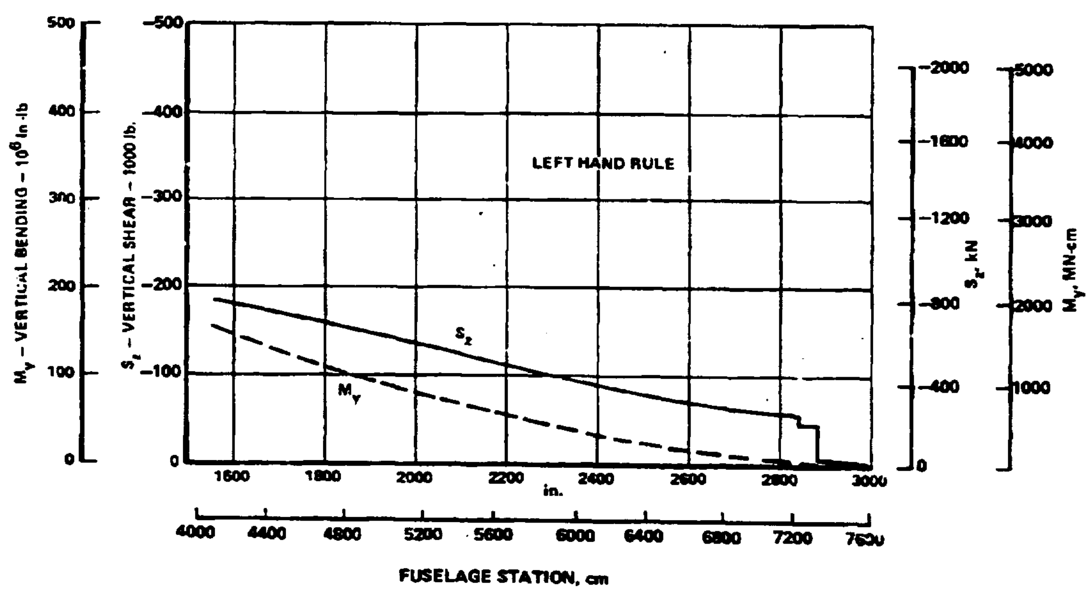

Figure 119. - LH_2 subsonic transport fuselage aftbody limit loads (1.0 g max. weight start of cruise, P_{zT} = 222 410 N (50 000 lb).

- Ground Test Differential Pressure - A proof pressure corresponding to the operating pressure multiplied by 1.33, was specified. No detrimental deformation shall result from this condition.

$$p_{proof} = 1.33 \times p_{op}$$

A burst pressure equivalent to the operating pressure multiplied by 2, was defined. Catastrophic failure of the tank shall not occur.

$$p_{burst} = 2.00 \times p_{op}$$

7.2.1.6 Emergency landing condition: The following ultimate inertia load factors (FAR 25.561) were applied to the tank suspension system and fuel within the tank.

upward: $n = 2.0$

forward: $n = 9.0$

sideward: $n = 1.5$

downward: $n = 4.5$

Each load factor was applied on ar arbitrary independent condition.

7.2.1.7 Thermal stress criteria: Thermal stresses reflecting the maximum individual or combination of through-the-wall, circumferential, and longitudinal temperature gradients were investigated. For the critical flight condition(s), the external loads were combined with the appropriate temperature gradients associated with the insulation system, tank suspension method, and tank ullage condition.

- Limit Thermal Stresses/Strains - For limit design purposes, thermal stresses were calculated for the design flight condition that are compatible with the limit-load design condition. No additional factor of safety was applied to the thermal stresses/strains.

- Ultimate Thermal Stresses/Strains - The stress-strain relationship may not be linear when ultimate design stress levels are being considered. In these cases the thermal strain was held invariant and the stress ($E \times \epsilon$) was combined with the load stress which is thickness dependent. Where the thermal strain was of the same sign as the load stress a factor of safety of 1.25 was applied to the thermal strain. A factor of 1.00 was applied when they were subtractive.

7.2.1.8 Combined Loads Criteria: Flight loads, tank pressure and thermal stresses were combined as specified.

The factor of safety, as defined for the loads, pressures, and thermal strains in the foregoing section, was used to combine the loads and form the final stress resultants.

For compression design, the tensile force produced by the internal pressure was ignored and only the shear and/or compressive forces produced by the external loads were considered with the temperature induced strains/stresses.

For tension design, the sum of the membrane forces produced by the internal pressure and external loads was considered with the appropriate thermal strain/stresses.

The flight and ground conditions considered are specified in Table 45 with the design levels (factors of safety) of the load and thermal environment defined.

7.2.1.9 Fatigue design criteria: Fatigue design requirements can be met by limiting the permissible design tension stress levels for static ultimate design and normal operating conditions.

An average flight time of approximately 5 hours per flight was used for the LH_2-fueled transport. For 2219-T851 Aluminum Alloy at -253°C (-423°F), Figure 120 presents the relationship between fuel tank circumferential design stress and fatigue quality for 50 000 hours of service with the average flight time, one internal pressure cycle per flight, and a life reduction factor of four. The upper curve reflects the ultimate design stress levels applicable to fuel tank substructure other than skin, such as frames, which are uniaxially loaded by pressure and thermal loads. The ultimate design stress levels to be applied to fuel tank skin hoop tension are represented by the second curve on this figure. These values are reduced, to approximately 71.5 percent of the substructure design allowable, because the skin is subjected to biaxial stresses from internal pressure, external loads, and thermal loads. The allowable gross area tension stress for the operating condition for 2219 aluminum is presented as the lower curve of Figure 120. For other materials, the tension allowables in other than fuel tank regions are related to prior experience and successful service experience with similar types of aircraft, such as the L-1011 commercial transport.

The fatigue life for the materials selected for the integral and non-integral tank designs are achieved by limiting the ultimate design stress values. Table 46 contains the allowable gross area tension stresses for 2024 and 2219 aluminum alloys with a fatigue quality index (K_t) of 5.0.

TABLE 45. - COMBINED LOADS AND THERMAL CRITERIA

Condition	External Loads	Internal Pressure	Thermal Stress/Strain
Operating (Cruise Cond.)	Limit	Limit	Limit
Limit Design	Limit	Limit	Limit
Ultimate Design	Ultimate	Ultimate	Ultimate
Fail-Safe Design	Limit	Limit	Limit
Emergency Landing	Ultimate	Ultimate	Ultimate
Proof Test	-	Proof	-
Burst	-	Burst	-

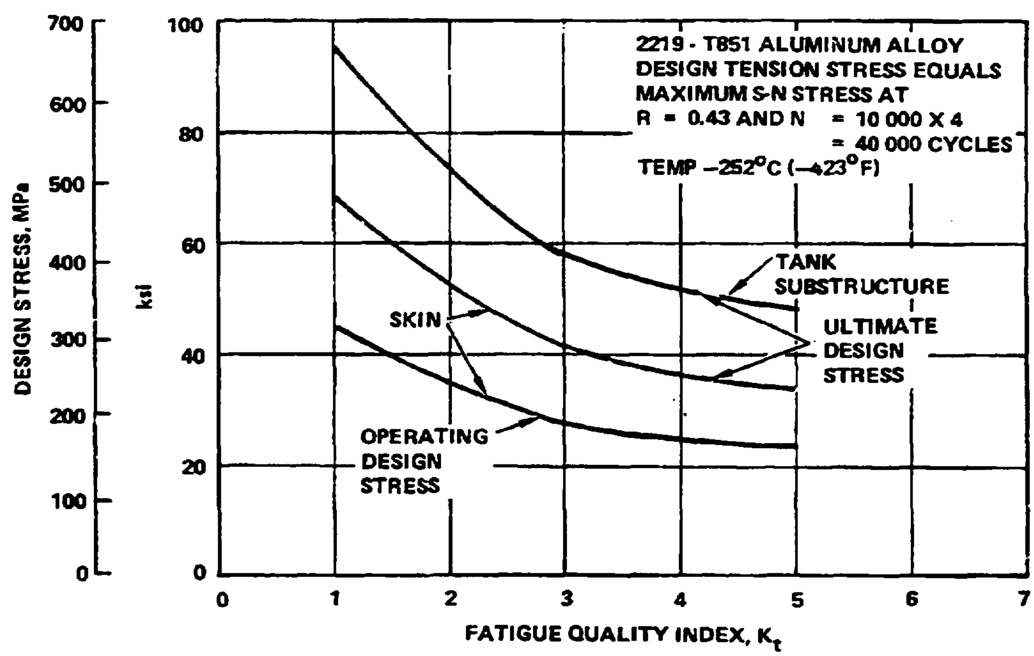

Figure 120. - Variation in circumferential design stress with fatigue quality for 10 000 flights including a life reduction factor of four on number of flights.

TABLE 46. - FUSELAGE ALLOWABLE GROSS AREA TENSION STRESSES FOR ULTIMATE DESIGN AND OPERATING CONDITIONS

	Nonintegral		Integral
	Shell	Tank (1)	Both (1)
	2024 Alum (RT)	2219 Alum -253°C (-423°F)	2219 Alum -253°C (-423°F)
Components	kPa (psi)	kPa (psi)	kPa (psi)
Ultimate Design Condition			
• General Structure	510 264 (45 000)	NA	NA
• Concentrated Loads and Biaxial Stress Areas	241 316 (35 000)	234 422 (34 000)	234 422 (34 000)
Operating Condition			
• Skin Hoop Tension at Operating Pressure, External Loads and Thermal Stress	NA	172 369 (25 000)	172 369 (25 000)

Notes:

1. Design allowables based on a fatigue quality index of 5.0, 50 000 hr of service life and a life reduction factor of 4.

For the nonintegral tank design, 2024 aluminum alloy was used for the fuselage bending material. The ultimate gross area tension stress for symmetrical flight and ground conditions was limited to 310 264 kPa (45 000 psi). In addition, the basic design allowable stress was further reduced to 241 316 kPa (35 000 psi) in local areas subjected to biaxial loading, regions adjacent to highly concentrated loads, blind areas and single load paths in primary structure. For the 2219 aluminum alloy which is used for the fuel tank design in both the integral and nonintegral designs, the allowable stress in areas subjected to concentrated loads and biaxial stresses was limited to 234 422 kPa (34 000 psi).

Table 46 presents the design allowables for the special fatigue considerations required for the operating design condition for pressurized fuel tank structure. For both integral and nonintegral tank designs, the allowable gross-area tension stress of 172 369 kPa (25 000 psi) (K_t = 5) for fuel tank skin circumferential stresses is related to fuel temperature, number of landings, and related values of life reduction and stress concentration factors. The allowable stress for fuel tank substructure, such as frames, would be higher than that required for fuel tank skins because the loading on the substructure is primarily uniaxial.

7.2.1.10 Fail-safe (damage tolerance) design criteria: The objective of the fail-safe (damage tolerance) design criterion is to ensure that flight safety is maintained in the event of structural damage of reasonable magnitude. Such damage may arise from fatigue as well as accidental impact or other sources. To meet the objective, a fracture control plan consisting of the following aspects was implemented.

Minimum requirements on material fracture properties shall be established for material selection. The required properties shall include fracture toughness, fatigue crack growth, and threshold for stress corrosion cracking. Materials in as received condition as well as after undergoing major fabrication processes such as cold work, welding, and heat treatment shall be tested.

Based on production inspection capabilities, the maximum size flaw that is likely to be missed shall not grow to critical proportions during the life of the structure; i.e., 10 000 flights or 50 000 hours. The inspection requirement shall be met by using a combination of quality control and NDI requirements.

The operating stress levels and material selection shall be chosen to ensure that under normal service conditions undetected flaws will remain as subcritical through-the-thickness cracks for a sufficiently long period. Thus, the detection of such flaws by leakage can be ensured.

For the above criteria, the critical damage size is that which can sustain the operating pressure in combination with the limit loads due to maneuvers or gusts.

For fail-safe, the tank structure must be capable of supporting the operating pressure loads and appropriate fail-safe loads for accidental damages equivalent to a 30.5 cm (12.0 in.) through-the-thickness crack anywhere in the structure, including members attached to the structure across the damaged section. The fail-safe loads shall be equal to the maneuver and gust loads that can reasonably be expected during completion of the flight in which the damage occurred.

Fail-safe for the remainder of the structure shall be designed to meet the fatigue and damage tolerance requirements of FAR 25.571.

Besides the customary quality control and NDI procedures which applied to the material received and during fabrication process, a leak test shall be conducted concurrently with the ground proof test discussed previously.

7.2.2 <u>Structural design concepts and materials</u>. - Two basic types of tank designs were considered for this study:

- Integral, where the tank serves both as the container of the fuel and also supports the body loads

- Nonintegral, in which the tank is simply a fuel container and does not participate in the support of the body loads which are carried by a separate shell structure.

Promising structural design concepts were evaluated for each of the above basic types of LH_2 tank designs and are shown in Table 47.

For the Integral tank design, three wall concepts were considered with all designs being restricted to one-piece configurations to minimize potential sources of leaks. These concepts were the blade-stiffened, zee-stiffened and tee-stiffened designs. In addition, an unstiffened wall design was included in the candidate concepts for the tank design.

The wall concepts considered for the nonintegral tank design were the conventional construction zee- and hat-stiffened concepts for the fuselage shell and the same one-piece wall designs as described for the integral tank used for the tank design.

For the fuselage shell structure of the nonintegral tanks, the conventional 2024 and 7075 aluminum alloys currently being employed on wide-bodied transport were used for the baseline material; whereas, the aluminum alloy 2219 was selected for the tank material for both basic types of tanks.

The 2219 aluminum alloy was selected because of its ductility at cryogenic temperatures, as well as its weldability, formability, stress corrosion resistance, and its high fracture toughness and resistance to flaw growth, References 27 and 28.

Table 48 presents a compilation of materials data applicable to the design of LH_2 fuel containment tankage and fuselage shell structure.

TABLE 47. - STRUCTURAL DESIGN CONCEPTS

Structural Component	Tank Design	
	Nonintegral	Integral
Fuselage	Zee-stiffened Hat-stiffened	Not applicable
Tank	Blade-stiffened Zee-stiffened Tee-stiffened Unstiffened	One-piece Configurations (Blade-, Zee-, Tee-stiffened)

TABLE 48. - MATERIALS DATA PERTINENT TO LH_2 FUELED SUBSONIC TRANSPORT FUEL CONTAINMENT TANKAGE/FUSELAGE STRUCTURES

Materials																	
Structural			Identity				Properties and Characteristics										
	Concept						F_{tu} (ksi)		F_{ty} (ksi)		F_{cy} (ksi)		e (%)		K_{IC} (2)(3) (ksi/in)		
Assy	Int.	Non-Int.	Type	Alloy	Prod. Form	Thickness (in.)	AMB.	LH_2	AMB.	LH_2	AMB.	LH_2	AMB.	LH_2	AMB.	LH_2	Comments
Tank	√	√	Alum. Alloy	2219-T8 or 2419-T8	Sht.	To .249	62	98	47	63	48		7	16	64	78	Density .102 lb/in[1], 2219 and 2419 properties the same except 2419 K_{IC} is guaranteed; hydrogen environment embrittlement is negligible.
					Plt.	To 1.0	62	98	47	63	48		8	15	-	47	
						1.0-2.0	62	98	47	63	47		7	15	34	-	
					Ext.	To .5	53	92	42	57	43		6	15	-	-	
						.5-3.0	58	92	42	57	42		6	15	-	-	
			Cres	21-6-9	Sht	To .249	100	234	60	181	60		40	58	-	-	Density 0.283 lb/in³; high resistance to hydrogen environment embrittlement.
					Bar	All	90	245	50	146	50		40	15	-	-	
				321	Sht	To .249	75	230	30	60	27		45	35	-	-	Density 0.286 lb/in³; high resistance to hydrogen environment embrittlement
					Bar	All	75	270	30	60	27		45	35	-	-	
Fus. Shell	N.A.	√	Alum. Alloy	2024-T3 Clad	Sht	To .128	64	110	47	74	39		15	17	83	-	Density 0.100 lb/in³; hydrogen environment embrittlement is negligible.
						.129-.249	65	110	47	74	39	(1)	15	17	87	-	
					Plt	.25-.49	65	97	47	80	40		12	10	-	-	
						.50-1.0	63	97	47	80	39		8	10	21	-	
				7075-T76 Clad	Sht	To .187	67	106	57	70	56		8	15	49	-	Density 0.101 lb/in³; hydrogen environment embrittlement is negligible
						.188-.249	69	106	59	70	58		8	15	53	-	
					Plt	To .449	68	95	58	80	57		8	9	25	-	
						.50-1.0	68	95	57	80	56		6	9	25	-	
				7075-T76 Bare	Sht	.64-.125	78	115	70	100	64		8	11	61	-	Density 0.101 lb/in³; hydrogen environment embrittlement is negligible.
						.125-.249	78	115	71	100	70		8	11	59	-	
					Plt	.25-.49	77	110	69	95	65		9	10	-	-	
						.50-1.0	77	110	70	95	68		9	10	23	-	
						1.0-2.0	76	110	69	95	66		6	10	23	-	
					Ext	.25-.49	81	117	73	100	73		7	20	-	-	
						.50-.74	81	117	72	100	72		7	20	24	-	
						.75-1.5	81	117	72	100	72		7	20	24	-	

(1) F_{cy} @ LH_2 temperature not available. $F_{cy} = F_{ty}$ @ $-423°$, assures a reasonable assumption.
(2) All facture toughness values are for L-T orientation.
(3) K_{IC} is the stress intensity factor applicable for conditions of plane strain and is the minimum threshold value for large thicknesses.

For fuselage shell structure, independent of the fuel containment system, data for the 2024 and 7075 materials indicate that such materials can remain in contention for independent fuselage shell structure of the LH_2 transport.

Comparison of data for 2219, 21-6-9 (Nitronic 40) and 321 materials for the tank structure show the strength/density advantage for the 2219 material in fuel containment applications.

7.2.3 Concept screening. - The design of an economically viable LH_2-fueled aircraft requires the lowest attainable structural mass-fraction commensurate with the assumed technology period. To achieve this goal-promising structural design concepts were evaluated for each basic tank configuration (i.e., integral and nonintegral) using a representative load/temperature environment and the design criteria specified in 7.2.1. The candidate structural design concepts are described in 7.2.2.

7.2.3.1 Evaluation procedure: To provide a rational basis for evaluating the candidate tank wall concepts for the integral and nonintegral tanks, a structural investigation was conducted which proceeded in parallel with that of the insulation system described in 7.1. The structural evaluation consisted of the following steps:

1. Baseline tank configurations were established for the integral and nonintegral tank designs. Structural configurations and a typical insulation system were postulated for a constant volume tank to define the basic tank dimensions.

2. A BOSOR4 finite difference structural model was established for the integral and nonintegral tanks using the basic dimensions defined for the above baseline tanks. A representative wall concept was selected for each tank from the candidate concepts which provided the property data for the models.

3. Using the external loads, static solutions were obtained using the BOSOR4 structural models. Displacements, inplane stress resultants, and bending moment resultants were defined for each tank design.

4. Point design regions were selected and typical structural components for each tank design were defined for conducting the detail analysis. The results of the BOSOR4 static solutions were used to define the load/temperature environment.

5. Detailed structural analyses were conducted on each candidate tank wall concept using the internal load/temperature environment corresponding to the basic tank design being investigated. These environments, in conjunction with computerized stress analysis programs, were used to define the minimum-weight proportions and corresponding weight of the candidate concepts. Included in this study were basic strength, stability, and fatigue and fail-safe analyses.

6. The total tank weight for each candidate concept was extrapolated from the results of the point design analysis. These results were then used to select the most promising tank wall concept for the integral and nonintegral tank designs.

7.2.3.2 Analytical methods: Established methods were employed to analytically evaluate the candidate tank concepts during the concept screening analysis; they were of two general types: (1) computerized shell programs to define the internal loads and conduct the general stability analysis, and (2) stress analysis programs and methods for sizing the major structural components. A description of these programs and analytical methods is presented in the following text.

7.2.3.2.1 Shell analysis: The computerized shell analysis program, BOSOR4 (Reference 29), was used to define the internal loads and conduct the stability analyses. This program uses a finite-difference solution method based on an energy formulation and can perform stress, stability, and vibration analyses of segmented, ring-stiffened shells. The BOSOR4 program is limited to shells of revolution.

7.2.3.2.2 Structural analysis: The basic strength and stability analyses of the candidate tank wall concepts were conducted using existing structural analysis computer programs. In addition to these programs, established methods were used to analyze the damage tolerance aspects of the wall concepts, as well as the basic strength of the other major structural components.

For the tank wall concepts a computer program which links general purpose random search algorithms with available stress analysis programs was used to define the minimum weight panel proportions. These stress analysis programs are similar to those reported in Section 12 of Reference 31. Included in these programs is a strength evaluation of the complex stress state, i.e., inplane and normal stress resultants. The search algorithm, entitled MONTE CARLO I, employed in these programs contains a sequence of two previously reported and well known approaches: Random Selection and Random Rays, Reference 32.

The sizing of the frames for this study were based on the theory derived by Shanley in Reference 33, which is premised on providing sufficient frame stiffness to preclude a general instability failure of the shell in bending. Shanley's expression for the required frame stiffness is:

$$(EI) = C_f MD^2/L$$

This expression relates the frame stiffness (EI) to the applied bending moment (M), the shell diameter (D), and frame spacing (L).

7.2.3.2.3 Fatigue analysis: A detailed description of the fatigue criteria is presented in 7.2.1.9. The intent of this section is to describe the application of this criteria to the structural components.

The fatigue design requirements are met by restricting the permissible design tension stress levels used for design. Design allowables for both the operational and ultimate design conditions were established and are shown in Figure 120.

For the operating condition, the limit loads for the cruise condition were used and the fuel tank skin circumferential stress was restricted to a stress level of 172 369 kPa (25 000 psi), $k_t = 5$.

The design allowables for the skin and substructure of the tank for the ultimate design conditions are also shown on Figure 120. The application is similar to that of the operating conditions, with the exception that the applied loads reflect the maximum ultimate design loads from any of the flight conditions.

7.2.3.2.4 Fail-safe analysis: The objective of the fail-safe analysis was to ensure that the structure in the presence of an assumed damage condition was capable of supporting the design load of 100-percent limit load. Both circumferential and longitudinal skin crack damages were assumed as specified in the design criteria, 7.2.1.10.

In general, for all wall concepts which have separately attached stiffeners (spot welded or mechanically fastened), the stiffener reinforces the skin and provides crack-arresting capability; conversely, for one-piece skin/stiffener designs, no reinforcement capability is provided by the stiffener. In the latter case, the fail-safe criteria is met by lowering the axial stress level (i.e., increasing the cross-sectional area) and/or by providing external straps.

The analysis methods used for conducting the fail-safe analysis are presented in Reference 34. Figures 121 and 122 outline the general equations used in determining the residual strength of the damaged structure for the circumferential and longitudinal crack conditions, respectively.

7.2.3.3 Baseline tank configurations: Baseline integral and nonintegral tank configurations were defined for use in the analysis and evaluation of the candidate structural concepts in the concept screening analysis. The size and geometry of these nominal tanks were established based on the following:

- The tank is of conical configuration with ellipsoidal closures having an aspect ratio (a/b) = 1.30
- The tanks are covered with an insulation having a thickness of 15.24 cm (6.00 in.)
- The tanks are sized by using an overall effective fuel density of 63.72 kg/m^3 (3.978 lb/ft^3).

For the baseline aircraft,

$$W_g = 177\ 690 \text{ kg } (391\ 740 \text{ lbm.})$$

$$\text{Usable fuel per tank} = \frac{27\ 955\ (61\ 630)}{2} = 13\ 978 \text{ kg } (30\ 815 \text{ lb})$$

$$\text{Tank volume (in as-built, warm condition)} = \frac{13\ 978\ (30\ 815)}{63.72\ (3.978)} = 219.3 \text{ m}^3\ (7\ 746 \text{ ft}^3)$$

As mentioned earlier, the basic analysis of both structure and insulation systems was performed using the aft tank of the aircraft as a model. The geometry of the aft tank and its relation to the aircraft was presented previously in Figure 87. Table 49 shows the assumed structural concepts and the major dimensions of the baseline integral and nonintegral aft tanks.

7.2.3.4 Structural models: BOSOR4 math models were constructed for each basic tank design (integral and nonintegral) to define the internal loads for the concept screening analysis. The tank dimensions used for the models reflected the size and geometry of the nominal baseline tank configurations. Representative wall concepts were selected from the list of candidate structural concepts and their corresponding stiffnesses were used as input to the structural models.

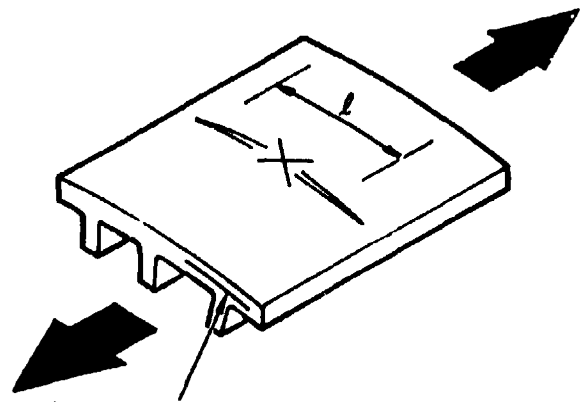

THE RESIDUAL STRENGTH OR ALLOWABLE STRESS IS DEFINED BY

$$F_g = \frac{\gamma \, n k_o}{\sqrt{\ell}}$$

WHERE:

γ = REINFORCEMENT EFFICIENCY PARAMETER

n = CURVATURE REDUCTION FACTOR, $n = 1/2$

k_o = STRESS INTENSITY FACTOR FOR CONDITIONS OF PLANE STRESS USED FOR THROUGH-THE-THICKNESS CRACKS, $k_o = k_c/\sqrt{\pi/2}$

k_c = PLANE STRESS FRACTURE TOUGHNESS (ASTM NOTATION)

ℓ = TOTAL CRACK LENGTH, $\ell = 2a$

Figure 121. - Fail-safe analysis of circumferential damage condition.

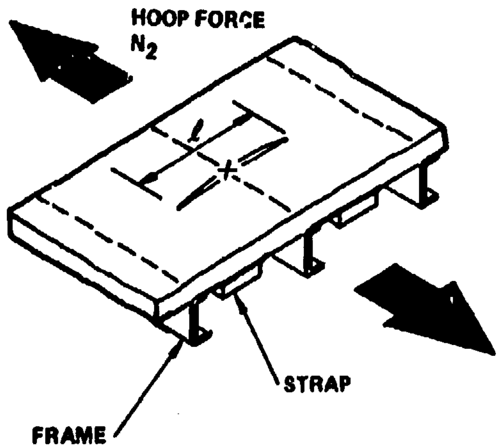

THE RESIDUAL STRENGTH OR ALLOWABLE STRESS IS DEFINED FOR A REINFORCED PANEL BY

$$F_{pg} = 1.2\, F_{tus} \left(\frac{2We + \sum \frac{Ae}{t_s}}{C_1 \ell + 2We} \right)$$

AND FOR AN UNREINFORCED PANEL BY

$$F_{po} = 1.2 \left(\frac{2We\, F_{tus}}{C_1 \ell + 2We} \right)$$

WHERE:

$2W_e$ = AN EFFECTIVE WIDTH PARAMETER

ℓ = TOTAL CRACK LENGTH, $\ell = 2a$

F_{tus} = ULTIMATE TENSILE STRENGTH OF THE SKIN MATERIAL

C_1 = LONGITUDINAL CRACK EXTENSION PARAMETER FOR PRESSURIZED FUSELAGE PANEL. A FUNCTION OF THE STRESS INTENSITY FACTOR K_Q.

$\left(\frac{\sum Ae}{t_s} \right)$ = EFFECTIVE REINFORCEMENT AREA DIVIDED BY SKIN THICKNESS.

Figure 122. - Fail-safe analysis of longitudinal damage condition.

TABLE 49. - CONCEPTS AND DIMENSIONS OF BASELINE INTEGRAL AND NONINTEGRAL TANKS

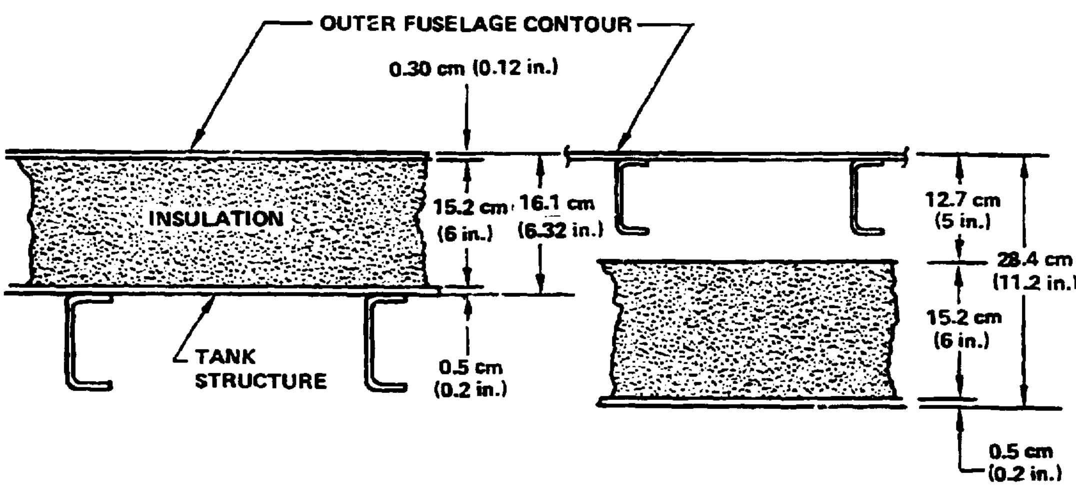

	Integral	Nonintegral
Vol - m^3(ft^3)	21 913 (7746)	219.3 (7746)
D_2 - m(ft)	4.216 (13.833)	4.216 (13.833)
D_1 - m(ft)	6.32 (20.75)	6.44 (21.12)
d_2 - m(ft)	3.90 (12.78)	3.65 (11.967)
d_1 - m(ft)	6.00 (19.697)	5.87 (19.254)
ℓ - m(ft)	8.39 (27.52)	9.32 (30.59)
h_1 - m(ft)	2.31 (7.58)	2.26 (7.41)
h_2 - m(ft)	1.50 (4.92)	1.41 (4.61)
L - m(ft)	12.20 (40.02)	12.99 (42.61)

7.2.3.4.1 Nonintegral tank model: The representative structural/material arrangement selected as a baseline for this design consisted of a zee-stiffened panel concept for the shell (the fuselage structure surrounding and supporting the tank) with sheet metal frames at approximately 50.8 cm (20-in.) spacing. The materials for the shell structure are the conventional 2024 and 7075 aluminum alloys. The structural configuration selected for the LH_2 tank was the blade-stiffened configuration fabricated from 2219 aluminum alloy.

A preliminary sizing of this representative concept was conducted to define the input properties for the model. For the fuselage, the shell wall and an area of 0.613 cm^2 (0.095 in^2) per stringer pitch which included an 0.084 cm (0.033 in.) thick skin. The internal frames were of conventional sheet metal construction with an area of approximately 4.19 cm^2 (0.65 in^2) (excluding any effective skin) at approximately 50.8 cm (20 in.) spacing.

The configurations used for modeling the tank reflected the baseline tank configuration, i.e., ellipsoidal closures and a conical tank. The tank closures were an unstiffened wall design with a constant thickness of 0.25 cm (0.10 in.). External rings were provided at the junction of the closures and the conical section for supporting the tank.

Pertinent dimensions of the baseline fuselage shell and tank are shown in the structural model represented in Figure 123. The tank was supported at the equators of the forward and aft tank closures. At the aft support, the tank and shell had compatible deflection (axial and radial) and rotational degrees of freedom; whereas, only radial deflection was permitted at the forward support.

The structural computer model is characterized by 150 axial node points in the tank, and 99 in the fuselage shell. Figure 124 shows the structural model with the components of the applied loads indicated. These loads reflect the limit loads components of the PLA symmetrical maneuver condition at 2.5 g. These components include the tail loads (moment and shear) applied at aft end of fuselage, the tank internal pressure and inertia loading, and the tank and fuselage temperatures. The tail loads applied at the aft fuselage were adjusted so that the combined effect of these loads and the tank inertia load would meet the specified shear and moment values at the forward end of the tank, FS 2335.

BOSOR4 static solutions were conducted to assess the internal membrane and bending forces associated with the tank and fuselage structure. Separate solutions were obtained using each component of the applied loads to assess the impact of the individual load components as well as providing the basis for defining other load conditions.

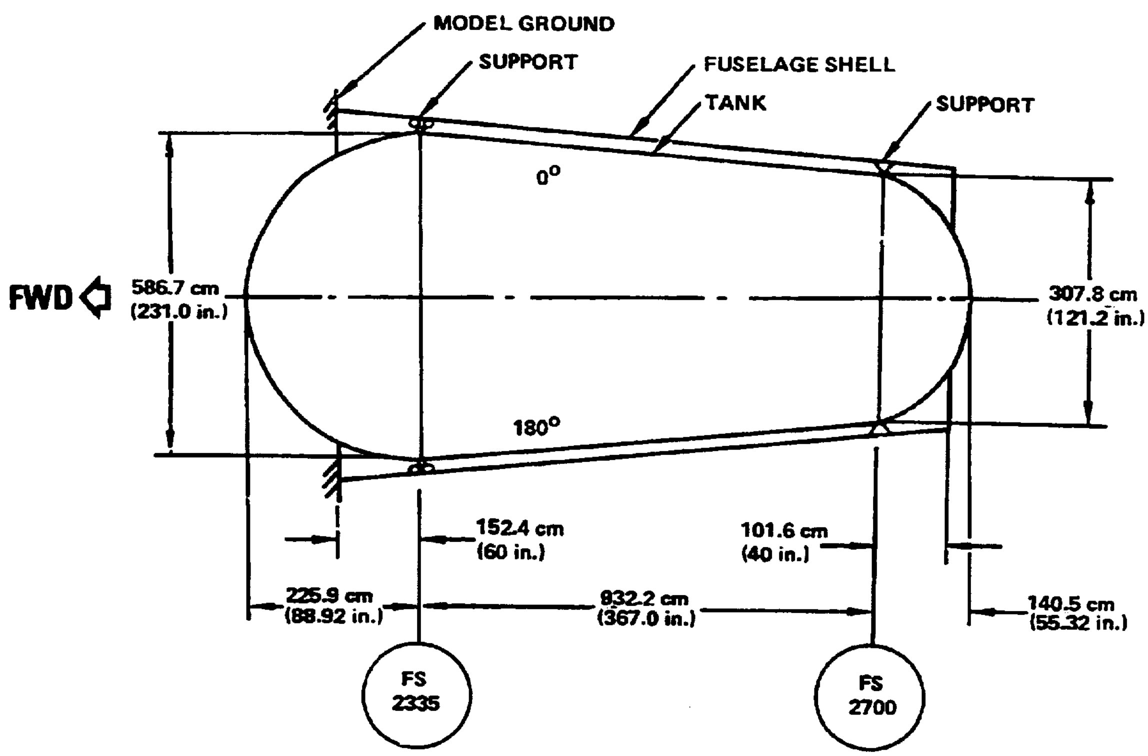

Figure 123. - Fuselage and tank dimensions used for the nonintegral tank structural model.

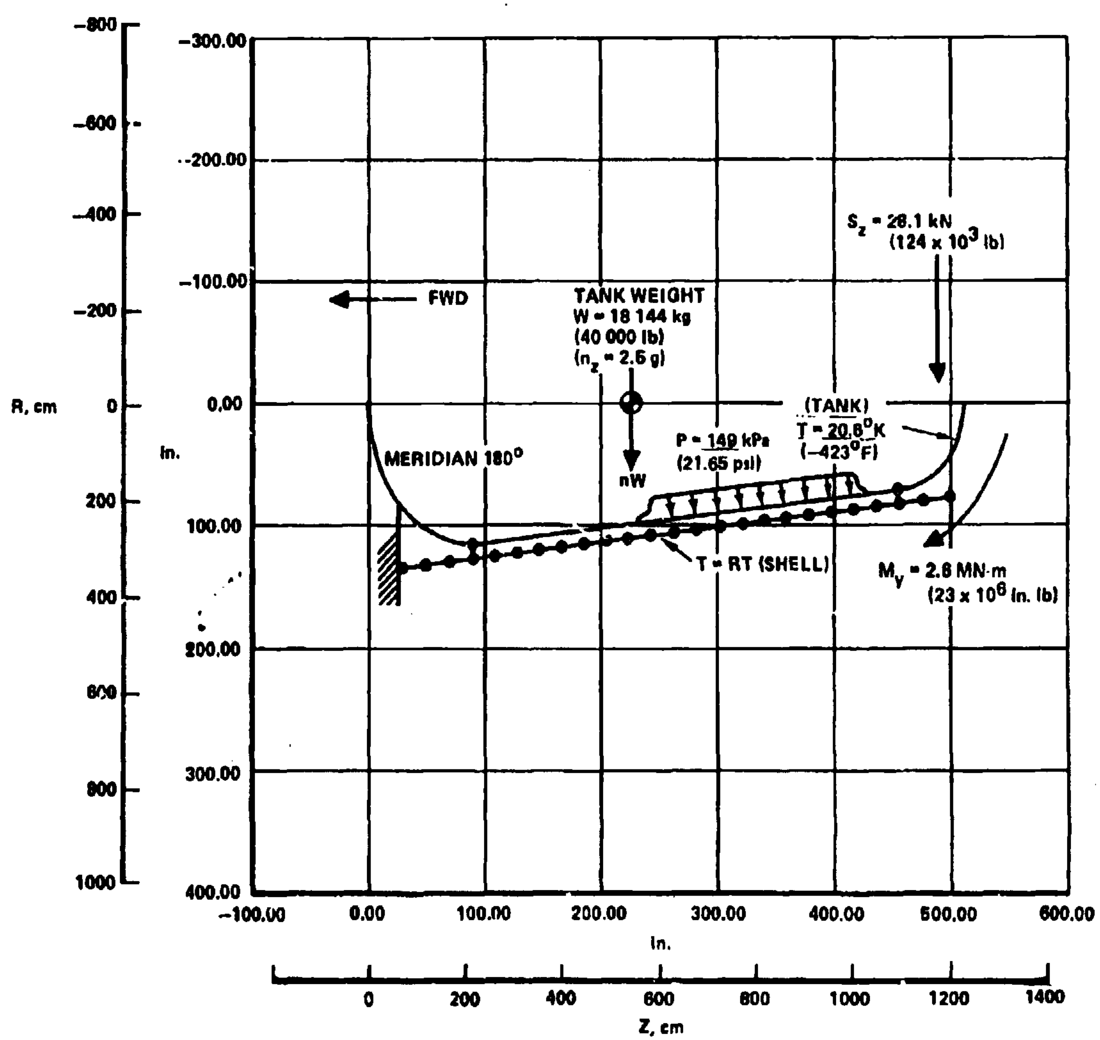

Figure 124. - Applied loads and structural model for the nonintegral tank design.

Results of the static solutions include both printout and plots of the displacements, membrane forces, and bending moments as a function of arc length. The arc length is measured from the apex of the forward tank closure aft along the tank meridian to the apex of the aft tank closure, approximately 1625.6 cm (640 in.). The plots then proceed to the forward end of the shell (fixed boundary) aft along the shell meridian.

The three displacement components: meridional (U), circumferential (V) and normal (W) were defined for each load component. Figure 125 displays a plot of the normal displacement (W) for each of the load components, i.e., the temperature, air load, and internal pressure conditions.

The inplane stress and bending moment resultants for each of the applied load conditions are shown in Figures 126 through 131. The meridional (N_1), hoop (N_2) and inplane shear (N_{12}) stress resultants are displayed in Figures 126, 128 and 130 for the internal pressure, airload and temperature conditions, respectively. The corresponding meridional (M_1), hoop (M_2) and twisting (M_T) moments are shown in Figures 127, 129, and 131. All stress resultants and moments are with reference to the outer skin surface, not the neutral axis of the shell.

7.2.3.4.2 Integral tank model: The representative structural candidate selected for the modeling effort on the integral tank design was the zee-stiffened panel concept with sheet metal frames at approximately 50.8 cm (20 in.) spacing. Tank material was 2219 aluminum alloy. Truss structures composed of Boron/Epoxy tubular members were provided as interface skirts between tank and fuselage. Conventional zee-stiffened structure using 2024 aluminum alloy was selected for the short segments of fuselage at both ends of the model.

The integral tank design represented in the structural model is shown in Figure 132. The tank was cantilevered from the forward end of the fuselage segment approximately 152.4 cm (60.0 in.) forward of the interface structure. The structural model for the integral tank design was characterized by approximately 150 axial node points for the tank and 72 points in the fuselage segment and interface skirts.

The preliminary sizing of the structural concepts provided the necessary input data for the model. For the small segments of fuselage at the forward and aft end of the model, conventional zee-stiffened structure was utilized with the same material properties as described for the nonintegral tank design. The input data for the interface trusses reflected Boron/epoxy tubular element having an area of 14.2 cm^2 (2.2 in^2) and a inertia value of 41.62 cm^4 (1.0 in^4). The input for the tank structure, which must support both the flight and internal pressurization loads, reflected the zee-stiffened design with an area of approximately 1.29 cm^2 (0.20 in^2) per stringer pitch. The tank closures were ellipsoidal in configuration and of unstiffened wall design with a constant thickness of 0.25 cm (0.10 in.).

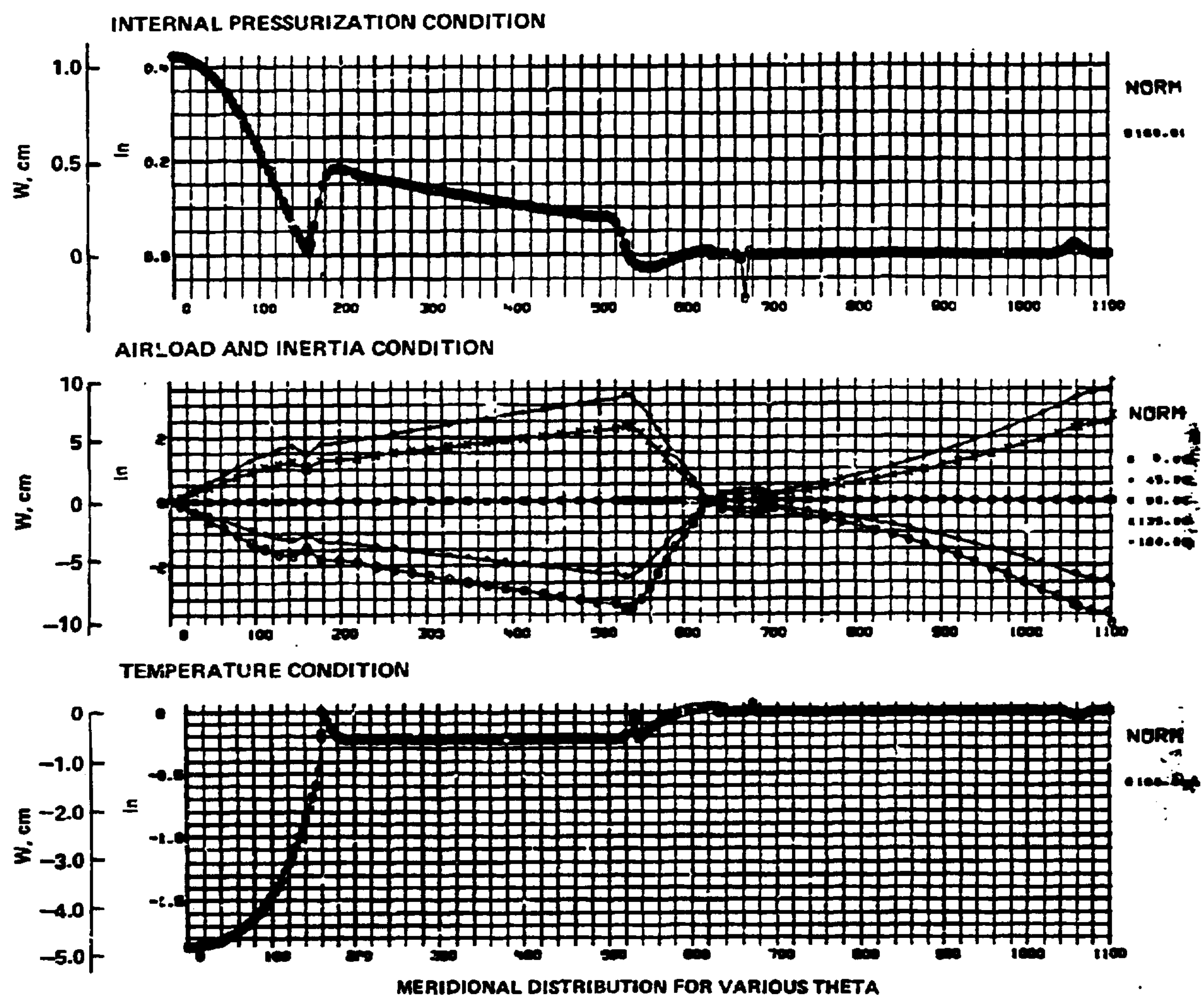

Figure 125. - Normal displacements of the nonintegral tank structural model.

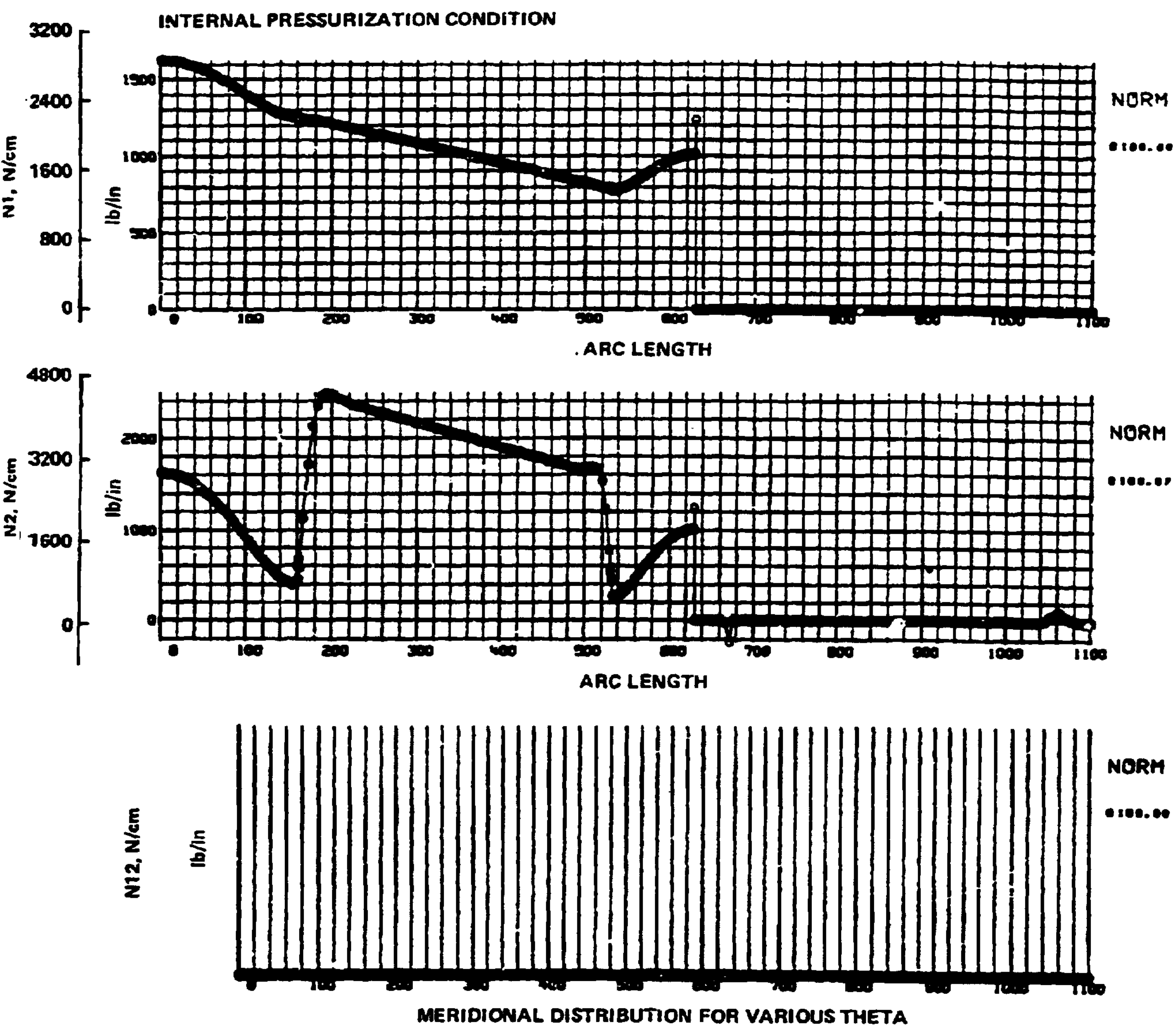

Figure 126. - Inplane stress resultants for the internal pressurization condition, nonintegral tank design.

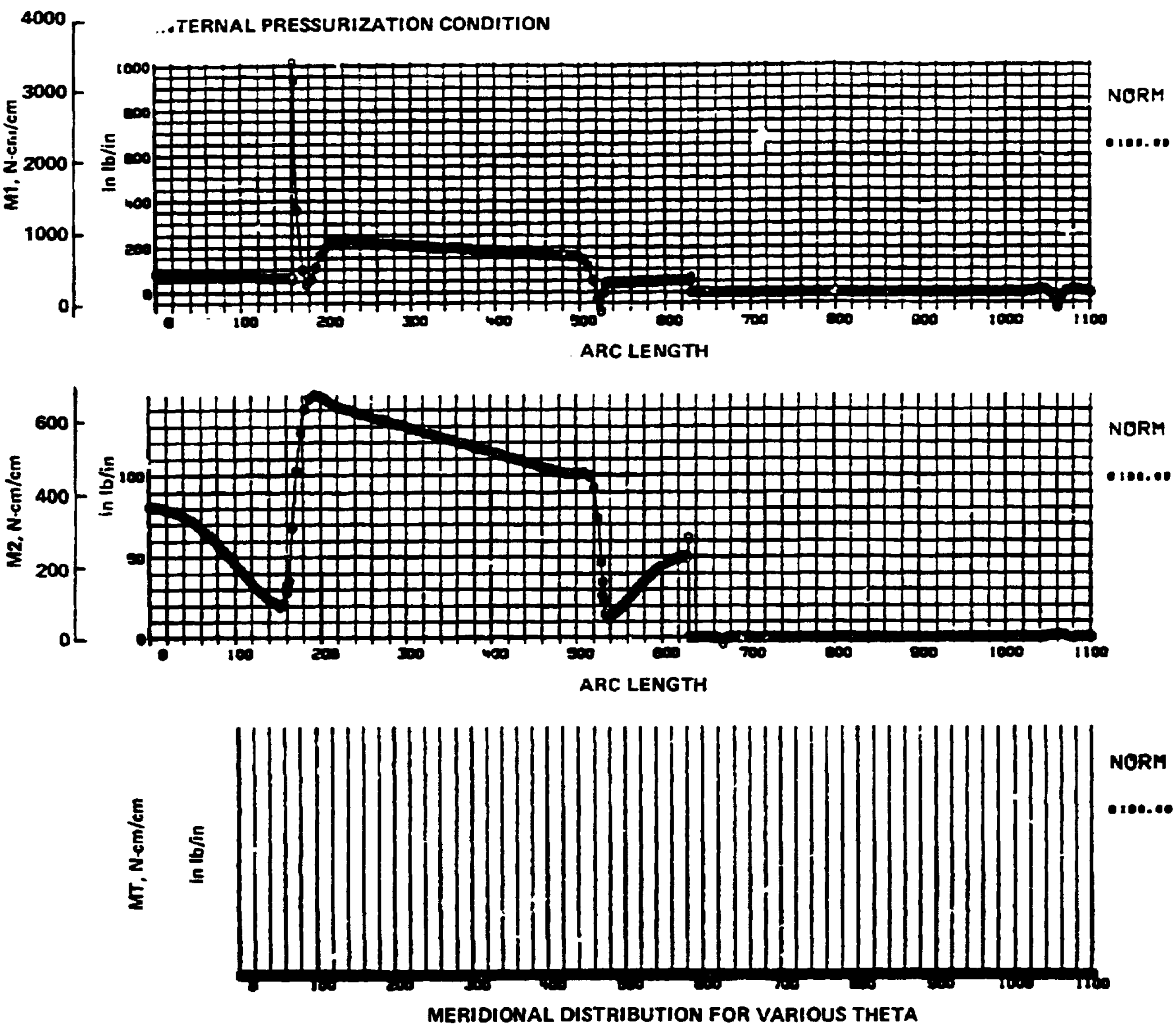

Figure 127. - Bending moments for the internal pressurization condition, nonintegral tank design.

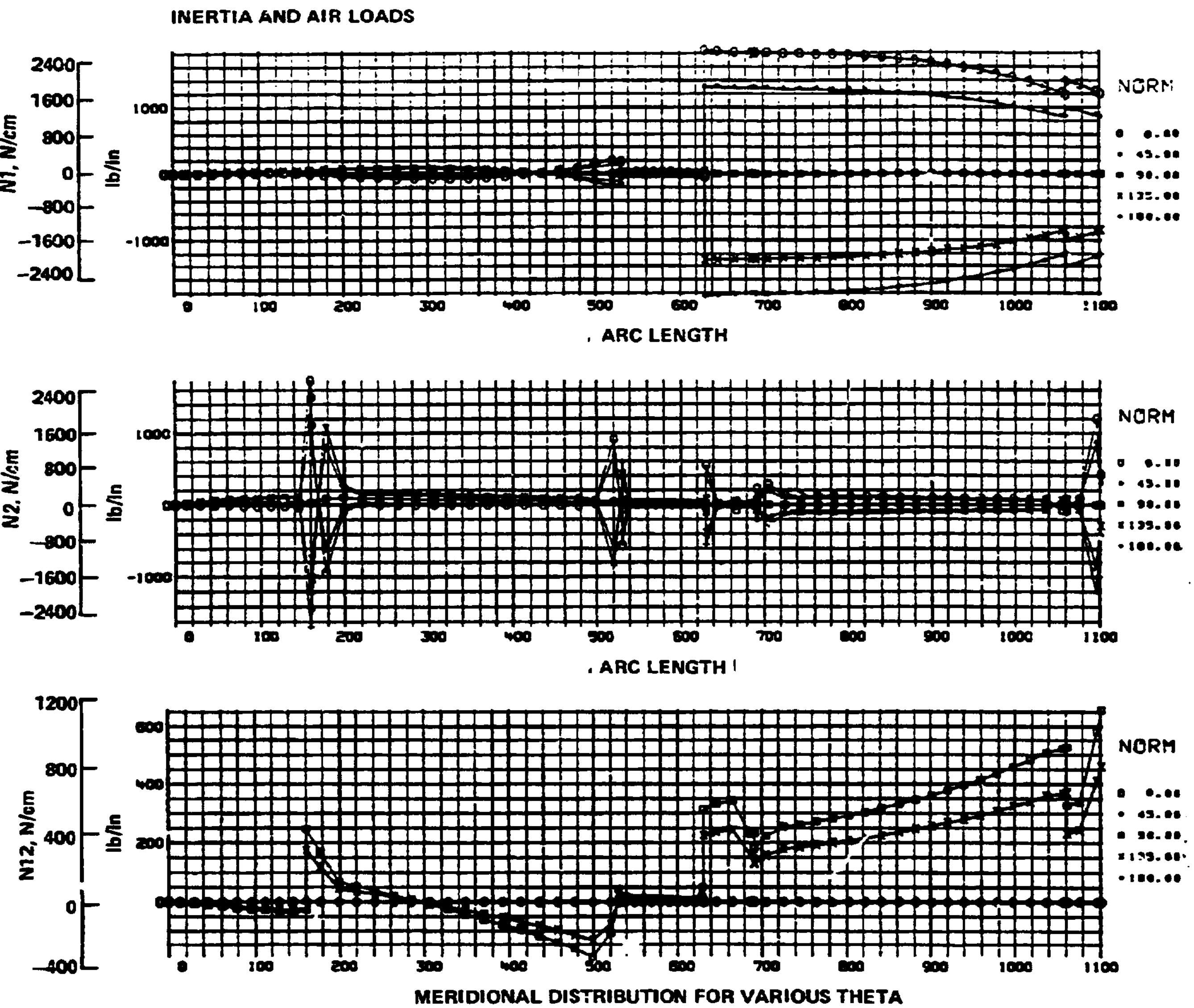

Figure 128. - Inplane stress resultants for the inertia and air load condition, nonintegral tank design.

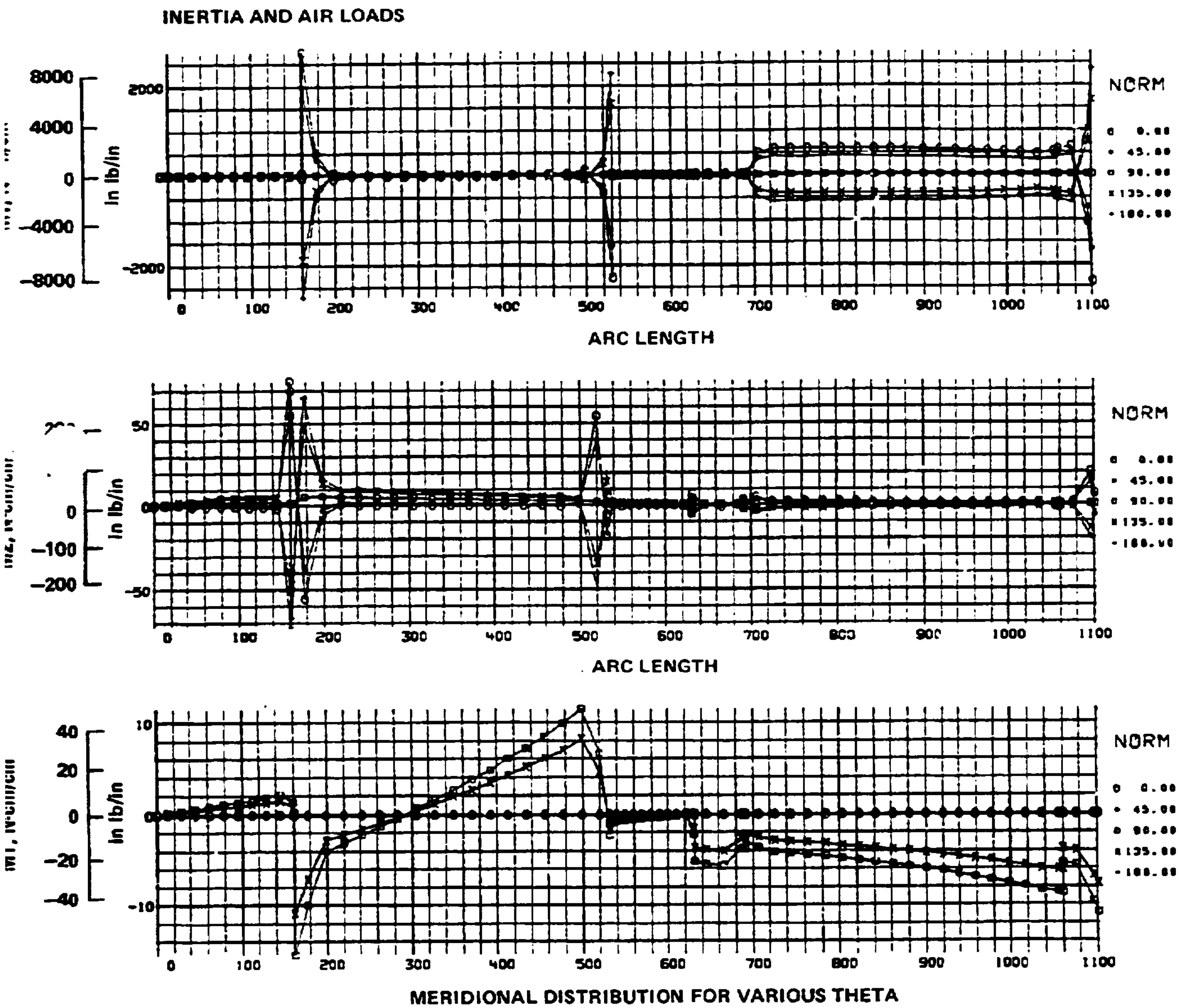

Figure 129. - Bending moments for the inertia and air load condition, nonintegral tank design.

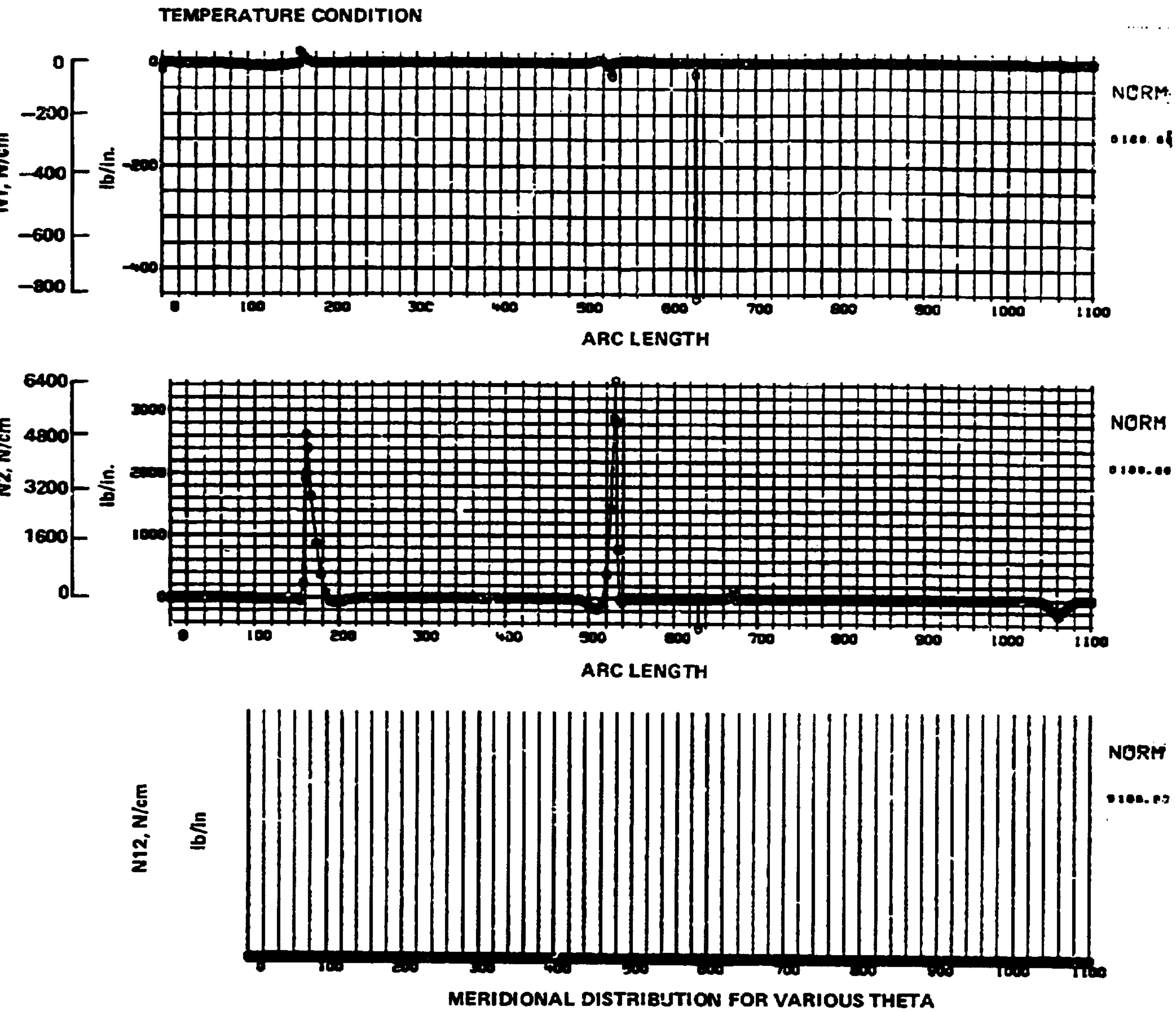

Figure 130. - Inplane stress resultants for the temperature condition, nonintegral tank design.

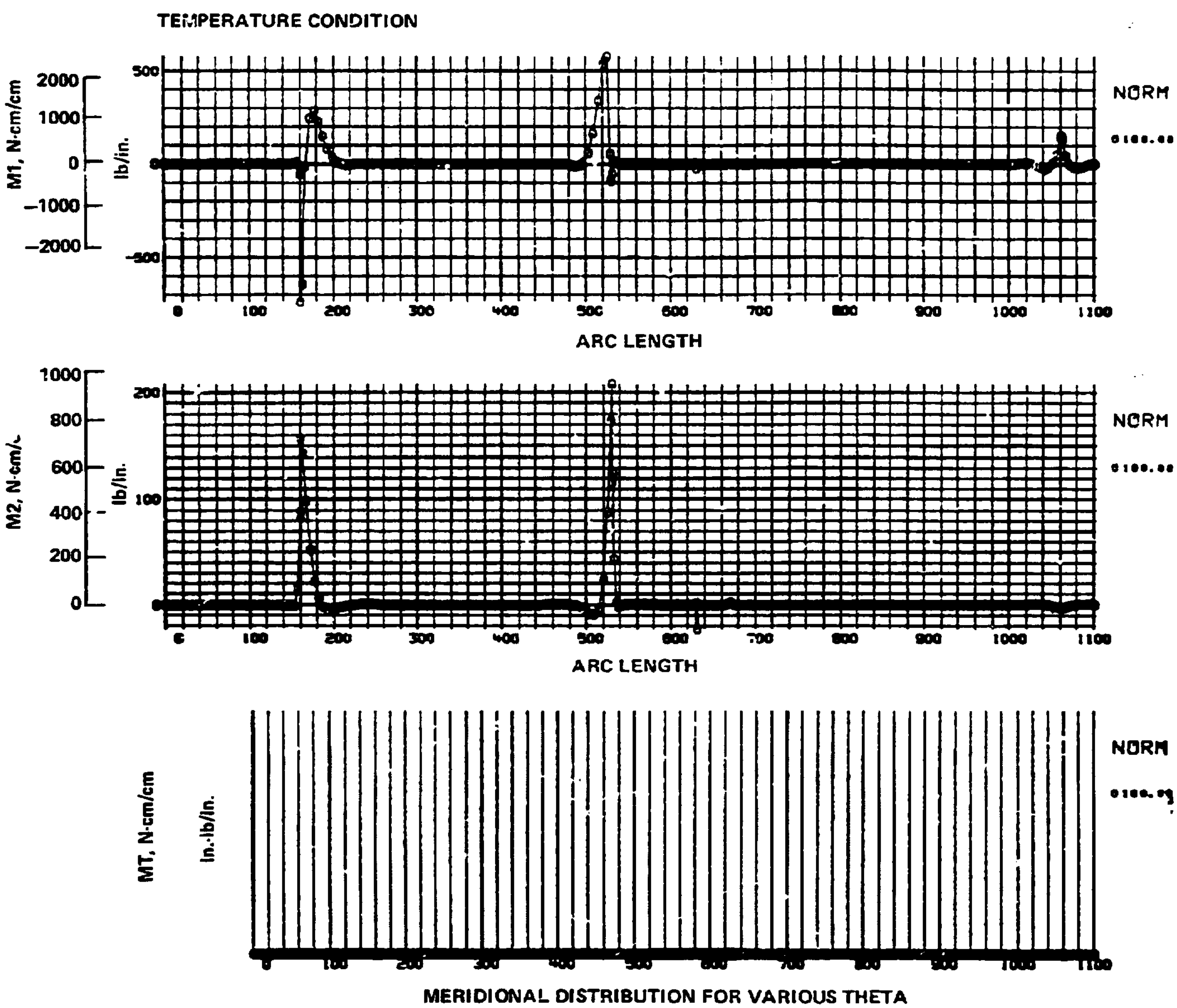

Figure 131. - Bending moments for the temperature condition, nonintegral tank design.

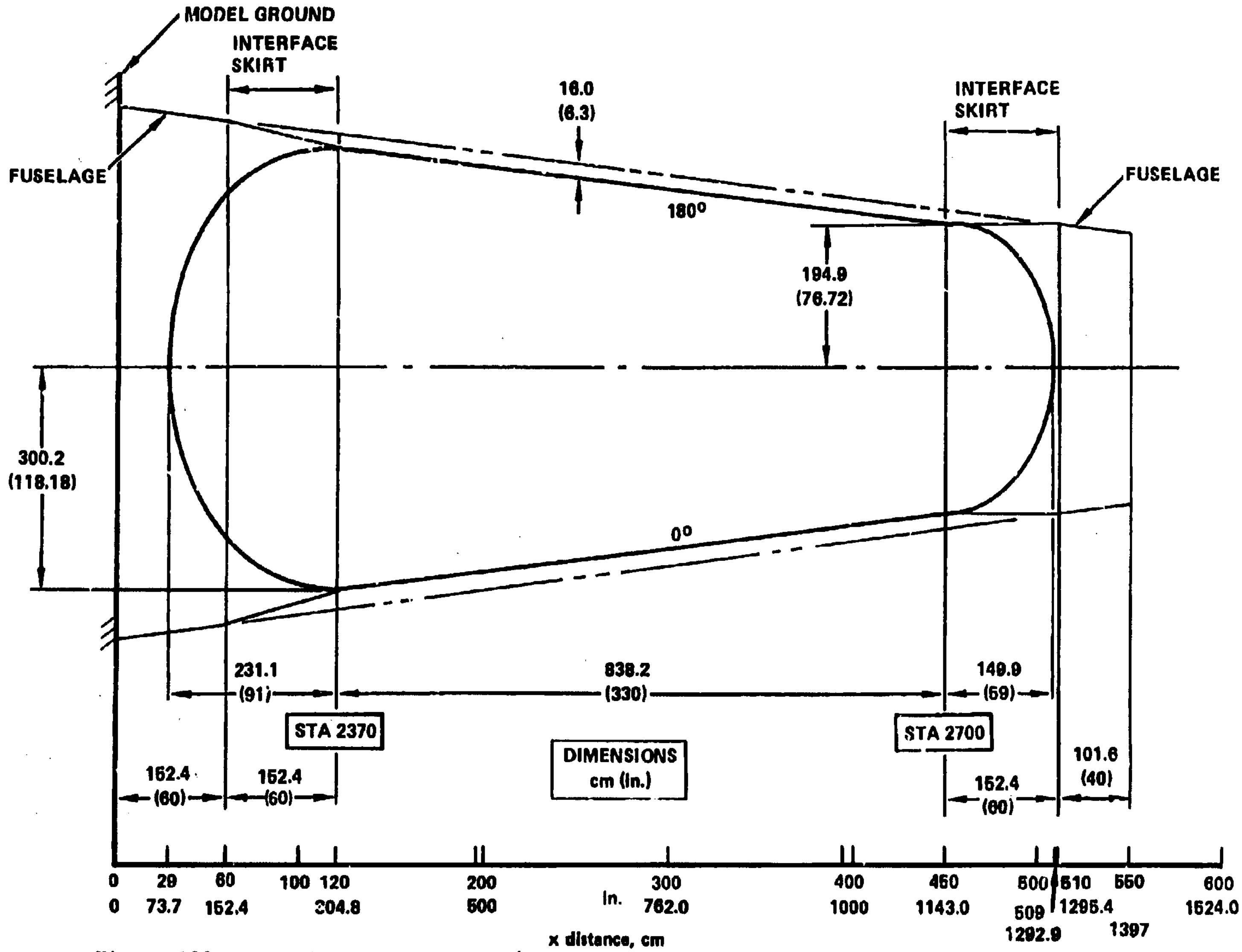

Figure 132. - Fuselage and tank dimensions used for the integral tank structural model.

Figure 133 presents a plot of the structural model with the applied loads simulating the PLA flight condition shown. Similar to the nonintegral tank design, static solutions were conducted on the integral tank model and displacements and stress resultants were obtained.

The normal displacements (W) for each component of the PLA flight condition are shown in Figure 134. The plots on this figure present the displacements due to the temperature condition, the airloads, and pressurization conditions, respectively, starting from the bottom. This figure presents the displacements as a function of arc length measured along the shell meridian. This measurement initiates at the forward end of the fuselage shell (fixed boundary) and proceeds aft along the meridian to the equator of the forward tank closure. The arc length is then measured from the apex of the forward tank closure to the equator, and then proceeds along the tank cylinder to the equator of the aft tank closure and continues to the apex of the aft closures. The arc length then proceeds from the forward end of the aft interface skirt through the skirt and aft fuselage shell. The arc length in Figure 134 is segmented and titled to indicate the various structural components.

The inplane stress and bending moment resultants for each of the applied load components are displayed in Figures 135 through 140. The first two figures present the stress and bending moment resultants for the internal pressurization condition, and the remaining figures present the resultants in the same order for the airload and temperature conditions, respectively. All stress resultants and moments are referenced to the outer skin surface, not the neutral axis of the shell.

7.2.3.5 Point design environment: The internal load environment imposed on the aft tankage of the liquid hydrogen-fueled subsonic transport was defined at selected locations, hereafter known as point design regions, and used as the basis for the evaluation of the candidate concepts.

The design conditions and their associated flight parameters were presented in 7.2.1.4. Also included were the resulting external loads (vertical shear and bending moment) imposed on the fuselage afterbody by these flight conditions. The load components for these conditions include the airloads (tail and inertial loads), the internal pressurization of the

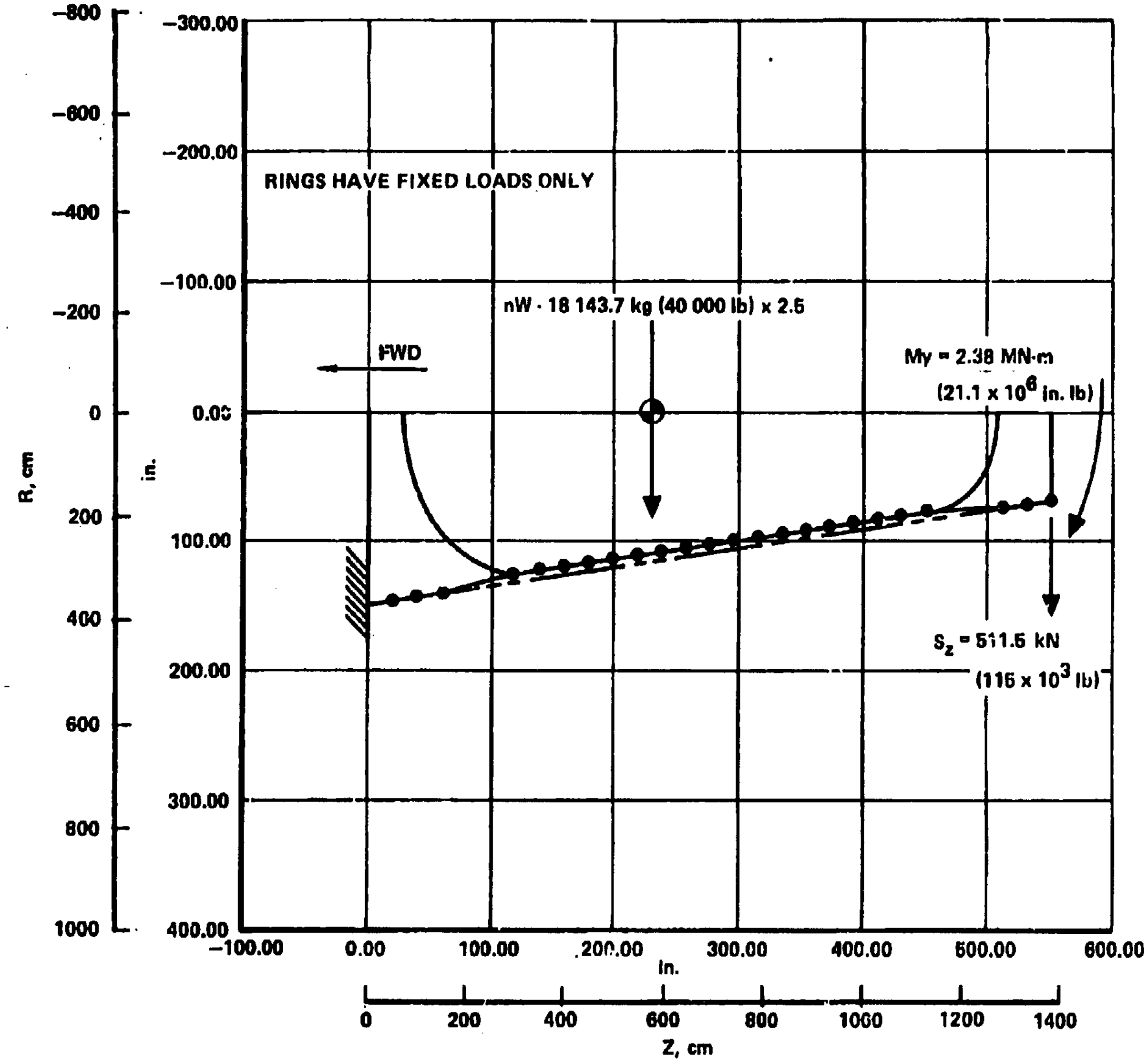

Figure 133. - Applied loads and structural model for the integral tank design.

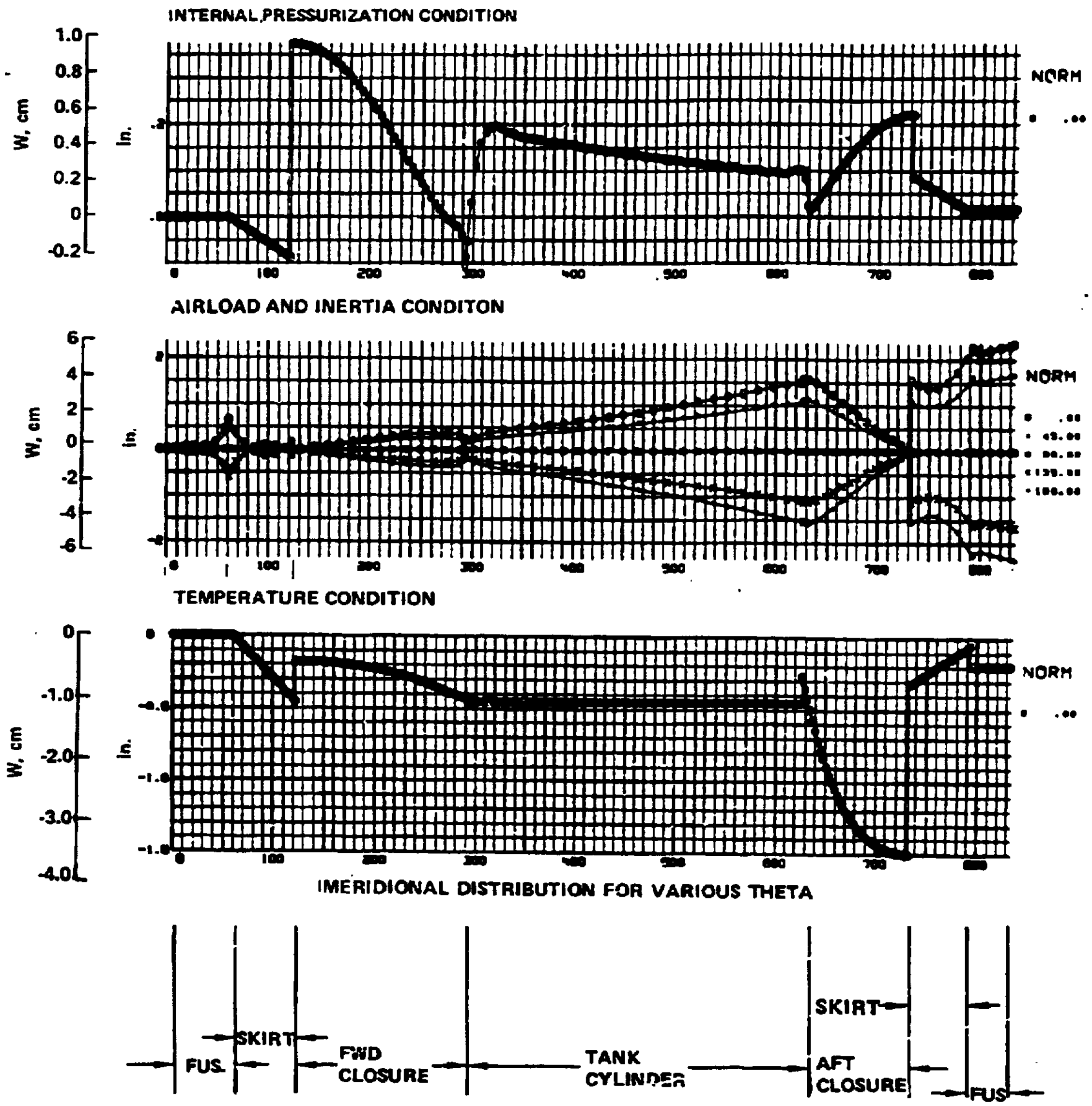

Figure 134. - Normal displacements of the integral tank structural model.

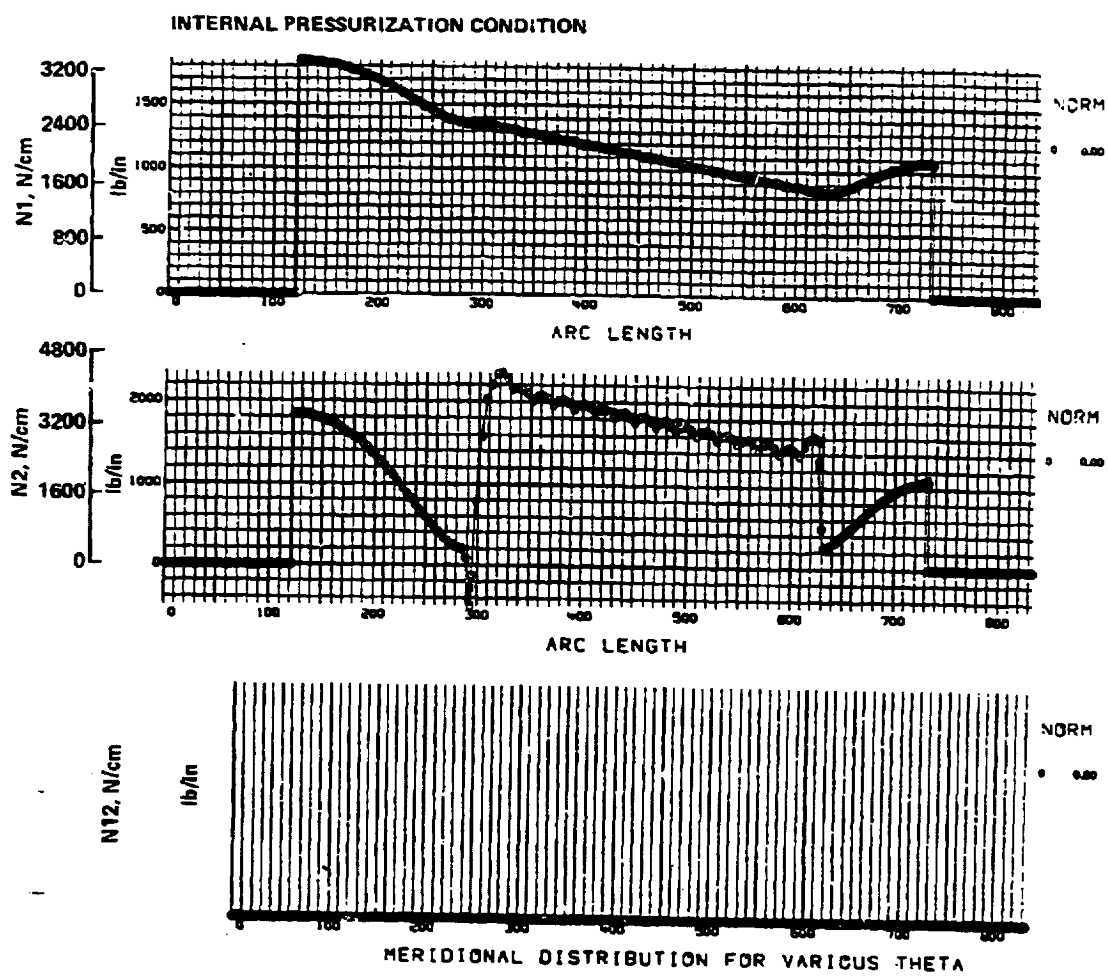

Figure 135. - Inplane stress resultants for the internal pressurization condition, integral tank design.

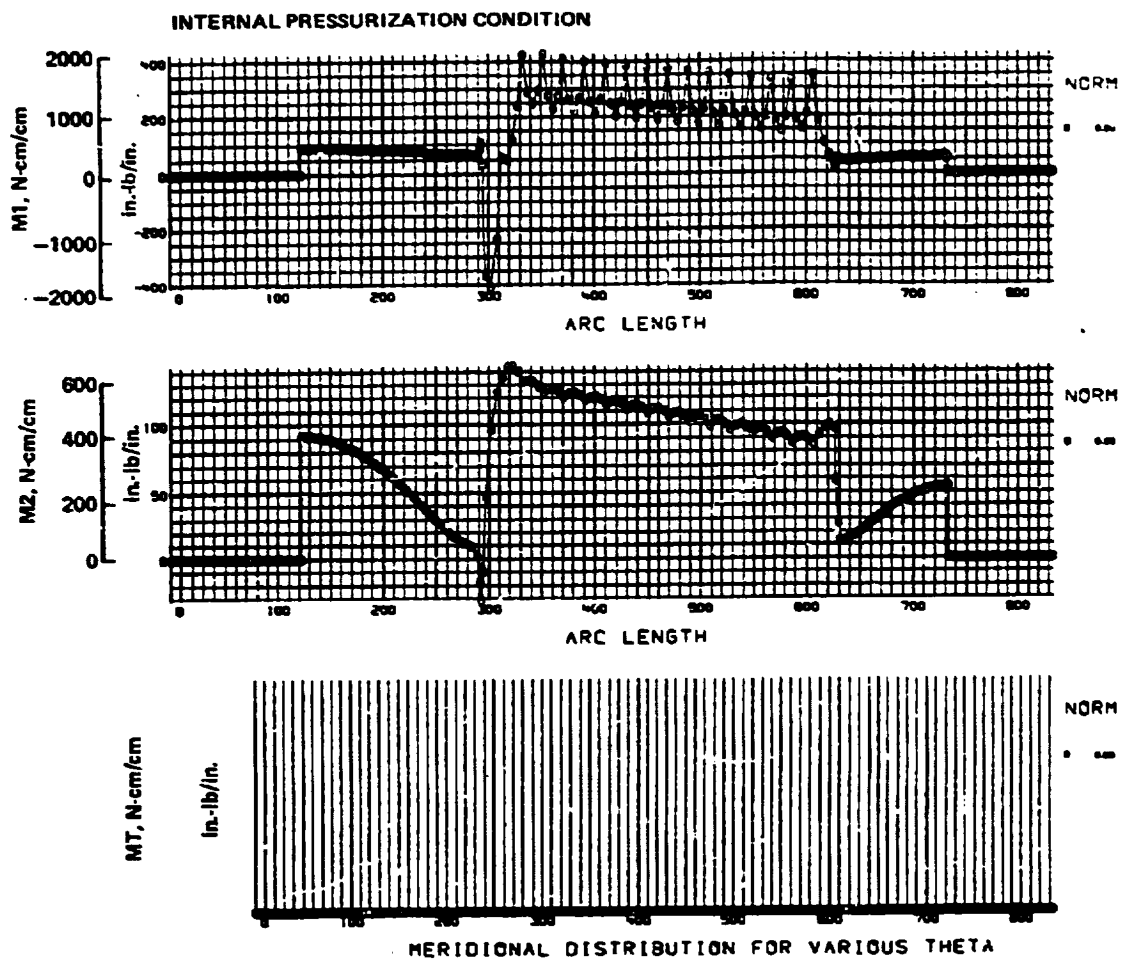

Figure 136. - Bending moments for the internal pressurization condition, integral tank design.

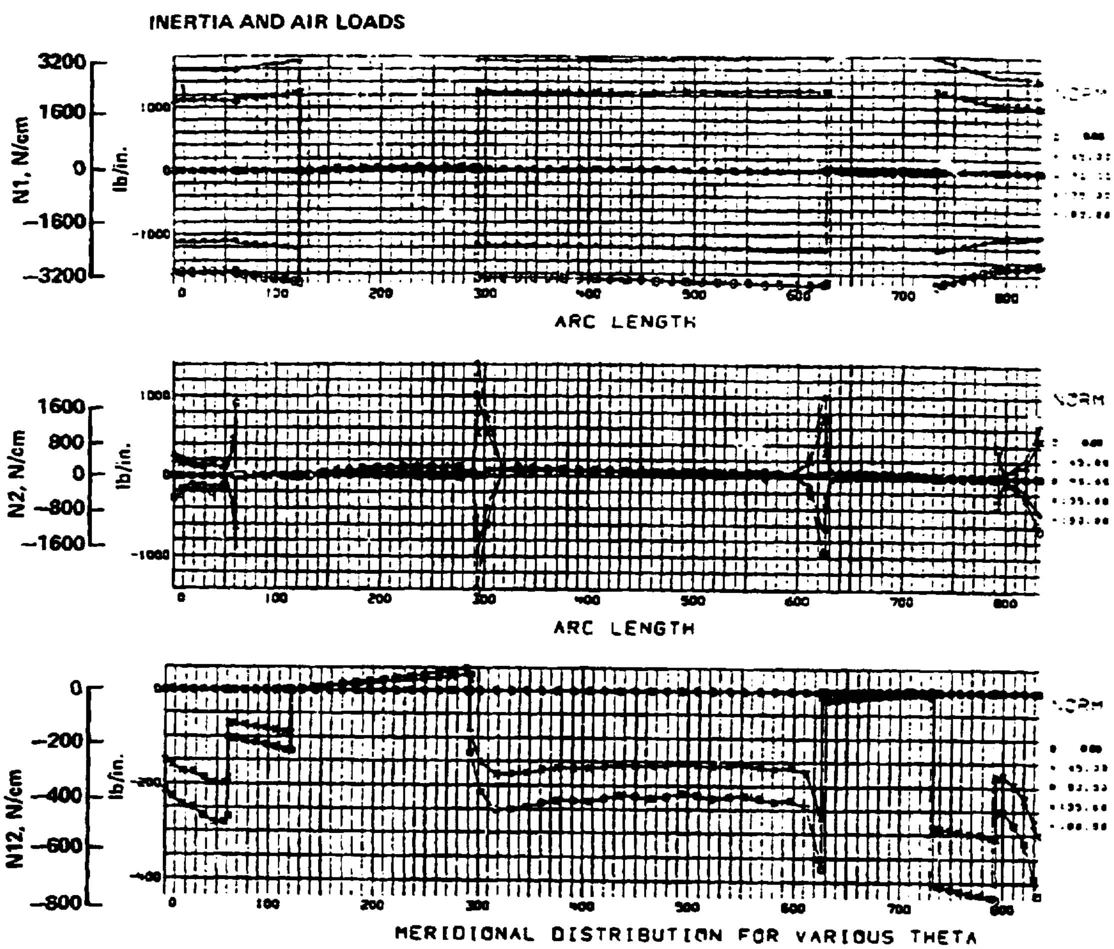

Figure 137. - Inplane stress resultants for the inertia and air load condition, integral tank design.

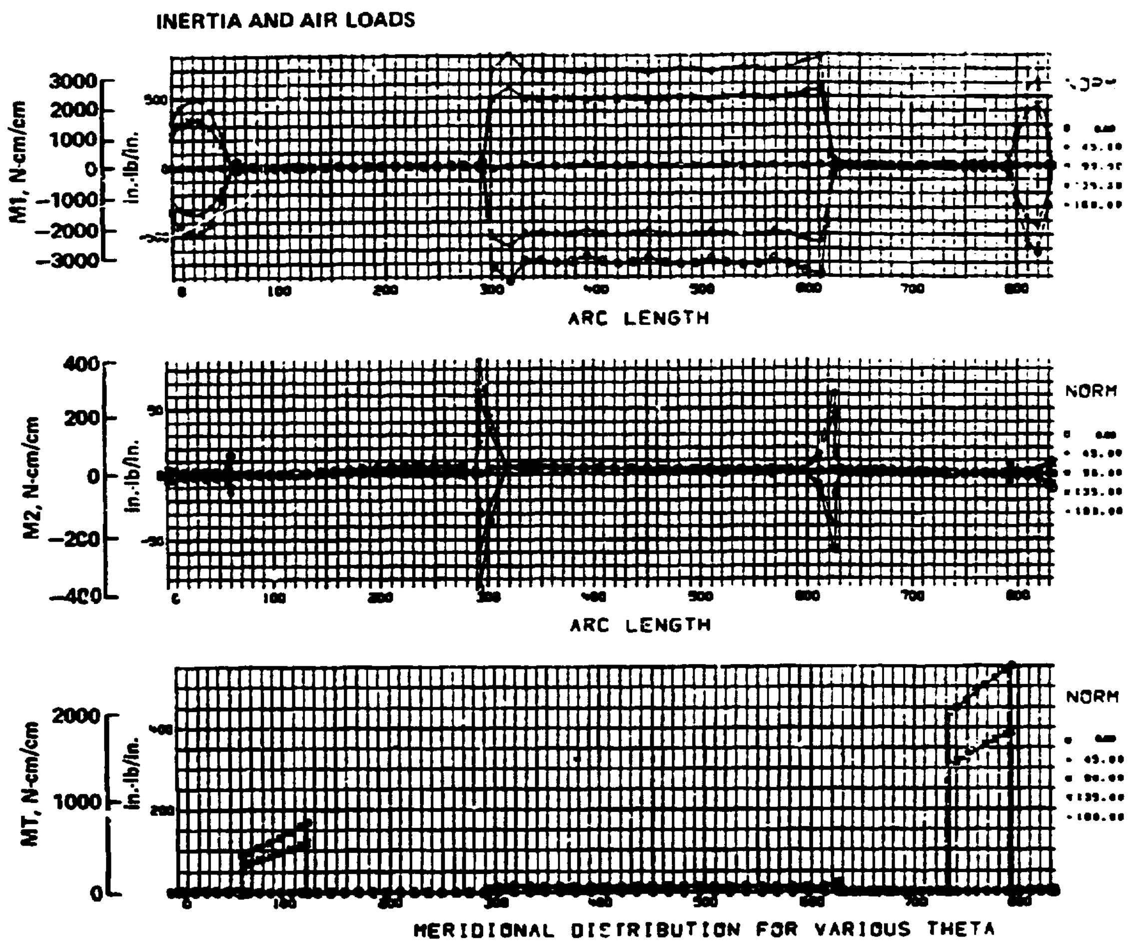

Figure 138. - Bending moments for the inertia and air load condition, integral tank design.

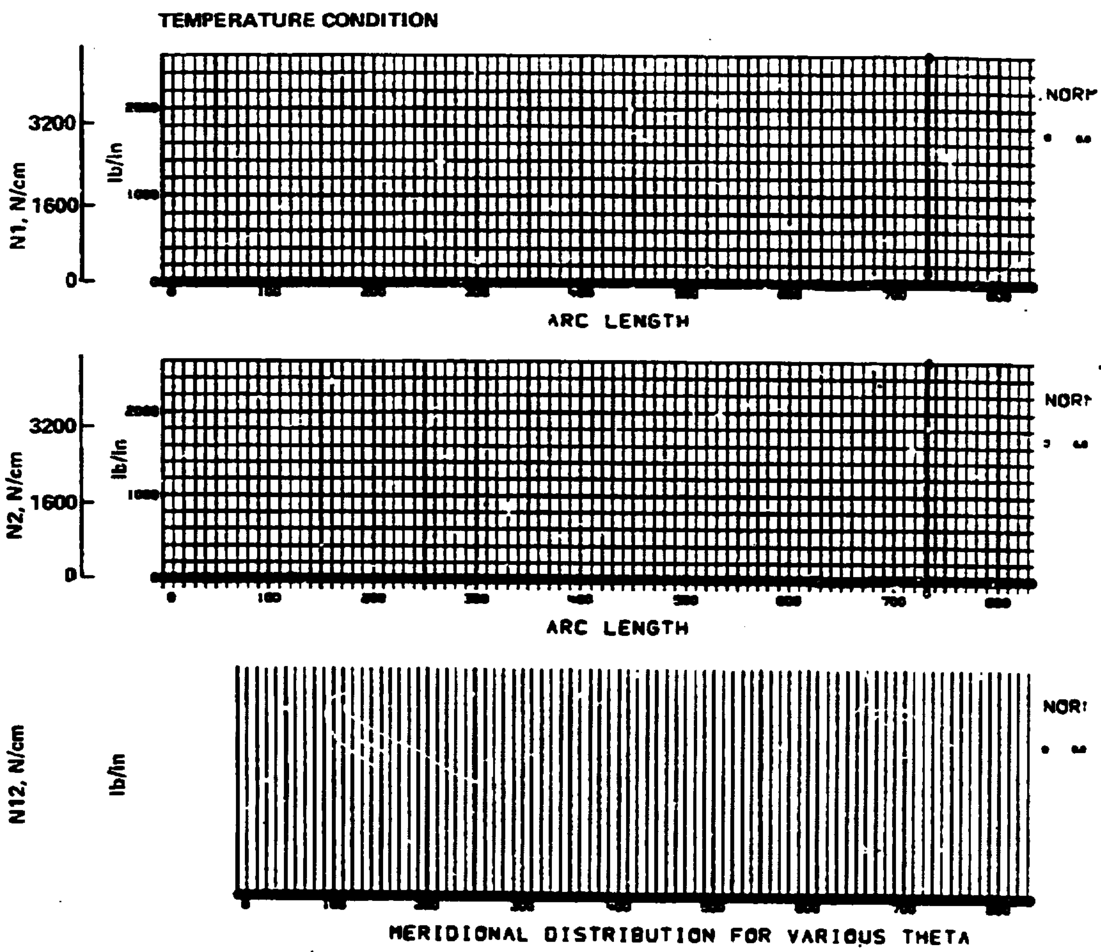

Figure 139. - Inplane stress resultants for the temperature condition, integral tank design.

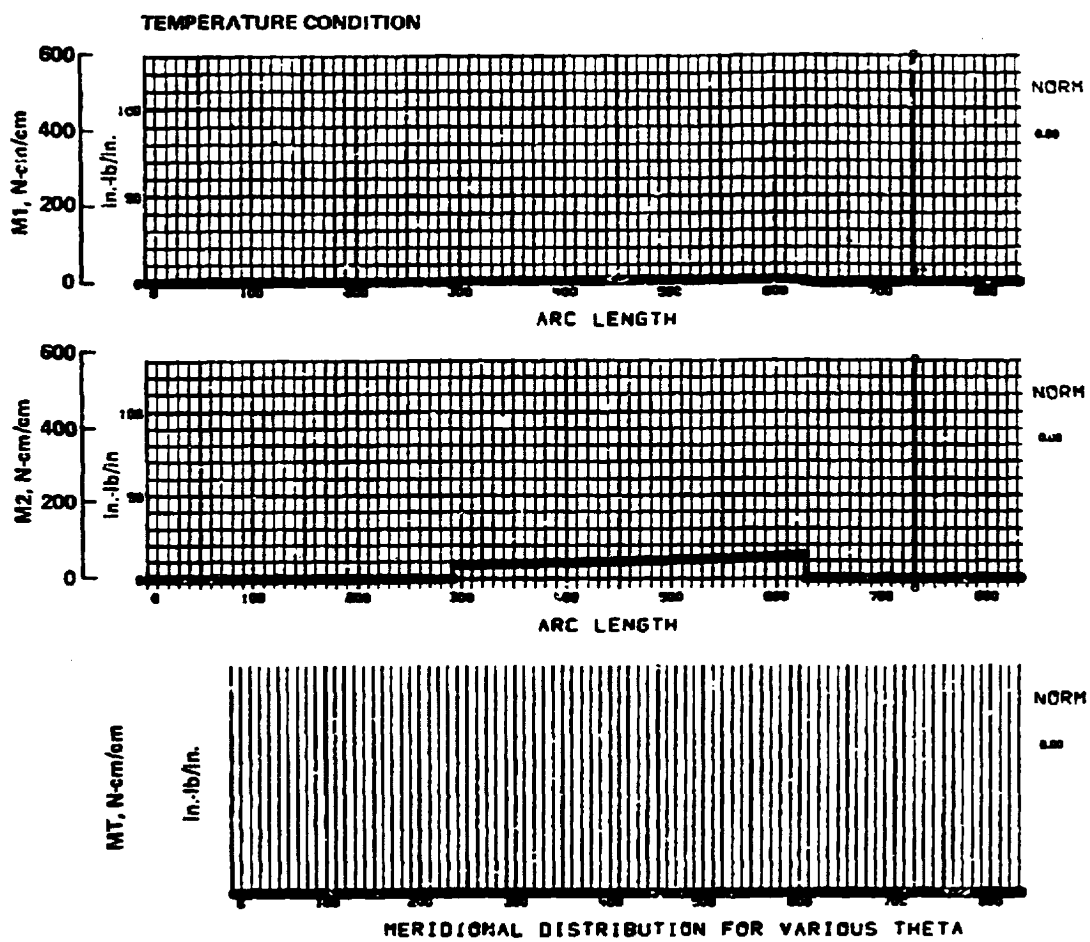

Figure 140. - Bending moments for the temperature condition, integral tank design.

tank, and the temperature environment. BOSOR4 static solutions were conducted for each of these load components to define the overall internal load distribution for each basic tank design, i.e., integral and nonintegral. These results are presented in (7.2.3.4), Structural Models. These internal loads were then used to define the point design environment for each flight condition. For example, the inplane and bending stress resultants due to the internal pressure condition from the structural model were multiplied by the pressure ratio to form the corresponding stress resultants for each flight condition.

The tank pressure schedule for each of the design flight conditions is presented in Table 50. The nomenclature and safety factors used in developing this schedule are described in 7.2.1.

The point design regions selected for the structural analysis of the nonintegral and integral tank designs are presented in Figure 141. These regions, which are shaded on this figure, correspond to the one-quarter and three-quarter lengths between the equators of the forward and aft tank closures.

The load/temperature environments were defined at three circumferential locations at each of the above design regions. Examples of these results are presented in Tables 51 through 53. These tables show the inplane stress resultants for the PLA, Negative Maneuver and Cruise conditions at the tank quarter-length point design region.

TABLE 50. - TANK PRESSURE SCHEDULE

Flight Cond.	Alt m (ft)	$P_{nom.}$ kPa (psia)	$P_{atm.}$ kPa (psi)	ΔP kPa (psi)	P_{op} kPa (psi)	P_{Limit} kPa (psi)	P_{ult} kPa (psi)
Positive Low Angle	6706 (22 000)	145 (21.0)	43 (6.2)	102 (14.8)	112 (16.3)	112 (16.3)	168 (24.4)
Pitching Maneuver	S.L.	145 (21.0)	101 (14.7)	43 (6.3)	48 (6.9)	48 (6.9)	72 (10.4)
Negative Maneuver	6706 (22 000)	145 (21.0)	43 (6.2)	102 (14.8)	112 (16.3)	112 (16.3)	168 (24.4)
Cruise	10 668 (35 000)	145 (21.0)	23 (3.4)	121 (17.6)	134 (19.4)	134 (19.4)	201 (29.1)

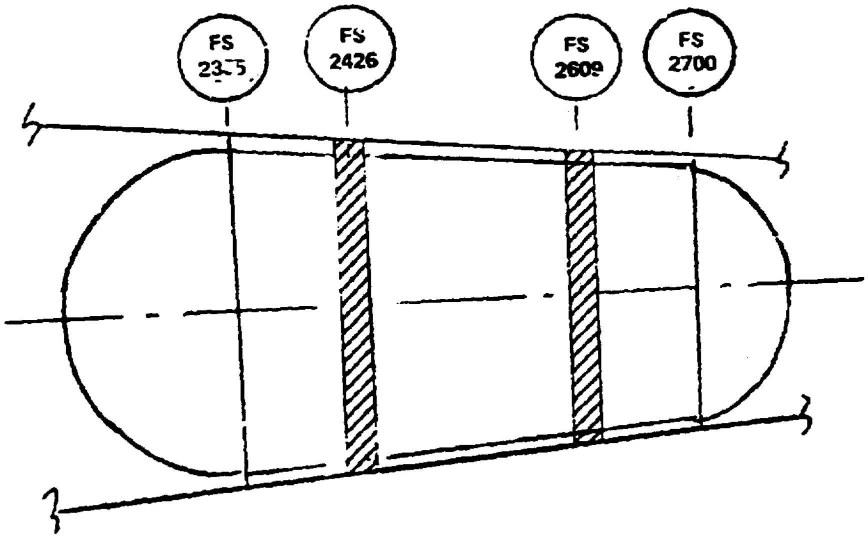

NONINTEGRAL TANK

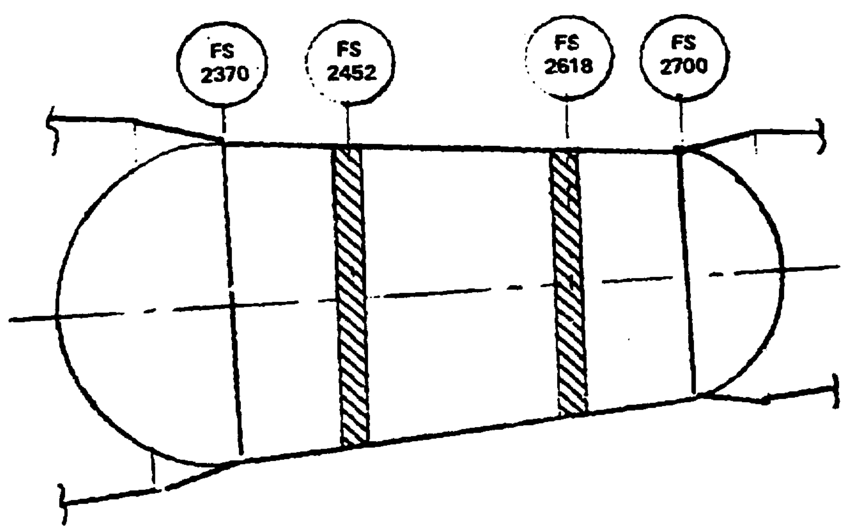

INTEGRAL TANK

Figure 141. - Point design regions

TABLE 51. - POINT DESIGN LOAD ENVIRONMENT, PLA FLIGHT CONDITION (1)(2)

Structural Component	Circumf. Location rad (deg)	Nonintegral Tank Design Membrane Forces (3) kN/m (lb/in)			Integral Tank Design Membrane Forces (3) kN/m (lb/in)		
		N_1	N_2	N_{12}	N_1	N_2	N_{12}
Fuselage	0 (0)	467 (2669)	30 (173)	0 (0)			
	1.57 (90)	0 (0)	0 (0)	74 (423)			
	3.14 (180)	-468 (-2670)	-30 (-174)	0 (0)			
Tank	0 (0)	207 (1184)	446 (2545)	0 (0)	698 (3983)	415 (2370)	0 (0)
	1.57 (90)	230 (1313)	467 (2667)	6 (33)	250 (1429)	416 (2378)	61 (347)
	3.14 (180)	252 (1442)	488 (2769)	0 (0)	-198 (-1129)	418 (2386)	0 (0)

1. Ultimate loads.
2. Tank quarter-length location from the forward head equator.
3. Meridional (N_1), hoop (N_2), and shear (N_{12}) forces.

TABLE 52. - POINT DESIGN LOAD ENVIRONMENT, NEGATIVE MANEUVER CONDITION (1)(2)

Structural Component	Circumf. Location rad (deg)	Nonintegral Tank Design Membrane Forces (3) kN/m (lb/in)			Integral Tank Design Membrane Forces (3) kN/m (lb/in)		
		N_1	N_2	N_{12}	N_1	N_2	N_{12}
Fuselage	0 (0)	-94 (-534)	-6 (-35)	0 (0)			
	1.57 (90)	0 (0)	0 (0)	15 (85)			
	3.14 (180)	94 (534)	6 (35)	0 (0)			
Tank	0 (0)	229 (1307)	446 (2545)	0 (0)	90 (514)	400 (2285)	0 (0)
	1.57 (90)	220 (1256)	437 (2497)	2 (13)	244 (1394)	401 (2287)	12 (69)
	3.14 (180)	211 (1204)	429 (2448)	0 (0)	395 (2256)	401 (2288)	0 (0)

1. Ultimate loads.
2. Tank quarter-length location from the forward head equator.
3. Meridional (N_1), hoop (N_2), and shear (N_{12}) forces.

TABLE 53. - POINT DESIGN LOAD ENVIRONMENT, CRUISE CONDITION (1)(2)

Structural Component	Circumf. Location rad (deg)	Nonintegral Tank Design Membrane Forces (3) kN/m (lb/in)			Integral Tank Design Membrane Forces (3) kN/m (lb/in)		
		N_1	N_2	N_{12}	N_1	N_2	N_{12}
Fuselage	0 (0)	187 (1067)	12 (70)	0 (0)			
	1.57 (90)	0 (0)	0 (0)	30 (169)			
	3.14 (180	-187 (-1067)	-12 (-70)	0 (0)			
Tank	0 (0)	277 (1582)	542 (3097)	--	471 (2692)	480 (2740)	0 (0)
	1.57 (90)	274 (1563)	551 (3145)	2 (13)	297 (1698)	480 (2743)	24 (139)
	3.14 (180)	283 (1615)	559 (3194)	--	113 (648)	481 (2746)	0 (0)

1. Ultimate loads.
2. Tank quarter-Length location from the forward head equator.
3. Meridional (N_1), hoop (N_2), and shear (N_{12}) forces.

7.2.3.6 Point design analysis results: The candidate structural concepts were subjected to point design analysis to define the most promising structural concept for each of the basic types of tanks, i.e., integral and nonintegral. The candidate concepts were presented in 7.2.2, with the analytical methods and point design environments described in 7.2.3.2 and 7.2.3.5, respectively. The structural components included in the point design analysis are represented in Figure 142. A typical insulation system is shown for reference purposes only.

7.2.3.6.1 Nonintegral design: The candidate wall concepts identified for the tank and fuselage were subjected to point design analyses to define the minimum-weight proportions. For the fuselage, zee-stiffened and hat-stiffened concepts fabricated from conventional aluminum material were investigated; whereas, for the tank, an unstiffened design (monocoque shell) was considered along with several stiffened designs (blade, zee, and tee), all based on the use of 2219 aluminum alloy

Two candidate shell configurations for the fuselage were sized for a range of frame spacings using the previously described analytical methods and point design environment.

The resultant panel cross-sectional data for the upper, mid, and lower fibers at the quarter-length location are shown in Figure 143. As can be

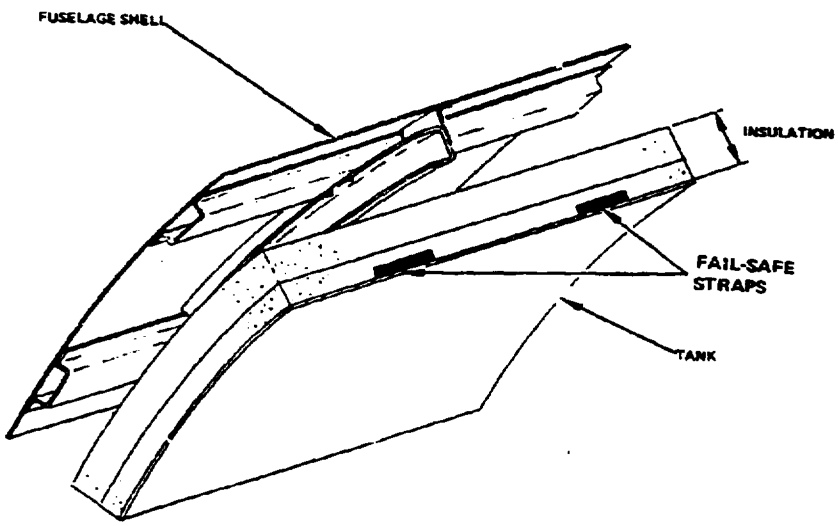

a) NONINTEGRAL TANK

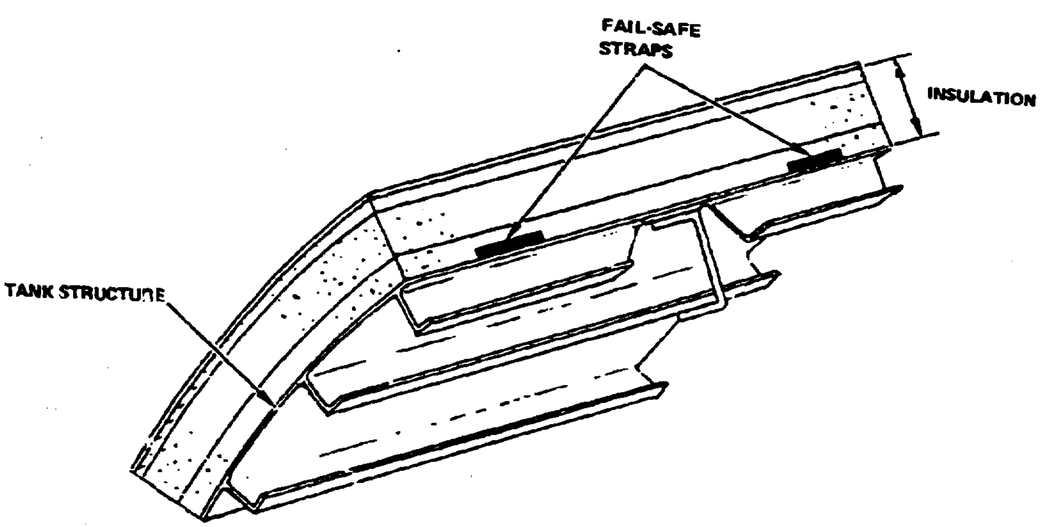

b) INTEGRAL TANK

Figure 142. - Point design structure.

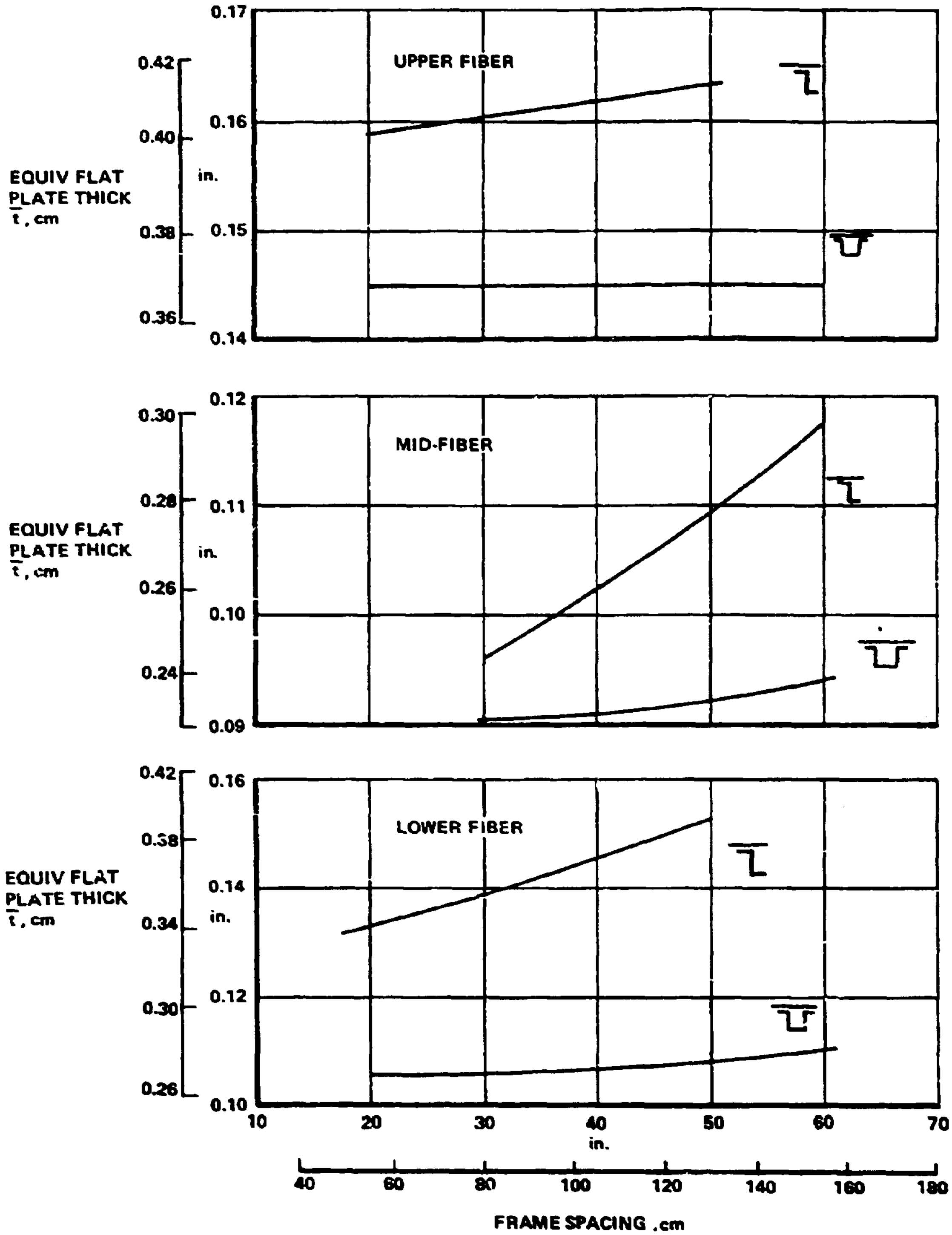

Figure 143. - Fuselage shell equivalent thickness, nonintegral design.

seen from this figure, the hat-stiffened design has smaller thicknesses than the zee-stiffened design at all of the circumferential locations investigated. The equivalent thickness curves for the hat-stiffened concept are relatively insensitive to frame spacing with approximate values of 3.683 mm (0.145 in.), 2.286 mm (0.090 in.), and 2.667 mm (0.105 in.) indicated for a frame spacing of 1016 mm (40.0 in.) for the upper, mid and lower fibers, respectively.

The minimum weight designs for the zee-stiffened concept occur at the minimum frame spacings studies and in general are very sensitive to changes in frame spacing. For comparison purposes, the corresponding thicknesses of the zee-stiffened design at 1016 mm (40.0 in.) spacing are 4.089 mm (0.161 in.), 2.616 mm (0.103 in.), and 3.708 mm (0.146 in.) for the upper, mid and lower fibers, respectively.

Representative sheet metal frames were sized for application to both fuselage shell concepts. The frame designs were evaluated for both strength and stiffness at the two point design regions on the fuselage.

The frame stiffness requirements were predicated using the criteria developed by Shanley in Reference 32, which ensures failure of the sheet-stringer panel between frames, i.e., prevents general instability. The frame bending stiffness (EI), and the corresponding area and equivalent panel thickness for various frame spacings at the two point design regions are shown in Table 54. The maximum bending moments and shell diameters are also indicated on this table.

The basic strength of the frames were assessed using the loads obtained from the BOSOR4 static analysis. Figure 144 displays the internal hoop forces acting in the frame as a function of the circumferential angle. The internal forces for both the maximum upbending (PLA condition) and downbending (negative maneuver) conditions are presented. At the fuselage quarter-length location, a maximum hoop force of ±10 676N (±2400 lb) (limit) is indicated; whereas, only ±7784N (±1750 lb) (limit) is shown at the three-quarter length location.

Table 55 presents the frame analysis conducted using the internal frame loads from the model. The frame hoop forces were adjusted for frame spacings greater than that used in the model. Representative tension and compression allowables and a minimum frame area were defined and are noted on the table.

A summary of the area requirements defined by the stiffness and strength analyses are presented in Table 56. The required design areas, i.e., the maximum value between stiffness and strength requirements, and their equivalent panel thicknesses are specified.

The combined results of the fuselage shell and frame analysis are presented in Tables 57 and 58 for the hat- and zee-stiffened fuselage concepts, respectively. These tables reflect the component and total equivalent thicknesses for the shell and frame as a function of frame spacing. The equivalent unit weights for these designs are also displayed graphically in Figure 145.

TABLE 54. - FUSELAGE FRAME STABILITY REQUIREMENTS, NONINTEGRAL TANK DESIGN

Point Design Region	Fuselage Bending Moment M, MN-cm (in-lb)	Shell Dia D, cm (in.)	Frame Spacing L, cm (in.)	(EI) MN-cm^2 (lb-in^2)	Frame Area A_f cm^2 (in^2)
Quarter Length (FS 2426)	1101.6 (97.5 X 10^6)	588 (231.6)	51 (20)	467.8 (16.3 X 10^6)	6.65 (1.03)
			76 (30)	312.8 (10.9)	4.45 (0.69)
			102 (40)	234.5 (8.17)	3.35 (0.52)
			127 (50)	187.7 (6.54)	2.71 (0.42)
			152 (60)	156.4 (5.45)	2.19 (0.34)
Three-Quarter Length (FS 2609)	677.9 (60 X 10^6)	477 (187.86)	51 (20)	189.9 (6.62 X 10^6)	2.71 (0.42)
			76 (30)	126.5 (4.41)	1.81 (0.28)
			102 (40)	94.9 (3.31)	1.35 (0.21)
			127 (50)	76.1 (2.65)	1.10 (0.17)
			152 (60)	63.4 (2.21)	0.90 (0.14)

$$(EI)_f = C_f \frac{MD^2}{L}$$

where: $C_f = 1/16\,000 = 6.25 \times 10^{-5}$

$E_f = 10.5 \times 10^6$

$A = 6.0t$

$I \approx 9t$

$I \approx 1.5A$

$$I_f = \frac{(EI)_f}{E}$$

or

$$A_f = \frac{(EI)_f}{1.5E}$$

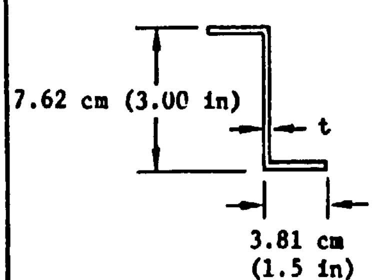

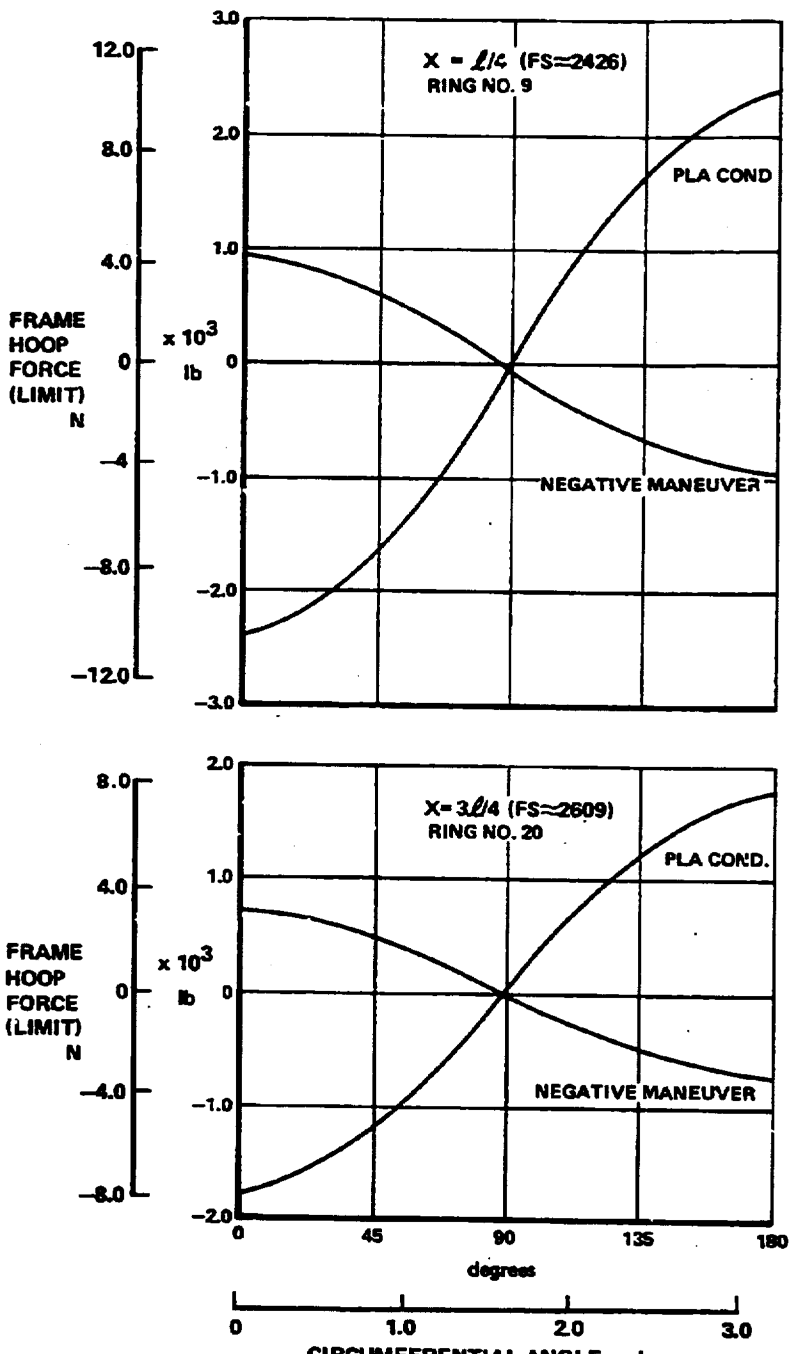

Figure 144. - Fuselage frame loads, nonintegral design.

TABLE 55. - FUSELAGE FRAME STRENGTH REQUIREMENTS, NONINTEGRAL DESIGN

Circum. Location		L = 50.8 cm (20 in.)[1]		L = 76.2 cm (30 in.)		L = 101.6 cm (40 in.)		L = 127.0 cm (50 in.)		L = 152.4 cm (60 in.)	
	rad (deg)	P N (lb)	A cm^2 (in^2)	P N (lb)	A cm^2 (in^2)	P N (lb)	A cm^2 (in^2)	P N (lb)	A cm^2 (in^2)	P N (lb)	A cm^2 (in^2)
ℓ/4	0 (0)	15 680 (3525)	1.9 (0.30)	23 522 (5288)	1.9 (0.30)	31 360 (7050)	1.9 (0.30	39 198 (8812)	1.9 (0.30)	47 040 (10 575)	1.9 (0.30)
	1.57 (90)	--	1.9 (0.30)	77	1.9 (0.30)	--	1.9 (0.30)	--	1.9 (0.30)	--	1.9 (0.30)
	3.14 (180)	-15 680 (-3525)	1.0 (0.30)	-23 522 (-5288)	2.3 (0.35)	-31 360 (-7050)	3.0 (0.47)	-39 198 (-8812)	3.8 (0.59)	-47 040 (-10 575)	4.6 (0.71)
	A_{AVG}		1.0 (0.30)		2.0 (0.31)		2.2 (0.34)		2.4 (0.37)		2.6 (0.40)
3ℓ/4	0 (0)	11 677 (2625)	1.9 (0.30)	17 517 (3938)	1.9 (0.30)	23 353 (5250)	1.9 (0.30)	29 189 (6562)	1.9 (0.30)	35 030 (7875)	1.9 (0.30)
	1.57 (90)	--	1.9 (0.30)	--	1.9 (0.30)	--	1.9 (0.30)	--	1.9 (0.30)	--	1.9 (0.30)
	3.14 (180)	-11 677 (-2625)	1.9 (0.30)	-17 517 (-3938)	1.9 (0.30)	-23 353 (-5250)	2.3 (0.35)	-29 189 (-6562)	2.8 (0.44)	-35 030 (-7875)	3.4 (0.52)
	A_{AVG}		1.9 (0.30)		1.9 (0.30)		2.0 (0.31)		2.2 (0.34)		2.3 (0.36)

1. Structural Model Data, Frame Spacing = 50.8 cm (20 in.)
2. $P_L = P_{20} \times \left(\frac{L}{20}\right)$
3. Allowables: Tension, F_t = 310 264 kPa (45 000 psi); Compression, F_c = 103 421 kPa (15 000 psi)
4. $A = P/F_{t,c}$ or $A = A_{min}$ = 1.9 cm^2 (0.30 in^2)
5. Average Area (A_{AVG}) = ($A_0/4 + A_{90}/2 + A_{180}/4$)

TABLE 56. - SUMMARY OF FUSELAGE FRAME REQUIREMENTS, NONINTEGRAL DESIGN

Sta.	Frame Spacing cm	(in)	Area cm^2 (in^2) Stiffness Reqmt.		Strength Reqmt.		A_{R_2} cm^2	(in^2)	$\overline{t}$ cm (A/L)	(in.)
$\ell/4$	50.8	(20)	6.65	(1.03)	1.94	(0.30)	6.65	(1.03)	0.132	(0.052)
	76.2	(30)	4.45	(0.69)	2.00	(0.31)	4.45	(0.69)	0.058	(0.023)
	101.6	(40)	3.35	(0.52)	2.19	(0.34)	3.35	(0.52)	0.033	(0.013)
	127.0	(50)	2.71	(0.42)	2.39	(0.37)	2.71	(0.42)	0.020	(0.008)
	152.4	(60)	2.19	(0.34)	2.56	(0.40)	2.58	(0.40)	0.018	(0.007)
$3\ell/4$	50.8	(20)	2.71	(0.42)	1.94	(0.30)	2.71	(0.042)	0.053	(0.021)
	76.2	(30)	1.81	(0.28)	1.94	(0.30)	1.94	(0.30)	0.025	(0.010)
	101.6	(40)	1.35	(0.21)	2.00	(0.31)	2.00	(0.31)	0.020	(0.008)
	127.0	(50)	1.10	(0.17)	2.19	(0.34)	2.19	(0.34)	0.018	(0.007)
	152.4	(60)	0.90	(0.14)	2.32	(0.36)	2.32	(0.36)	0.015	(0.006)

In similar fashion the candidate structural concepts for the tank of the nonintegral design were subjected to point design analysis to assess the relative merit of each concept. General instability analysis of the tank was conducted using BOSOR4 to ascertain if frames were required to prevent this failure mode. The concepts and associated stiffnesses used for this model were described in Section 7.2.3.4. The tank design for this model contained no frames except at the forward and aft suspension points. The results of the BOSOR4 bifurcated stability analysis showed that internal frames were not required to stabilize the tank design; therefore, they were not considered in the evaluation of the candidate concepts.

The tankage of the nonintegral design experiences only minor thermal loadings and flight inertia loads; therefore, the predominate loading was caused by the internal pressurization. Since the tank wall is tension designed, the structural concepts were designed by applying the fatigue and damage tolerance criteria. The basic tank wall cross-sectional data defined using this criteria was in all cases sufficiently strong to meet the basic strength requirements.

In general, the fatigue allowable defined for the operating condition established the minimum skin gage, whereas the fail-safe criteria was used to define the cross-sectional area and strap requirements. Both circumferential

TABLE 57. - SUMMARY OF FUSELAGE WEIGHT DATA FOR THE HAT-STIFFENED DESIGN, NONINTEGRAL TANK

Sta	Location	Frame Spacing cm	(in.)	Equiv. Thk., $\bar{t}$, cm (in.) Shell		Frame		Total		Total[a] Unit Wt. kg/m²	(lbm/ft²)
$\ell/4$	Upper Fiber	50.8	(20)	0.368	(0.145)	0.032	(0.052)	0.500	(0.197)	13.87	(2.84)
		76.2	(30)	0.368	(0.145)	0.058	(0.023)	0.427	(0.168)	11.82	(2.42)
		101.6	(40)	0.368	(0.145)	0.033	(0.013)	0.401	(0.158)	11.13	(2.28)
		127.0	(50)	0.368	(0.145)	0.020	(0.008)	0.389	(0.153)	10.74	(2.20)
		152.4	(60)	0.368	(0.145)	0.018	(0.007)	0.386	(0.152)	10.69	(2.19)
$\ell/4$	Mid Fiber	50.8	(20)			0.132	(0.052)				
		76.2	(30)	0.231	(0.091)	0.058	(0.023)	0.290	(0.114)	8.01	(1.64)
		101.6	(40)	0.231	(0.091)	0.033	(0.013)	0.264	(0.104)	7.32	(1.50)
		127.0	(50)	0.234	(0.092)	0.020	(0.008)	0.254	(0.100)	7.03	(1.44)
		152.4	(60)	0.239	(0.094)	0.018	(0.007)	0.257	(0.101)	7.08	(1.45)
$\ell/4$	Lower Fiber	50.8	(20)	0.269	(0.106)	0.132	(0.052)	0.401	(0.158)	11.13	(2.28)
		76.2	(30)	0.269	(0.106)	0.058	(0.023)	0.328	(0.129)	9.08	(1.86)
		101.6	(40)	0.272	(0.107)	0.033	(0.013)	0.305	(0.120)	8.45	(1.73)
		127.0	(50)	0.274	(0.108)	0.020	(0.008)	0.295	(0.116)	8.15	(1.67)
		152.4	(60)	0.279	(0.110)	0.018	(0.007)	0.297	(0.117)	8.20	(1.68)

(a) $w = 144\ \rho\bar{t} = 14.4\ x\bar{t}$

TABLE 58. - SUMMARY OF FUSELAGE WEIGHT DATA FOR THE ZEE-STIFFENED DESIGN, NONINTEGRAL TANK

Sta	Location	Frame Spacing cm (in.)	Equiv. Thk., $\bar{t}$, cm (in.)			Weight (a) kg/m^2 (lb/ft^2)
			Shell	Frame	Total	
$\ell/4$	Upper Fiber	50.8 (20)	0.404 (0.159)	0.132 (0.052)	0.536 (0.211)	14.84 (3.04)
		76.2 (30)	0.409 (0.161)	0.058 (0.023)	0.467 (0.184)	12.94 (2.65)
		101.6 (40)	0.409 (0.161)	0.033 (0.013)	0.442 (0.174)	12.25 (2.51)
$\ell/4$	Mid Fiber	76.2 (30)	0.244 (0.096)	0.058 (0.023)	0.302 (0.119)	8.35 (1.71)
		101.6 (40)	0.262 (0.103)	0.033 (0.013)	0.295 (0.116)	8.15 (1.67)
		127.0 (50)	0.282 (0.111)	0.020 (0.008)	0.302 (0.119)	8.35 (1.71)
		152.4 (60)	0.297 (0.117)	0.018 (0.007)	0.315 (0.124)	8.69 (1.78)
$\ell/4$	Lower Fiber	50.8 (20)	0.340 (0.134)	0.132 (0.052)	0.472 (0.186)	13.08 (2.68)
		76.2 (30)	0.356 (0.140)	0.058 (0.023)	0.414 (0.163)	11.47 (2.35)
		101.6 (40)	0.371 (0.146)	0.033 (0.013)	0.404 (0.159)	11.18 (2.29)

(a) $w = 144\ \rho\bar{t} = 14.1\ \bar{t}$

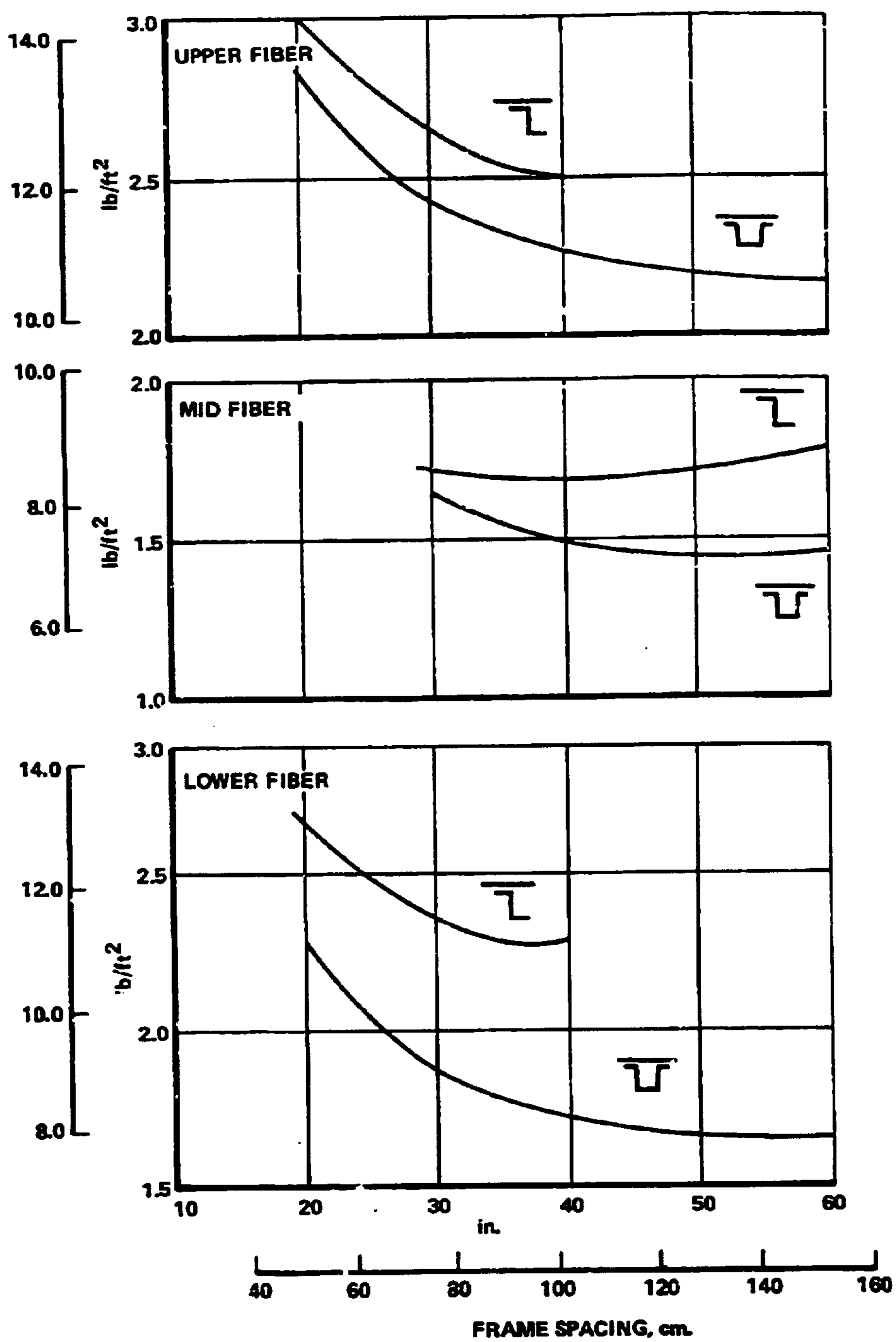

Figure 145. - Fuselage unit weight at the quarter-length location, nonintegral design.

and longitudinal crack damages were considered for the fail-safe analysis. Table 59 presents the fatigue and fail-safe analysis (circumferential damage condition) conducted at the two point design regions. This data reflects all the stiffened wall designs as well as the unstiffened design at these two locations. All designs require the same equivalent axial thickness ($\bar{t}$), whereas the skin thickness of the stiffened concepts can approach the minimum thickness dictated by the fatigue criteria.

The requirement for hoop straps was investigated using the longitudinal damage fail-safe criteria, see 7.2.3.2. Table 60 presents an example of the analysis conducted at the upper fiber location of the quarter-length point design region. This table presents the strap requirements for both the stiffened and unstiffened designs as a function of a variable strap spacing. The strap areas and their equivalent thicknesses for the stiffened skin designs are slightly higher than those of the unstiffened design for all strap spacing investigated. This situation is caused by accepting the minimum skin thickness and the correspondingly higher hoop stress dictated by the fatigue criteria.

Integral weld lands are provided on the tank wall for the attachment (spot welds) of the hoop fail-safe straps. The dimensions of these weld lands were postulated to be the width of the strap 5.08 cm (2.0 in.) and one-quarter the thickness of the skin ($t_{s/4}$). Typical equivalent thickness calculations for these lands are included on Table 60.

Table 61 summarizes the results of the point design analysis conducted on the upper fibers at the quarter-length location on the tank. These unit weights reflect the component and total weights of the fuselage and tank as a function of hoop strap spacing. Insignificant weight differences are noted between the candidate concepts at any of the strap facings. The weight for any of the concepts is approximately 23.9 kg/m^2 (4.90 lbm/ft^2) and is relatively insensitive to the placement of the tank hoop fail-safe straps. The corresponding unit weight data for the lower fiber is shown in Table 62. The same insensitive weight trends are noted between concepts with all concepts weighing approximately 21.5 kg/m^2 (4.4 lbm/ft^2).

The average circumferential unit weight and the component unit weights at the upper, mid and lower fibers are shown in Figure 146 as a function of fail-safe strap spacing for the tank quarter-length location. Because of the very little variation in weight between any of the concepts, it reflects both the stiffened and the unstiffened designs. An average unit weight of 22.6 kg/m^2 (4.62 lb/ft^2) is noted at this tank location.

7.2.3.6.2 Integral design: The candidate wall concepts for integral tank design were subjected to point design analysis. These concepts included the blade-stiffened and the zee-and tee-stiffened concepts. All concepts are one-piece configurations to minimize the potential sources of leaks.

TABLE 59. - TANK FATIGUE AND FAIL-SAFE REQUIREMENTS, NONINTEGRAL TANK DESIGN

Point Design Region	Fiber Location	Limit Loads N1 kN/m (lb/in.)	Limit Loads N2 kN/m (lb/in.)	Minimum[(1)] Skin Thk. t_s, cm (in.)	Equivalent[(2)] Axial Thk. t, cm (in.)
X = ℓ/4	Upper	185 (1 055)	362 (2 065)	0.229 (0.090)	0.389 (0.153)
	Mid	182 (1 042)	367 (2 097)	0.231 (0.091)	0.384 (0.151)
	Lower	189 (1 077)	373 (2 129)	0.236 (0.093)	0.396 (0.156)
X = 3ℓ/4	Upper	147 (839)	290 (1 658)	0.183 (0.072)	0.307 (0.121)
	Mid	146 (837)	294 (1 679)	0.185 (0.073)	0.307 (0.121)
	Lower	146 (836)	298 (1 700)	0.188 (0.074	0.307 (0.121)

1. Fatigue Criteria (Operating Conditions)

$$t_s = \frac{N_2}{F} = \frac{N_2}{23\ 000}$$

2. Fail-safe Criteria (Circumferential Damage)

$$\overline{t} = \frac{N1}{Fg} \quad \text{where:}$$

$$Fg = \frac{1\ K}{2\sqrt{\ell}} = \frac{47\ 870}{2\ \sqrt{12}} \approx 6910$$

$$= 47\ 643\ \text{kPa}$$

STIFFENED

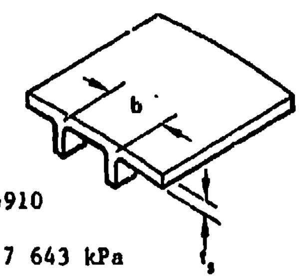

t_s = Skin Thk.

$\overline{t}$ = A/b

UNSTIFFENED

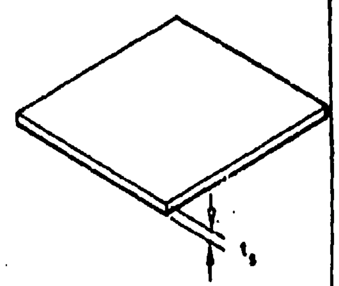

$\overline{t} = t_s$

TABLE 60. - TANK FAIL-SAFE STRAP AND WELD LAND REQUIREMENTS
NONINTEGRAL TANK DESIGN - QUARTER LENGTH POINT

Structural Concepts	Location Fiber	Skin Thk. t_s cm (in)	N_2 kN/m (lb/in.)	f_2 kPa (psi)	Strap Spacing b cm (in.)	Crack Length $\ell = 2b$ cm (in.)	Fail-Safe Straps: Area A_s cm² (in²)	Fail-Safe Straps: Equiv. Thk., $\bar{t}$ cm (in.)	Weld Land $\bar{t}$ cm (in.)
All Stiff.	Upper	0.229 (0.090)	362 (2065)	152 890 (22 000)	15 (6)	30 (12)	0.923 (0.143)	0.061 (0.024)	0.0191 (0.0075)
Skin					25 (10)	51 (20)	1.677 (0.260)	0.066 (0.026)	0.0114 (0.0045)
Concepts					38 (15)	76 (30)	2.619 (0.406)	0.069 (0.027)	0.0076 (0.0030)
1, Z, T					51 (20)	102 (40)	3.568 (0.553)	0.071 (0.028)	0.0058 (0.0023)
Unstiff	Upper	0.389 (0.153)	362 (2065)	93 079 (13 500)	15 (6)	30 (12)	0.710 (0.110)	0.046 (0.018)	0.0325 (0.0128)
Skin					25 (10)	51 (20)	1.465 (0.227)	0.058 (0.023)	0.0193 (0.0076)
Concept					38 (15)	76 (30)	2.413 (0.374)	0.064 (0.025)	0.0130 (0.0051)
					51 (20)	102 (40)	3.355 (0.520)	0.066 (0.026)	0.0097 (0.0038)

1. Fail-safe requirements (refer to 7.2.3.2.4)

$$f_2 = F_{PR} = 1.2\,F_{tu}\left(\frac{2We + \Sigma Ae/ts}{C_1\ell + 2We}\right)$$

where:

$2We = 1.05 \qquad 1.20\,F_{tu} = 74\ 400$

$C_1 = 1.055 \qquad \Sigma A_e = 2A_s$

then:

$$A_s = \left[\frac{f_2}{74{,}400}(1.055\,\ell + 1.05) - 1.05\right]\frac{t_s}{2}$$

2. Weld land requirement

$$\bar{t} = A_{LAND}/b$$

where:

$$A_{LAND} = 2.00\times t_s/4$$

then:

$$\bar{t} = t_s/2b$$

TABLE 61. - SUMMARY OF UPPER FIBER UNIT WEIGHTS AT THE QUARTER-LENGTH LOCATION, NONINTEGRAL TANK DESIGN

Hoop Strap Spacing cm (in.) [a]		25.4 (10)	38.1 (15)	50.8 (20)
Unstiffened Design	Fuselage[b], kg/m^2 (lbm/ft^2)	11.068 (2.267)	11.068 (2.267)	11.068 (2.267)
	Shell	10.224 (2.094)	10.224 (2.094)	10.224 (2.094)
	Frame	0.845 (0.173)	0.845 (0.173)	0.845 (0.173)
	Tank, kg/m^2 (lbm/ft^2)	12.865 (2.635)	12.836 (2.629)	12.831 (2.628)
	Shell	10.736 (2.199)	10.736 (2.199)	10.736 (2.199)
	Straps	1.597 (0.327)	1.753 (0.359)	1.826 (0.374)
	NOF	0.532 (0.109)	0.352 (0.072)	0.273 (0.056)
	Total, kg/m^2 (lbm/ft^2)	23.934 (4.902)	23.905 (4.896)	23.900 (4.895)
Integral Stiffened Design[c]	Fuselage[b], kg/m^2 (lbm/ft^2)	11.068 (2.267)	11.068 (2.267)	11.068 (2.267)
	Shell	10.224 (2.094)	10.224 (2.094)	10.224 (2.094)
	Frame	0.845 (0.173)	0.845 (0.173)	0.845 (0.173)
	Tank, kg/m^2 (lbm/ft^2)	12.875 (2.637)	12.846 (2.631)	12.836 (2.629)
	Shell	10.736 (2.199)	10.736 (2.199)	10.736 (2.199)
	Straps	1.714 (0.351)	1.826 (0.374)	1.889 (0.387)
	NOF	0.420 (0.086)	0.283 (0.058)	0.210 (0.043)
	Total, kg/m^2 (lbm/ft^2)	23.943 (4.904)	23.914 (4.898)	23.904 (4.896)

(a) Tank fail-safe straps.

(b) Fuselage represents least-weight concept (hat stiffened) and corresponding frame spacing 101.6 cm (40.0 in.).

(c) All integral designs (blade-, zee-, and tee-stiffened concepts).

At the point design regions, each component associated with the definition of a unit segment of structure was sized as a function of frame spacing. These components included the basic panel, frame, fail-safe strap and non-optimum factor; and were sized using the previously discussed design criteria, analytical methods and point design environment.

The resultant panel cross-sectional data for the upper and lower fibers at the quarter-length location are shown in Figure 147. This figure presents the equivalent thicknesses of the blade, zee and tee-stiffened designs as a function of frame spacing. Due to the fail-safe requirements (circumferential crack condition) all designs had the same thickness at the smaller frame spacings; whereas. when the compression loads became dominant, the less efficient compression design (blade) required a greater thickness at the higher frame spacings.

TABLE 62. - SUMMARY OF LOWER FIBER UNIT WEIGHTS AT THE QUARTER-LENGTH LOCATION, NONINTEGRAL TANK DESIGN

	Hoop Strap Spacing cm (in.) [a]	25.4	(10)	38.1	(15)	50.8	(20)
Unstiffened Design	Fuselage[b] kg/m^2 (lbm/ft^2)	8.354	(1.711)	8.354	(1.711)	8.354	(1.711)
	Shell	7.509	(1.538)	7.509	(1.538)	7.509	(1.538)
	Frame	0.845	(0.173)	0.845	(0.173)	0.845	(0.173)
	Tank, kg/m^2 (lbm/ft^2)	13.153	(2.694)	13.129	(2.689)	13.119	(2.687)
	Shell	10.956	(2.244)	10.956	(2.244)	10.956	(2.244)
	Straps	1.650	(0.338)	1.806	(0.370)	1.889	(0.387)
	NOF	0.547	(0.112)	0.366	(0.075)	0.273	(0.056)
	Total, kg/m^2 (lbm/ft^2)	21.507	(4.405)	21.483	(4.400)	21.473	(4.398)
Integral Stiffened Designs[c]	Fuselage[b] kg/m^2 (lbm/ft^2)	8.354	(1.711)	8.354	(1.711)	8.354	(1.711)
	Shell	7.509	(1.538)	7.509	(1.538)	7.509	(1.538)
	Frame	0.845	(0.173)	0.845	(0.173)	0.845	(0.173)
	Tank, kg/m^2 (lbm/ft^2)	13.163	(2.696)	13.139	(2.691)	13.119	(2.687)
	Shell	10.956	(2.244)	10.956	(2.244)	10.956	(2.244)
	Straps	1.787	(0.366)	1.899	(0.389)	1.953	(0.400)
	NOF	0.420	(0.086)	0.283	(0.058)	0.210	(0.043)
	Total, kg/m^2 (lbm/ft^2)	21.517	(4.407)	21.492	(4.402)	21.473	(4.398)

(a) Tank fail-safe straps.

(b) Fuselage represents least-weight concept (hat-stiffened) and corresponding frame spacing 101.6 cm (40.0 in.).

(c) All integral designs (blade-, zee-, and tee-stiffened concepts).

For each of these concepts, unstiffened skin panels were found to be the lightest concept for the design of the mid-panels at the quarter-length location. A panel thickness of 4.166 mm (0.164 in.), invariant with frame spacing, was used for these designs.

The frames for these designs were analyzed in a manner similar to that of the fuselage frames for the nonintegral design. Both strength and stability were considered. Figure 148 presents these results along with added requirements imposed by the fail-safe criteria. An example of this fail-safe analysis is summarized in Table 63 for the 762 mm (30.0 in.) frame spacing design. Note that the assumbed location and size of the damage dictates the respective area of the frame or strap. The methods employed in this analyses are described in the Analytical Methods Section.

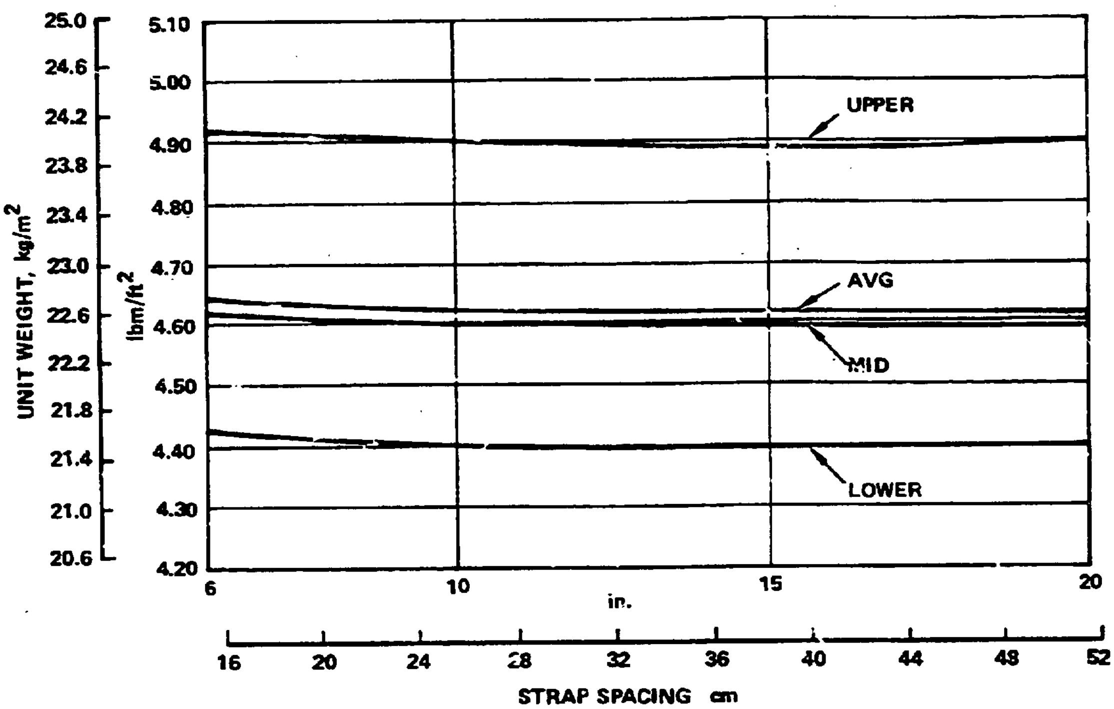

Figure 146. -. Unit weights vs strap spacing for nonintegral tank (quarter-length point design region).

Table 63 describes the frame and strap requirements as a function of the number of straps, but does not indicate the selection process used in defining the spacing for the minimum weight design. Table 64 summarizes the frame area requirements due to stability, strength, minimum gage and fail safe. In addition, the strap area requirements for fail safe and the total area of the frame and straps are presented. It can be seen from this table that the fail safe requirements dictate the areas of the frames when no straps or one strap is used; whereas, the stability requirements design the higher strap spacings. Using these frame areas and combining them with the required strap areas a total equivalent thickness was obtained. Minimum-weight designs are indicated for the two and three strap designs. The smaller number of straps was chosen for the 762 mm (30.0 in.) frame spacing design.

The results of the analyses conducted on the hoop straps and frames dictated the minimum-weight combination for each of the frame spacings investigated. Table 65 summarizes these results and indicates the unit strap areas, total strap areas and the equivalent thickness for each design.

Integral strap weld lands and panel closeouts were postulated for each tank design. The strap weld lands were similar to those described for the nonintegral tank. To provide for attachment of the frames the panel stiffeners were assumed to be tapered-out with a flat land of sufficient thickness provided to carry the axial and bending stresses. These results are presented in Tables 66 and 67 under the heading of nonoptimum factor (NOF).

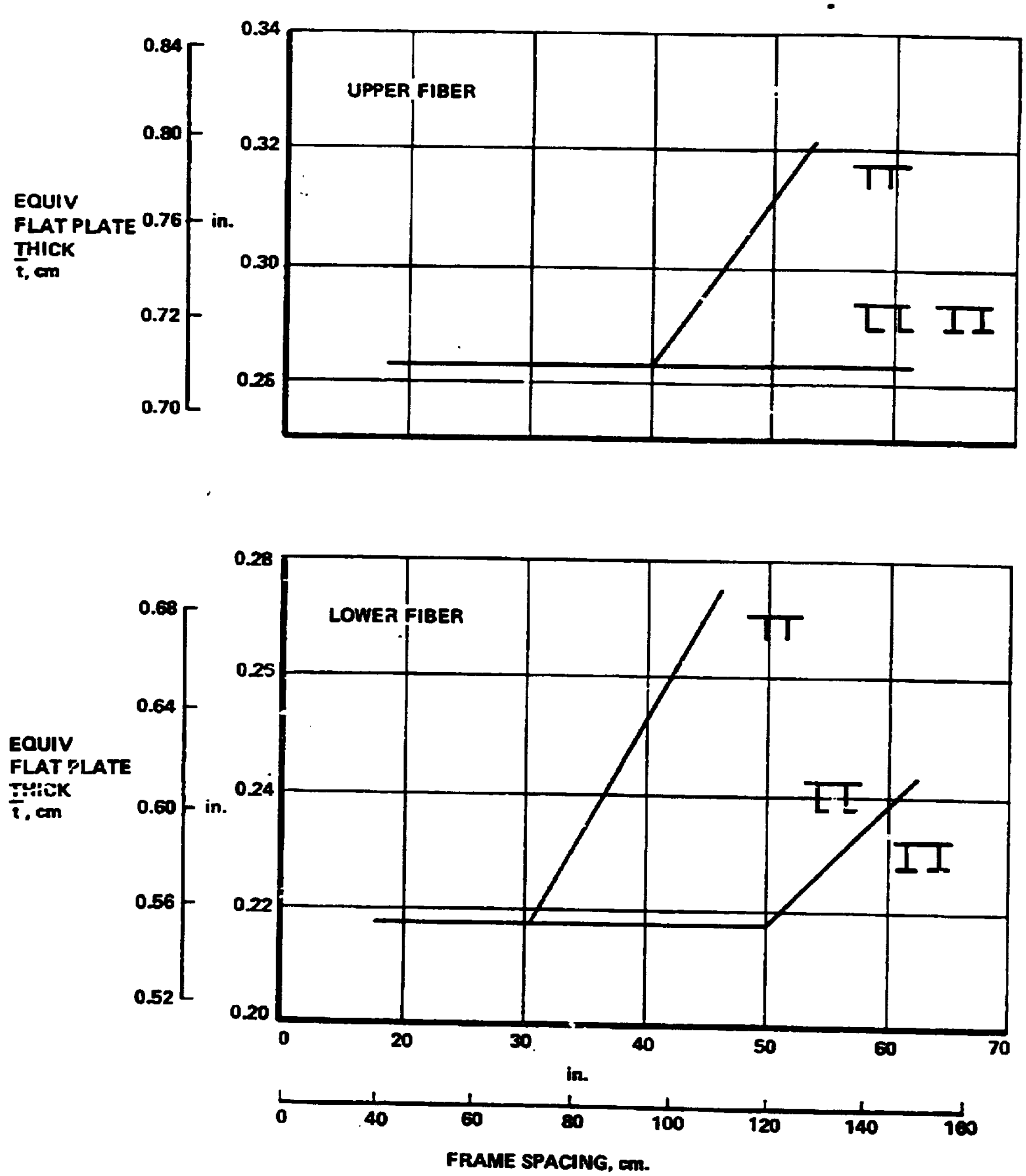

Figure 147. - Tank equivalent thickness, integral design.

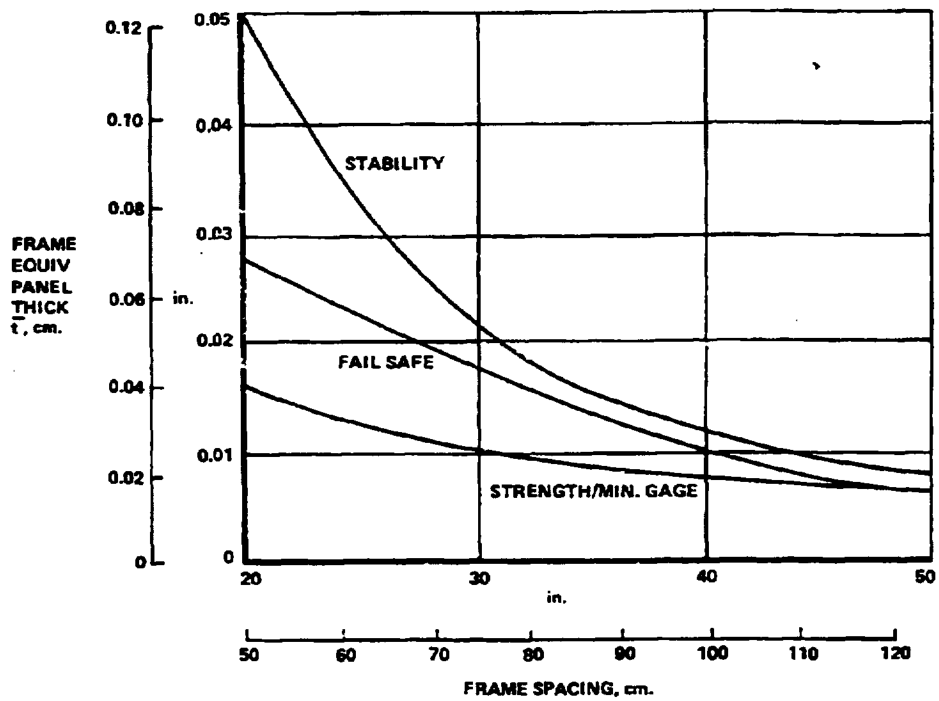

Figure 148. - Frame equivalent thickness as a function of spacing, integral design.

Tables 66 and 67 summarize the results of the point design analysis conducted on upper and lower fibers at the quarter-length location. These weights reflect the component and total weights of the tank as a function of the variable frame spacing. In general, at both locations the blade-stiffened designs are competitive from a weight standpoint with the tee- and zee-stiffened designs at the lower frame spacings and are much heavier at the larger spacings.

Figure 149 presents the total unit weight for the upper and lower fibers. The total cross-sectional unit weight for each candidate concept of the integral tank design was defined by averaging the unit weights calculated at the upper, side and lower circumferential locations. These results are presented in Figure 150 as a function of frame spacing. A minimum weight design of approximately 19.0 kg/m^2 (3.90 lb/ft^2) is indicated for the blade-stiffened pane panel concept at a frame spacing of approximately 101.6 cm (40.0 in.). The corresponding minimum weight designs for both the zee- and tee-stiffened concepts occur at a frame spacing of approximately 127 cm (50.0 in.). The associated average circumferential weight for both of these designs is 18.3 kg/m^2 (3.75 lb/ft^2). This affords a 1.0 kg/m^2 (0.20 lb/ft^2) weight saving over the blade-stiffened design.

TABLE 63. - FRAME AND STRAP FAIL-SAFE REQUIREMENTS FOR 76.3 cm (30.0 in.) FRAME SPACING DESIGN, INTEGRAL TANK

Point Design Region	Frame Spacing b, cm (in.)	No. Straps n	Strap Spacing cm (in.)	Crack Length cm (in.)	A_e cm^2 (in.)	Strap(1) Requirement A_s cm^2 ($in.^2$)	Strap(1) Requirement ΣA_s cm^2 ($in.^2$)	Strap(1) Requirement $\bar{t}$ cm (in.)	Frame(2) Requirement A_F cm^2 ($in.^2$)	Frame(2) Requirement $\bar{t}$ cm (in.)
X = ℓ/4 (FS 2452)	76.2 (30.0)	0	76.2 (30.0)	152.4 (60.0)	13.87 (2.15)	0 (0)	0 (0)	0 (0)	13.87 (2.15)	0.183 (0.072)
	↓	1	38.1 (15.0)	76.2 (30.0)	2.06 (0.32)	2.06 (0.32)	2.06 (0.32)	0.028 (0.011)	6.19 (0.96)	0.081 (0.032)
	↓	2	25.4 (10.0)	50.8 (20.0)	1.16 (0.18)	1.16 (0.18)	2.32 (0.36)	0.030 (0.012)	3.48 (0.54)	0.046 (0.018)
	↓	3	19.1 (7.5)	38.1 (15.0)	0.77 (0.12)	0.77 (0.12)	2.32 (0.36)	0.030 (0.012)	2.32 (0.36)	0.030 (0.012)
	76.2 (30.0)	4	15.2 (6.0)	30.5 (12.0)	0.65 (0.10)	0.65 (0.10)	2.58 (0.40)	0.033 (0.013)	1.94 (0.30)	0.025 (0.010)

1. STRAP REQUIREMENT

- Longitudinal crack arrested by hoop straps

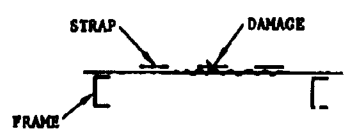

$A_S = A_e$

where:

A_s = Strap area, cm^2 ($in.^2$)

A_e = Reinforcement area, cm^2 ($in.^2$)

2. FRAME REQUIREMENT

- Longitudinal crack arrested by a frame

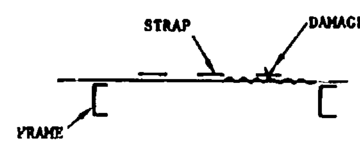

$A_F = 3A_e$

This assumes one third of the area of the frame is effective in resisting skin cracks

TABLE 64. - FRAME AND STRAP REQUIREMENTS FOR A 76.2 cm (30.0 in.) FRAME SPACING DESIGN, INTEGRAL DESIGN

Frame Spacing cm (in.)	No. Straps	Frame Equivalent Thickness cm (in.)					Strap Equiv. Thk. cm (in.)	Total Equiv. Thk. cm (in.)
		Stability Reqmts	Strength Reqmts	Min. Gage	Fail-Safe Reqmts	Design		
76.2 (30.0)	0	0.053 (0.021)	0.025 (0.010)	0.025 (0.010)	0.183 (0.072)	0.183 (0.072)	0 (0)	0.183 (0.072)
	1	0.053 (0.021)			0.081 (0.032)	0.081 (0.032)	0.028 (0.011)	0.109 (0.043)
	2	0.053 (0.021)			0.046 (0.018)	0.053 (0.021)	0.030 (0.012)	0.084 (0.033)
	3	0.053 (0.021)			0.030 (0.012)	0.053 (0.021)	0.030 (0.012)	0.084 (0.033)
76.2 (30.0)	4	0.053 (0.021)	0.025 (0.010)	0.025 (0.010)	0.025 (0.010)	0.053 (0.021)	0.033 (0.013)	0.086 (0.034)

TABLE 65. - SUMMARY OF MINIMUM-WEIGHT STRAP DESIGNS, INTEGRAL TANK DESIGN

Frame Spacing b, cm	(in.)	No. Straps	Strap Spacing cm	(in.)	Strap Area A_s, cm^2	(in.^{2})	Total Strap Area A_s cm^2	(in.^{2})	$\overline{t}$ cm	(in.)
50.8	(20.0)	2	16.94	(6.67)	0.65	(0.10)	1.29	(0.20)	0.025	(0.010)
76.2	(30.0)	3	19.05	(7.50)	0.77	(0.12)	2.32	(0.36)	0.030	(0.012)
101.6	(40.0)	4	20.32	(8.00)	0.77	(0.12)	3.10	(0.48)	0.030	(0.012)
127.0	(50.0)	5	21.16	(8.33)	0.65	(0.10)	3.23	(0.50)	0.025	(0.010)

TABLE 66. - SUMMARY OF UPPER FIBER UNIT WEIGHTS AT THE QUARTER-LENGTH LOCATION, INTEGRAL DESIGN

	Unit Weight, kg/m^2 (lbm/sq ft)							
Frame Spacing cm (in.)	50.8	(20)	76.2	(30)	101.6	(40)	127.0	(50)
Blade-Stiffened Design	27.88	(5.71)	24.95	(5.11)	23.58	(4.83)	24.80	(5.08)
Shell	19.92	(4.08)	19.92	(4.08)	19.92	(4.08)	21.97	(4.50)
Frames	3.37	(0.69)	1.51	(0.31)	0.83	(0.17)	0.54	(0.11)
Straps	0.63	(0.13)	0.83	(0.17)	0.83	(0.17)	0.83	(0.17)
NOF	3.91	(0.80)	2.64	(0.54)	1.95	(0.40)	1.46	(0.30)
Zee-Stiffened Design	28.56	(5.85)	25.39	(5.20)	23.92	(4.90)	23.14	(4.74)
Shell	19.92	(4.08)	19.92	(4.08)	19.92	(4.08)	19.92	(4.08)
Frames	3.37	(0.69)	1.51	(0.31)	0.83	(0.17)	0.54	(0.11)
Straps	0.63	(0.13)	0.83	(0.17)	0.83	(0.17)	0.83	(0.17)
NOF	4.64	(0.95)	3.08	(0.63)	2.29	(0.47)	1.86	(0.38)
Fee-Stiffened Design	28.71	(5.88)	25.44	(5.21)	24.02	(4.92)	23.24	(4.76)
Shell	19.92	(4.08)	19.92	(4.08)	19.92	(4.08)	19.92	(4.08)
Frames	3.37	(0.69)	1.51	(0.31)	0.83	(0.17)	0.54	(0.11)
Straps	0.63	(0.13)	0.83	(0.17)	0.83	(0.17)	0.83	(0.17)
NOF	4.78	(0.98)	3.22	(0.66)	2.39	(0.49)	1.90	(0.39)

7.2.3.7 Screening results: The tank weight for each candidate concept of the integral and nonintegral tanks was calculated using the results of the point design analysis. From these results the most-promising concept was selected for each basic type of tank and used as the baseline configuration for conducting the parametric studies and the investigation of the four candidate fuel containment systems.

Caution should be exercised in interpreting these results since the purpose was to screen the candidate wall concepts and not to conduct a comparison study between the two basic types of tanks.

The total tank cross-sectional weight for each candidate concept of the integral tank design was defined by using the average circumferential unit weights at the two point design regions. Figure 150 presents the average circumferential unit weight as a function of frame spacing for the quarter-length location. From these data the minimum weight designs were selected and used to extrapolate the total weight of the tank conical section.

Table 68 presents a summary of the unit weights of the upper, mid and lower fibers at each point design region. In addition, the average unit weight of the tank at the point design regions and at the ends of the tank cone are defined. This unit weight data was then converted to pounds per foot of

TABLE 67. - SUMMARY OF LOWER FIBER UNIT WEIGHTS AT THE QUARTER-LENGTH LOCATION, INTEGRAL DESIGN

	Unit Weight, kg/m^2 (lbm/sq ft)							
Frame Spacing cm (in.)	50.8	(20)	76.2	(30)	101.6	(40)	127.0	(50)
Blade-Stiffened Design	22.17	(4.54)	19.58	(4.01)	20.60	(4.22)	22.70	(4.65)
Shell	15.28	(3.13)	15.28	(3.13)	17.63	(3.61)	20.46	(4.19)
Frames	3.37	(0.69)	1.51	(0.31)	0.83	(0.17)	0.54	(0.11)
Straps	0.63	(0.13)	0.83	(0.17)	0.83	(0.17)	0.83	(0.17)
NOF	2.83	(0.58)	1.90	(0.39)	1.27	(0.26)	0.88	(0.18)
Zee-Stiffened Design	21.97	(4.50)	19.43	(3.98)	18.36	(3.76)	17.77	(3.64)
Shell	15.28	(3.13)	15.28	(3.13)	15.28	(3.13)	15.28	(3.13)
Frames	3.37	(0.69)	1.51	(0.31)	0.83	(0.17)	0.54	(0.11)
Straps	0.63	(0.13)	0.83	(0.17)	0.83	(0.17)	0.83	(0.17)
NOF	2.69	(0.55)	1.81	(0.37)	1.32	(0.27)	1.07	(0.22)
Tee-Stiffened Design	21.87	(4.48)	19.33	(3.96)	18.26	(3.74)	17.72	(3.63)
Shell	15.28	(3.13)	15.28	(3.13)	15.28	(3.13)	15.28	(3.13)
Frames	3.37	(0.69)	1.51	(0.31)	0.83	(0.17)	0.54	(0.11)
Straps	0.63	(0.13)	0.83	(0.17)	0.83	(0.17)	0.83	(0.17)
NOF	2.54	(0.52)	1.71	(0.35)	1.27	(0.26)	1.03	(0.21)

conical length (average unit weight times mean diameter) and used to derive the weight of the tank cylinders which are shown in Figure 151.

The zee- and tee-stiffened aft tank cones have approximately equal weights of 2401 kg (5293 lb) each with the blade-stiffened design weighing 2500 kg (5512 lb). A weight saving of approximately 100 kg (220 lb) is indicated for the zee- and tee-stiffened designs. Table 69 displays a tank weight for these designs which includes the weight of typical closures in addition to the cone weight.

The zee-stiffened design was selected as the most promising concept for the integral tank design since no appreciable variation in weight is noted between the zee- and tee-stiffened designs. The zee-stiffened tank would be slightly less complicated to manufacture, i.e., lower cost.

The unit weights for the unstiffened and stiffened concepts of nonintegral tanks are approximately equal. The unit weights of the upper and lower fibers at the quarter-length location were previously shown in Tables 61 and 62. The average unit weights were derived by the same methods described for the integral tank design. Table 70 contains the unit weights used for this analysis.

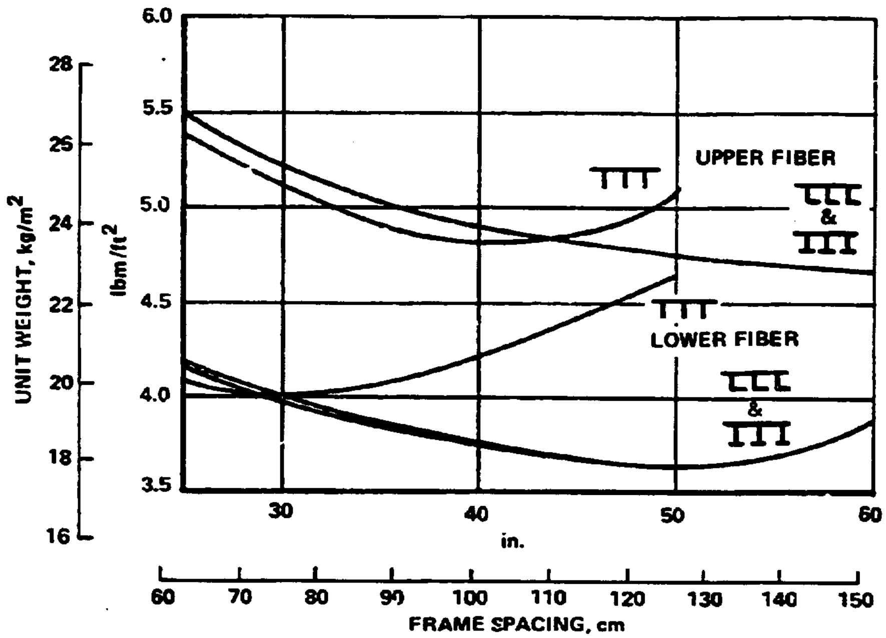

Figure 149. - Total unit weight comparison of structural candidates, integral tank design.

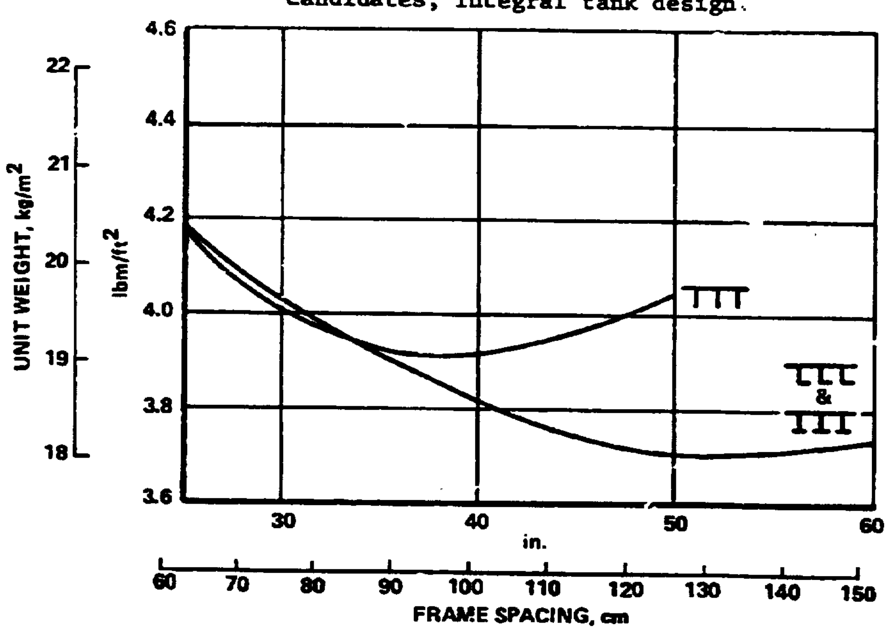

Figure 150. - Average circumferential weight comparison of structural candidates, integral tank design.

TABLE 68. SUMMARY OF UNIT WEIGHTS FOR INTEGRAL TANK DESIGN

Concept	Unit Weights kg/m^2 (lbm./sq.ft.)							
	X=0		X= /4		X=3 /4		X=	
Blade-Stiffened	20.26	(4.15)	19.04	(3.90)	16.60	(3.40)	15.38	(3.15)
Upper fiber		—	23.44	(4.80)	22.07	(4.52)		—
Mid fiber		—	16.11	(3.30)	13.18	(2.70)		—
Lower fiber		—	20.51	(4.20)	18.06	(3.70)		—
Zee- and Tee-Stiff.	19.53	(4.00)	18.31	(3.75)	15.92	(3.26)	14.65	(3.00)
Upper fiber		—	23.19	(4.75)	21.82	(4.47)		—
Mid fiber		—	16.11	(3.30)	13.18	(2.70)		—
Lower fiber		—	17.82	(3.65)	15.62	(3.20)		—

Figure 152 presents the development of the tank and fuselage cone weights for a typical aft tank. Similar to the integral design, a tank and body weight was estimated and is shown on the previously presented Table 70.

All the candidate concepts for the nonintegral tank design exhibited approximately the same weight when compared on a theoretical unit weight basis; where in reality, the tanks fabricated with the stiffened wall configuration would have a higher degree of complexity involved in the design of discrete regions, i.e., head/cone junctures, suspension points, tank penetrations, etc. In addition, the unstiffened wall concept has a decisive cost advantage over the stiffened concepts when the basic problem of fabrication stiffened one-piece wall designs on a conical surface are addressed. If modification of the minimum-weight proportions are attempted to ease the fabrication problems additional weight penalties are incurred for the integrally stiffened concepts.

In conclusion, the unstiffened wall concept was selected for the nonintegral tank design because of its equal or lighter weight and its lower cost.

7.2.4 Parametric studies. - Structural parametric studies were conducted to appraise various aspects related to the design of LH_2 fuel containment tanks. In general these studies encompassed basic design studies on the dome shape and suspension systems, and investigations to assess the effects of pressure (higher tank operating pressures and pressure stabilization) and a variable life on the tank design.

7.2.4.1 Dome shape study: Candidate dome configurations applicable to a constant volume liquid hydrogen tank containment system are described in this

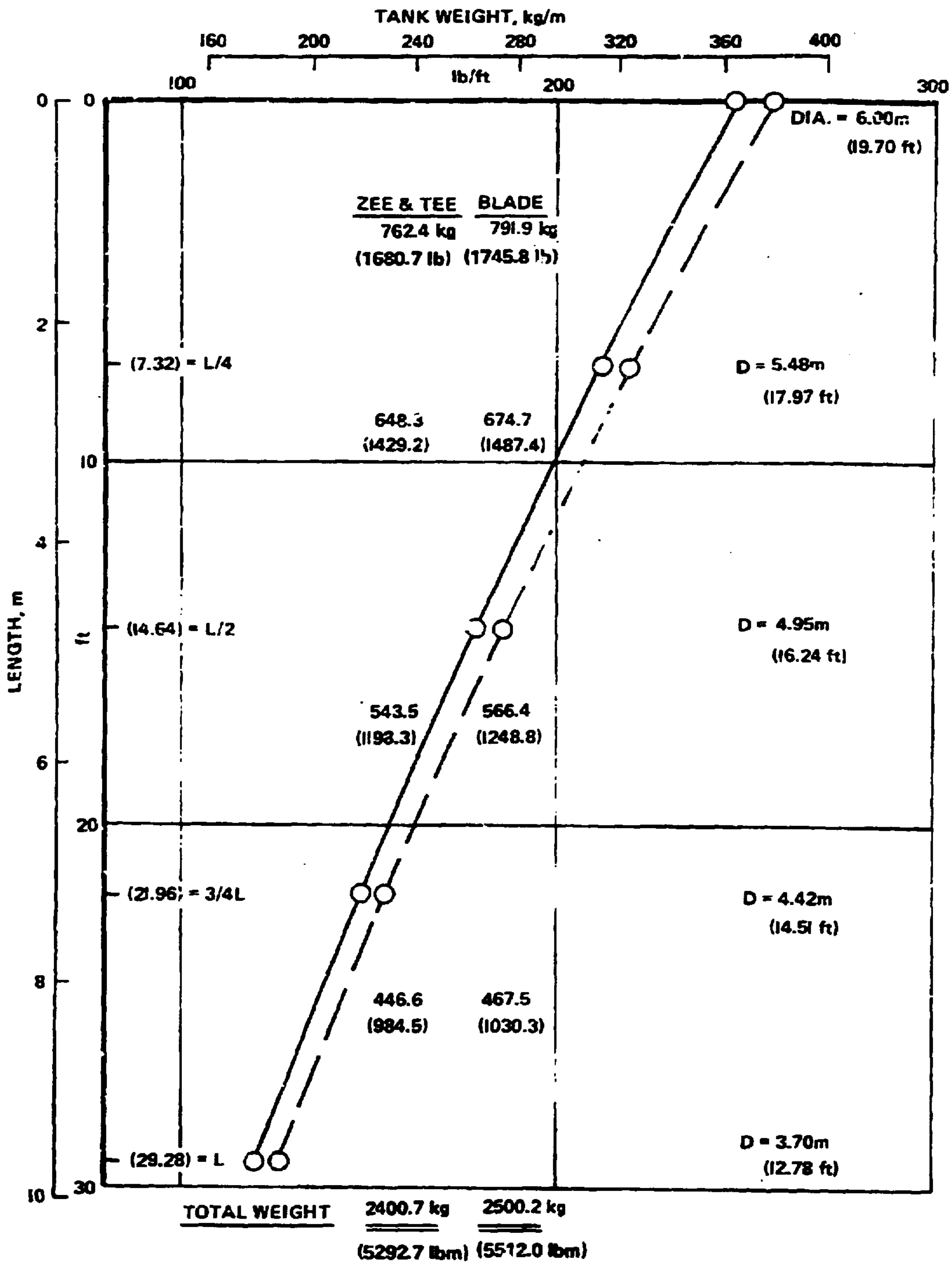

Figure 151. - Integral LH_2 tank wall, optimum weight including fail-safe straps and weld lands.

TABLE 69. - AFT TANK WEIGHT

Item	Weight kg (lbm)		
	Nonintegral	Integral	
	All Concepts	Zee and Tee	Blade
Tank	2253 (4968)	2942 (6485)	3041 (6704)
Cylindrical section	1746 (3850)	2401 (5293)	2500 (5512)
Domes	337 (743)	371 (817)	371 (817)
Divider dome	170 (375)	170 (375)	170 (375)
Body Shell	1516 (3342)	-- --	-- --
Total	3769 (8310)	2942 (6485)	3041 (6704)

TABLE 70. - SUMMARY OF UNIT WEIGHTS FOR THE NONINTEGRAL TANK DESIGN

All Concepts	Unit Weight kg/m^2 (lbm/sq ft)			
	X=0	X=$\ell/4$	X=3$\ell/4$	X=ℓ
Tank	13.96 (2.86)	12.89 (2.64)	10.69 (2.19)	9.57 (1.96)
Upper fiber	13.96 (2.86)	12.84 (2.63)	10.64 (2.18)	9.52 (1.95)
Mid fiber	13.77 (2.82)	12.74 (2.61)	10.69 (2.19)	9.67 (1.98)
Lower fiber	14.35 (2.94)	13.13 (2.69)	10.69 (2.19)	9.47 (1.94)
Body	10.30 (2.11)	9.72 (1.99)	8.54 (1.75)	7.96 (1.63)
Upper fiber	11.77 (2.41)	11.08 (2.27)	9.72 (1.99)	9.03 (1.85)
Mid fiber	10.30 (2.11)	9.72 (1.99)	8.54 (1.75)	7.96 (1.63)
Lower fiber	8.84 (1.81)	8.35 (1.71)	7.37 (1.51)	6.88 (1.41)

section. Specifically, the geometric proportions and the associated weight, internal volume, and surface area of the candidate dome configuration are studied. For each dome configuration, total tank weight is calculated and evaluated with respect to airplane direct operating cost (DOC). By selecting the DOC as the objective function, the proportions of the least-costly dome-tank configuration are determined.

The nonintegrated tank design shown in Figure 153 was selected as the baseline for the study. The three candidate dome configurations as depicted in Figure 154 include a hemispherical head and the general families of ellipsoidal and torispherical heads. For the preliminary analysis of the candidate

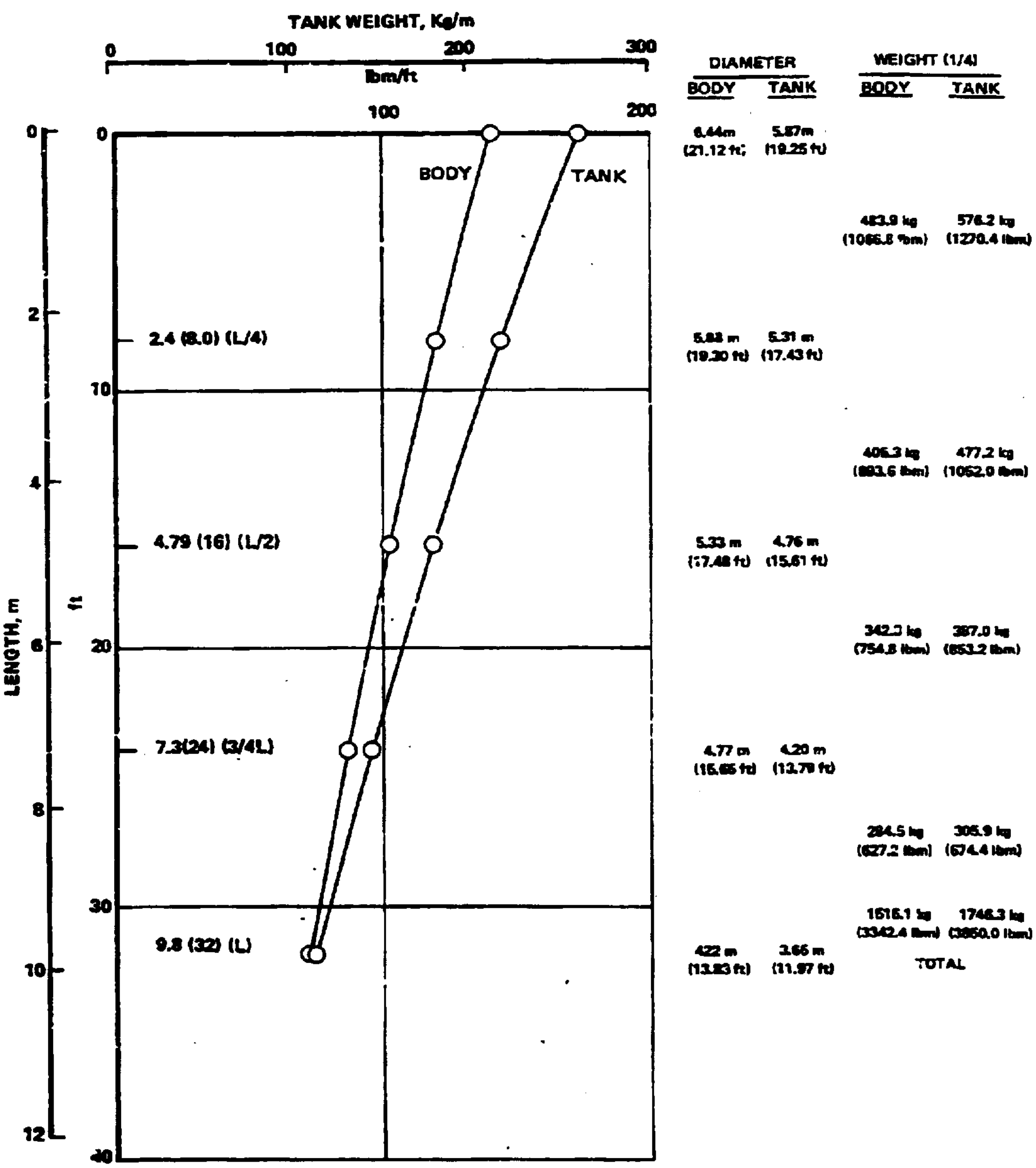

Figure 152. - Nonintegral LH_2 tank wall, optimum weight including fail-safe straps and weld lands.

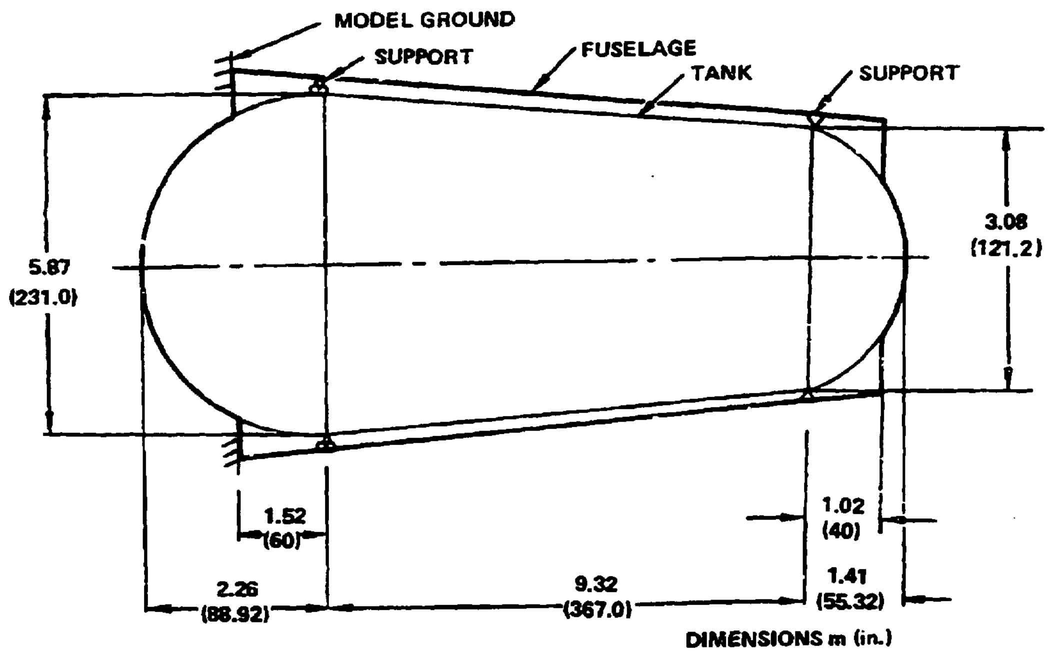

Figure 153. - Fuselage shell and tank configuration, nonintegral design.

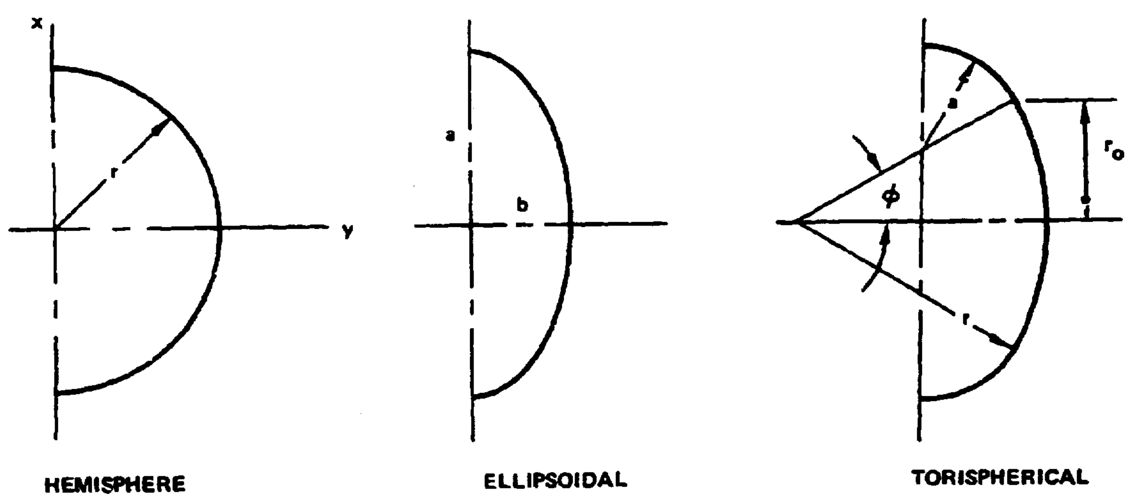

Figure 154. - Candidate configurations for dome shape study.

head configurations, thin-shell theory (membrane) was used. The dome shells were considered to be constructed of isotropic material with variable wall-thickness and subject only to internal pressurization. The operating design stress curves indicated that a fatigue allowable of 158 579 kPa ([illegible] 000 psi) was most suitable for the analysis. The von-Mises failure criter[illegible]

$$\bar{\sigma}^2 = \sigma_1^2 + \sigma_2^2 - \sigma_1\sigma_2$$

was used. In this expression, σ_1 and σ_2 are the meridional and hoop stress, respectively. For axisymmetric shells of revolution subject only to internal pressure, these stresses are given by the relationships:

$$\sigma_1 = pr_2/2t$$

$$\sigma_2 = p(r_2 - r_2^2/2r_1)/t$$

where p is the internal pressure and t is the wall thickness. The meridional radius of curvature r_1 and the hoop radius of curvature r_2 for the candidate dome configurations are given in Table 71.

Parametric studies were conducted to define the proper dome shape, considering both tank weight and volumetric efficiency. Candidate dome configurations were applied to the large diameter dome of the nonintegral tank design. Standard numerical techniques were used in the preliminary strength analysis to size the variable wall thickness requirements and obtain needed parameters such as dome radii of curvature, surface area and volume, and dome weight.

Figures 155 and 156 show the variation of surface area, volume, and weight as a function of the specific geometry parameter for the families of ellipsoidal and torispherical heads, respectively. The hemispherical dome is represented in Figure 155 by an a/b = 1.0. For the ellipsoidal configuration, minimum weight of 215 kg (4[illegible] pounds) is obtained at an a/b = 1.3. The torispherical design yields a minimum weight of 222 kg (489 pounds) at an angle ϕ of 0.95 radians. The hemispherical dome is approximately 17-percent heavier than the leastweight ellipsoidal dome.

Tank and fuselage geometric proportions were determined for a constant volume tank. The weights were calculated for these constant volume tank configurations and included the tank, fuselage shell, insulation and fuel for the nonintegral tank design. The fuel boiloff weight was accounted for as the length/surface area varied. Figure 157 shows the resultant weights of the

TABLE 71. - RADII OF CURVATURE OF CANDIDATE DOME CONFIGURATIONS

Configuration	Radii of Curvature	
	Meridional (r_1)	Hoop (r_2)
Hemispherical	r	r
Elliptical	$r_2{}^3(b^2/a^4)$	$((a/b)^4y^2+x^2)^{1/2}$
Torispherical (toridal segment)	a	$a(1 + b/r_o)$
See Figure 153 for geometry.		

forward and aft tanks as a function of dome parameter. Using these weights and their corresponding length and associated diameter changes, the ASSET program was used to assess the effects on aircraft L/D for a constant payload-range mission. The cost comparison date (DOC) for the resultant aircraft are shown in Figure 158 as a function of the specific dome parameters. A summary of the minimum aircraft DOC configuration for each dome shape is shown in Table 72. The aircraft utilizing ellipsoidal heads on the tanks display a minimum DOC of 0.9852 ¢/s km (1.8246 ¢/seat-nmi) for a dome aspect ratio of 1.60. The associated total weight and fuselage length are 37065 kg (81 715 pounds) and 67.97 m (223.0 feet), respectively. The corresponding minimum DOC for the torispherical head design is 0.9852 ¢/s km (1.8245 ¢/seat-nmi). for a ϕ = 0.36 radian dome. A total weight of 36 902 kg (81 355 pounds) and a fuselage length of 68.2 m (223.7 feet) are noted for this design.

Since the DOC for both the elliptical dome and torispherical dome is approximately 0.9854 ¢/s km (1.825 ¢/seat-n.mi.), these designs were subject to a more detailed analysis using the BOSOR 4 computer program. This analysis included the bending as well as the membrane thickness requirements of a shell under internal pressure load. The von Mises failure criteria was also used in this analysis. Figures 159 and 160 present the undeformed shapes of the elliptical and torispherical domes, respectively.

These models were subjected to a nonlinear elastic analysis using the BOSOR program with internal pressurization being the only loading considered. As an example of the results, the stresses associated with the elliptical dome are shown in Figure 161. The arc length is measured from the apex to the equator of the dome, and along the cylinder. The upper plot reflects the hoop stress on the outer fiber (s_{20}) as the function of the meridian length; whereas, the two lower plots depict the equivalent stresses (von Mises criteria) on the innter S_{EI} and outer S_{EO} fibers, respectively. Maximum equivalent stresses of 158 585 kPa (23 000 psi) and 137 900 kPa (20 000 psi) are noted for the dome and cylinder, respectively.

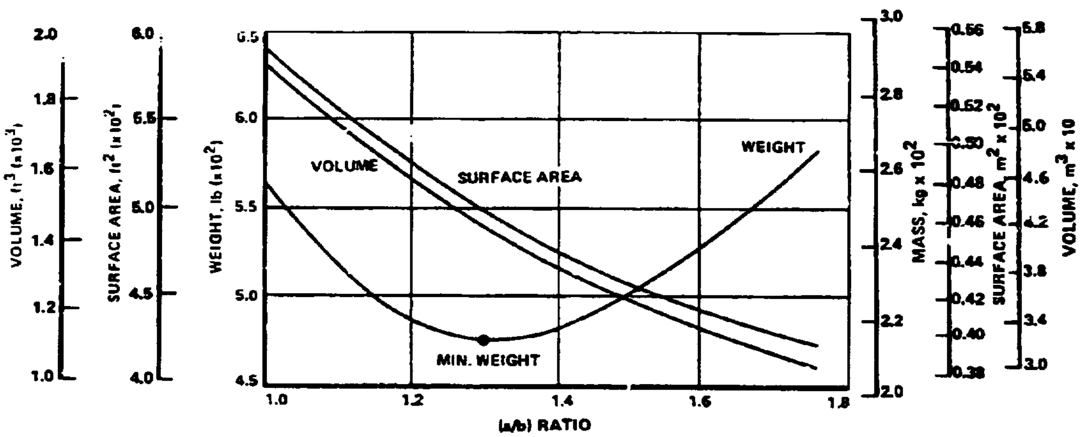

Figure 155. - Elliptical dome design data.

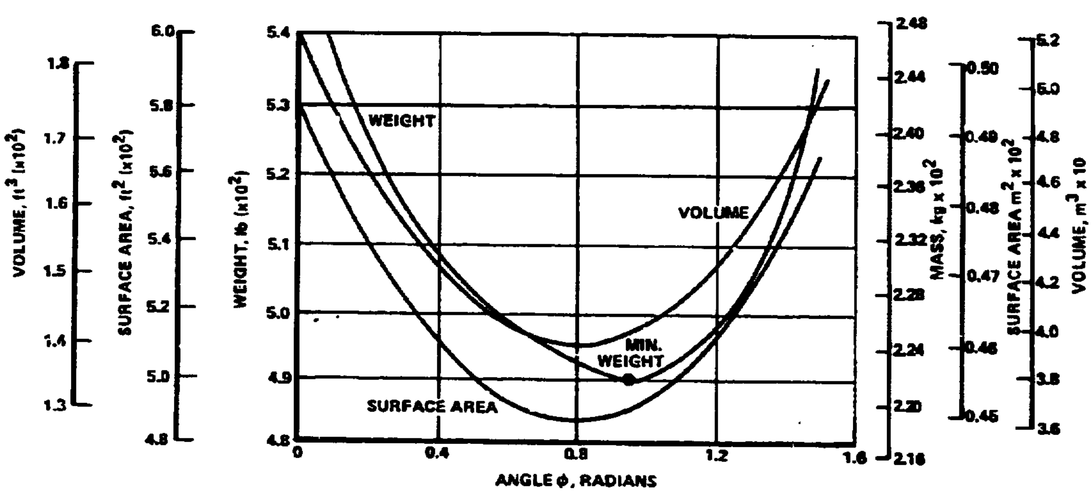

Figure 156. - Torispherical dome design data.

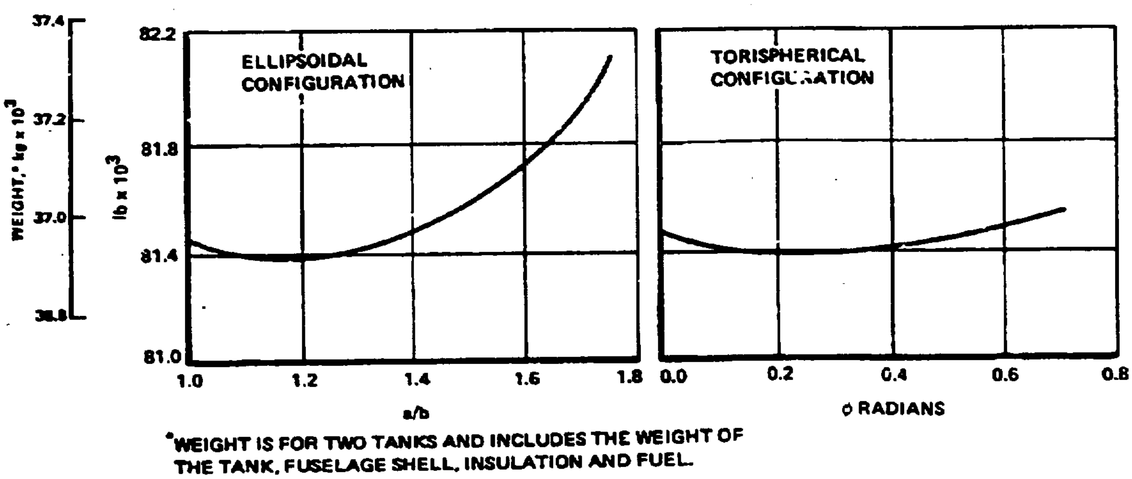

Figure 157. - Tank weight comparison dome shape study.

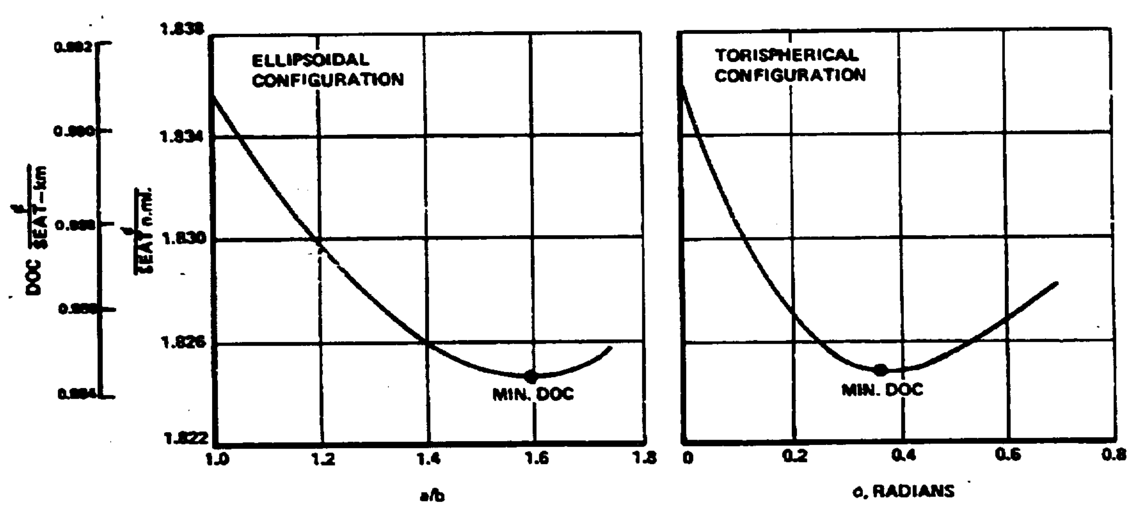

Figure 158. - Cost comparison date, dome shape study.

TABLE 72. - COMPARISON OF DATA FOR MINIMUM DOC DOMES CONFIGURATION

Item	Ellipsoidal	Torispherical
Dome Geometry		
Proportions	a/b = 1.6	ϕ = 0.36
Height m (ft)	1.83 (6.01)	2.29 (7.51)
Weight kg (lb)	37 065 (81 715)	36 902 (81 355)
(Incl- tank, shell, insul. and fuel)		
Fuselage Length m (ft)	67.97 (223.0)	68.18 (223.7)
DOC ¢/seat km (¢/Seat n.mi.)	0.9852 (1.8246)	0.9852 (1.8245)

The maximum equivalent stresses for the torispherical dome are 124 990 kPa (25 600 psi) and 111 319 kPa (22 800 psi) for the dome and cylinder, respectively. Additional evaluation indicates a weight penalty required to sustain a 112 296 kPa (23 000 psi) allowable of approximately 2.3 kg (5 lb) per head or a total weight increment of approximately 9.1 kg (20.0 lb) for the combined forward and aft tanks.

A summary of the results of this study are presented in the following table.

Concept	Evaluation Function	
	Minimum Wt.	Minimum DOC
Ellipsoidal Design		
a/b Weight, kg (lb)	1.30 215.0 (474)	1.60 240.4 (530)
Torispherical Design		
ϕ, radians Weight, kg (lb)	0.95 221.8 (489)	0.36 234.1 (516)

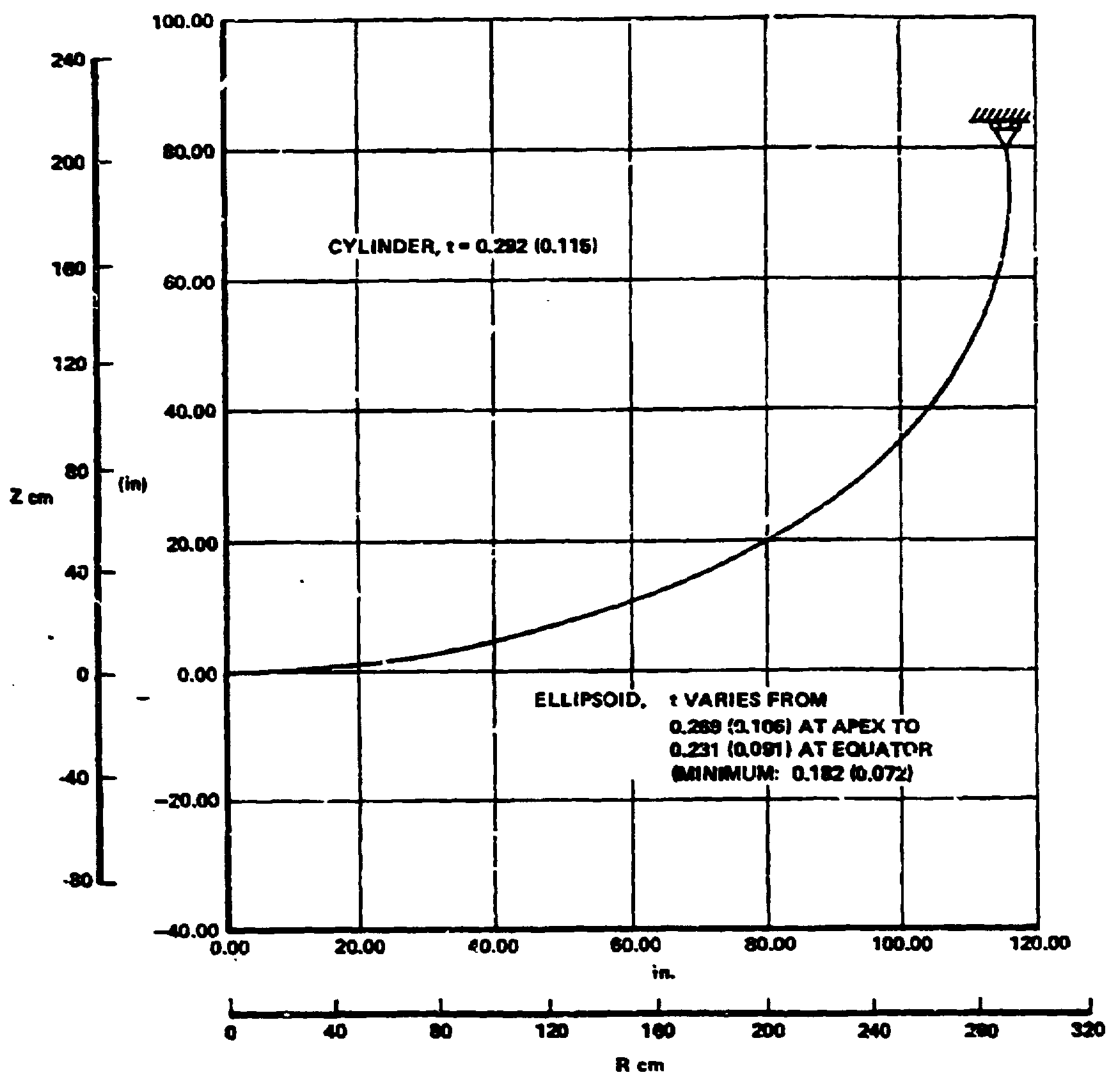

Figure 159. - Elliptic dome-nonlinear stress initial undeformed structure.

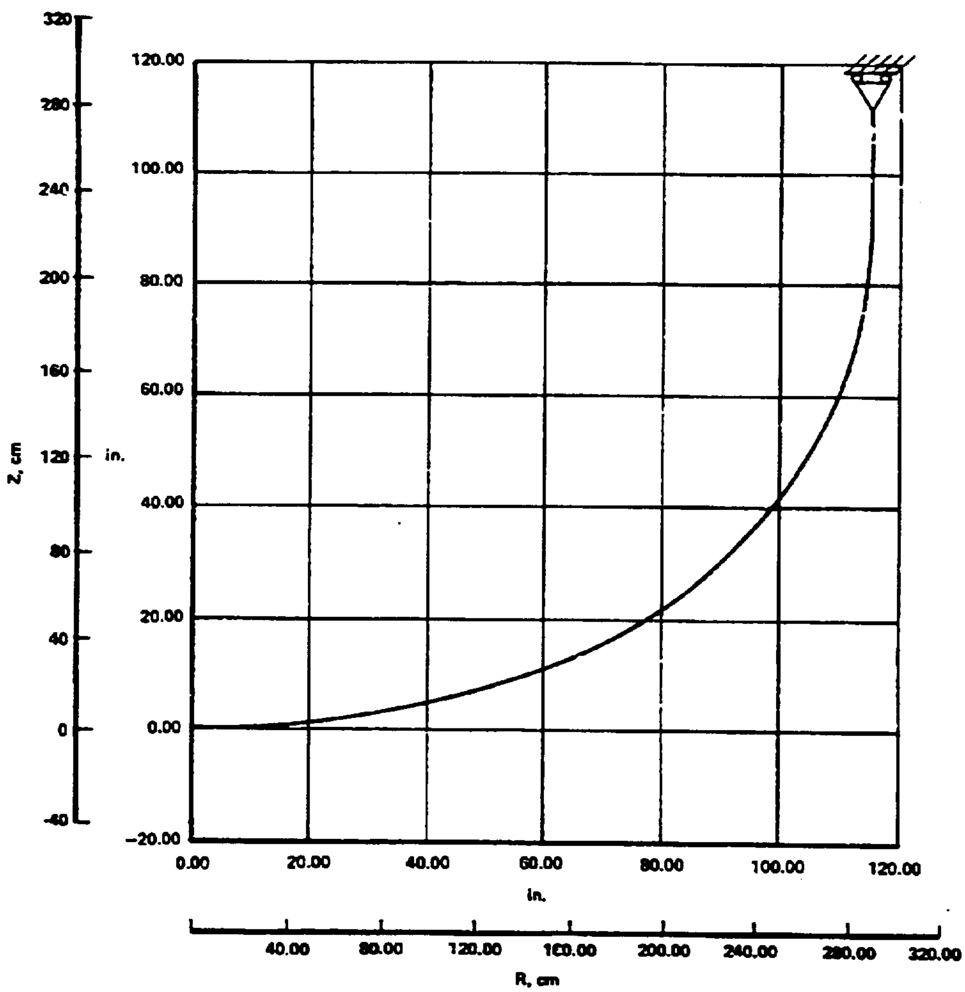

Figure 160. - Torispherical dome-nonlinear stress initial undeformed structure.

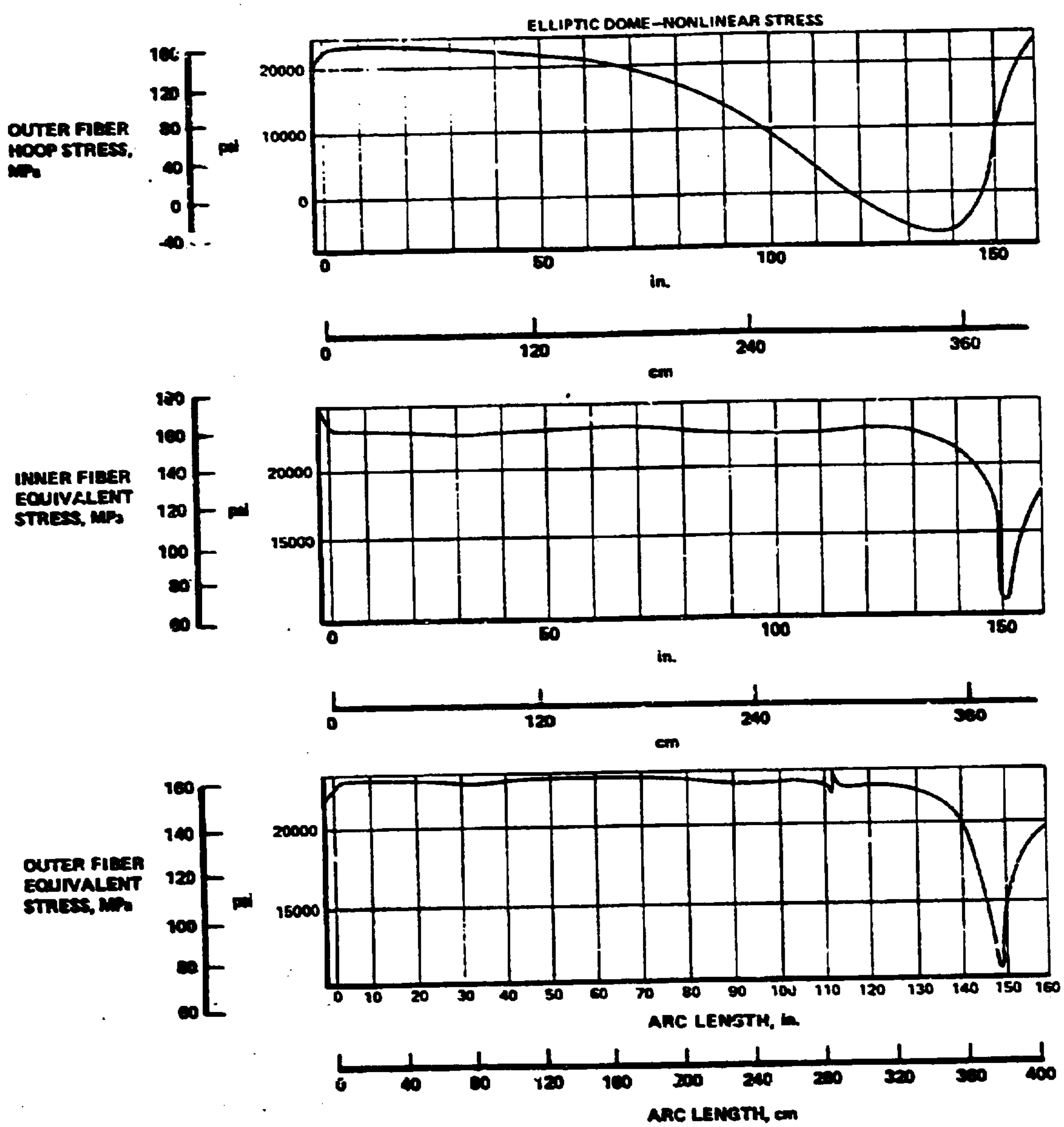

Figure 161. - Elliptical dome stresses.

Considering minimum-weight dome designs the ellipsoidal design is the least weight design and indicates a weight saving of 6.8 kg (15 lb) (5-percent) over the equivalent torispherical design.

When DOC is the object function and the dome weight of the two designs are compared, the torispherical design offers the least weight with a weight saving of approximately 3-percent over the ellipsoidal design. There is no appreciable difference in the aircraft DOC between the two minimum DOC designs. Both designs have a DOC of approximately 0.9854 ¢/S km (1.825 ¢/S n.mi.).

Based on these results, neither design affords a clear cut decision as to the preferred dome configuration. The elliptical dome with the minimum DOC configuration (a/b = 1.6) was arbitrarily selected.

7.2.4.2 Tank life investigation: A structural study was conducted to assess the mass trend associated with varying the tank design life, i.e., planning on replacing the tank during the 50 000 hours of service life required of the aircraft.

Representative tank wall and closure concepts were selected for each basic tank design (integral and nonintegral configurations) using the results of the prior concept screening analysis and dome shape study. These representative tanks were sized at selected point design regions using the applied loads and pressure schedule defined for the concept screening analysis and the criteria specified in Section 7.2.1.

The three tank lives considered were the full aircraft life (50 000 hr), one half-life (25 000 hr) and one-third life (16 700 hr). For fatigue considerations both limit and ultimate tension design allowables were determined for each respective tank life. These allowables are presented in Figure 162 for baseline aluminum alloy 2219-T851. All allowables dealing with unpressurized fuselage shell structure are the same as those presented in the concept screening study.

The minimum weight tank wall designs were determined using the same methods described in the analytical methods section of the concept screening study. Using these methods, point designs were determined for a range of frame spacings for the integral tank design and as a function of the hoop fail-safe strap spacing for the nonintegral tank. The wall thicknesses of the tank closures were defined using the theory described in the dome shape study. The results of this study are presented in the following sections.

7.2.4.2.1 Nonintegral Tank Design: An unstiffened skin design, the most-promising concept resulting from the concept screening study, was used in the life study evaluation for nonintegral tanks. Due to the predominance of the fail-safe requirement, no change was found as a result of the life criterion. Subcomponents, straps, and NOF also were found to be invariant with length of service life. The fuselage shell was not considered as a replacement item; hence, it was not effected by a change in life criterion. Consequently, the non-integral tank weight remains constant as a function of design life and is

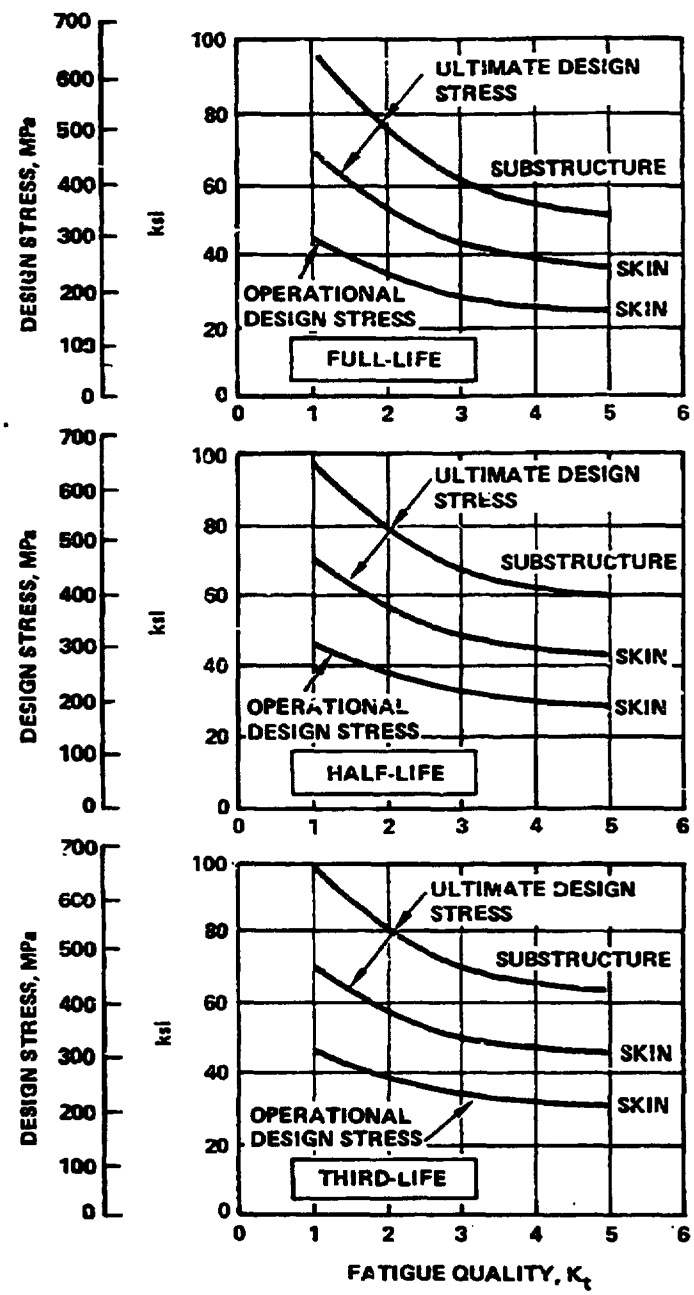

Figure 162. - Variation in circumferential design stress with life, 2219-T851 aluminum alloy

identical to the data presented in the concept screening study for all circumferential locations at both quarter point stations.

Closures similar in design to those used for the integral tank were incorporated into this design also. Ellipsoidal domes with an aspect ratio (a/b) = 1.6 were used in addition to restricting the minimum gage to 1.27 mm (0.050 in).

Thus, the only variation due to design life specification results from the change in the tank heads. Adding the tank head variation to the constant tank body weights, a total tank weight for each life is evolved and may be evaluated to find the minimum DOC life concept.

7.2.4.2.2 Integral Tank Design: As a result of the concept screening analysis, a hybrid structural approach utilizing both the zee-stiffened and unstiffened wall concepts was used for the integral tank design. Circumferentially, the stiffened wall concept was incorporated in the design at the relatively highly loaded upper and lower quadrants; while the unstiffened skin was employed at the side quadrants due to the lower loadings.

An example of the type of data obtained is summarized in Figure 163. This figure displays a summary of the point design data for the upper fiber at the tank quarter-length station. The upper figure shows the variation in wall thickness with life, the center figure displays the component and total unit weight for a representative life, and the lower figure depicts the total unit weight of the tank for each life investigated.

The wall thickness variations shown in the above figure incorporate longitudinal straps in the design to meet the fail-safe requirements imposed by the high tension loads. These fail-safe straps have an area of 1.29 cm^2 (0.2 in^2) and are centered between the stiffeners. The variations in the tank wall thicknesses are primarily attributable to the change in minimum skin thickness as a function of fatigue life. Dominance of the fail-safe requirements results in a constant equivalent thickness over the range of frame spacings.

The equivalent panel thicknesses were then combined with the calculated thicknesses of the frames, circumferential fail-safe straps and non-optimum factors (NOF) to obtain a total panel weight. All of the subcomponents; frames, straps and NOF, vary with length of service life. A typical plot of the components and total unit weights for the full-life condition are shown in the middle plot of Figure 163.

The total weights for each life are shown in the lower plot of Figure 163 as as a function of frame spacing. This plot reveals continuously decreasing values which are due to the effect of the subcomponents as the panels remain constant over the range of frame spacing. Thus, for this range of frame spacings, each life has a minimum value at a frame spacing of 177.8 cm (70 in.) with the third-life tank the lightest at 22.5 kg/m^2 (4.61 lb/ft^2), followed by the half- and full-lives at 22.6 kg/m^2 (4.63 lb/ft^2) and 22.8 kg/m^2 (4.68 lb/ft^2), respectively. Note the maximum variation in weight at this spacing is only 0.3 kg/m^2 (0.07 lb ft^2).

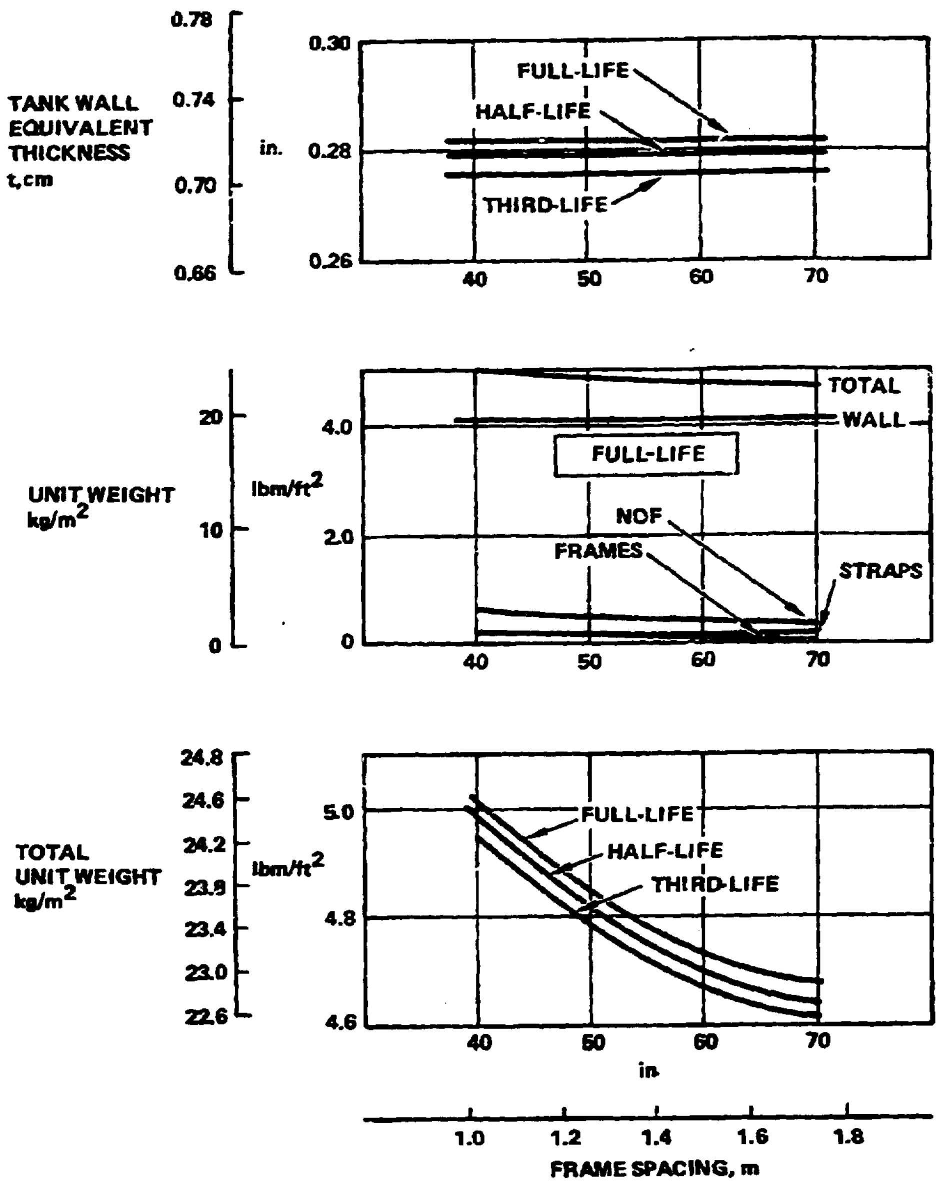

Figure 163. Upper fiber point design data at the quarter length station, integral tank

An unstiffened panel design of 2.03 cm (0.164 in.) thickness was employed at midfiber location. Fail-safe considerations design these panels; hence there was no variation in thickness with life. Panel thicknesses were combined with the various applicable subcomponents to obtain both the unit and total weight for this location. As with the upper fiber location, the mid fiber location exhibits the same continuously decreasing total weight trend with tank life. Thus again, a minimum spacing of 177.8 cm (70.0 in.) provided the lightest structure with all designs weighing approximately 12.9 kg/m^2 (2.65 lb/ft^2). A weight variation of only 0.1 kg/m^2 (0.02 lb/ft^2) is noted between designs.

A summary of the results of the lower fiber point design analysis is presented in Figure 164. The variation in wall thickness for each tank-life (upper plot) is constant for frame spacings less than 127 cm (50 in.) with no variation due to change in life because of the circumferential damage fail-safe requirements. Unlike the upper fiber location, where longitudinal straps were employed, the lower fiber analysis indicated that increasing the skin thickness was a more efficient (i.e., lower weight) method of meeting the fail-safe requirements. The maximum lower fiber meridional tension load is approximately one-half of that on the upper fiber. Thus, for this region, the skin was not held to the minimum thickness dictated by fatigue for the respective life but was maintained at a level commensurate with the fail-safe requirements. The frame spacing region above 127 cm (50 in.) shows an increasing thickness with a variation from one life criterion to the next. Designs within these spacings are primarily controlled by local buckling with the fail-safe requirements becoming less critical as the frame spacing is increased.

Similar to the upper fiber analysis, plots of the component and total unit weights for the lower fiber were constructed for each tank life. The component unit weights for the full-life condition are presented in the center of Figure 164. The total weights are shown in the lower figure and indicates minimum weight designs at 127 cm (50.0 in.) frame spacing for each of the life intervals investigated. The corresponding total unit weights for these designs are approximately the same, i.e., the heaviest weight design (full-life) has a weight of 18.5 kg/m^2 (3.78 lb/ft^2), which is only 0.05 kg/m^2 (0.01 lb/ft^2) heavier than those designed for half- and third-life intervals.

An average equivalent thickness for the circumference at the quarter length station was calculated using the results of the analysis conducted on the upper, mid and lower fibers. These data were plotted as a function of frame spacing, as presented in Figure 165. Minimum-weight frame spacings of 134.6 cm (53.0 in.), 137.2 cm (54.0 in.) and 142.2 cm (56.0 in.) are noted for the full-, half- and third-life designs, respectively. The lightest weight tank is the third-life design which weighs 16.9 kg/m^2 (3.47 lb/ft^2). It is only 0.15 kg/m^2 (0.03 lb/ft^2) lighter than the heaviest design (full-life).

The minimum weight design data at the quarter-length station were used in association with the corresponding data at the three-quarter length station to calculate the weight of the tank cyclinder for each design life.

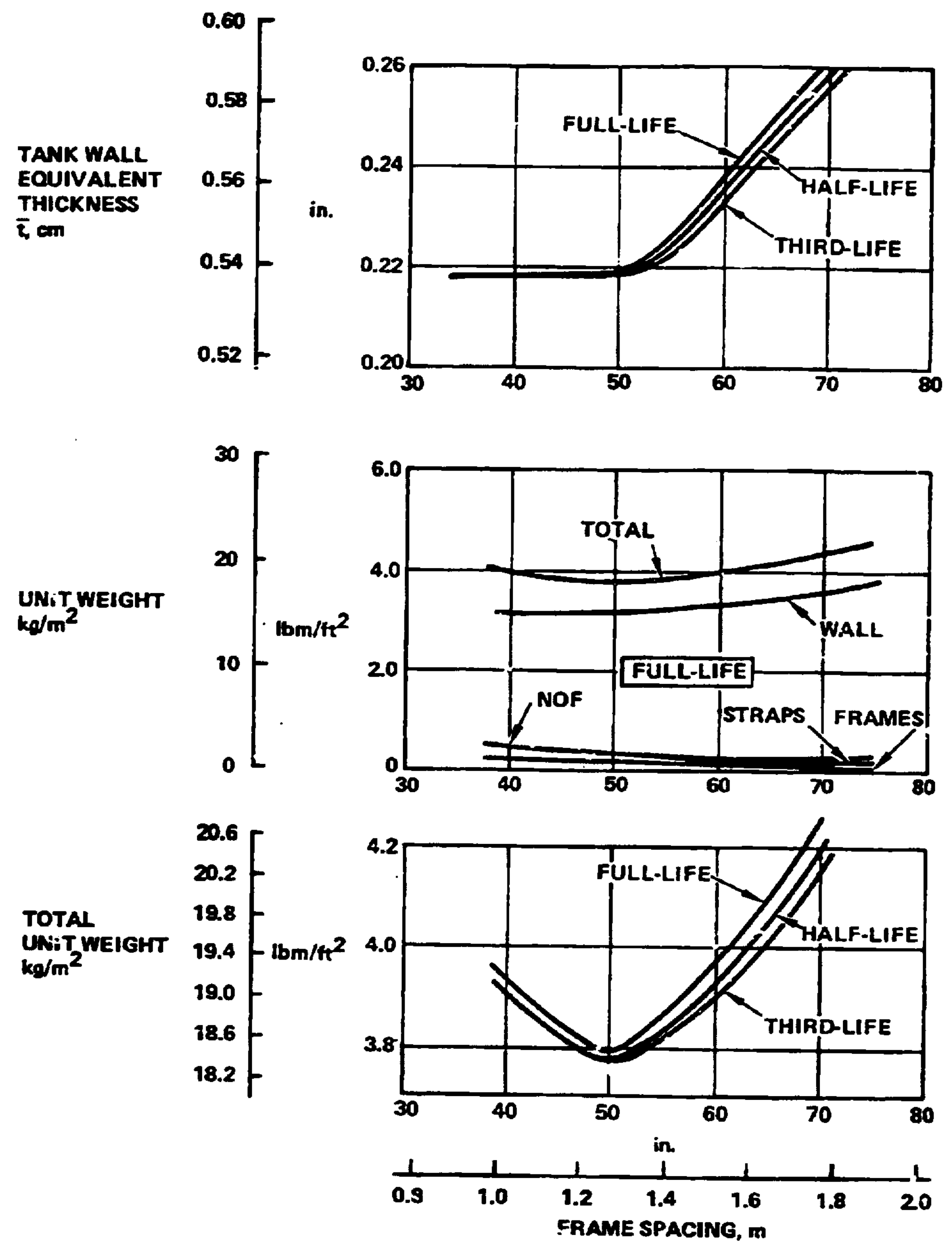

Figure 164. Lower Fiber point design data at quarter-length station, integral tank

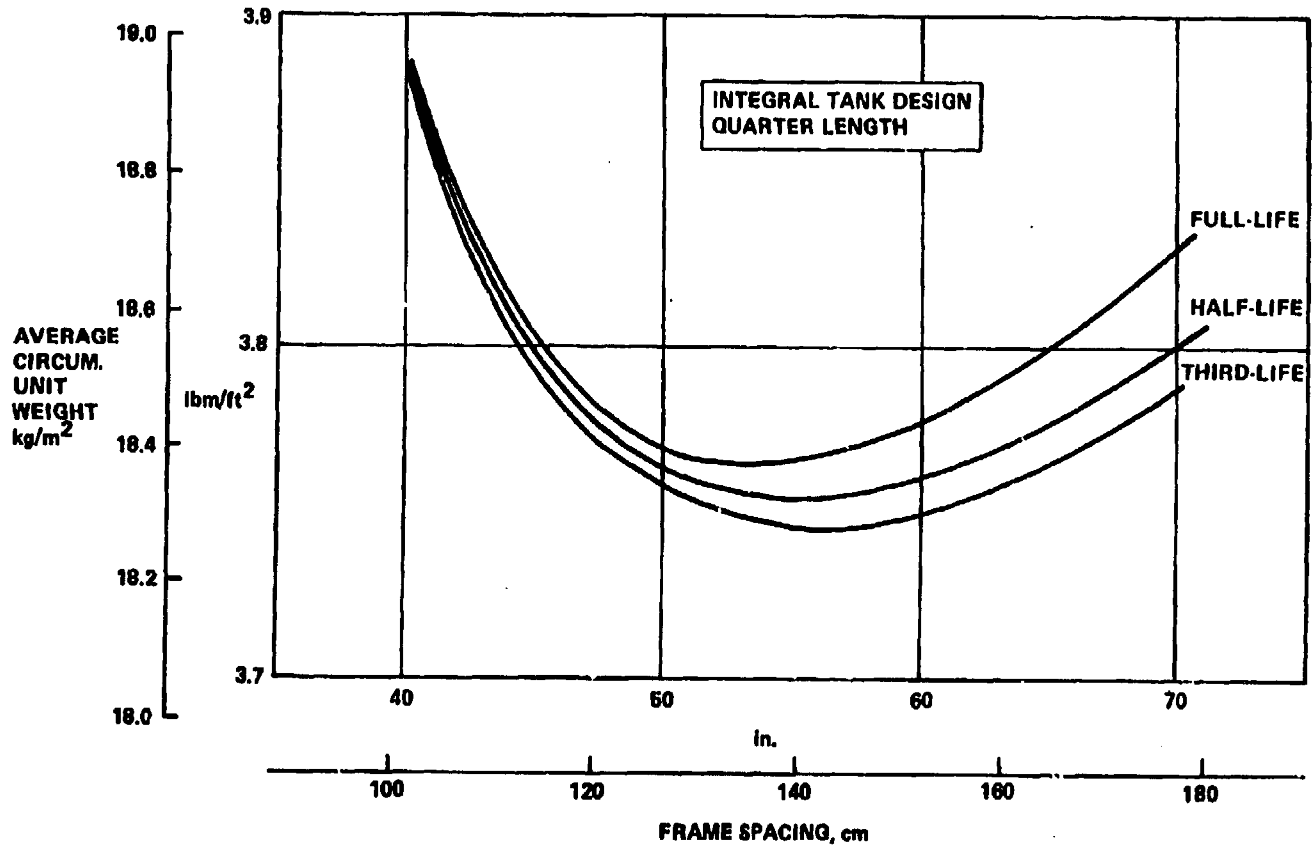

Figure 165. Variation in average circumferential unit weight with life, integral tank

In addition to calculating the cylinder weights, the weights of ellipsoidal tank domes with an a/b ratio of 1.6 and a minimum wall thickness of 0.13 cm (0.05 in.) were estimated. Combining the cylinder weight results with the fore and aft tank dome head designs provided a total tank weight. The results are reported in 7.2.4.2.3.

7.2.4.2.3 Conclusions: The following table presents the tank weights, excluding insulation, for the integral and nonintegral tank designs. The values shown reflect the weight of both the forward and aft tanks.

	Tank Weight kg (lb)	
Tank Design	Nonintegral Design	Integral Design
Full-Life	9218 (20 322)	7081 (15 612)
Half-Life	9181 (20 240)	7039 (15 518)
Third-Life	9135 (20 140)	6989 (15 408)

For both tank designs, only small changes in weight are noted as the life varies. A weight decrement of 83 kg (182 lb) is noted for the third-life design when compared to the full-life design for the nonintegral tank. Similarly, a weight decrement of 93 kg (204 lb) is noted when the same life designs are compared for the integral tank. These small weight savings offered by the reduced life tank designs translate into an insignificant decrement in aircraft DOC that would not off-set the initial investment and installation costs for replacing the tanks.

7.2.4.3 Tank Pressurization Study: This study was undertaken to assess the impact on airplane weight and DOC elicited by using higher tank pressures. Three pressures were studied, including the baseline nominal tank pressure of 145 kPa (21 psia). The two higher nominal tank pressures were 207 kPa (30 psia) and 276 kPa (40 psia.)

Both integral and nonintegral designs were investigated in this study. For the integral tank design, the one-piece zee-stiffened configuration was employed; whereas, for the nonintegral tank an unstiffened wall design was utilized. These configurations were the most-promising concepts surviving the concept screening analysis. Ellipsoidal tank domes, with their associated minimum DOC parameters, were used for both tank designs based on the results of the previously reported dome shape study. Total tank weights were thus defined for both basic types of tanks.

The tension loads corresponding to the three pressure cases are shown in Table 73. These loads are combined loads (airload, pressure and thermal) where only the membrane forces due to the internal pressurization are multiplied by the ratio of pressures. The criteria and analytical methods are defined in Section 7.2.1 and 7.2.3.2.

TABLE 73. MEMBRANE LOAD VARIATION WITH TANK PRESSURE, TANK PRESSURIZATION STUDY

Nominal Tank Pressure kPa (psia)	Type of Tank	Membrane Loads (Ultimate)								
		Upper Fiber			Mid Fiber			Lower Fiber		
		Cond.	N_1 kN/m (lb/in)	N_2 kN/m (lb/in)	Cond.	N_1 kN/m (lb/in)	N_2 kNm (lb/in)	Cond.	N_1 kNm (lb/in)	N_2 kNm (lb/in)
145 (21.0)	Nonintegral	Cruise	277 (1582)	542 (3097)	Cruise	274 (1563)	551 (3145)	Cruise	283 (1615)	559 (3194)
	Integral	PLA	690 (3983)	415 (2370)	Cruise	297 (1698)	482 (2753)	Neg Man	395 (2256)	401 (2288)
207 (30.0)	Nonintegral	Cruise	412 (2356)	813 (4645)	Cruise	409 (2337)	822 (4694)	Cruise	418 (2388)	830 (4741)
	Integral	PLA	846 (4830)	658 (3755)	Cruise	442 (2524)	718 (4103)	Neg Man	544 (3105)	645 (3684)
276 (40.0)	Nonintegral	Cruise	562 (3211)	1114 (6359)	Cruise	559 (3195)	1122 (6406)	Cruise	568 (3244)	1130 (6455)
	Integral	PLA	1010 (5772)	927 (5295)	Cruise	597 (3411)	981 (5602)	Neg Man	709 (4049)	915 (5227)

7.2.4.3.1 Nonintegral Tank Design: The pressurization study conducted on the nonintegral tank design was performed using the minimum-weight design from the concept screening study, i.e., an unstiffened wall configuration for the tank with a hat-stiffened fuselage. The same panels designed for the concept screening study were used as the baseline (145 kPa (21 psia)) tank design. A different set of panels was sized for each higher pressure case. The various wall thicknesses at the quarter length station are presented in Table 74. All of these designs are fail-safe critical at each circumferential location for each nominal tank pressure. As such, they are constant over the range of strap spacings. The subcomponents (straps and NOF) are increased from the baseline case by means of load ratios for each higher pressure with variations circumferentially but not longitudinally. The various components are combined to define the total unit weights. There is an insignificant variation in unit weight with strap spacing at each circumferential location. Table 75 presents the minimum weights for each pressure and circumferential location, all of which occur at the largest strap spacing 50.8 cm (20.0 in.). The average circumferential weights are also shown. These average unit weights are plotted versus strap spacing in Figure 166. All of the nonintegral designs reveal small variations with strap spacing and minor effects of the subcomponents with the design being dominated by the weight of the panel.

The designs of the three-quarter length station were extrapolated, via load ratios applied to the one quarter length location. The weights of these two point design regions were then combined with weights of the tank domes to obtain a total tank weight for each pressure intensity.

7.2.4.3.2 Integral Tank Design: At the quarter length station the zee-stiffened panel concept was evaluated at the upper fiber location with respect to frame spacing for each candidate pressure. The wall thicknesses for these designs are constant at 0.721 cm (0.284 in.), 0.853 cm (0.336 in.), and 1.036 (0.408 in.), for the design pressures of 145, 207, and 276 kPa (21, 30, and 40 psia), respectively, regardless of frame spacing. As noted previously, all of the upper fiber designs contain longitudinal fail-safe straps centered between the stiffeners with an area of 1.29 cm^2 (0.20 in^2).

The dominance of the fail-safe requirements at 145 kPa (21 psia) and the combination of fail-safe and complex stress requirements at the higher pressures, accounts for the constant equivalent thickness over the range of frame spacings. The panel equivalent thicknesses are combined with the subcomponents (straps and frames) and the nonoptimum factor to obtain the total unit weights which are shown in Figure 167.

The only subcomponent variation experienced was the increase of the circumferential strap equivalent thickness which was found by means of load ratios applied to the baseline case. The strength consideration in the frame design is generally not a controlling factor, especially at larger spacings, nor is the nonoptimum factor (NOF) variation of great enough magnitude to be accounted for.

TABLE 74. - VARIATION OF TANK WALL THICKNESS WITH INTERNAL PRESSURE, NONINTEGRAL DESIGN

Nominal Tank Pressure kPa (psia)	Tank Wall Equivalent Thickness, cm (in.)[1]			
	Upper Fiber	Mid Fiber	Lower Fiber	Average
145 (21.0)	0.389 (0.153)	0.384 (0.151)	0.396 (0.156)	0.386 (0.152)
207 (30.0)	0.577 (0.227)	0.572 (0.225)	0.584 (0.230)	0.577 (0.227)
276 (40.0)	0.787 (0.310)	0.782 (0.308)	0.795 (0.313)	0.787 (0.310)

(1) Quarter length point design region.

TABLE 75. - VARIATION OF TANK UNIT WEIGHT WITH INTERNAL PRESSURE, NONINTEGRAL DESIGN

Nominal Tank Pressure kPa (psia)	Tank Unit Weight, kg/m^2 (lb/sq ft)[1][2]			
	Upper Fiber	Mid Fiber	Lower Fiber	Average
145 (21.0)	23.92 (4.90)	22.46 (4.60)	21.48 (4.40)	22.56 (4.62)
207 (30.0)	30.08 (6.16)	28.76 (5.89)	27.73 (5.68)	28.86 (5.91)
276 (40.0)	37.11 (7.60)	35.74 (7.32)	34.71 (7.11)	35.84 (7.34)

(1) Quarter length point design region

(2) All data reflects a fail-safe strap spacing of 50.8 cm (20.0 in.)

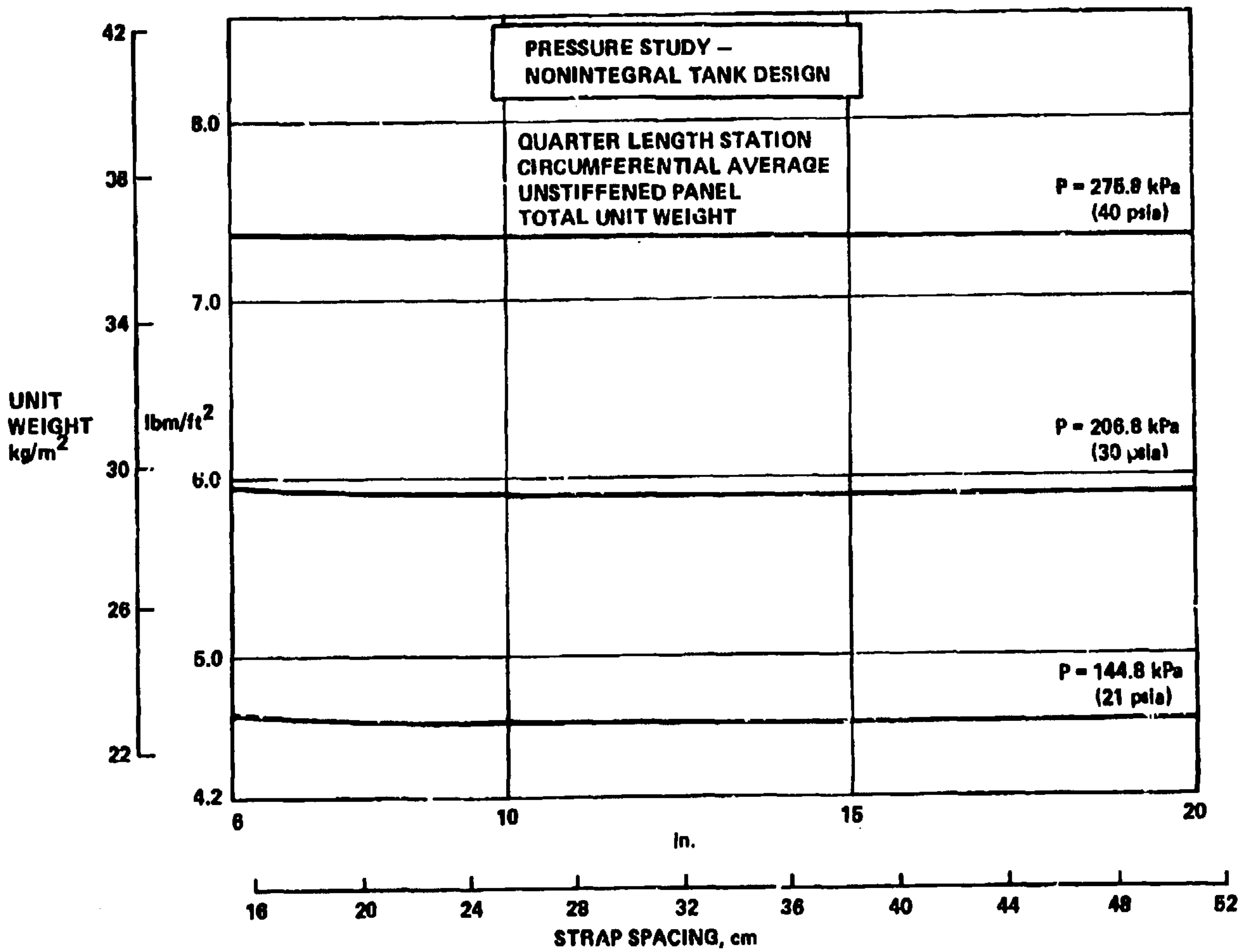

Figure 166. Variation in average circumferential weight with internal pressure, nonintegral tank design

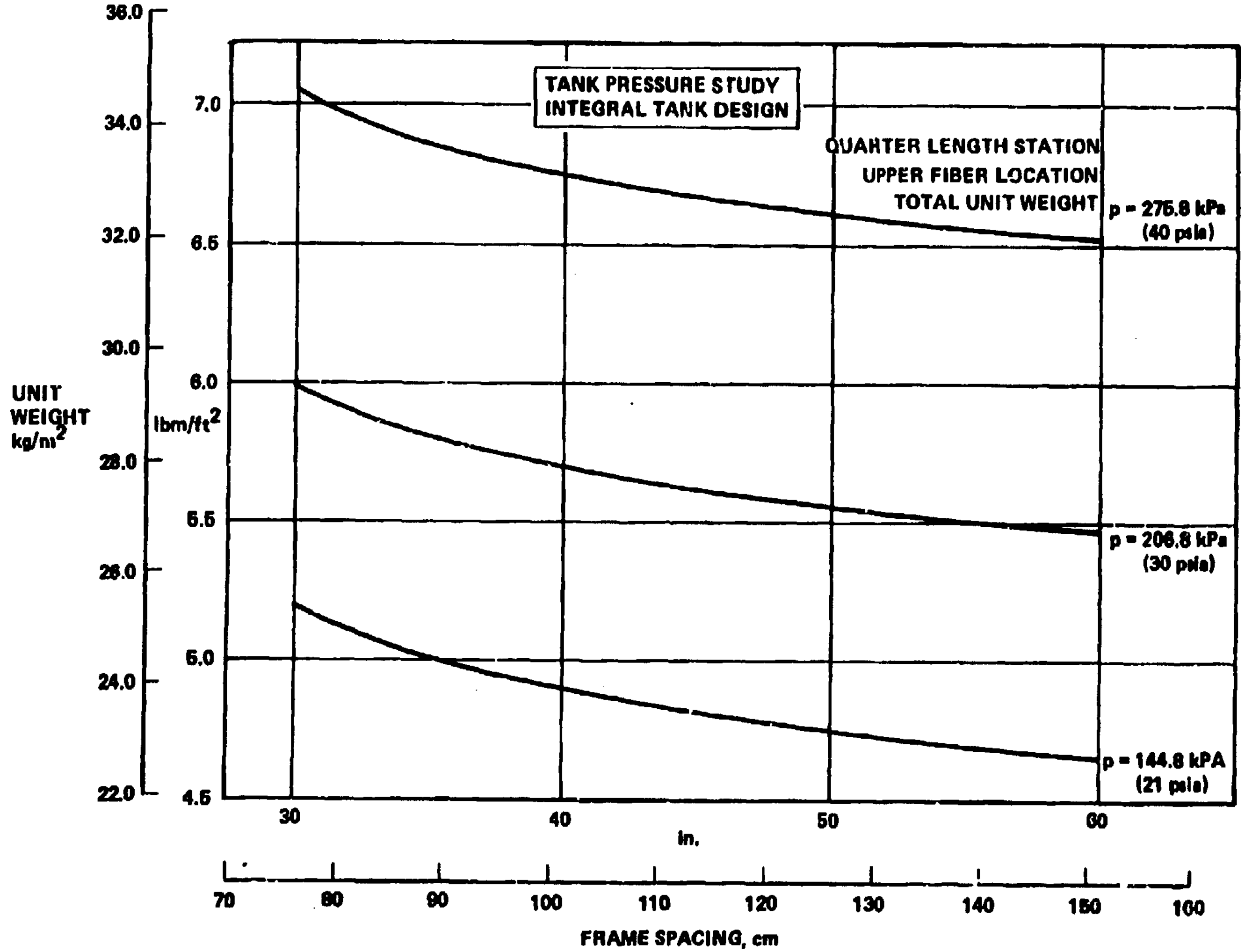

Figure 167. Variation in tank unit weight with internal pressure, integral design

The unit total weight plots display continuously decreasing curves with a decelerating rate as frame spacing increases. A drop-off of the subcomponent effect is indicated by the decreasing curves for a constant panel weight. Minimum-weight panel designs are found at the maximum frame spacing investigated, 152.4 cm (60 inches). As expected, the panel designed for 145 kPa (21 psia) is the lightest and the 276 kPa (40 psia) the heaviest. Minimum-weight designs for the 145 kPa (21 psia), 207 kPa (30 psia) and 276 kPa (40 psia) are 22.8 kg/m^2 (4.66 lb/ft^2), 26.7 kg/m^2 (5.46 lb/ft^2) and 31.9 (6.53 lb/ft^2), respectively.

The panel concept at the mid-fiber location is the fail-safe critical, unstiffened skin configuration with thicknesses of 0.417 cm (0.164 in.), 0.622 cm (0.245 in.) and 0.851 cm (0.335 in.) representing 145 kPa (21 psia.), 207 kPa (30 psia.), and 276 kPa (40 psia.), respectively. These thicknesses are constant over the range of frame spacings. Similar to the upper fiber total weight curves, the mid-fiber location has a minimum-weight spacing of 152.4 cm (60 in.) and corresponding weights of 13.1 kg/m^2 (2.68 lb/ft^2), 19.3 kg/m^2 (3.96 lb/ft^2) and 26.3 kg/m^2 (5.38 lb/ft^2) for 145 kPa (21 psia.), 207 kPa (30 psia.), and 276 kPa (40 psia.), respectively.

The variation of the panel thicknesses for the lower fiber location at the quarter length station are presented in Figure 168. Note that the 145 kPa (21 psia.) case does not employ longitudinal fail-safe straps but that they are included in the 207 kPa (30 psia) and 276 kPa (40 psia) cases. This situation is necessitated by the added tension load brought on by the higher pressures. The straps are centered between stiffeners with an area of 1.29 cm^2 (0.2 in^2). The use of straps for the 145 kPa (21 psia.) case, or the deletion of straps for the higher pressures, would result in much higher equivalent thicknesses. Although the usage indicated in Figure 164 does not alter the one-to-one comparison, the designs represented are minimum weights.

With reference to Figure 168, the nonlinearities between the panel thickness curves can best be explained by describing the critical failure modes for each design. The panels designed for the baseline pressure case (145 kPa (21 psia)) are fail-safe critical at the lower frame spacings with local buckling becoming predominate as frame spacing increases. For the 207 kPa (30 psia) design condition, fail safe, strength, and local buckling modes are active at various frame spacings. The fail-safe criteria are dominate at the lower frame spacings, whereas the basic strength and local buckling modes constrain the designs at higher spacings.

The further increase of pressure to 276 kPa (40 psia) results in fail-safe dominance for all frame spacings. The cross-sectional geometry is proportioned by basic strength and local buckling requirements.

Plots of the total weight at the lower fiber location are presented in Figure 169. A minimum weight frame spacing is noted for each pressure condition. The corresponding weights for these designs are 17.8 kg/m^2 (3.64 lb/ft^2), 20.5 kg/m^2 (4.19 lb/ft^2) and 25.1 kg/m^2 (5.14 lb/ft^2) for the 145 kPa (21 psia), 207 kPa (30 psia) and 276 kPa (40 psia) conditions, respectively.

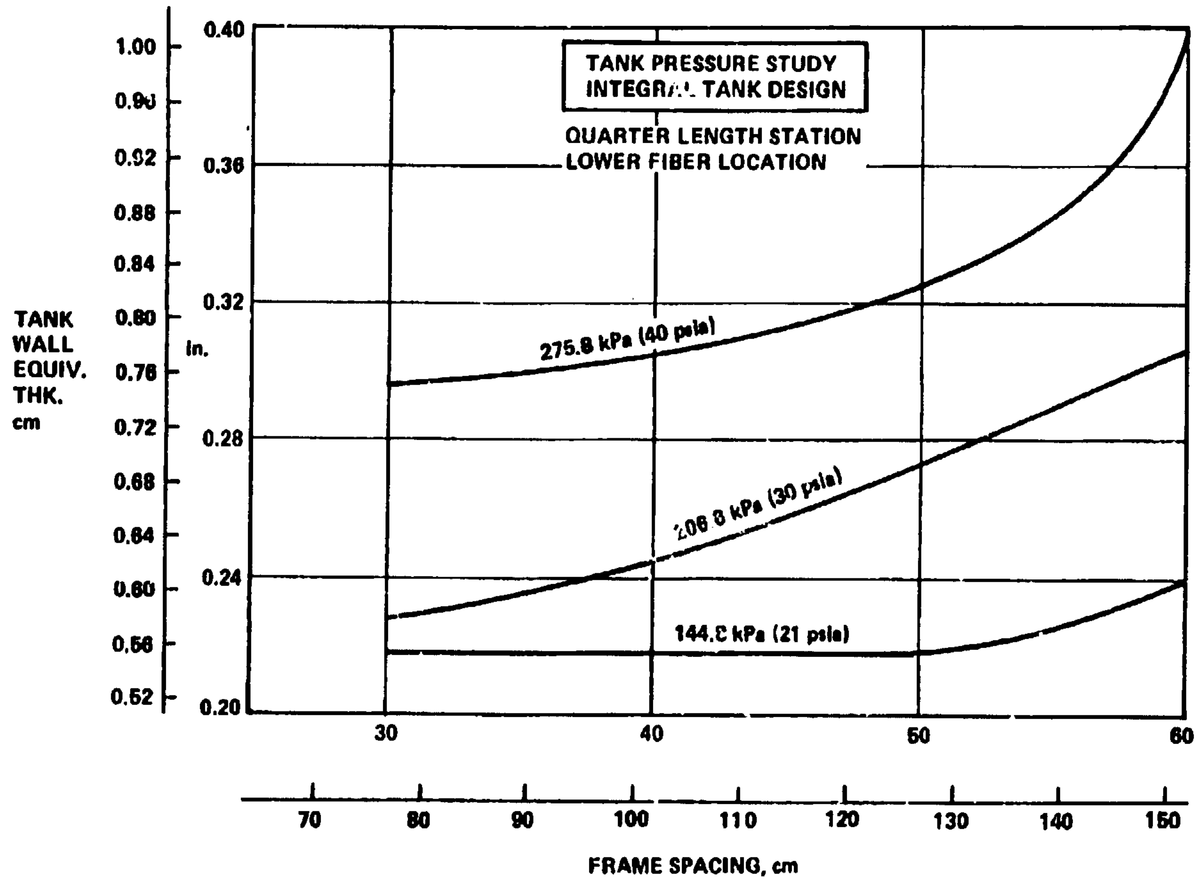

Figure 168. Variation in tank wall equivalent thickness with internal pressure, integral tank design

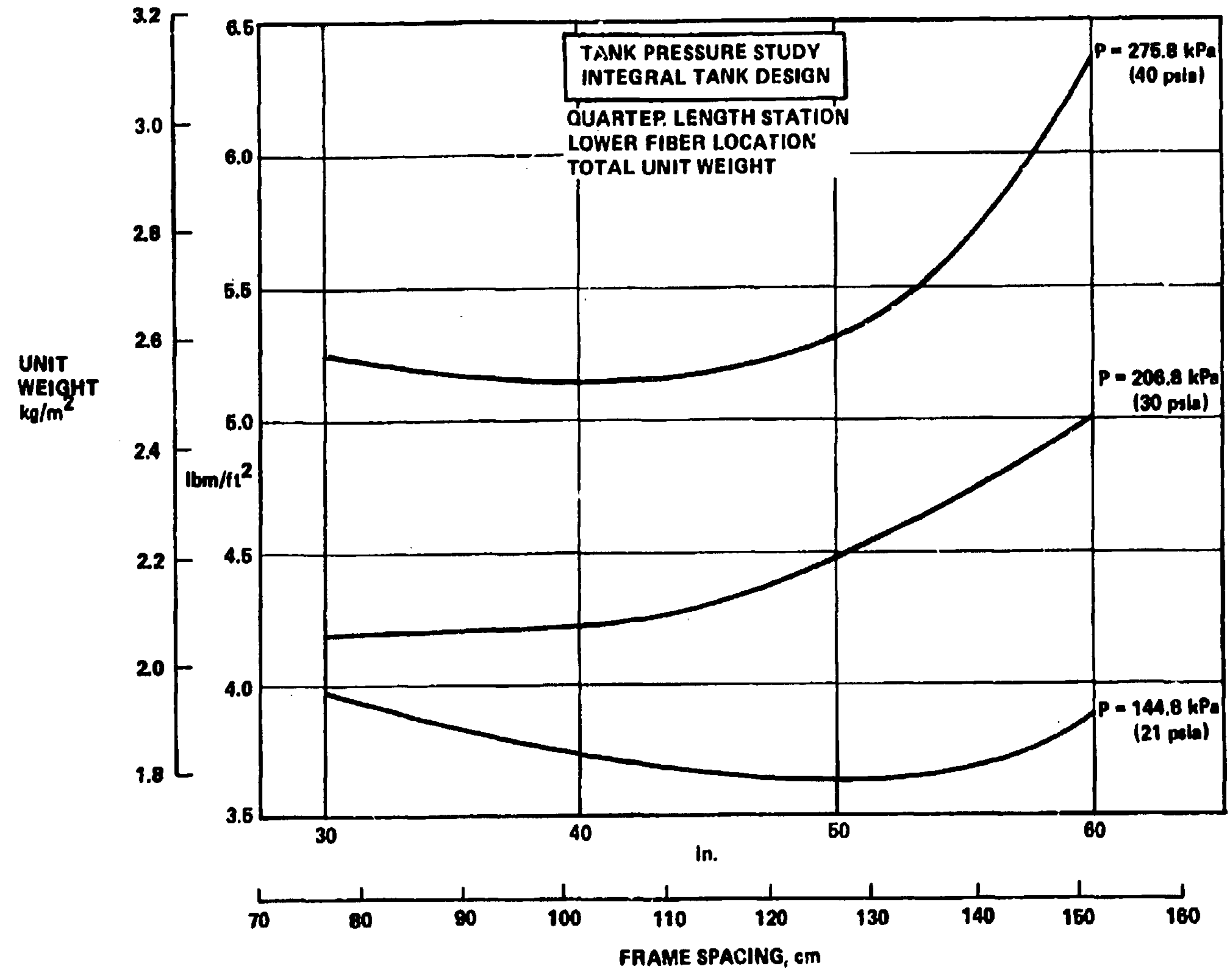

Figure 169. - Variation in tank unit weight with internal pressure, integral design

At the quarter-length station, the unit weights of the panel designs at the three circumferential locations are averaged to obtain a unit weight for the complete cross-section which is presented in Figure 170. Optimum frame spacings of 137 cm (54 in.), 127 cm (50 in.), and 127 cm (50 in.) are noted for the 145 kPa (21 psia), 205 kPa (30 psia) and 276 kPa (40 psia) pressures cases, respectively. The corresponding weights are 16.7 kg/m^2 (3.43 lb/ft^2), 21.9 kg/m^2 (4.49 lb/ft^2) and 27.7 kg/m^2 (5.67 lb/ft^2), respectively.

The unit weights at the three-quarter length station were obtained by extrapolating, using load ratios, the unit weights at the quarter length station. These data were then combined with the weights of the tank domes designed for the various pressure cases to calculate the total tank weights which are presented in Section 7.2.4.3.3.

7.2.4.3.3 Conclusions: The results of the tank pressurization study are shown in Table 76 for both the nonintegral and integral tanks. Optimum tank weights are shown, in addition to weight of the body shell required in conjunction with nonintegral tanks over the tank conical section. As would be expected, the weight of the nonintegral tank is very nearly directly proportional to nominal design pressure. This is not the case for the integral tanks, where a significant portion of the tank cylinder is designed by body shear and bending loads in addition to tank pressure loads. The results are also plotted in Figure 171 and show that as tank pressure is increased the tank weights tend to converge. This is due to the reduced influence of body loads on the integral tank at higher pressures.

Table 77 shows the optimum tank and body shell thicknesses along with tank dimensions used in this study. Using the results of the concept screening study, it was found that the weight of the tank conical section could be approximated (within 1%) by the following equation:

$$W_{\text{tank cone}} = (W_{0.25L} + W_{0.75L}) \left(\frac{L\ \text{tank cone}}{2}\right)$$

The above equation was used to calculate the weight of the tank conical section and body shell.

The effect of higher tank pressures on liquid hydrogen boiloff is reported in section 7.1.6.2.3. That analysis shows that approximately 213 kg (470 lb) of LH_2 could be saved from being vented in flight if a tank pressure of 276 kPa (40 psia) is used instead of the nominal value of 145 kPa (21 psia). A similar weight of LH_2 could be saved from being vented during the tank filling operation, however that is a less valuable saving because the vent gases are recovered and reliquefied.

In any event, design for the higher tank pressure is not a worthwhile proposition because the tremendous weight penalty associated with the structural design makes the cost saving afforded by the reduced boiloff trivial by comparison.

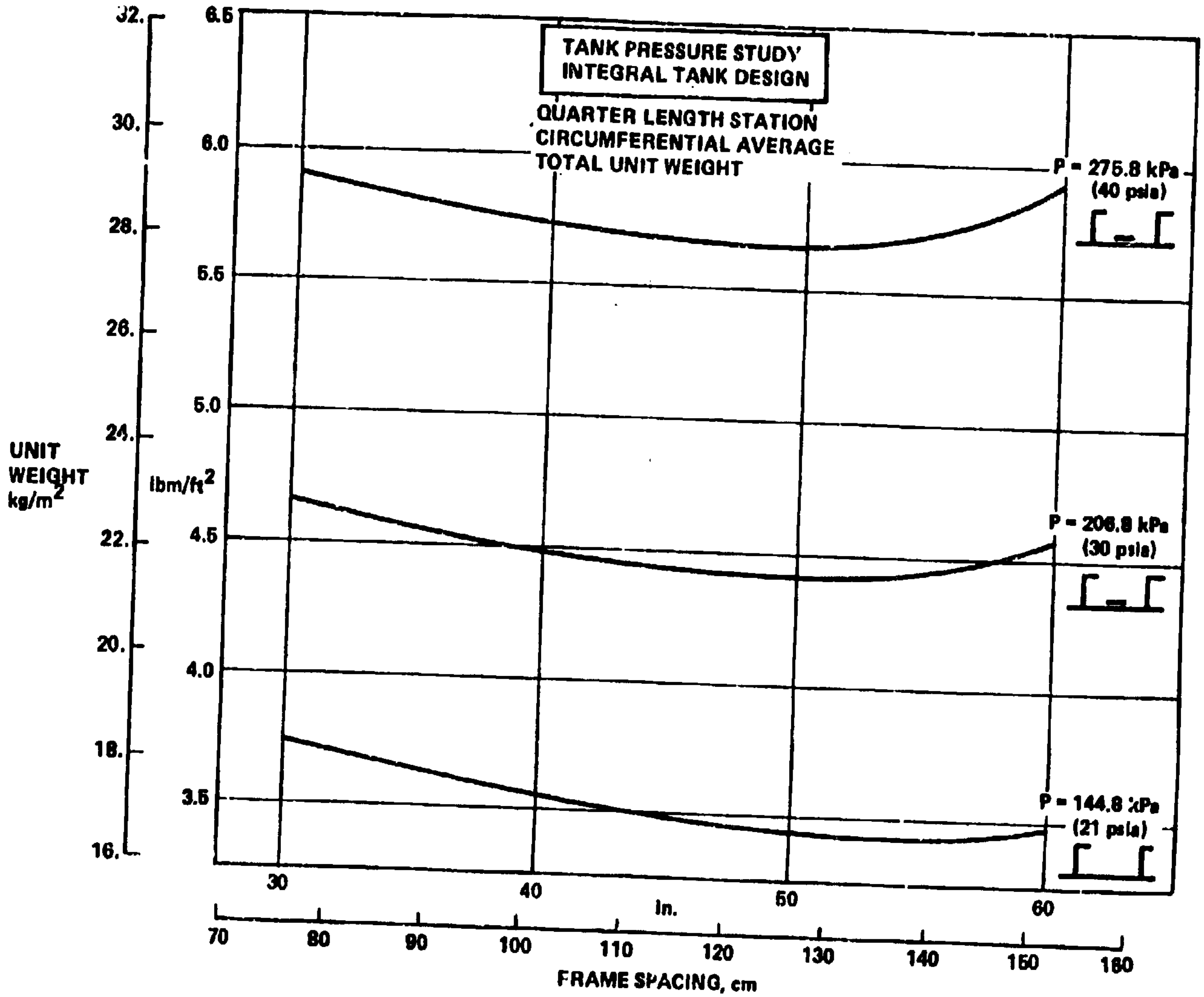

Figure 170. Variation in average circumferential weight with internal pressure, integral design

TABLE 76. - LH_2 AFT TANK PRESSURIZATION STUDY RESULTS

Item	Nonintegral, kg (lbm)			Integral, kg (lbm)		
Nominal Pressure, kPa (psia)	145 (21)	207 (30)	276 (40)	145 (21)	207 (30)	276 (40)
Tank	2154 (4749)	3138 (6918)	4252 (9374)	2669 (5884)	3476 (7663)	4390 (9678)
Cylindrical Section	1723 (3799)	2558 (5640)	3504 (7726)	2201 (4852)	2843 (6267)	3572 (7876)
Dome Ends	303 (669)	452 (997)	620 (1367)	332 (732)	497 (1096)	681 (1502)
Divider Dome	127 (281)	127 (281)	127 (281)	136 (300)	136 (300)	136 (300)
Body Shell (over tank conical section only)	1328 (2928)	1328 (2928)	1328 (2928)	—	—	—
Total	3482 (7677)	4466 (9846)	5580 (12 302)	2669 (5884)	3476 (7663)	4390 (9678)

TABLE 77. - TANK PRESSURIZATION STUDY AFT TANK

NONINTEGRAL - Optimum $\bar{t}$, cm (in.) (including frames and fail-safe straps)									
Location on Tank Circumference		Body Shell		Nominal Pressure kPa (psia)					
				145 (21)		207 (30)		276 (40)	
		L/4	3/4L	L/4	3/4 L	L/4	3/4 L	L/4	3/4 L
Upper		0.399 (0.157)	0.358 (0.141)	0.465 (0.183)	0.368 (0.145)	0.686 (0.270)	0.546 (0.215)	0.942 (0.371)	0.752 (0.296)
Mid		0.264 (0.104)	0.231 (0.091)	0.460 (0.181)	0.368 (0.145)	0.688 (0.271)	0.546 (0.215)	0.940 (0.370)	0.752 (0.296)
Lower		0.302 (0.119)	0.269 (0.106)	0.475 (0.187)	0.368 (0.145)	0.701 (0.276)	0.546 (0.215)	0.953 (0.375)	0.752 (0.296)
Avg.	$\bar{t}$ cm (in.)	0.307 (0.121)	0.272 (0.107)	0.465 (0.183)	0.368 (0.145)	0.691 (0.272)	0.546 (0.215)	0.945 (0.372)	0.752 (0.296)
	$\bar{w}$ kg/m^2 (psf)	8.50 (1.74)	7.52 (1.54)	12.89 (2.64)	10.20 (2.09)	19.14 (3.92)	15.14 (3.10)	26.17 (5.36)	20.80 (4.26)
Dia. - m (ft)		5.88 (19.30)	4.77 (15.65	5.31 (17.43)	4.20 (13.79)	5.31 (17.43)	4.20 (13.79)	5.31 (17.43)	4.20 (13.79)
Tank Unit Wt-kg/m (lb/ft)		157.0 (105.5)	112.7 (75.7)	215.2 (144.6)	134.7 (90.5)	319.5 (214.7)	199.9 (134.3)	436.8 (293.5)	274.7 (184.6)
Tank Cone Wt. - kg (lb) (L Tank Cone = 9.85m (32.32'))		1328 (2928.4)		1723 (3799.2)		2558 (5639.8)		3505 (7726.1)	

INTEGRAL - Optimum $\bar{t}$, cm (in.) (including frames and fail-safe straps)						
Location on Tank Circumference	Nominal Pressure - kPa (psia)					
	145 (21)		207 (30)		276 (40)	
	L/4	3/4 L	L/4	3/4 L	L/4	3/4 L
Upper	0.836 (0.329)	0.798 (0.314)	0.975 (0.384)	0.904 (0.356)	1.166 (0.459)	1.057 (0.416)
Mid	0.475 (0.187)	0.384 (0.151)	0.701 (0.276)	0.561 (0.221)	0.950 (0.374)	0.762 (0.300)
Lower	0.643 (0.253)	0.559 (0.220)	0.790 (0.311)	0.676 (0.266)	0.922 (0.363)	0.787 (0.310)
Avg. cm (in.) $\bar{t}_{AVG}$	0.607 (0.239)	0.531 (0.209)	0.792 (0.312)	0.676 (0.266)	1.001 (0.394)	0.843 (0.332)
kg/m^2 (psf) $\bar{w}_{AVG}$	16.80 (3.44)	14.70 (3.01)	21.92 (4.49)	18.70 (3.83)	27.68 (5.67)	23.34 (4.78)
Dia. ~ m (ft)	5.48 (17.97)	4.42 (14.51)	5.48 (17.97)	4.42 (14.51)	5.48 (17.97)	4.42 (14.51)
Tank Unit Wt. (W) - kg/m (lb/ft)	289.0 (194.2)	204.2 (137.2)	377.2 (253.5)	259.8 (174.6)	476.4 (320.1)	324.3 (217.9)
Tank Cone Wt.~kg(lb) (L = 8.92 m (28.28 ft))	2201 (4851.7)		2843 (6267.4)		3573 (7876.3)	

C-3

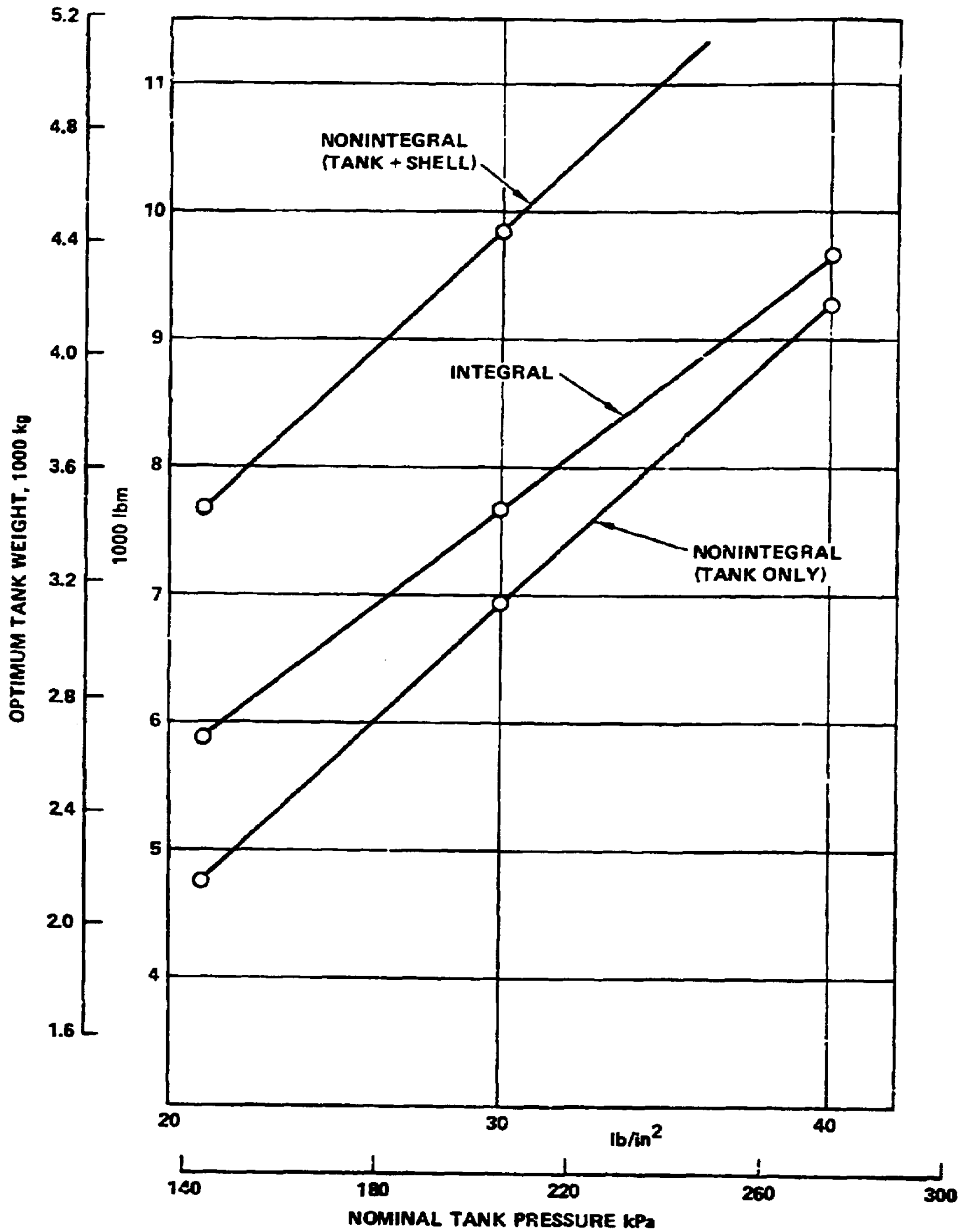

Figure 171. Weight vs nominal pressure for integral and nonintegral tanks.

7.2.4.4 Pressure stabilization study: The objective of the pressure stabilization study was to investigate the effect of internal tank pressurization on the buckling strength of typical LH_2 tanks. Based on the results of the concept screening analysis, the tankage for the baseline nonintegral tank design is tension designed; hence, stability is not a critical design factor. Therefore, only the integral tank design was considered for this study.

7.2.4.4.1 Approach: A BOSOR4 structural model was established using the baseline integral tank configuration (Section 7.2.3.3) and the tank wall data resulting from the concept screening analysis (Section 7.2.3.6). Using this model as the foundation for this study the following approach was taken, illustrated in Figure 172.

1. The tank was analyzed for the ultimate load condition, without internal pressurization, to ascertain if the basic design criteria is met. Point A in Figure 172.

2. The above step was repeated using limit loads, without internal pressurization, to assess the structural margin available in this design. Point B in Figure 172.

3. The stiffness of the structure was reduced so that the buckling load exactly equals the limit load. This stiffness reduction was accomplished by a reduction in the modulus of elasticity, which is approximately equivalent to a reduction in the thicknesses of the various shell components. Point C in Figure 172.

4. A constant internal pressure was added to the reduced stiffness configuration (step 3) until the buckling load equals 1.5 times the limit loads; i.e., the structure meets the ultimate load criteria. Curve $C\text{-}D_3$ in Figure 172.

5. The damage tolerance criteria was applied to the reduced stiffness tank wall configuration of step 4.

6. The amount of weight savings was assessed.

7.2.4.4.2 Model definition: The geometric configuration for the selected tank (the aft tank) is shown in Figure 173. Fore and aft of the tank a short segment of the fuselage structure is added to the mathematical model to insure that the boundaries are properly accounted for. The forward end of the model is assumed to be clamped, the aft end is free.

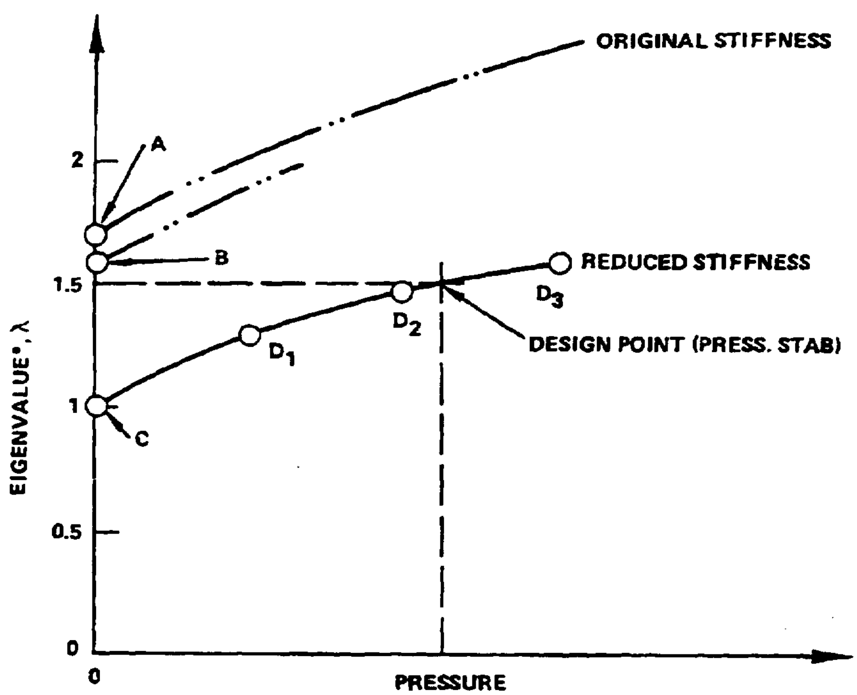

*THE EIGENVALUE BASED ON ULTIMATE LOAD IS ASSUMED TO BE MULTIPLIED BY 1.5

Figure 172. Analysis sequence - pressure stabilization study

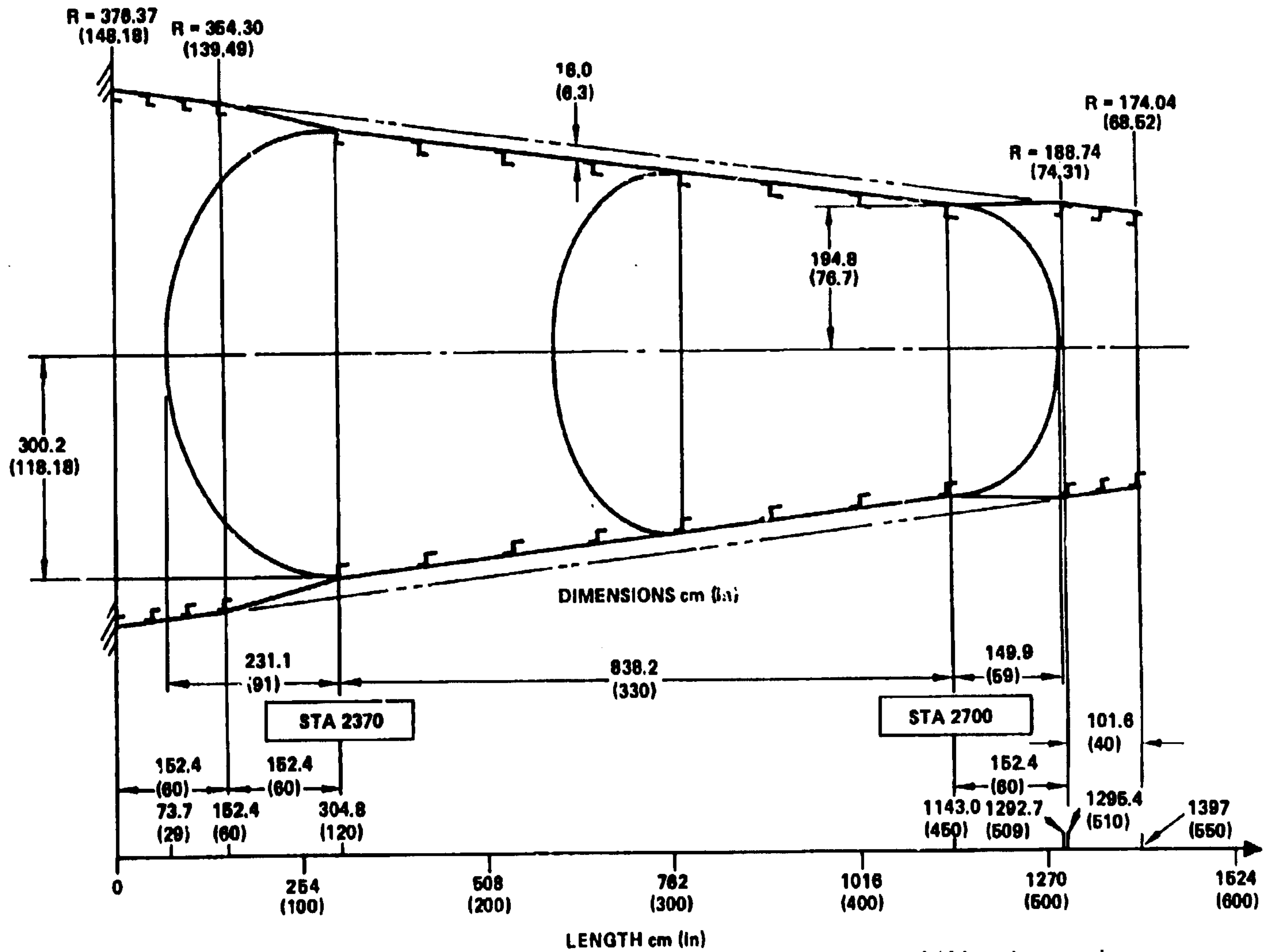

Figure 173. Integral tank configuration used for pressure stabilization study

The loading consists of air loads and inertial loads. At sta 2370 (see Figure 173) the total limit moment is 9.3 MN-m (82×10^6 in lb) and the limit shear 95.6 kN (215 000 lb). At sta 2700 the moment is 3.69 MN-m (32.7×10^6 in. lb) and the shear is 511.5 kN (115 000 lb). The structure is assumed weightless, except for the tank, where the structure and fuel weigh 18 144 kg (40 000 lb). With a load factor of 2.5 the inertia mass of the tank is 45 359 kg (100 000 lb) which was distributed axially in proportion to the diameter of the tank. In addition to this inertia contribution, the pressure head of the tank and fuel were included in the analysis.

Representative temperatures used on the model components were: 20°C (68°F) for the fuselage, -134°C (-210°F) for the truss structure and -253°C (-423°F) for the tank.

The structure in general consists of ring- and stringer-stiffened shells. The tank-to-fuselage interface, however, consists of a tubular truss work. In the computer model the rings are modelled as discrete elements but the stringers are smeared; i.e., their various stiffnesses are added to the skin stiffness. Thus, buckling may take place between rings, but buckling between stringers is prevented. The skirts are modelled as an equivalent orthotropic shell, so that in the computer model the individual tubes cannot buckle.

The fuselage consists of a zee-stiffened 0.630 cm (0.036 in.) 0.348 cm^2 skin. The zee-stiffeners are approximately 2.54 cm (1.00 in.) high with an area of 0.348 cm^2 (0.054 $in.^2$) and a moment of inertia of 3.288 cm^4 (0.079 in^4). The sheet metal frames are spaced at 50.8 cm (20 in.), and are 10.16 cm (4 in.) deep with an area of 4.200 cm^2 (0.651 in^2) and a moment of inertia of 85.3 cm^4 (2.05 in^4). The skin and stringers are 2024-T3 aluminum, the rings of 7075-T6 aluminum.

The forward and aft interface skirts are made of tubing arranged to form a triangular truss. The angle between the tubes is approximately 0.35 rad (20°). The tubes are made of a boron/epoxy composite with an OD of 5.72 cm (2.25 in.) and an ID of 3.81 cm (1.50 in.). The modulus of elasticity is 124 GPa (18×10^6 psi). The truss members are hinged to the fuselage and to the tank, so that differential expansion or contraction of the various structures can take place without the inducement of stress.

The conical shell of the tank is made of 2219-T851 aluminum alloy with zee-stiffeners. Since BOSOR4 has the capability to handle only rotationally symmetric structures, the hoop variation of the stringer configuration was omitted. However, to compensate for the slight 3 to 8 percent deviation of the neutral axis from the center of the circular cross-section, the applied loads were adjusted to give the proper stress resultant in the critical buckling area. The section properties resulting from the concept screening analysis were used for the tank. The properties were supplied at the quarter and three-quarter length stations of the tank, and interpolated linearly between those points.

In addition to the stringers, the tank is also stiffened by frames, each with an area of 2.477 cm^2 (0.385 in^2), a moment of inertia of 23.31 cm^4 (0.560 in^4), and a depth of 7.62 cm (3 in.). The frames are made of 2219-T851 aluminum. The three domes are of monocoque design and are made of 2219-T851 aluminum. The closures are both 0.254 cm (0.1 in.) thick, the divider 0.127 cm (0.05 in.) thick. All three domes have an a/b ratio of 1.3 because this analysis was initiated before the dome shape study, section 7.2.4.1, was completed.

7.2.4.4.3 Results: The lower half of the math model showing the fuselage and tank is presented in Figure 174. The model is broken down into nine structural segments, as shown in the figure. The directions of increasing arch lengths are indicated by the arrows in the righthand part of the figure. The deformed shape of the lower portion of the structure under the ultimate load condition, unpressurized, is shown in Figure 175. The deformations are exaggerated; the aft dome does not penetrate the aft truss support structure. Note that the differential lateral displacement of the investigated structure is 6.35 cm (2.5 in.), and the axial shortening, caused by a combination of the temperature distribution and the inertia head of the fuel, is 7.11 cm (2.8 in.). The deformations are also plotted in Figure 176, where U is the meridional and W is the normal displacement.

The circumferential displacement V is zero, since the deformations are plotted for the lower extreme fiber of the structure which is a symmetry line. The stress resultants and moments, referred to the outer skin surface (not the neutral axis of the shell) are shown in Figures 177 and 178. N1 and N2 the meridional and hoop normal stress resultants, N12 is the shear stress resultant (zero, due to symmetry); M1, M2, and MT are the meridional, hoop and shear moments.

In the BOSOR4 buckling analysis the number of circumferential buckles which gives a minimum buckling load is obtained. Figure 179 shows the buckling loads (corresponding to points A and B in Figure 172) as a function of the circumferential wave number. The buckling loads are represented by the eigenvalue λ, so that

$$\text{Buckling Load} = \lambda\ (\text{Applied Load Set}) + \Delta p$$

Note that the eigenvalue is multiplied by all loads, except the internal pressure Δp. Thus, the temperature is also multiplied by λ. (However, a subsequent check showed that the buckling loads are only affected in the fourth figure by the temperature, which is due to the hinged connections between the supporting structure and the tank.)

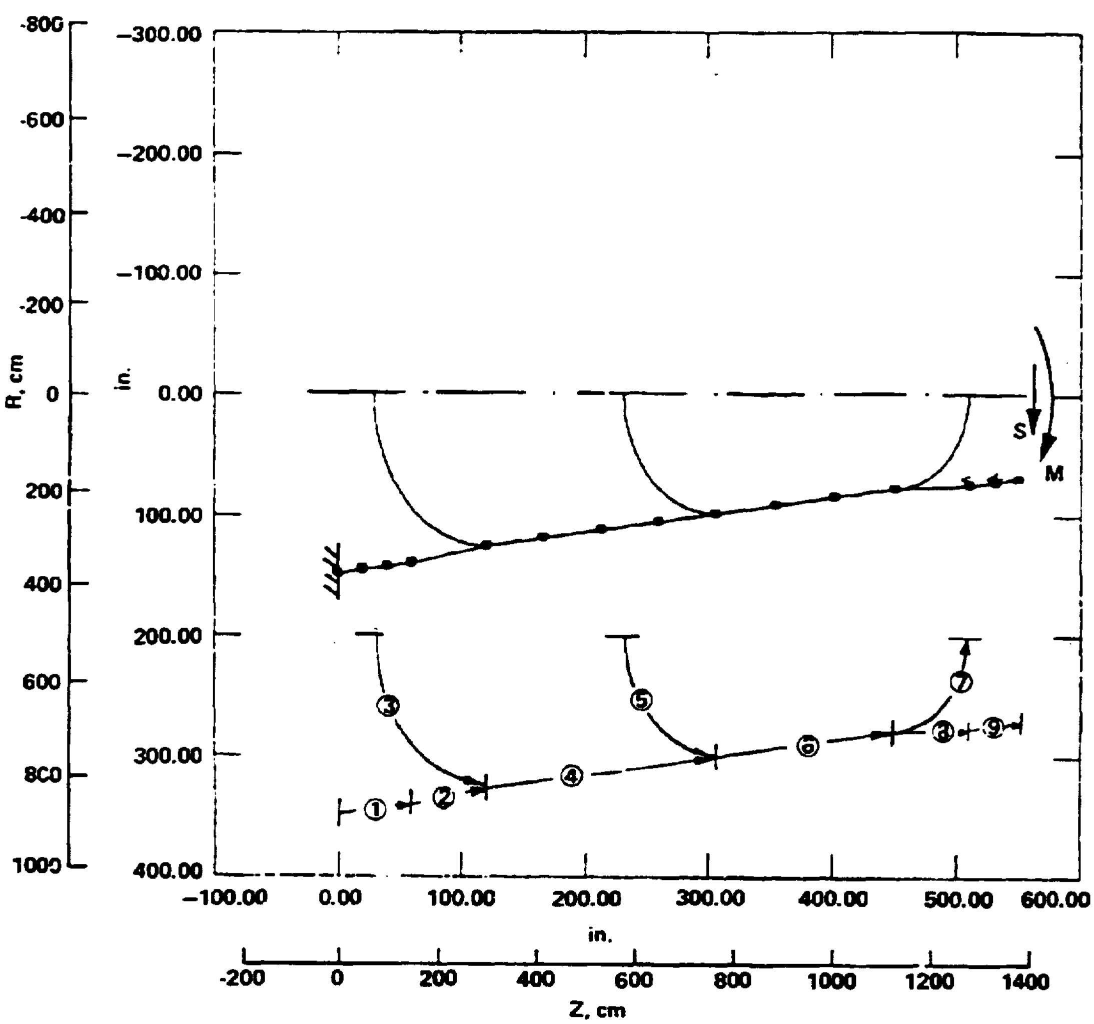

Figure 174. Computer model.

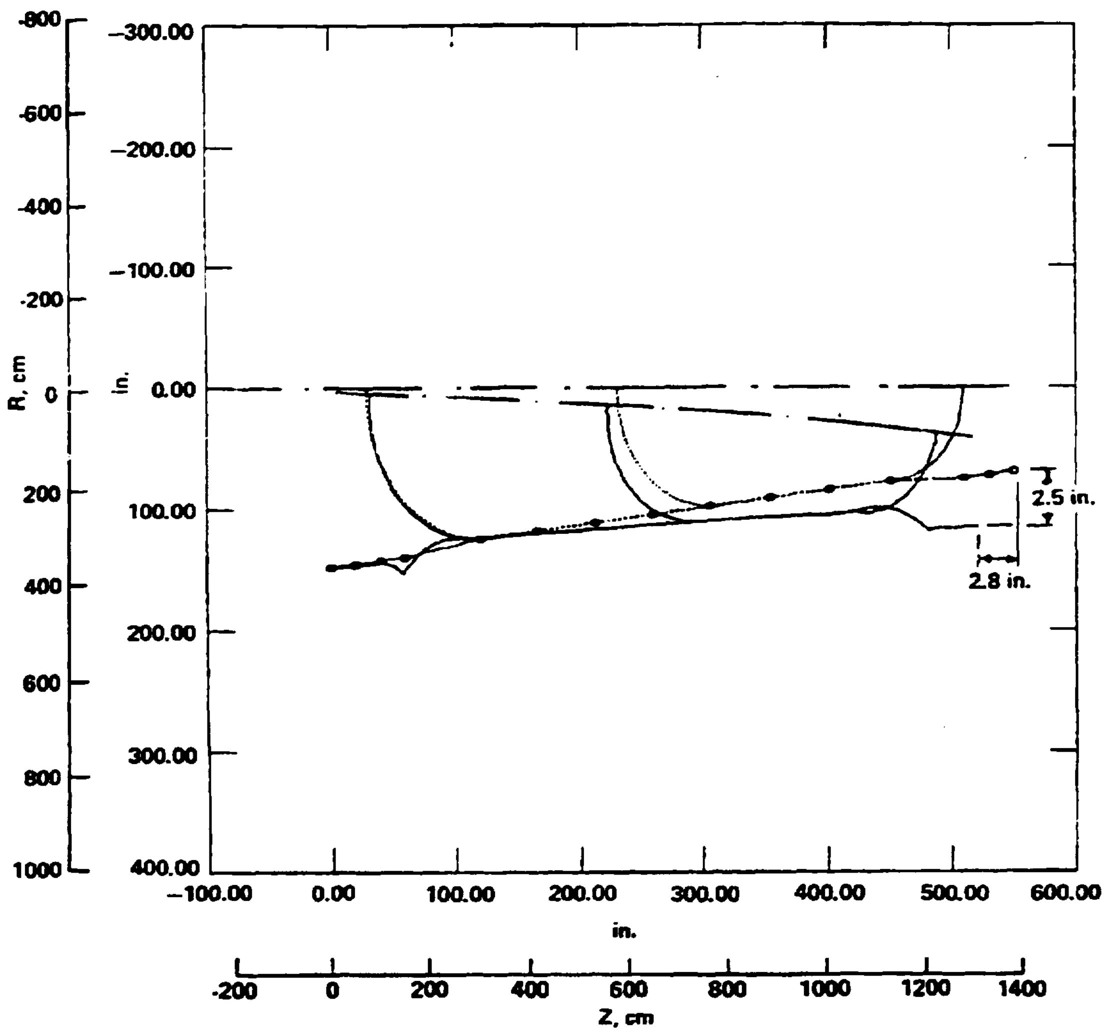

Figure 175. Deformed structure - ultimate load.

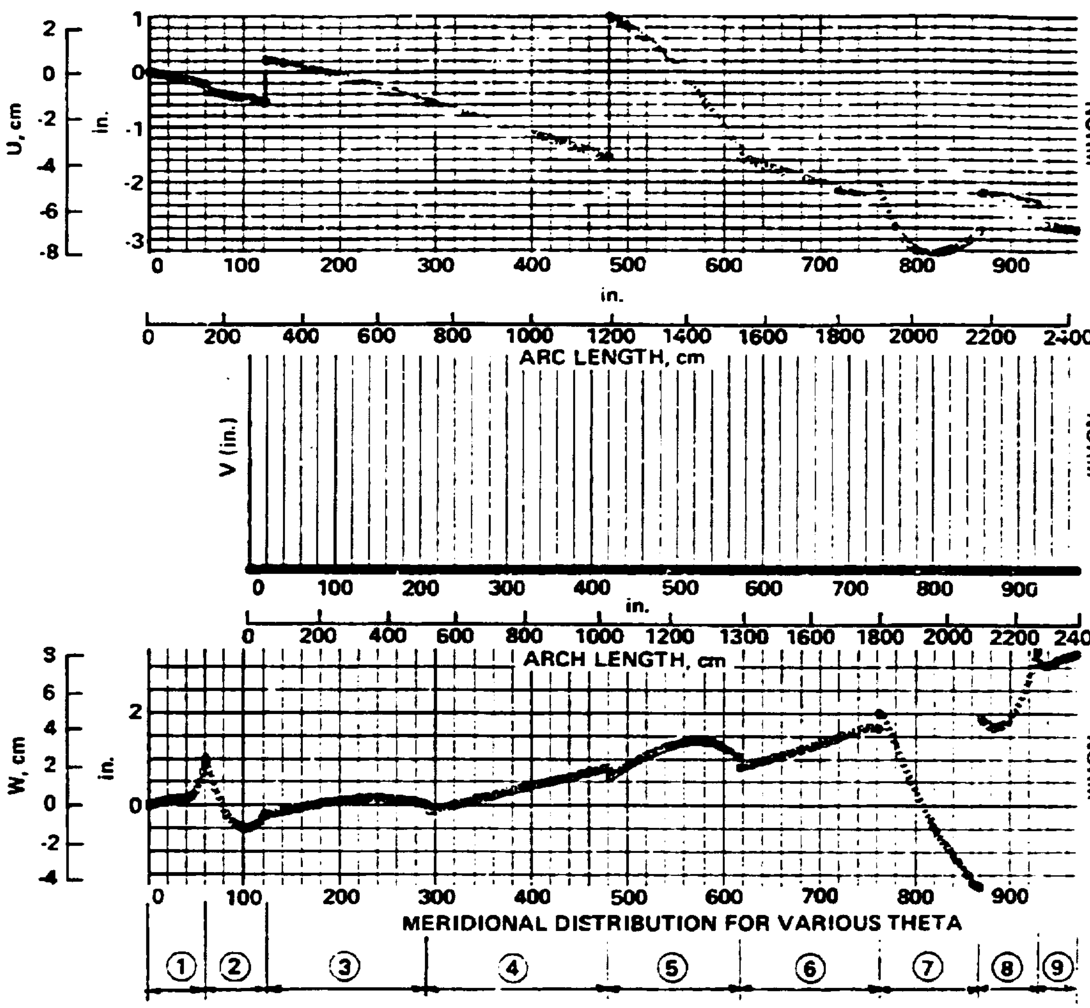

Figure 176. Deformations - ultimate load

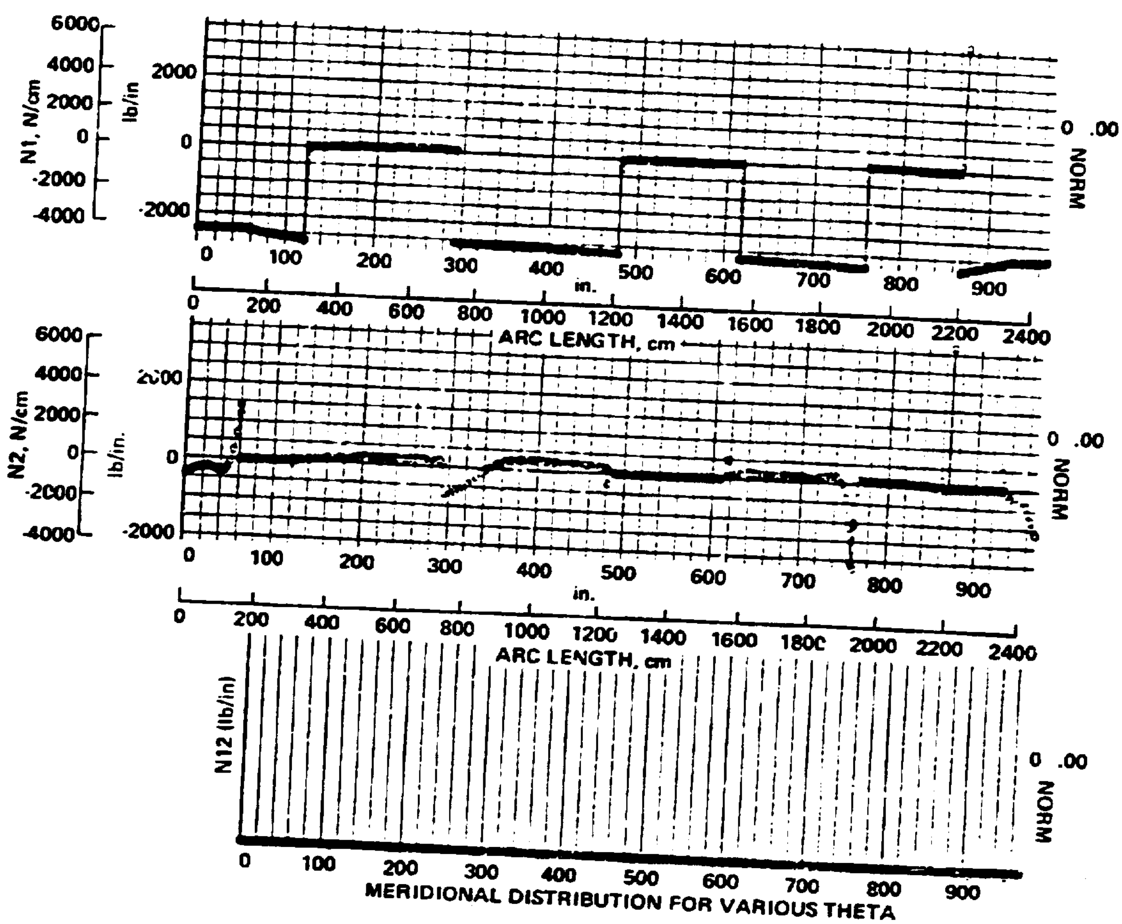

Figure 177. Stress resultants - ultimate load

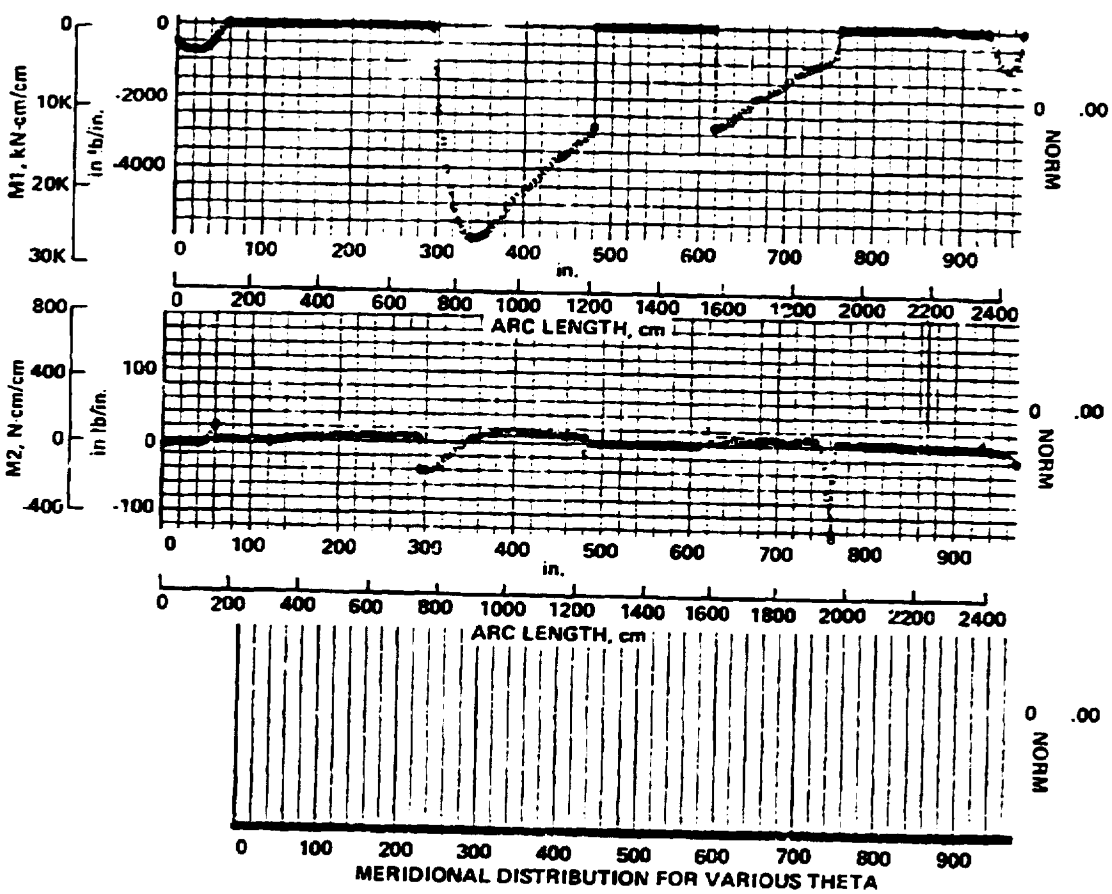

Figure 178. Moments - ultimate load

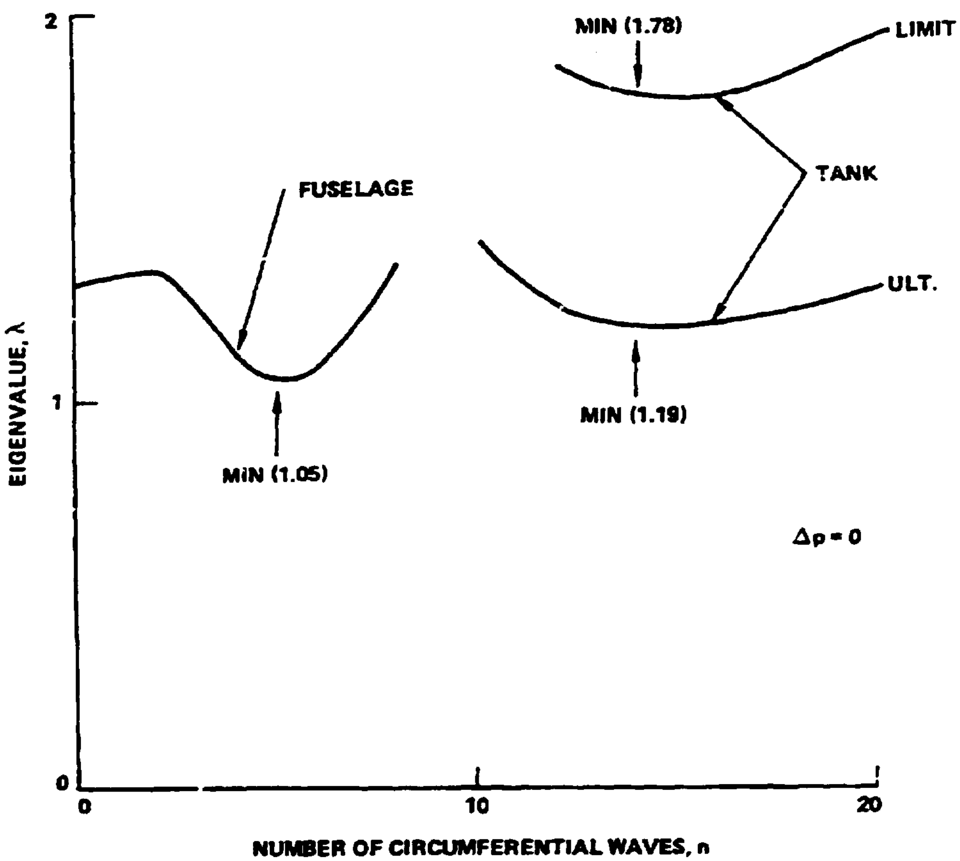

Figure 179. Initial buckling analysis, unpressurized.

There are two minima in the buckling load: one for the fuselage (λ = 1.05 ult.) and one for the tank (λ = 1.19 ult.). The axial wave shape for the fuselage is shown in Figure 180 and for the tank in Figure 181. We note that the fuselage buckling load is smaller than the buckling load for the tank. However, the present study is only concerned with the tank, so a further investigation of the fuselage is not discussed here.

Based on the results shown in Figure 179, and following the approach previously outlined, the modulus of elasticity of the skin and stringers in the tank was reduced by the limit factor 1/1.78, which results in an eigenvalue of λ = 1 for the limit design condition (see Figure 172, Point C). A subsequent series of analyses with increasing internal pressurization, Δp, was run and is shown in Figure 182. With the pressure added, the number of circumferential buckles changed from 14 to 12, but the axial mode shape remained as in Figure 181.

The addition of the internal pressure is very effective in restoring the buckling load capability to the tank wall, with a stiffness reduction of more than 40 percent (1 - 1/1.78 = 0.438) an internal pressure of only 9.3 kPa (1.35 psi) is required to increase the eigenvalue to the required value of 1.5.

The circumferential variation in wall thickness is shown in Figures 183 and 184 for the tank quarter and three-quarter length stations. These figures display the thicknesses used for the initial input to the model, the resulting reduced thicknesses when pressure stabilization is accounted for, and the thickness requirements dictated by the damage tolerance criteria.

Neglecting the damage tolerance requirements, the results of BOSOR4 bifurcated buckling analysis indicates a weight savings, corresponding to a 44 percent reduction in the tank wall thickness, is possible if pressure stabilization is utilized. However, the magnitude of this weight saving (as indicated by the increment of thickness between the initial and pressure stabilized curves on Figures 183 and 184) is too high, since the wall thicknesses input into the BOSOR4 model reflect the maximum thickness requirements at the very localized critical buckling area at the upper fibers of the tank. Hence, the thickness corresponding to this area has to be used for the entire circumference due to BOSOR's limitation of analyzing only axisymmetric structure.

Based on the results of the concept screening analysis the cross-sectional areas dictated by the damage tolerance requirements (see Figure 183 and 184) are also adequate for any local buckling modes; therefore, little or no real weight saving is indicated since these thickness values exceed those predicated on pressure stabilizing the tank.

Based on the depth of analysis of this study no significant weight saving is indicated when the tank is pressure stabilized. In the example studied, the damage tolerance requirements are the dominant design factors with stability, in most cases, only being a secondary effect. Even if a sizable weight payoff were possible, other questions would have to be answered prior to

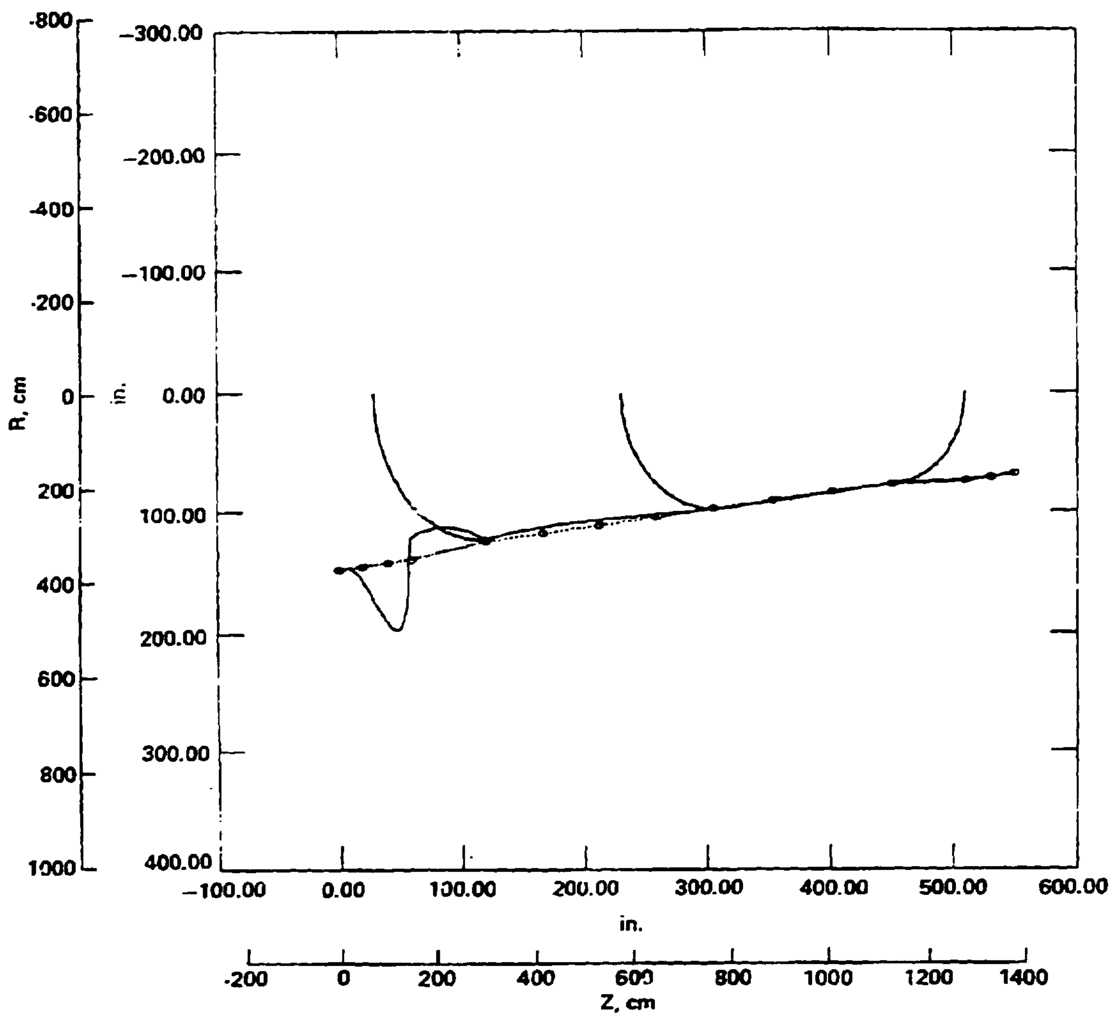

Figure 180. Fuselage buckling mode

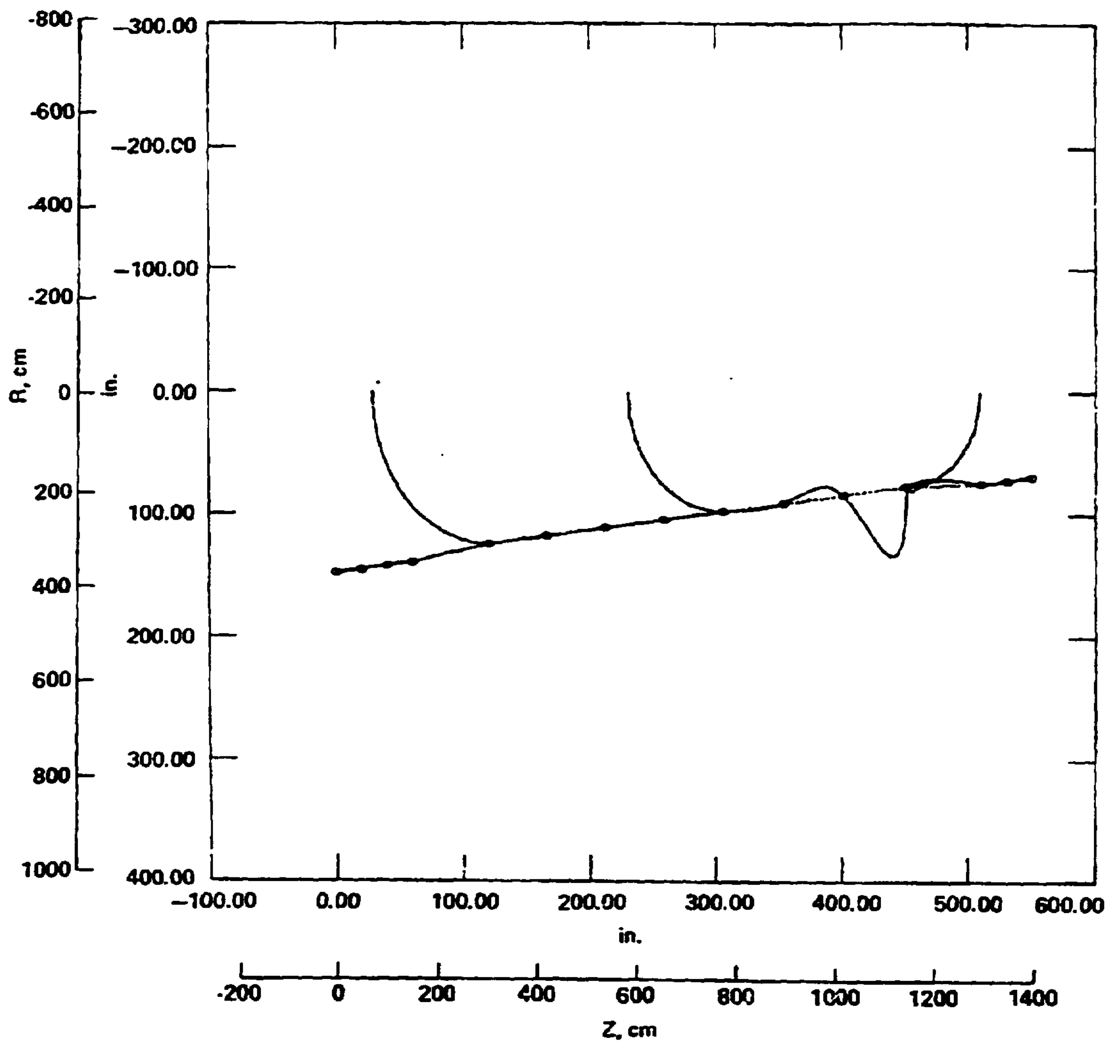

Figure 181. Tank buckling mode

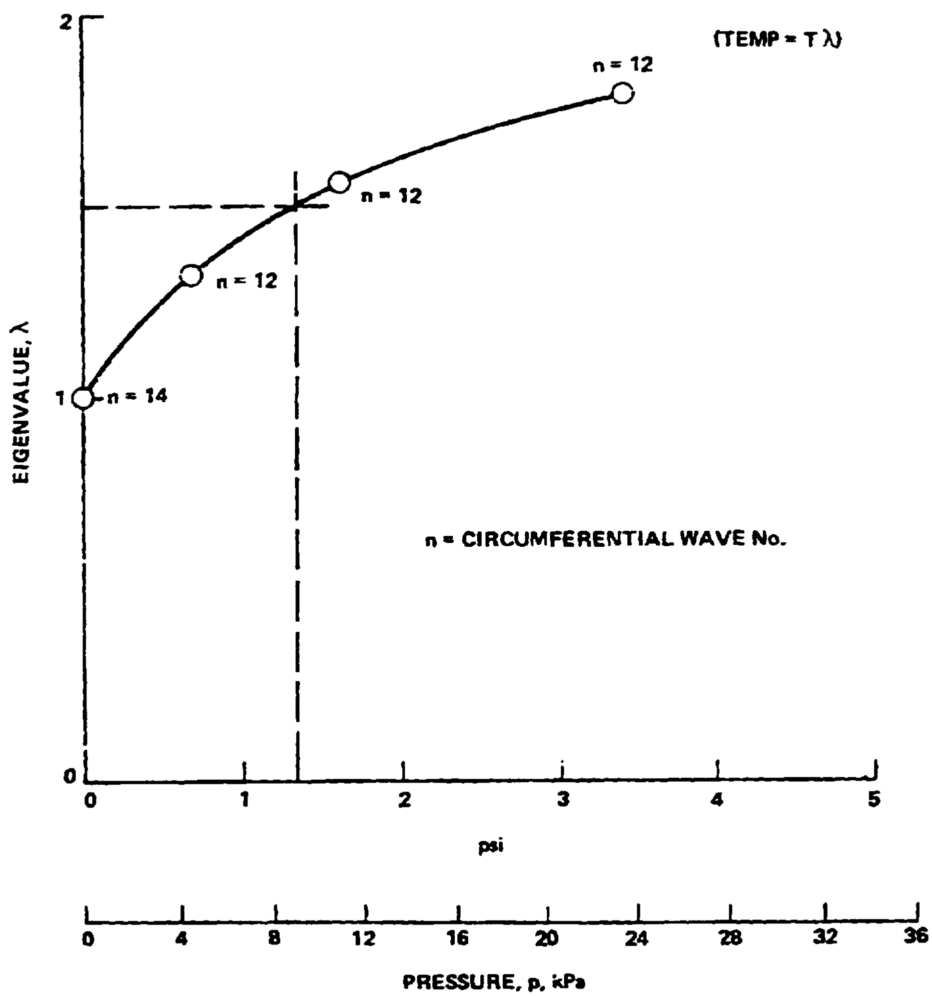

Figure 182. Variation in eigenvalue with pressure.

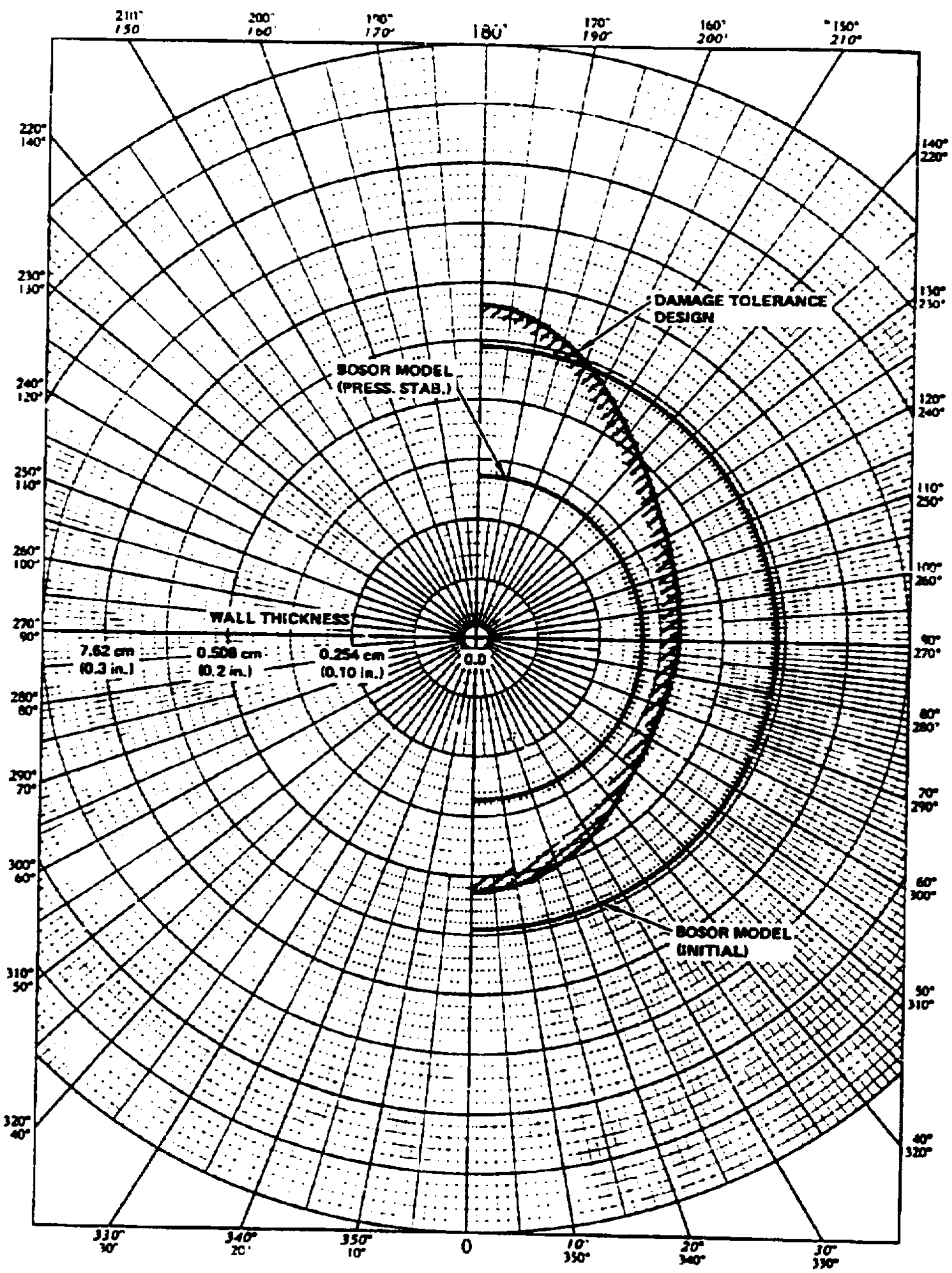

Figure 183. Circumferential variation in wall thickness at tank quarter length station.

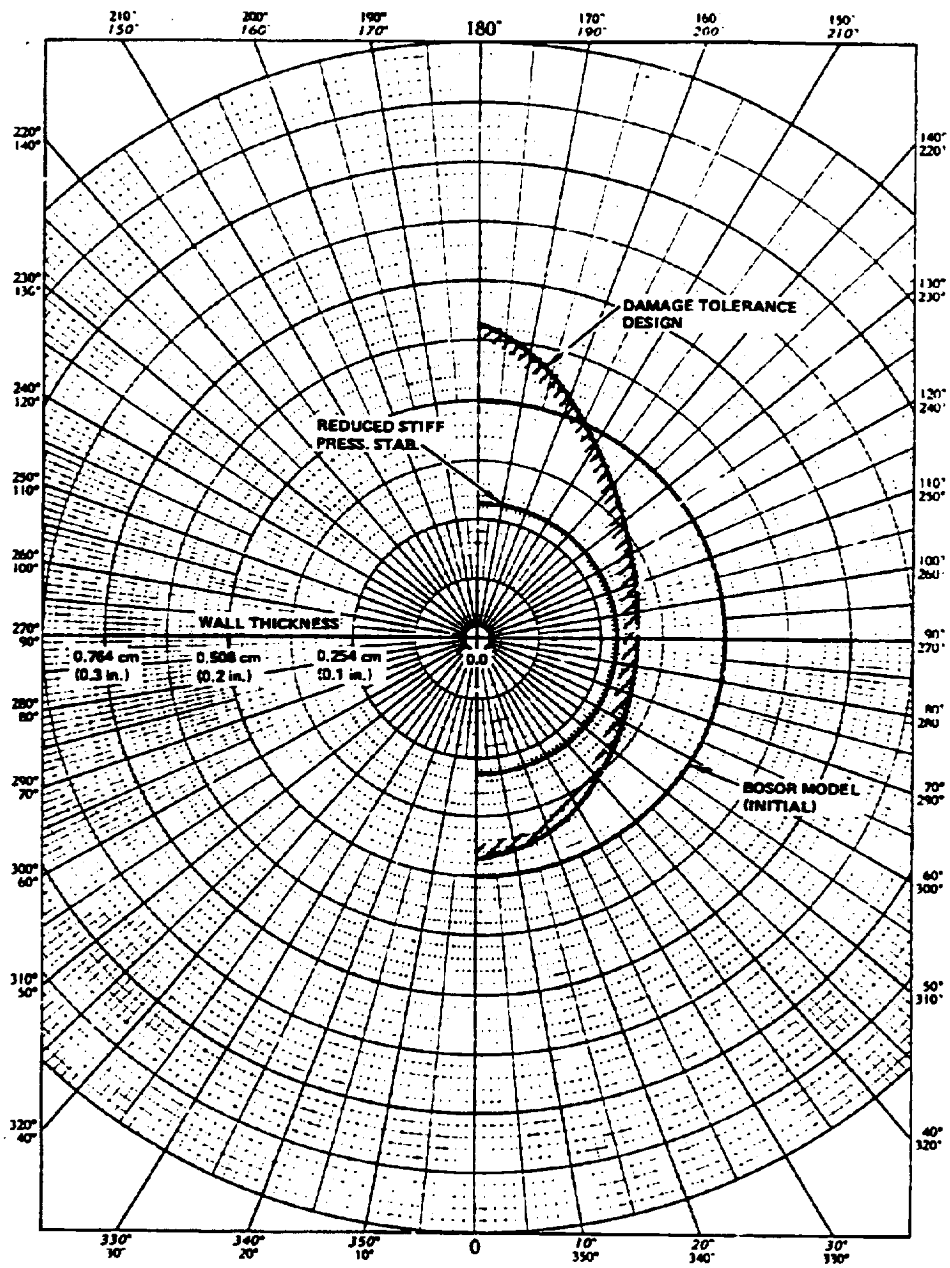

Figure 184. Circumferential variation in wall thickness at tank three-quarter length station.

incorporating pressure stabilized structure in commercial airframe design. Some of these are:

- The acceptance of the philosophy of pressure stabilizing structure by the FAA, airlines, and the airframe manufacturers themselves.
- The added fail-safe burden of "loss of tank pressure - possible loss of airplane."
- An assessment of the additional redundancies required in the components to accurately monitor the tank pressures.

Accordingly, it was decided that the tank design to be incorporated in the final LH_2-fueled airplane would not be pressure stabilized.

7.2.4.5 Tank Suspension Study: This study consisted of an analysis of methods proposed for supporting the nonintegral and the integral tanks.

7.2.4.5.1 Nonintegral Tank: A four point support system was investigated for the nonintegral tank design. The general attachment scheme is depicted in Figure 185, sheet 2. All points are capable of supporting the vertical forces with only the forward points used for reacting the forward/aft inertia forces.

Both circumferential and longitudinal placement of these support points were studied. For the circumferential placement study, several angular locations, included the 1.57 rad (90 deg) location (tank side), were investigated to define their impact on the design of the tank and the insulation system. The results indicated that the placement of the support at other than the 1.57 rad (90 deg) location could result in lower applied loads on the tank but the additional linkage requires a smaller diameter tank for maintaining the proper insulation clearance. In addition, the linkage will have a longer penetration of the insulation system which could provide additional sources of heat leaks. Based on these considerations the most direct approach was taken for the design of the support system, i.e., the side location.

The longitudinal location of the support points was investigated by assuming the tank was a simple beam with overhangs at both ends. The applied vertical loads reflected a full tank with a 4.5 g load factor. Figure 186 presents the beam nomenclature and the magnitude and type of loads. Using this model, the location of the beam reaction points was varied until equivalent membrane forces were obtained at the maximum moment location of each beam segment. The resultant locations for the support points were approximately 1.143 m (45.0 in.) aft of the equator of the equator of the forward dome and 1.905 m (75.0 in.) forward of the equator of the aft dome.

A sketch of the components included in the design of the support system for the nonintegral tank design is shown in Figure 187, sheet 2, view D-D. These components were subjected to a preliminary structural sizing in order to define the material distribution for estimating the weight of the support system. In general, the critical design condition was the emergency landing

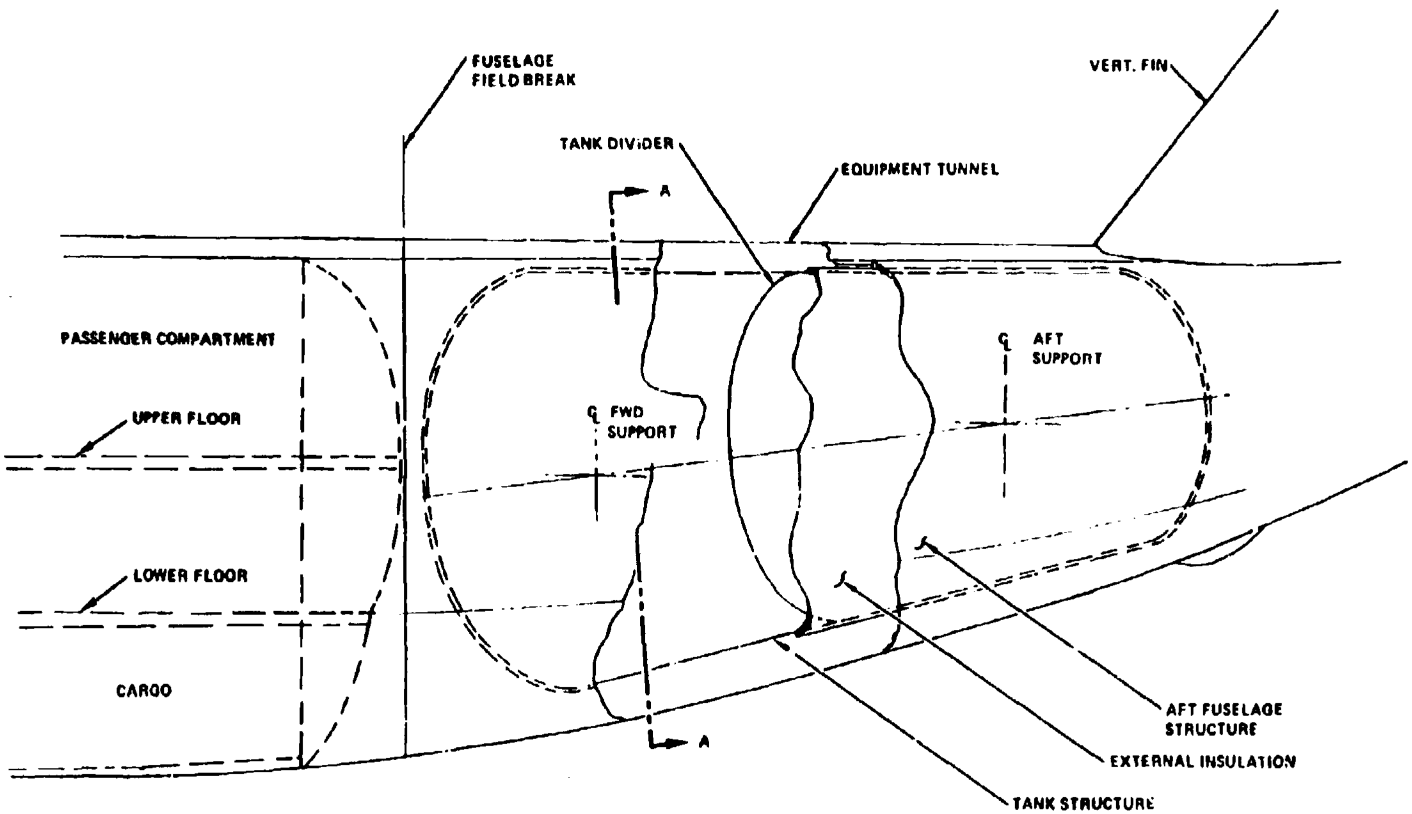

Figure 185. - Candidate A, nonintegral tank - external foam.

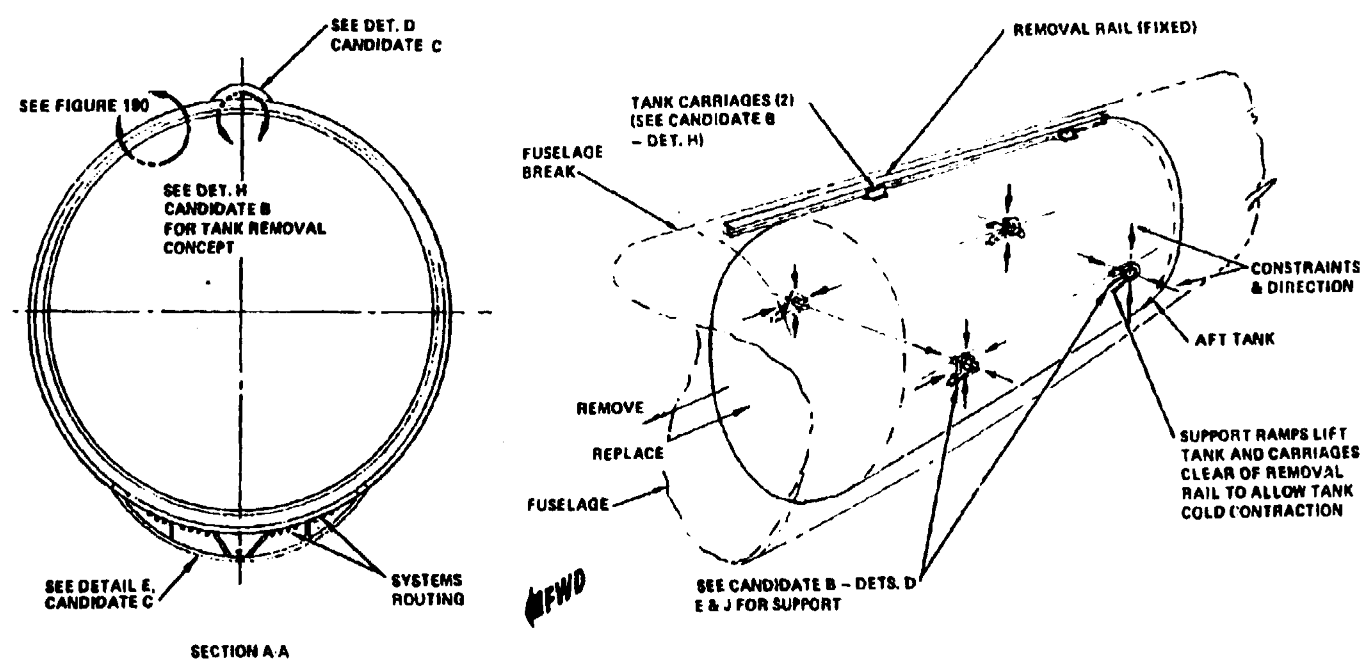

Figure 185. - Concluded.

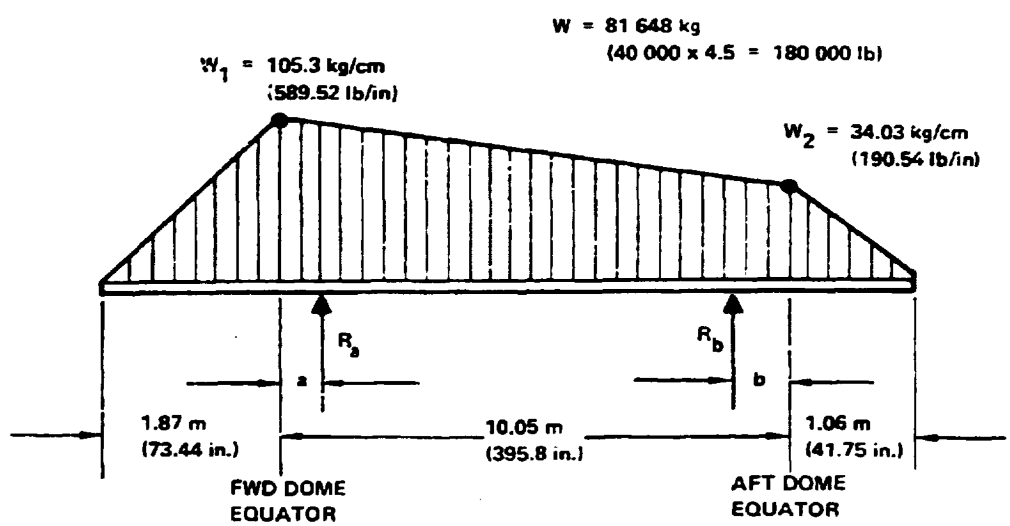

Figure 186. - Beam model for longitudinal placement study, nonintegral tank.

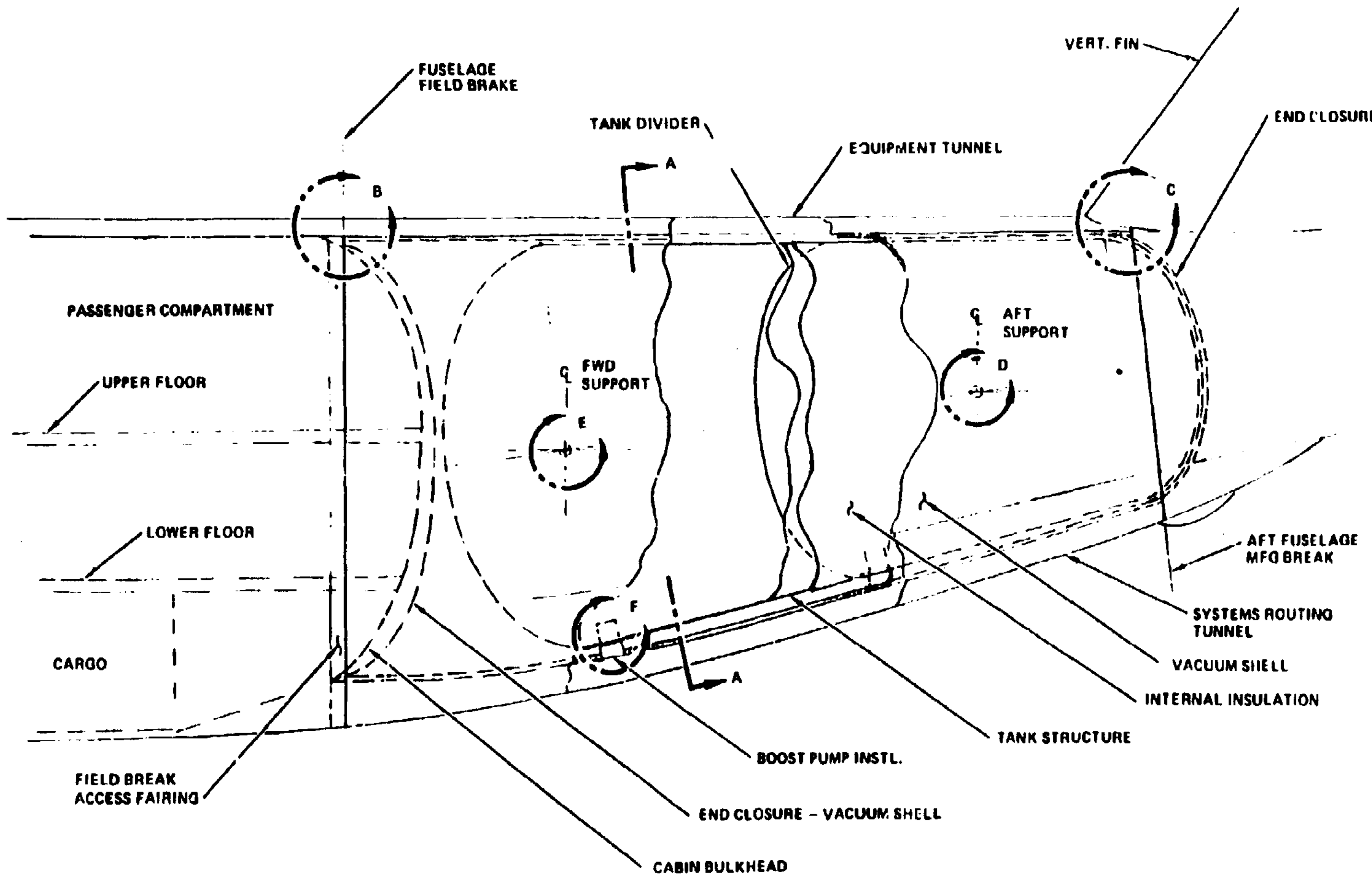

Figure 187. - Candidate B, nonintegral tank - hard shell vacuum.

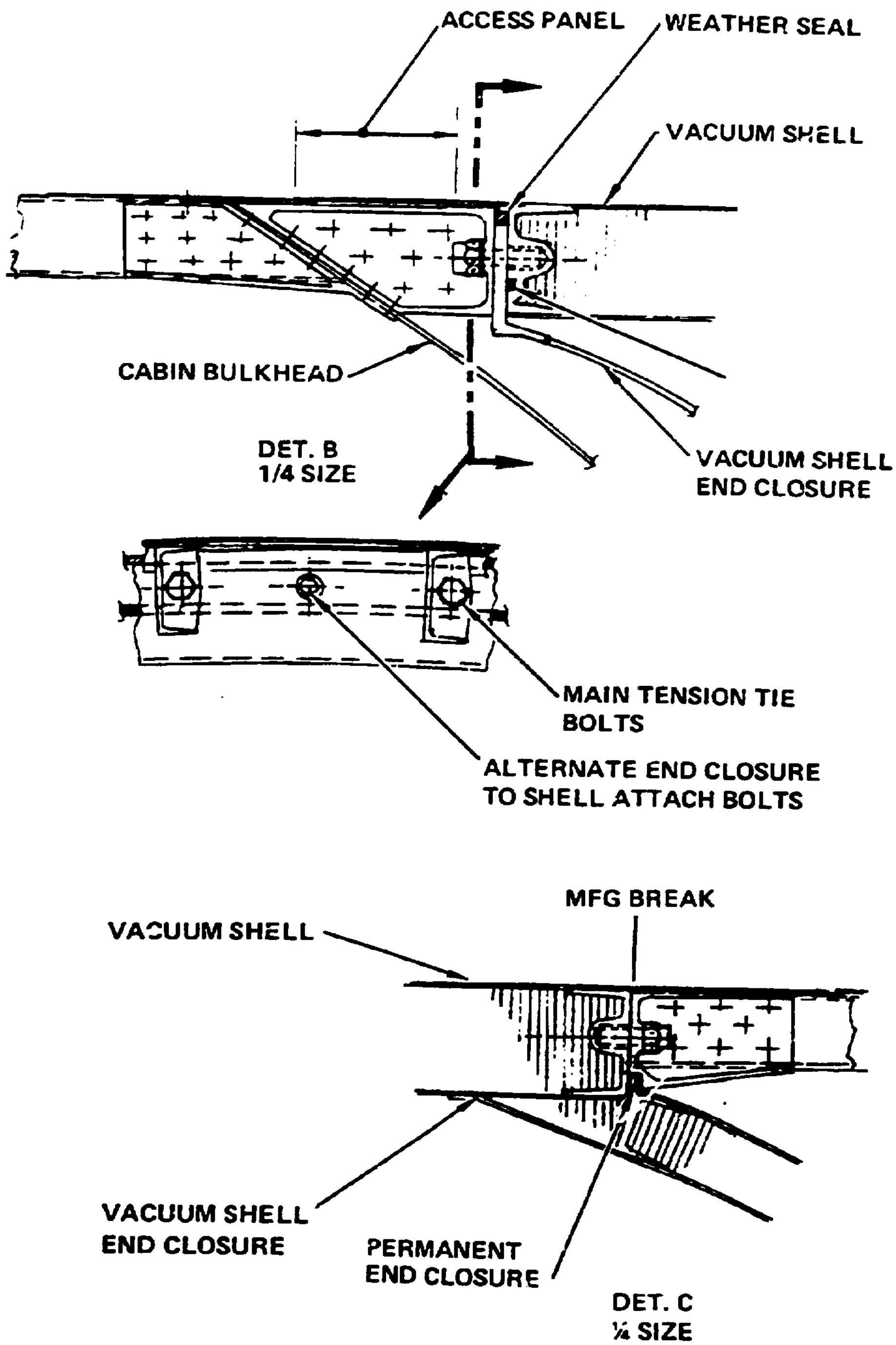

Figure 187. - Continued,

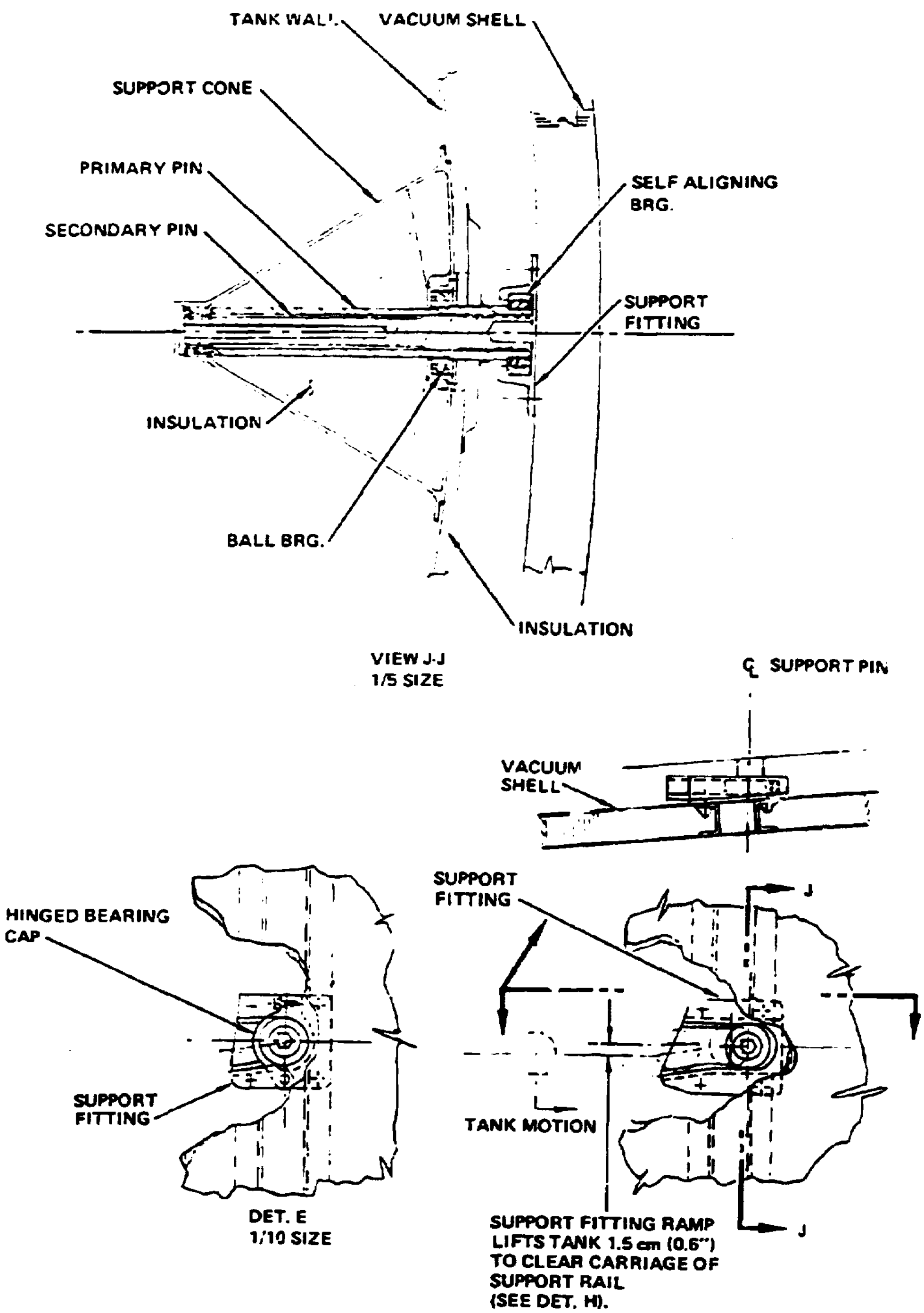

Figure 187. - Continued.

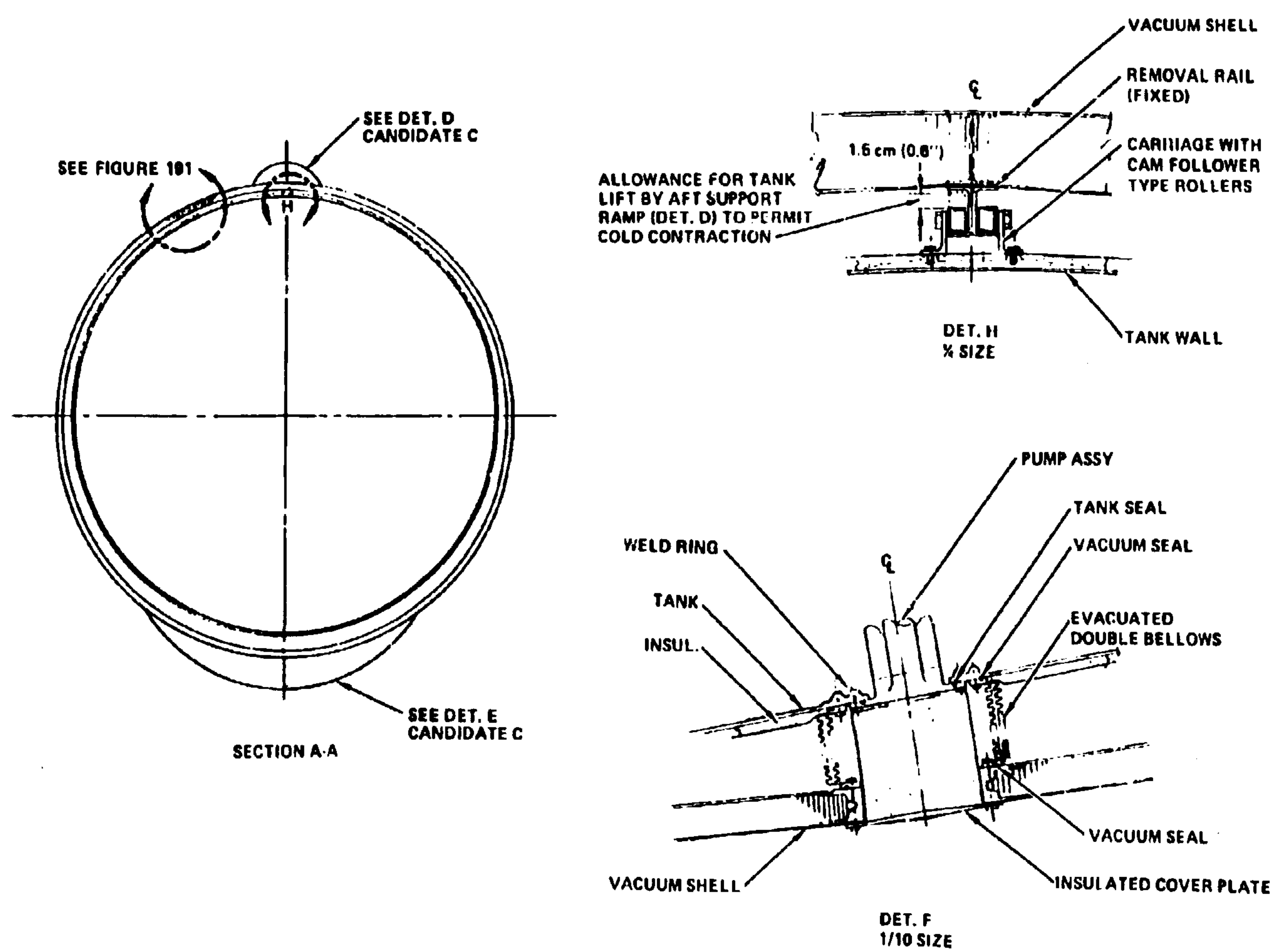

Figure 187. - Concluded.

condition. Section 7.2.1.6 defines the ultimate inertia load factors for this condition.

With reference to Figure 187, primary and secondary pins are provided for fail-safe purposes with bearings defined at the tank wall and exterior attachment point. The pin assembly is screwed into the internal threaded portion of the support cone. The structure adjacent to both the tank and fuselage support points is reinforced to provide for the redistribution of the concentrated forces. Lateral loads imposed by the tank would be resisted by suitable structure at the fuselage support points. The design shown in Figure 187, view J-J, uses self-aligning thrust bearings to transmit the loads to the fuselage.

7.2.4.5.2 Integral Tank: A tubular truss design was investigated for the structural connection to the fuselage at both ends of the integral tank design. A schematic drawing showing the location and design of this support system is presented in Figure 187.

Tapered tubular Boron/epoxy struts with titanium end fittings (see Sheet 2 of above figure) were selected for the design of the truss structure. Each strut is bolted to the adjacent tank and fuselage structure to allow some relative displacement between the structural components. This helps to alleviate the thermal stresses induced in the strut and tank skirt caused by the contraction of the cryogenic tank. In addition, foamed-in-place insulation is provided over part of the length of the strut to reduce the thermal leakage from the tank, as well as to protect the adjacent structure from the cryogenic temperatures.

The Boron/epoxy diagonal elements of the truss were analyzed for the maximum loads imposed during flight. A maximum element load of 182.4 kN (41 000 lb) and 62.3 kN (14 000 lb) (ultimate) was defined for the forward and aft truss structure, respectively, for the 'PLA' flight condition. Euler buckling and basic material strength (tension and compression) were considered in the selection of the cross-sectional dimensions and ply orientation. In addition, a minimum value of extensional stiffness, equivalent to the stiffness of the adjacent aluminum fuselage structure was imposed on the design of the truss elements.

Using these analytical procedures and criteria, the cross-sectional dimensions and material ply orientation of the truss elements were established. An average tubular cross section of (5.72 cm (2.25 in.) O.D. X 3.81 cm (1.50 in.) I.D.) was defined for the elements of the forward truss structure. Correspondingly, a (5.08 cm (2.00 in.) O.D. X 3.81 cm (1.50 in.) I.D.) cross-section was indicated for the elements of the aft truss structure. A Boron/epoxy strut composed of 70% 0° plies, 20% 0.785 rad (45°) plies and 10% 1.57 rad (90°) plies satisfies the strength and stiffness requirements of both the forward and aft truss structure.

Transition panels are provided at the forward and aft ends of the tank, as shown in Figure 187 (sheet 2), to cover the truss structure and maintain aerodynamics smoothness. These panels are removable to allow access to the internal truss structure. A Kevlar faced sandwich with Nomex core was premised for the design of these panels. Basic strength and buckling of these panels were investigated for an external pressure condition of 5.17 kPa (0.75 psi). The results of this evaluation defined a forward transition panel with 0.762 mm (0.030 in.) Kevlar face sheets and a 25.4 mm (1.00 in.) core thickness. The corresponding design data for the aft transition panel is 0.508 mm (0.020 in.) face sheets with 19.05 mm (0.75 in.) core thickness.

7.3 Evaluation of Preferred FCS Candidates

Evaluation of the four preferred fuel containment systems to determine which is best for application in a commercial transport aircraft was based on comparison of performance and cost characteristics of aircraft designed specifically to use each of the candidate systems. In addition, the evaluation was influenced by judgment concerning aspects such as safety, producibility, maintainability, reliability, etc.

Each of the candidate fuel containment systems (FCS) was incorporated into an aircraft design which was then subjected to the sizing routine using the ASSET computer program. The result was definition of four aircraft, one for each candidate FCS, each of which was optimized to perform the design mission at the lowest direct operating cost while still meeting all design and operational constraints such as the following:

- Maximum engine-out takeoff field length of 2438 m (8000 ft)
- Minimum initial cruise altitude of 9449 m (31 000 ft)
- Maximum approach speed of 69.4 m/s (135 kt) EAS at end of mission.

All of the aircraft designs incorporated the results of the studies and investigations reported previously herein, relative to the LH_2-fueled engine and fuel system elements. Thus, the aircraft used to evaluate the four preferred fuel containment systems represent complete, final designs (in a parametric sense and within the usual limitations of time and budget) of LH_2-fueled vehicles.

7.3.1 Weight considerations. - Evaluation of the weight of each of the candidate FCS was a critical aspect in the process of selecting a preferred design. It may be seen from Figures 190, 191, 192, and 193, scale drawings of typical cross sections of each of the candidates representing the top of the aft tank at the quarter length point, that there was a wide variation in the designs which were to be considered. Figures 185, 187, 188, and 189 show installation arrangements for each system.

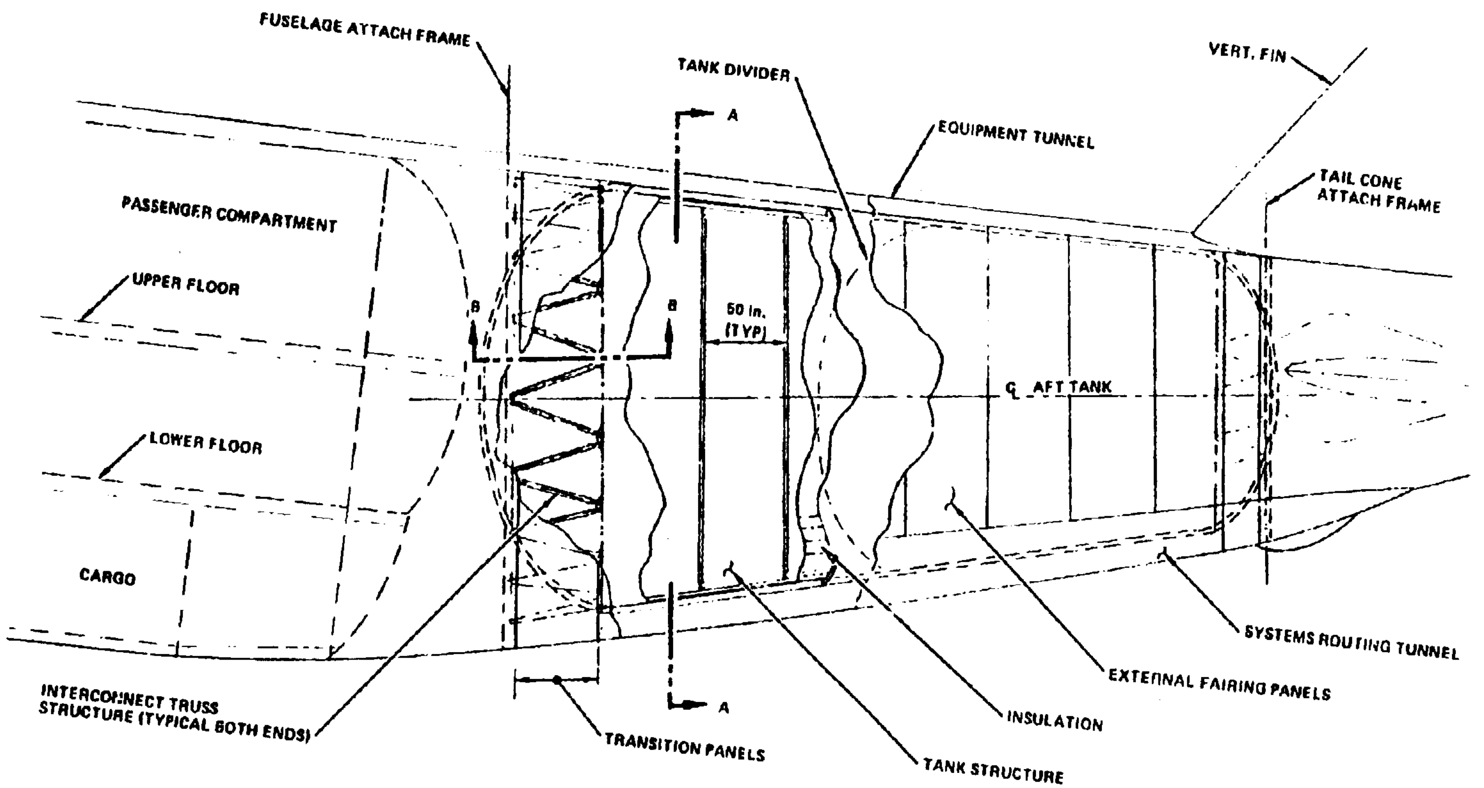

Figure 188. - Candidate C, integral tank - external foam.

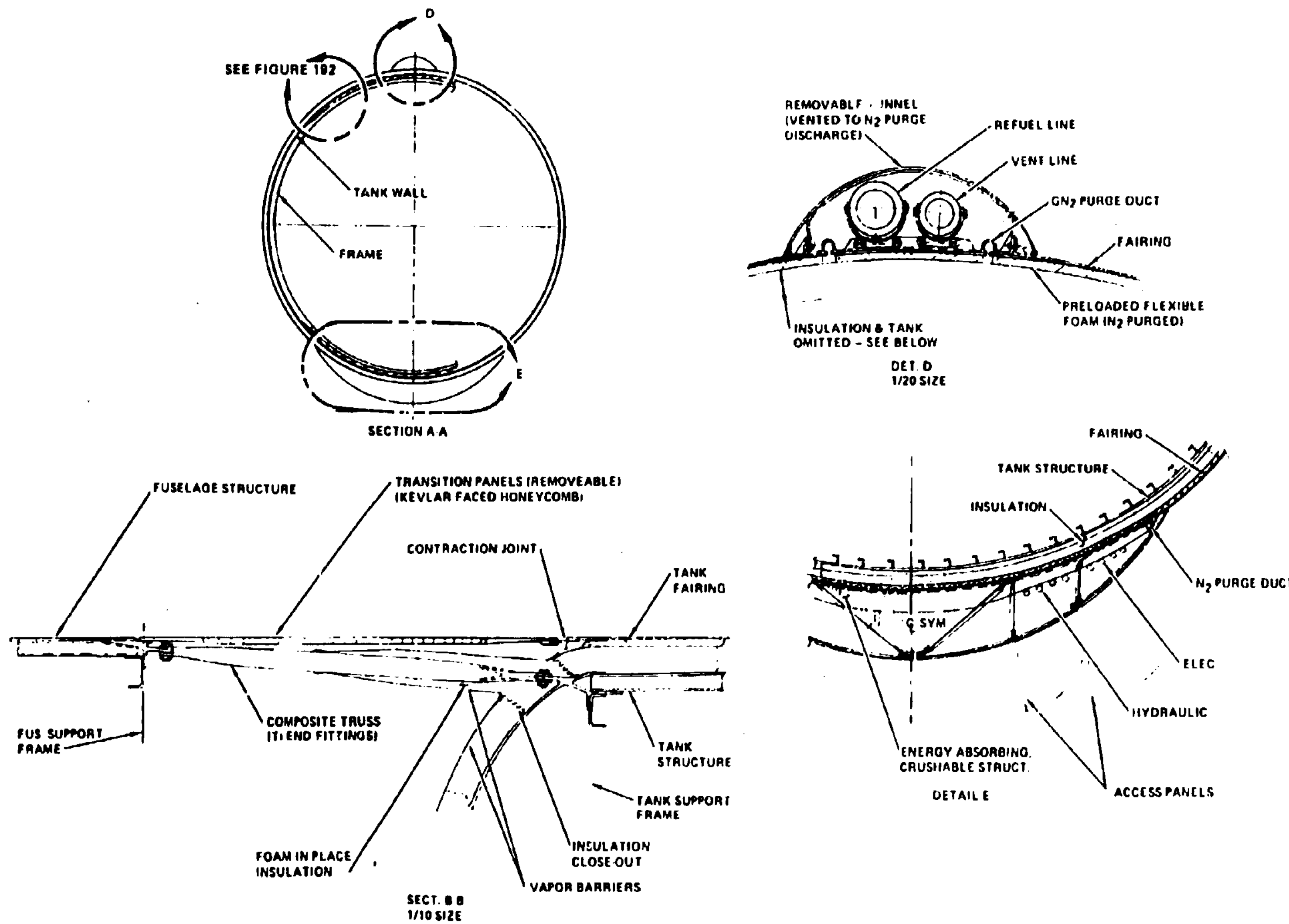

Figure 188. - Concluded.

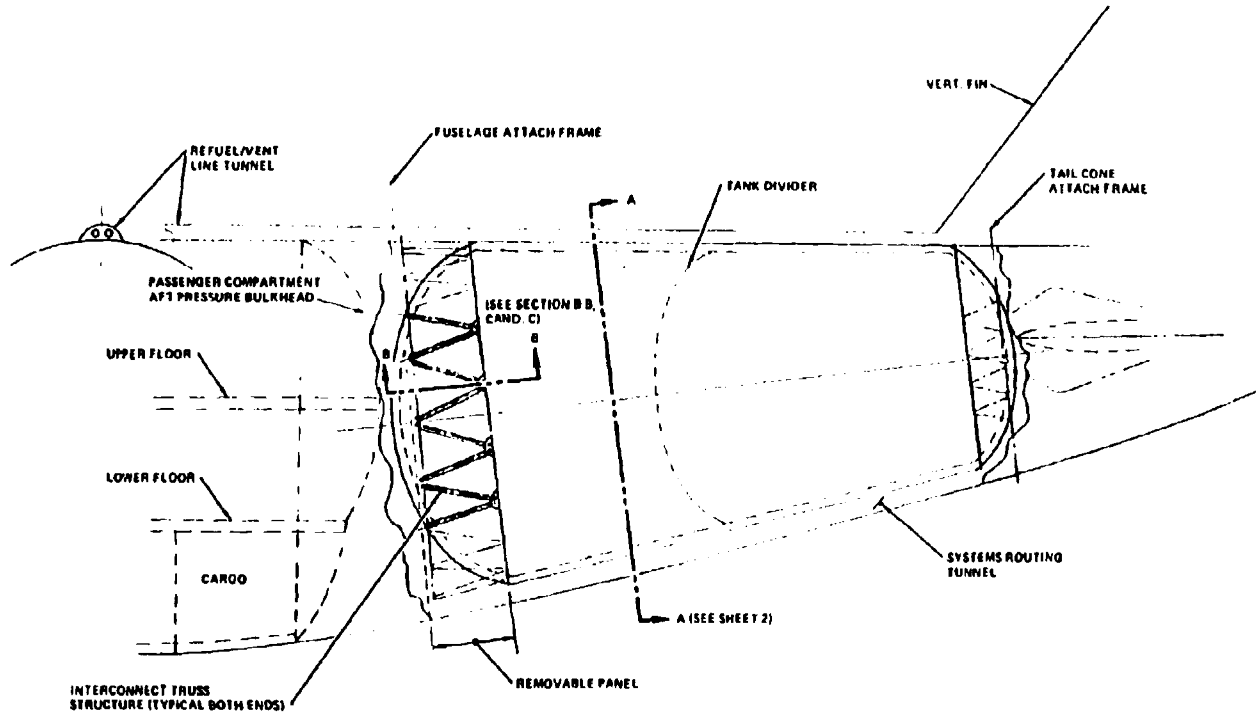

Figure 189. - Candidate D, integral tank - external microsphere insulation.

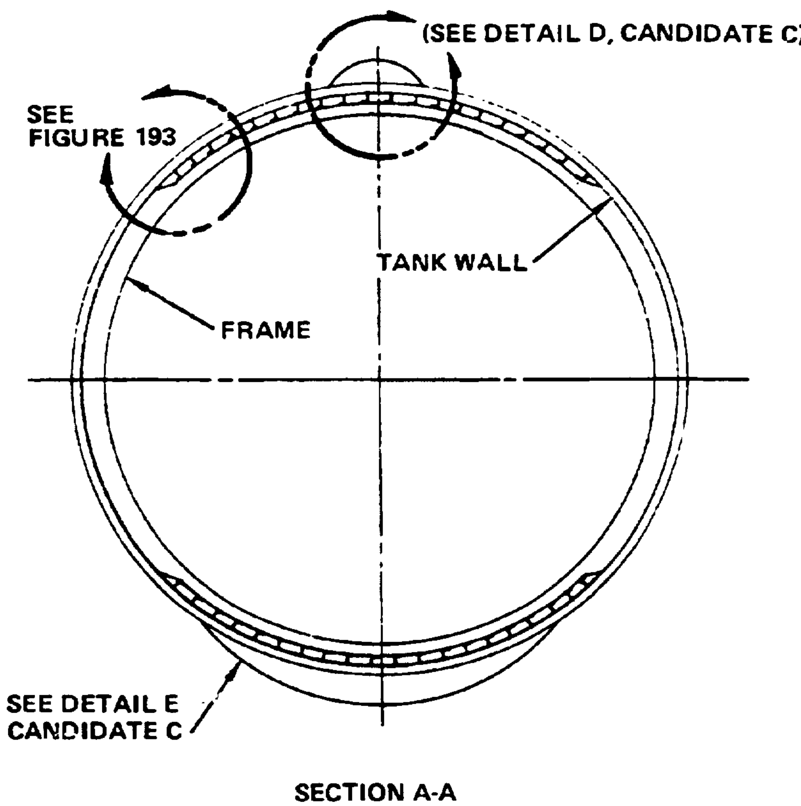

Figure 189. - Concluded

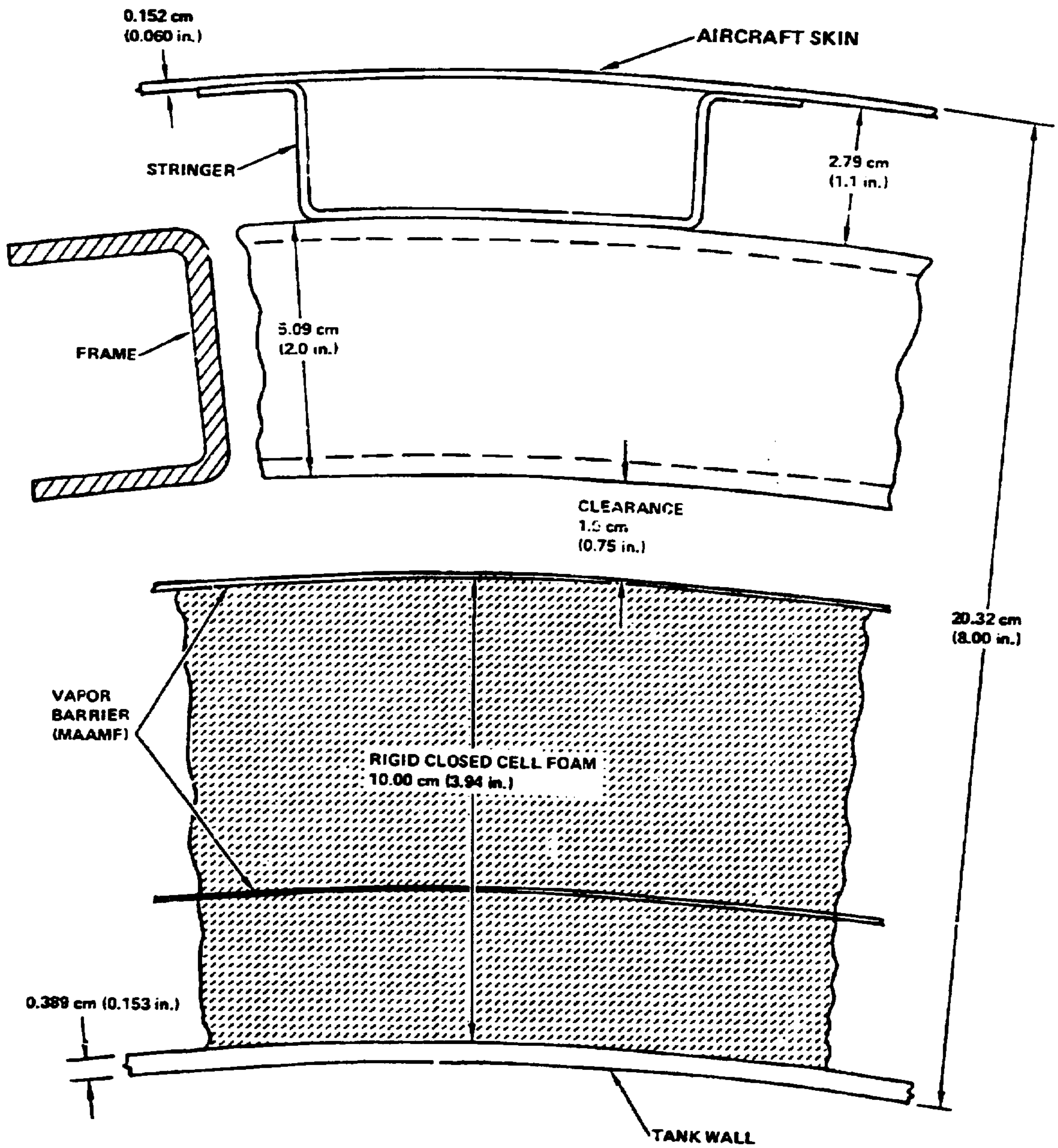

Figure 190. - Representative cross section, FCS candidate A (nonintegral tank - external foam).

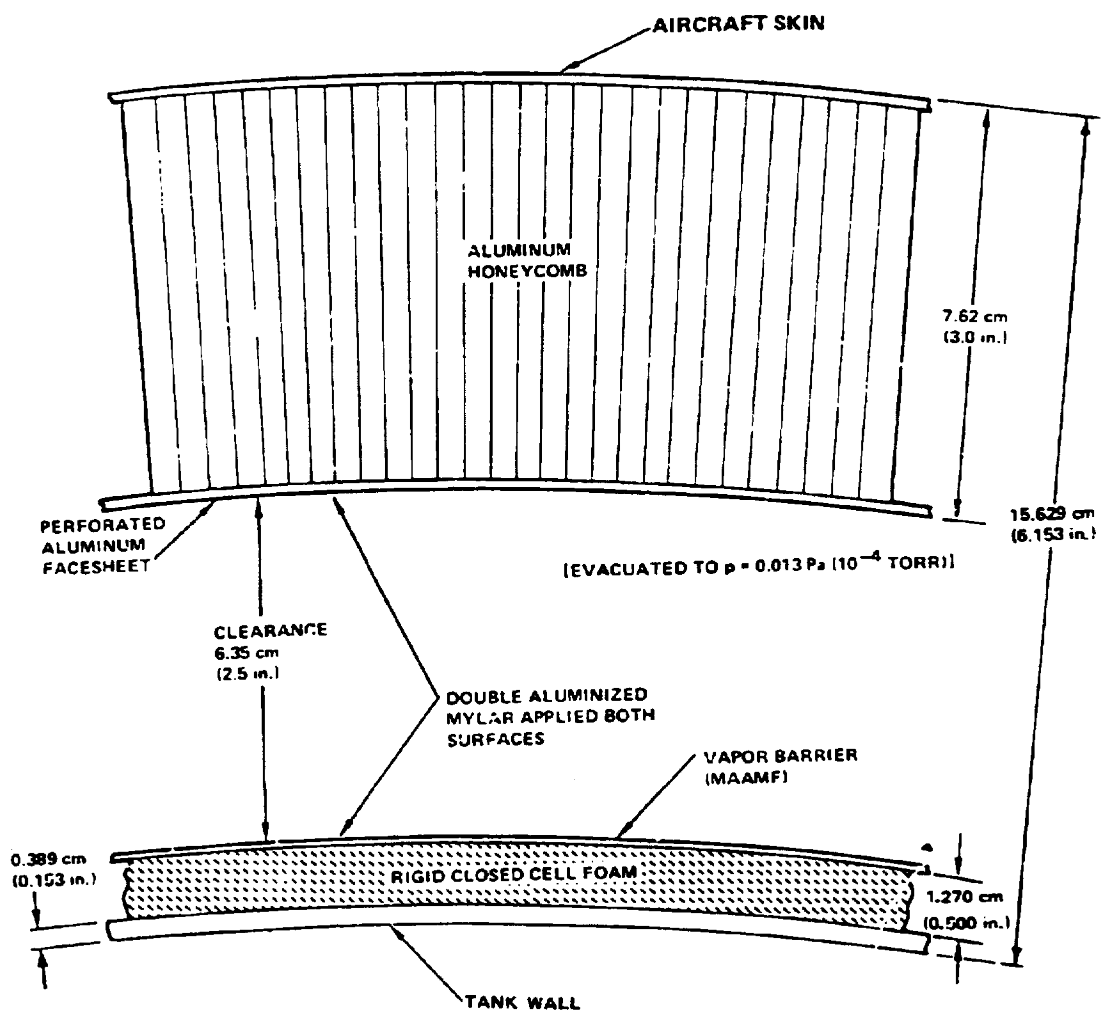

Figure 191. - Representative cross section, FCS candidate B (nonintegral tank - hard shell vacuum).

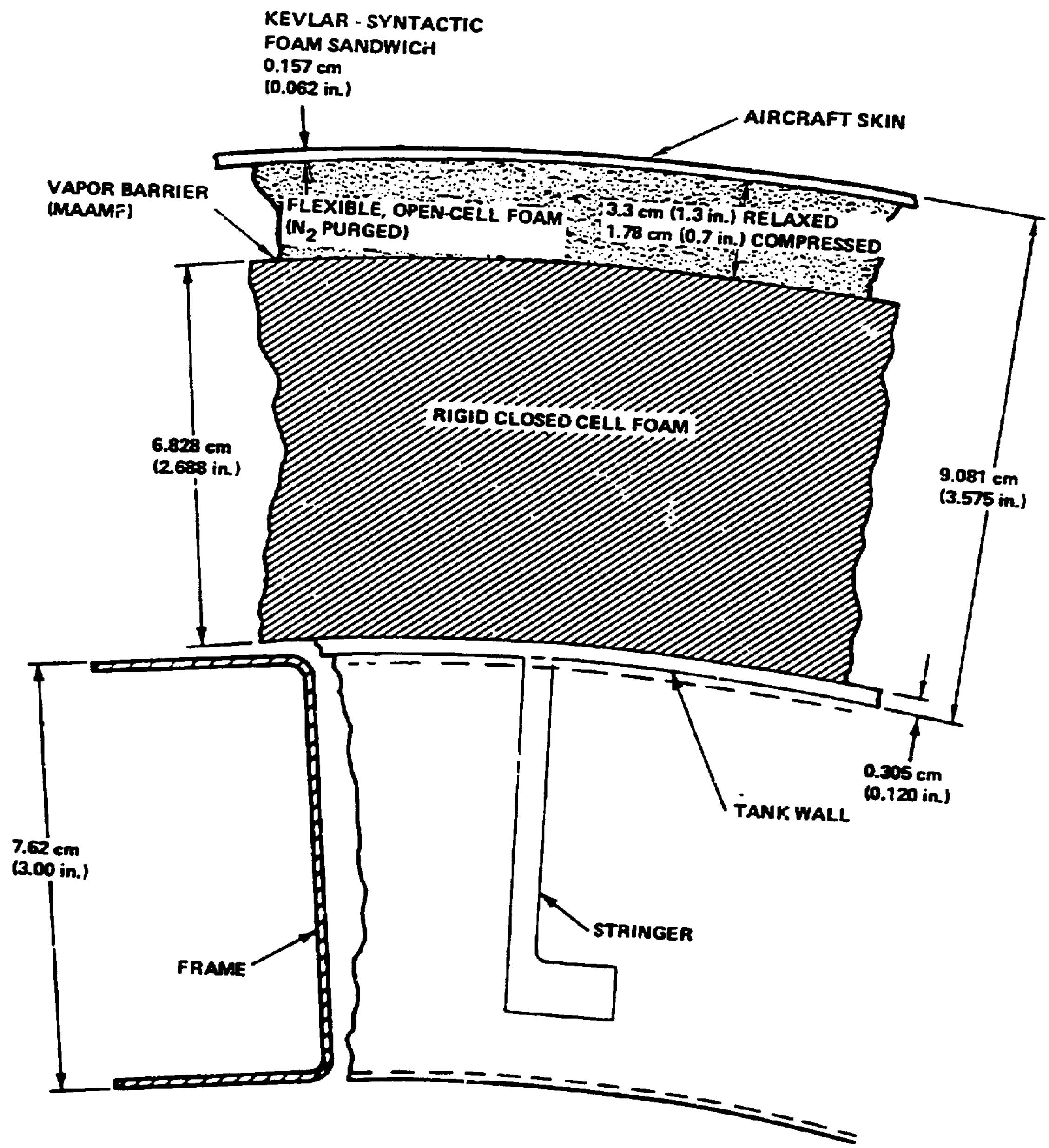

Figure 192. - Representative cross section, FCS candidate C (integral tank - external foam).

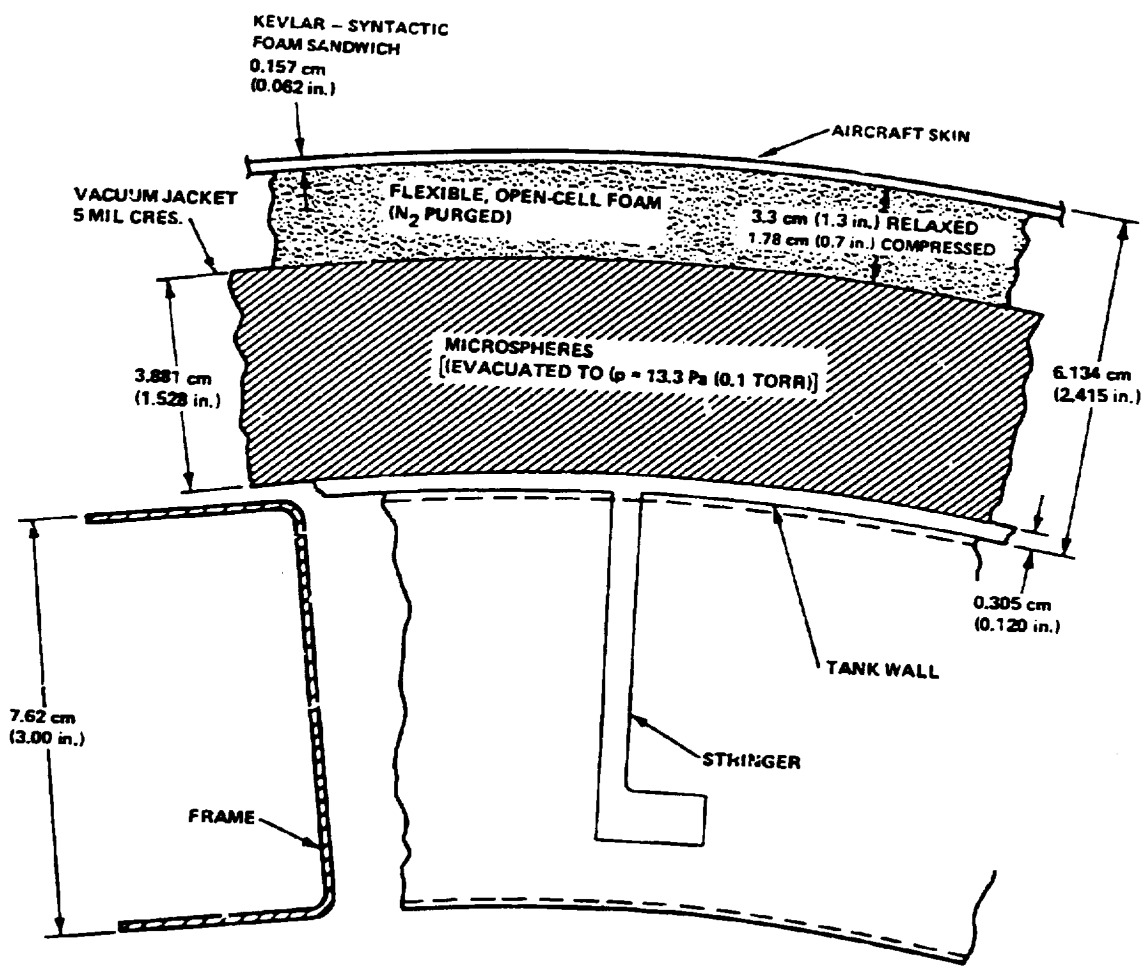

Figure 193. - Representative cross section, FCS candidate D (integral tank - microsphere insulation).

Because of the significance of inert weight as a multiplying factor on the gross weight and cost of transport aircraft, great care was taken to assure that consistent calculation methods were used for all candidates so that the weight comparisons would be as representative as possible.

A comparison of the weights of the four preferred candidate fuel containment systems is presented in Table 78. The basic design of all structural components, such as tank, suspension system, body shell, vacuum jacket, truss and fairing, was derived from stress analyses as explained in Section 7.2. An allowance of eight percent was added to the calculated structural weight to provide for manufacturing tolerances, joints, weld lands, margins of safety, access, and systems provisions. A similar allowance was applied to the insulation weight for all candidates to provide for manufacturing tolerance, density variations, access and systems provisions.

Detailed stress analysis was performed for the aft tanks with only random analysis on the forward tanks to support the weight estimates. It was found that, where tank pressures were the same, the following equations could be used to predict the forward tank weight:

$$W_{DOME_1} = W_{DOME_2} \left(\frac{D_1}{D_2}\right)^3$$

$$W_{CYL_1} = W_{CYL_2} \left(\frac{D_1}{D_2}\right)^2 \left(\frac{L_1}{L_2}\right)$$

where subscripts 1 and 2 refer to the forward and aft tanks, respectively, for the same candidate.

Candidate fuel containment systems C and D require nitrogen purge of the open cell foam just under the fairing cover. The total purge system requirement of 95 kg (210 pounds) is divided equally between the forward and aft tanks. Accordingly, the insulation system weights shown in Table 78 include 95 kg (210 pounds) for nitrogen purge systems for those systems. The nitrogen is assumed to be stored in liquid form in an insulated tank.

Similarly, vacuum pumping systems are required for Candidates B and D. The system required for Candidate B weighs 136 kg (300 pounds) per tank. It consists of a combination of Roots blowers, fore-pumps and turbomolecular pumps. For Candidate D the pumping system consists of just two Roots blowers in series and the weight is 91 kg (200 pounds) per tank.

To assure a fair comparison between integral and nonintegral candidates, the body shell weight has been included. In the case of the forward tanks, the body shell length is measured from the tank forward end to the forward

TABLE 78. SYSTEM WEIGHT COMPARISON OF FUEL CONTAINMENT SYSTEM CANDIDATES (SI Units, kg)

Item	Candidate No.			
	A	B	C	D
Fuel Containment System:[a]	10 595	13 416	9 359	9 647
• Tank and Body Shell:	(9 099)	(12 714)	(7 422)	(7 328)
Dome Ends - Fwd	503	564	552	564
Dome Ends - Aft	377	423	419	433
Divider Bulkhead	313	321	332	337
Cylinder	3 445	5 410	3 842	3 716
Suspension System and Removal Rail	665	665	-	-
Truss-Tank to Body Shell	-	-	837	845
Body Shell	3 794	4 314	1 439	1 433
Vacuum Jacket Dome Ends	-	1 017	-	-
• Insulation:	(1 496)	(702)	(1 937)	(2 319)
Aero. Fairing	-	-	325	313
Vapor Barrier and Adhesive	456	235	316	92
Open Cell Foam	-	-	246	239
Closed Cell Foam	1 040	195	954	-
Microspheres	-	-	-	982
N_2 Purge System	-	-	95	95
Vacuum Pump System	-	272	-	181
Vacuum Jacket		included above		417
Fuel Systems:	1 046	1 055	1 026	1 019
Engine Supply	412	415	403	400
Fueling/Defuel	320	323	314	312
Pressurization/Vent	314	317	308	307
Total System Weight	11 641	14 471	10 384	10 666
Total Fuel Wt.	27 887	28 281	27 302	27 134
Frac. of Total Fuel Wt. $\frac{\Sigma W_{SYS}}{W_{FUEL}}$	0.4174	0.5117	0.3803	0.3931

(a) Sum of forward and aft tanks

TABLE 78. - Concluded. (U.S. Customary Units, lb)

Item	Candidate No. A	B	C	D
Fuel Containment System:[a]	23 357	29 577	20 632	21 269
• Tank and Body Shell:	(20 059)	(28 030)	(16 362)	(16 156)
Dome Ends - Fwd	1 110	1 244	1 216	1 243
Dome Ends - Aft	832	932	924	955
Divider Bulkhead	690	707	732	744
Cylinder	7 596	11 927	8 471	8 192
Suspension System and Removal Rail	1 466	1 466	-	-
Truss-Tank to Body Shell	-	-	1 846	1 862
Body Shell	8 365	9 511	3 173	3 160
Vacuum Jacket Dome Ends	-	2 243	-	-
• Insulation:	(3 298)	(1 547)	(4 270)	(5 113)
Aero. Fairing	-	-	717	691
Vapor Barrier and Adhesive	1 006	517	697	203
Open Cell Foam	-	-	542	526
Closed Cell Foam	2 292	430	2 104	-
Microspheres	-	-	-	2 164
N_2 Purge System	-	-	210	210
Vacuum Pump System	-	600	-	400
Vacuum Jacket		included above		919
Fuel Systems:	2 307	2 325	2 261	2 246
Engine Supply	909	915	888	882
Fueling/Defuel	706	712	693	688
Pressurization/Vent	692	698	680	676
Total System Weight	25 664	31 902	22 893	23 515
Total Fuel Wt.	61 480	62 350	60 190	59 820
Frac. of Total Fuel Wt. $\frac{\Sigma W_{SYS}}{W_{FUEL}}$	0.4174	0.5117	0.3803	0.3931

(a) Sum of forward and aft tanks

cabin pressure bulkhead frame. For the aft tanks, body shell length is measured from the aft cabin pressure bulkhead frame to the aft end of the tank. Body shell weight is greater for the nonintegral Candidates A and B since the entire tank is enclosed within the body. For Candidates C and D, part of the body shell is integral with and included in the tank cylinder weight. The remaining body shell weight is for that portion covering the dome ends and the area between tank end and cabin pressure bulkhead.

7.3.2 Cost considerations. - Cost estimates were prepared for each of the candidate fuel containment systems, as well as for the basic fuel system components required for engine supply, fueling/defuel, and vent/pressurization systems. The data developed during this study were parametric cost factors to represent each design or candidate system in terms of production labor hours and material dollars per pound of total fuel system weight. The data were for use in the production cost subroutine of the Lockheed proprietary computer models, ASSET.

The production cost subroutine of ASSET contains individual cost factors for each type of material (up to five) which might be used in any of the individual structural mass groups (i.e., wing, tail, body, landing gear, nacelles, surface controls, and air induction and exhaust systems.) Labor and material cost factors are also included for the airframe and propulsion systems (including the fuel system) and avionics and engine installations. In addition, the subroutine includes provisions for learning curves, sizing factors, quality assurance, other recurring manufacturing support activities, warranty, and profit. The engine costs are estimated using modified Rand formulas and the avionics equipment are based on equipment requirements. These latter costs are estimated separately and added to that of the airframe to arrive at the total recurring cost. Production costs are used in the calculation of investment cost, DOC, IOC, and ROI.

7.3.2.1 Premises and assumptions: The basic premises and assumptions used in the cost study were as follows:

- These are engineering cost estimates for relative ranking of alternate configurations. Price quotes are neither implied or intended
- Costs are stated in constant 1976 dollars
- Costs include production (factory) labor and material only
- Estimated costs represent the cumulative average cost per aircraft based on a program quantity of 350 aircraft
- An 80-percent learning curve was used for labor
- A 95-percent learning curve was used for material
- Prime contractor profit is not included

7.3.2.2 Cost methodology: The first step in the cost analysis task was to define each system to the level required for estimating purposes, consistent with overall program requirements. A summary of the general characteristics, structural concepts, materials, and manufacturing methods for major items weighed individually was prepared in matrix form. Basic parametric cost factors in terms of production labor hours and material dollars per pound of weight were selected for conventional metal skin/stringer/frame construction, as well as for composite laminated, sandwich, and hybrid structures. These basic data were suitably modified to account for individual design concepts for each applicable major item. Cost factors previously developed for wide body transports for fabrication, assembly, and installation of plumbing; and for checkout of valves, pumps, and various other components of the engine supply, fueling/defuel, and vent/pressurization systems were appropriately used. Cost of pumps required for the vacuum pumping systems were estimated by LMSC. The estimated cost of microspheres in production quantities $4.41/kg ($2.00 per lb) was supplied informally by the 3M Corporation.

The basic cost factors in the form of labor hours and material dollars per pound were prepared so as to represent the cumulative average for 100 aircraft. The appropriate cost factors were applied to each item individually weighed, and all labor hours and material dollars were summed. Appropriate learning curves were applied, as well as labor rates, to arrive at the total cumulative average cost for 350 aircraft.

It should be noted that derivation of these cost factors required a certain amount of judgment and extrapolation of available data. Therefore, these estimates should not be construed as absolute values; however, the relative ranking of each system should be fairly consistent and representative within the framework of this study.

7.3.3 <u>Evaluation results</u>. - A matrix of computer runs was made with the ASSET program to determine the optimum wing loading and thrust-to-weight ratio for LH_2-fueled aircraft using each of the candidate fuel containment systems. As stated earlier, minimum DOC was the measure of merit but each aircraft was required to meet certain operational constraints while performing the design mission.

The results are shown in Table 79. The parameters listed are those considered particularly relevant to the objective of selecting a preferred FCS. On the basis of gross weight, fuel weight, OEW, fuselage length, engine size, aircraft price, DOC, and energy utilization, candidate D, the integral [illegible]nk design with microsphere insulation would be considered the best choice. [illegible]ndidate C [illegible]he integral tank design with closed cell foam insulation, would be [illegible]nd. The nonintegral tank designs are severely penalized by their great[illegible]ess and weight. A summary of the weight of individual elements of th[illegible]ucture and insulation systems of the respective aircraft, plus the w[illegible]their engine fuel supply systems, fueling/defuel systems, and pressu[illegible]n/vent systems, was shown in Table 78.

TABLE 79. - CHARACTERISTICS OF AIRCRAFT DESIGNED FOR FOUR PREFERRED FUEL CONTAINMENT SYSTEMS

[LH_2 fuel; 400 passengers; 10 190 km (5500 n.mi.); M = 0.85]

Tank Type / Insulation Concept		PCS Candidate No.			
		A	B	C	D
		Nonintegral Closed Cell Foam	Nonintegral Hard Vacuum	Integral Closed Cell Foam	Integral Microspheres
Gross weight	kg (lb)	175 903 (387 800)	179 441 (395 600)	172 138 (379 500)	171 367 (377 800)
Fuel weight (total)	kg (lb)	27 887 (61 480)	28 281 (62 350)	27 302 (60 190)	27 134 (59 820)
Payload weight	kg (lb)	39 916 (88 000)	39 916 (88 000)	39 916 (88 000)	39 916 (88 000)
Operating empty weight	kg (lb)	108 109 (238 320)	111 244 (245 250)	104 920 (231 310)	104 000 (229 280)
Fuel Containment System					
Weight	kg (lb)	10 596 (23 360)	13 417 (29 580)	9 358 (20 630)	9 640 (21 270)
Thickness*	cm (in.)	20.32 (8.00)	15.24 (6.0)	9.14 (3.6)	6.12 (2.41)
System Wt. Fraction	(W_{PCS}/W_f)	0.380	0.474	0.343	0.356
Fuel Systems Weight	kg (lb)	1 046 (2 307)	1 055 (2 325)	1 026 (2 261)	1 019 (2 246)
Fuselage length	m (ft)	68.3 (224.2)	67.9 (222.9)	66.6 (218.5)	65.7 (215.6)
Thrust per engine	N (lb)	10 996 (2472.0)	112 184 (25 220)	107 602 (24 190)	107 113 (24 080)
Lift/Drag (cruise)	-	16.42	16.53	16.41	16.43
Specific Fuel Consump. (cruise)	$\frac{kg}{hr}$/daN ($\frac{lb}{hr}$/lb)	0.206 (0.202)	0.206 (0.202)	0.206 (0.202)	0.206 (0.202)
Aircraft Price	$\$10^6$	39.1	40.0	38.3	38.1
LH_2 Systems Cost	$\$10^6$	0.95	1.43	0.86	0.89
Block DOC	¢/S km (¢/S n.mi.)	0.878 (1.626)	0.891 (1.650)	0.867 (1.598)	0.859 (1.591)
Total DOC (incl ground boiloff)	¢/S km (¢/S n.mi.)	0.884 (1.638)	0.894 (1.656)	0.869 (1.609)	0.863 (1.599)
Energy Utilization	kJ/S km (Btu/S n.mi.)	696 (1 222)	705 (1 238)	681 (1 196)	677 (1 189)

*From inside surface of tank skin to external surface of aircraft at tank quarter-length point

As obvious as it may seem from consideration of these quantitative values of aircraft parameters that the integral tank candidates are the superior choice, there are other considerations which need to be taken into account. These include such items as safety, producibility, maintainability, reliability, and operational considerations which are measures of the practicability of a design. These factors are subjective in nature and therefore are not amenable to being quantified. Accordingly, an evaluation scheme was established wherein each of these indicators of practicability could be considered on a relative basis.

An evaluation scale ranging from 1 to 10 was used, with 10 being best. To encourage a wide spread between the candidates in the final total, the system which was preferred for each parameter being evaluated was awarded the maximum rating of 10. It was not necessary that the lowest rated system be given a 1, this was a matter of judgment concerning the significance of the difference between the best and the worst systems.

The fuel containment systems were evaluated for their relative practicability on the basis of considerations which were discussed throughout Section 7 and in Appendix E and F. The results are presented in Table 80. Candidates C and D are again the preferred designs with the difference between them being too small to be meaningful. The nonintegral designs were considered deficient, particularly in their capability for being repaired and replaced.

Accordingly, on the basis of the small advantage shown in direct operating cost and energy utilization, Candidate D, the integral tank with the microsphere insulation system, is designated the preferred fuel containment system. However, it is emphasized that further development of both Candidate C and Candidate D is strongly recommended. It would be a serious mistake if future development of LH_2-fueled aircraft was tied exclusively to only one FCS concept when a) there is so little experimental data on either the foam or the microsphere system in connection with LH_2, b) the evaluation procedure involved so much subjective judgment and resulted in so little difference between the first and second choices, and c) the fuel containment system is such an important element in the design of a satisfactory aircraft.

The fundamental risk involved with Candidate C, an integral tank with closed cell foam applied on the external surfaces, pertains to the useful life which might be realizable with the foam and its vapor barrier. With Candidate D, it is a question of the degree of difficulty which will be encountered in fabrication and maintenance of the flexible stainless steel vacuum jacket, and questions of safety concerning the effect of a major fracture or penetration of the vacuum jacket during service. These questions can only be resolved by further development of both concepts.

TABLE 80. - EVALUATION OF PRACTICABILITY OF PREFERRED FCS CANDIDATES
(Scale of 1 to 10, 10 being best)

	Candidate			
	A	B	C	D
Safety	6	8	6	10
Producibility	8	2	10	9
Maintenance				
Inspection	7	10	7	10
Repair	3	1	10	7
Replacement	3	1	10	7
Reliability	10	3	10	7
Operations	8	8	8	10
Total	45	33	61	60

8. LH_2-FUELED AIRCRAFT CHARACTERISTICS

The results of all the analyses and studies described in foregoing sections were put together into the design of a final liquid hydrogen fueled aircraft which conforms to all the guidelines and meets all the requirements established at the beginning of the program.

In this section, the airplane and its operational characteristics are described; and the implications of its fuel system with regard to malfunctions, reliability, safety and fire protection, and FAR and industry standards are discussed.

It is important to note that before the final characteristics of the LH_2-fueled aircraft were generated, the Lockheed Aircraft Systems Synthesis Evaluation Technique (ASSET) computer program was revised to incorporate updated information in the aerodynamic, propulsion, weight, and cost subroutines. The changes were relatively minor except for modifications in the aerodynamic and propulsion programs which are worthy of note because they caused significant differences in the values of parameters previously listed herein.

The aerodynamic subroutine was modified to reflect use of more advanced supercritical wing technology. This led to increased L/D of the aircraft and a reduction in the fuel required for the mission. The propulsion subroutine was changed to use sea level static, uninstalled characteristics of the engine (rather than installed) as a basis for reference to reflect engine manufacturer practice in specifying engine size. This change resulted in higher apparent values of T/W for the aircraft even where there was no physical difference in the size of the engine relative to the aircraft gross weight.

These changes are significant in accounting for the differences between the aircraft parameters listed in Table 79 and those presented in Tables 81 and 87 for the final designs of the LH_2-fueled and the Jet A-fueled aircraft.

8.1 LH_2 Aircraft Description

The final airplane design is the one described in Section 7 which uses fuel containment system D, the integral tank design with microsphere insulation system. It also incorporates the LH_2-fueled turbofan engine discussed in Section 4.3.3; the design of engine fuel supply system with its boost pumps, feed lines, engine pump, and fuel control system as selected in Section 5; and the fuel subsystems defined in Section 6.

Significant characteristics of the aircraft are listed in Table 81. Its general description is fundamentally the same as that of the baseline aircraft from Reference 1. The general arrangement shown in Figure 2 (Section 3) is an accurate representation of the configuration; however,

TABLE 81. CHARACTERISTICS OF FINAL DESIGN, LH_2-FUELED TRANSPORT AIRCRAFT [400 PAX; 10 190 km (5500 n.mi.); MACH 0.85]

	SI Units		U.S. Units	
Gross Wt.	kg	168 829	lb	372 200
Total Fuel Wt.	kg	25 608	lb	56 460
Block Fuel Wt.	kg	21 621	lb	47 670
Operating Empty Weight	kg	103 305	lb	227 750
Aspect Ratio	-		-	9
Wing Area	m^2	296.8	ft^2	3 195
Sweep	rad	0.524	deg	30
Span	m	51.7	ft	169.6
Fuselage Length	m	65.7	ft	215.6
L/D Cruise	-	17.4	-	17.4
SFC Cruise	(kg/hr)/daN	0.206	$\frac{lbm}{hr}$/lbf	0.202
Initial Cruise Alt.	m	11 580	ft	38 000
Wing Loading (takeoff)	kg/m^2	568.8	lb/ft^2	116.5
Thrust/Weight	N/kg	3.20	-	0.326
No. Engines	-	4	-	4
Thrust per Engine	N	135 000	lbf	30 350
FAR Takeoff Dist.	m	2 440	ft	8 000
FAR Landing Dist.	m	1 768	ft	5 800
2nd Seg Climb Grad (Eng. Out)	-	0.0300	-	0.0300
Approach Speed	m/s	71.2	KEAS	138.4
Weight Fractions				
Fuel	-	15.17	-	15.17
Payload	-	23.64	-	23.64
Structure	-	32.39	-	32.39
Propulsion (includes tanks & fuel systems)	-	9.07	-	9.07
Price	$\$10^6$	43.39	$\$10^6$	43.39
DOC[(a)]	¢/Skm	0.869	¢/S n.mi.	1.609
Energy Utilization	kJ/Skm	636	Btu/S n.mi.	1118

(a) DOC based on LH_2 cost = \$5.69 per GJ (\$6/10^6 Btu = 31¢/lb) the overall dimensions are different. As listed in Table 81, the wing span is now 51.7 m (169.6 ft) and the body length is 65.7 m (215.6 ft). Internally, the 400 passengers are located in the central portion of the fuselage in a double-deck arrangement with the fuel tanks located forward and aft. The fuselage is basically circular in cross-section with a lower lobe attached which contains cargo and baggage.

The wing has a supercritical section and incorporates high lift devices including 15 percent leading edge slats and 35 percent double-slotted Fowler flaps out to the outboard engines. Conventional ailerons are attached to the outboard wing panel. Spoilers are provided for direct lift control in flight and for deceleration during landing ground run. Active controls are employed to minimize gust loading, provide a smoother ride and minimize tail size. The wing and body structure incorporates nearly 50 percent by weight of advanced composite materials.

The differences in performance and weight of the present design, relative to the Reference 1 aircraft, are due to small changes in specific fuel consumption in various engine settings and flight conditions resulting from the work reported herein to define a more realistic LH_2-fueled engine, and to changes in weight of various components of the LH_2 fuel system and the engine.

The engine used in the previous study (Reference 1) was flat rated to provide the same takeoff thrust under hot day (32.6°C) conditions as at standard day conditions. The engine was sized by the requirement to provide an aircraft thrust-to-weight ratio (T/W) that would meet the initial cruise altitude specification of 9449 m (31 000 ft).

The engine from the present study is not flat rated. In addition, it has a lower thrust lapse with altitude than did the original engine. For example; at 10 668 m (35 000 ft) Mach 0.85, the original engine produced 21.3 percent of its hot day, sea level static thrust while the present engine produces 28.7 percent, or in other words, 34.7 percent more thrust at altitude. The net effect of this is that while the reference aircraft required a 0.293 (installed) sea level static thrust-to-weight ratio to meet the minimum cruise altitude, the present engine can meet this with ease at a lower T/W. As a result, the engine-out takeoff field length requirement became critical in the present study in determining the thrust-to-weight ratio of 0.326 uninstalled (equivalent to 0.255 installed) which was selected as optimum for the final aircraft design.

8.2 Weight Estimating Relationships

Weight estimating relationships normally used for conventional subsonic passenger transport aircraft were employed in the present study, except as it was found necessary to modify them to account for features associated with use of LH_2 fuel. The changes included the following:

- Body — The body weight estimating equation was modified to account for the large volume required for the low density LH_2 which is equally distributed in tanks forward and aft of the passenger cabin. This distribution causes greater shear and bending loads in the body shell than for a conventional passenger transport which carries its Jet A fuel in the wing box. Although the wing equation was not modified for this study, the absence of fuel in the wing for bending relief would cause the wing specific weight to be somewhat heavier for an LH_2 design than for a conventional Jet-fueled aircraft.

- Fuel Tanks — The weight of the fuel containment system was calculated as described in Section 7.3.1. For the subject, final design aircraft, the weight of the integral tank design with microspheres contained in a soft vacuum annulus for insulation was represented.

- Engine Fuel Supply System — The engine fuel supply system weight was based on use of 2.54 cm diameter x 0.406 mm thick (1.0 in. dia. x 0.16 in. thick) stainless steel lines wrapped with 3.81 cm (1.5 in.) of closed cell foam. A 10.16 cm diameter x 0.406 mm thick (4.0 in. dia. x 0.016 in. thick) aluminum tube enclosed the foam insulation to provide a vapor seal and mechanical protection. The weight of the engine fuel supply system including boost pumps, lines, and valves was calculated as outlined in Section 5.6. Similarly, the aircraft fuel subsystems weights were taken from Section 6. Table 82 is a summary of the weight of the LH_2 fuel system.

- Propulsion — The LH_2 fueled turbofan engine weight was scaled from the baseline engine described in Section 4.3 which weighs 2082 kg (4589 pounds) and delivers 136.6 kN (30 706 lb) of thrust at sea level static, standard day conditions.

  The engine weight includes

  - Engine accessories and gearbox
  - Engine mounts and pylon splitter fairing
  - Gas generator cowl and tailpipe
  - Fan duct acoustic ring

  Installed engine weight per aircraft is expressed in pounds as:

$$WENG = (0.17839)\ (NENG)\ (TSLS)$$

TABLE 82. LH_2 FUEL SYSTEM WEIGHT SUMMARY

			kg	(lbm)
Engine Supply System			420.9	(928)
Plumbing - Tank to Engine				
Tank 1			68.9	(152)
Tank 2			54.4	(120)
Tank 3			77.6	(171)
Tank 4			91.6	(202)
Valves			26.8	(59)
Boost Pumps (3/Tank) and Housing (1/Tank)			53.1	(117)
Electrical System for Pumps and Valves			48.5	(107)
Refuel/Defuel System			328.0	(723)
Transfer Lines to Defuel Manifold			37.2	(82)
Refuel Lines Inside Tank			28.6	(63)
Refuel/Defuel Manifold			239.5	(528)
Valves and Fueling Adapter			22.7	(50)
Vent/Pressurization System			321.6	(709)
Vent Lines and Fittings			235.4	(519)
Valves			20.4	(45)
Adapter, NACA Scoop, Vent Extension			8.6	(19)
Alternate Pressurization System			57.2	(126)
Lines	49.0	(108)		
Heat Exchanger	3.6	(8)		
Regulator Installation	4.5	(10)		
Total LH_2 Fuel System Weight			1070.5	(2360)

NOTE: Fuel system instruments (fuel quantity, flowmeters, pressure gages, GH_2 sensors, etc.) are estimated to weigh 187 pounds, and are included in "instruments" on the ASSET weight statement.

where

NENG = Total number of engines

TSLS = Installed sea level static thrust/engine

Nacelle and pylon weight per aircraft, before applying a weight reduction factor for advanced composite usage, is equal to 31.66 percent of the total installed engine weight. On the same basis, the air inlets are 16.12 percent of the engine weight. The remaining propulsion group items, including fan thrust reversers, engine controls, and starting and oil systems weigh approximately 10 percent of the installed engine weight.

- Advanced Composites — Weight reduction factors were applied to the estimating equations to reflect the benefits expected from advanced composites usage in the 1990-1995 time period. These weight reduction factors were taken from the Advanced Technology Transport Study (Reference 38), performed by the Lockheed - Georgia Company, and are based on the intermediate technology level discussed therein. Table 83 lists the weight reduction factors as well as the estimated materials distribution for each group.

TABLE 83. - ADVANCED TECHNOLOGY WEIGHT REDUCTION FACTORS AND ESTIMATED MATERIALS DISTRIBUTION

Group	Weight Reduction Factors	Materials Distribution (% of Total Wt.)				
		Alum.	Ti.	Steel	Compos.	Other
Wing	0.635	44	4	2	48	2
Tail	0.730	49	15	2	32	2
Body	0.664	38	4	2	50	6
Landing Gear	0.848	8	15	20	20	37
Nacelles, pylon	0.787	5	30	30	35	0
Air Ind.	0.787	45	5	4	41	5
Flight Controls	0.950	20	5	20	5	50

8.3 Operational Requirements of LH_2 Fuel System

A detailed accounting of all of the flight and maintenance crew operational requirements for the airplane is beyond the scope of this program; however, some of the requirements which can be addressed in this conceptual phase of the airplane design are discussed in the following paragraphs.

8.3.1 Fueling and defueling - Because it is cryogenic and is also very easily ignited, hydrogen must be handled in a different manner than hydrocarbon fuel during fueling operations.

8.3.1.1 Recommended practices for fueling procedure:

1. Operating personnel should be suitably attired in protective apparel including thermally insulated gauntlet type gloves, head and body splash protective clothing, and nonconductive footwear.

2. Bond the airplane and ground fueling equipment to each other and to a permanently installed airport grounding terminal. (It is assumed that all parts of the airframe are bonded together electrostatically so that no unbonded components can cause a static discharge in the presence of a combustible mixture of hydrogen and air.)

3. Determine the total quantity of fuel required to accomplish the intended flight including normal reserve.

4. Set the "bug" on the fuel quantity indicator for each tank on the refuel panel (see Figure 194) at the fuel load required.

5. Insert the vapor recovery nozzle into the vapor recovery adaptor making sure that no contaminants are on the mating surfaces at the interfaces of the nozzle and adaptor.

6. Insert the fueling nozzle into the fueling adaptor taking the same precautions as in (5).

7. Place the actuating linkage for the vapor recovery nozzle in the open position.

8. Place the refueling valve switches on the fueling panel in the open position.

9. Initiate fueling by placing the actuating linkage of the fueling nozzle in the open position. (The fueling time for a full load of fuel starting from a 15 percent reserve quantity remaining from a previous flight should be approximately 20 minutes).

10. Close the actuating linkage of the fueling nozzle.

11. Place the refueling valve switches in the refuel panel in the closed position.

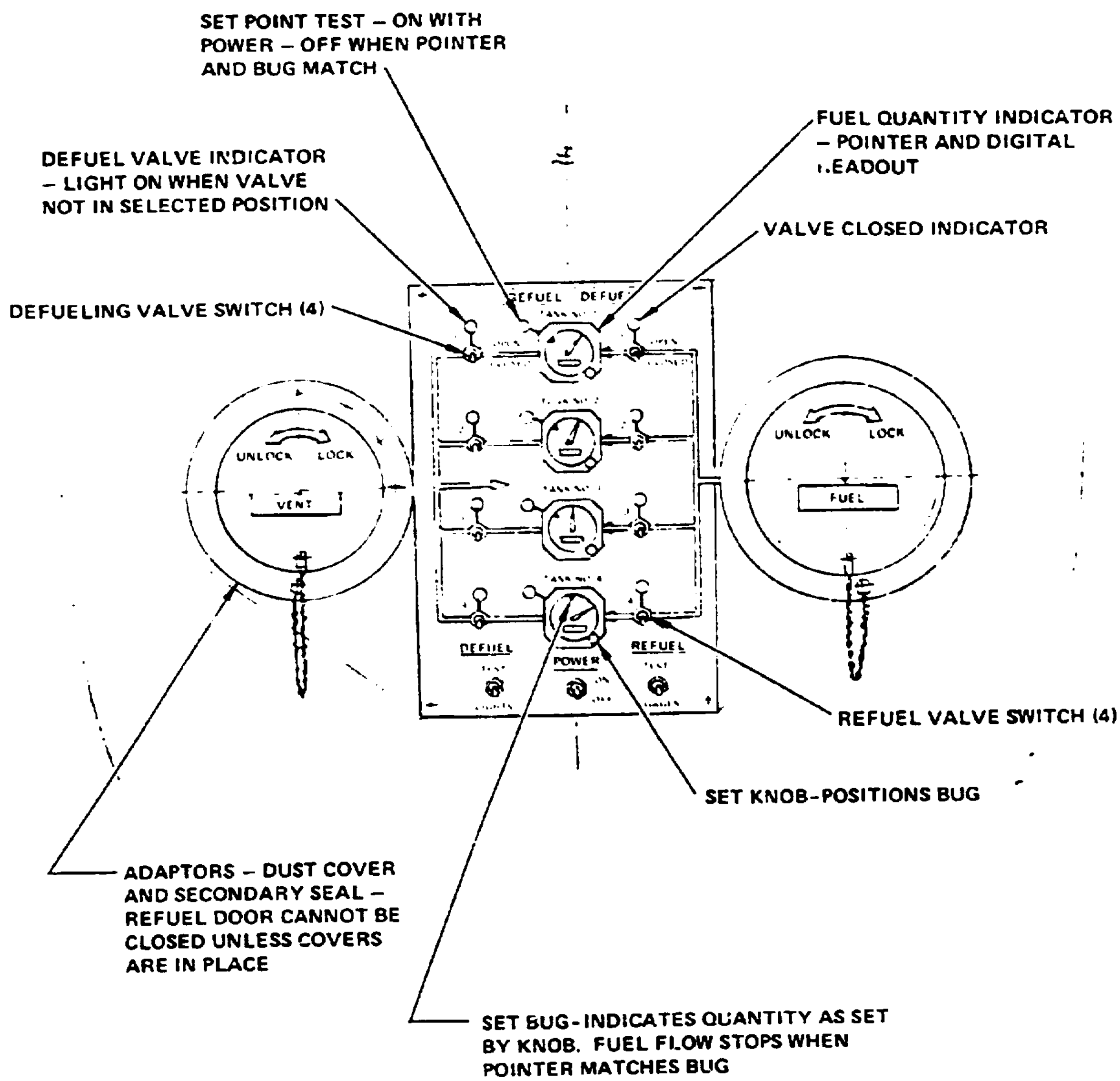

Figure 194. - Refuel panel.

12. Remove the fueling nozzle.

13. Remove the dust cover.

14. Close the actuating linkage of the vapor recovery nozzle.

15. Remove the vapor recovery nozzle.

16. Replace the dust cover.

8.3.1.2 Defueling procedure: Defueling is not a normal operation since it usually results from the need for maintenance activities. This usually involves emptying the tanks completely which is a specialized activity requiring special procedures to ensure that no impurities get into the tanks while the tanks are being:

1. emptied,

2. warmed to ambient temperature,

3. purged of hydrogen gas,

4. purged of air after maintenance activities are complete,

5. cooled to cryogenic temperatures, and

6. refueled.

These specialized procedures are discussed in some detail in Section 4.5.5 of Reference 2 and will not be discussed herein.

8.3.2 Flight engineer's panel. - Figure 195 shows the flight engineer's panel arranged in a functional manner to permit visualization of the essential features of the system. The diagram is self explanatory with the exception of the "press-relief" and "vent" push-to-test buttons. When depressed, these close the primary tank and vent line (back pressure) valves respectively. Continued depression will allow the tank (or vent line) pressure to rise to the higher setting of the secondary valves at which time the pressures should stabilize at the higher pressure. In this manner, it can be determined that both primary and secondary tank pressure and vent line valves are functional.

Fuel quantity gauges are backed by fuel totalizers which indicate the total quantity of fuel used by each engine by means of integration of the engine mounted fuel flowmeter.

The optional fuel jettison valves are also shown. To jettison fuel, all 12 pumps should be turned on, the jettison chute or boom extended and the jettison valve opened.

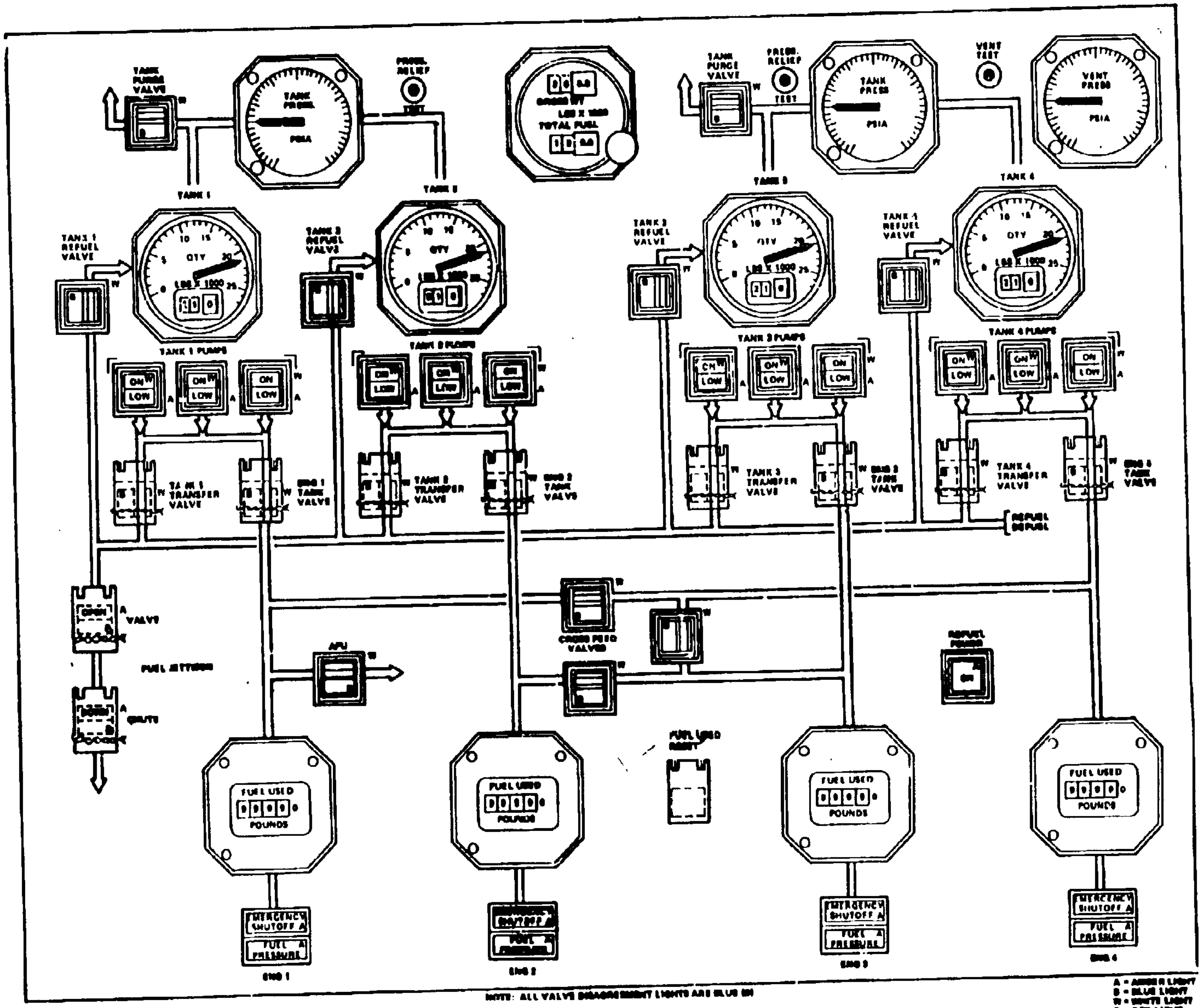

Figure 195. - Fuel system control panel - flight engineer.

8.3.3 Fuel management. - Installation of fuel tanks at the forward and aft locations in the fuselage provides obvious advantages in control of aircraft center-of-gravity. In normal operation, aircraft balance is maintained by having equal tank capacities with approximately equal moment arms for the forward and aft tanks. To illustrate this point, Figure 196 was prepared to show c.g. travel based on a typical weight and balance sheet. At gross take-off weight, the aircraft c.g. is at 41.5 percent MAC, well within the limits of 30 to 47 percent MAC at that weight. For normal fuel usage, the c.g. moves forward to 36.8 percent MAC at zero fuel weight creating a minimum requirement for aircraft trim adjustment.

However, a failure of the fuel line tank isolation valve in any one tank to the closed position could make fuel trapped in that tank unavailable for engine consumption if an alternate path for fuel to be removed from the tank were not provided. The consequences of such a condition, illustrated on the figure for fuel trapped in either Tank 1 or Tank 4, are not tolerable.

To preclude this possibility, the fuel transfer system described in Section 6.5 and illustrated in Figure 80 was incorporated in the fuel system design. An example of the effectiveness of the system can be illustrated by the following example. If the fuel valve in Tank No. 1 fails in the closed position the corrective action is to open the fuel transfer valve in Tank 1 and close its refuel control valve (see Fig. 80). Fuel immediately begins to flow from Tank 1 to Tank 2 through the Tank 2 fueling manifold. This does entail some nominal shift in c.g., but the amount is less than two percent as can be seen in Figure 196. In the other extreme situation, where the feed line from Tank 4 is blocked, requiring transfer to Tank 3, the forward c.g. shift is still less than two percent and entails an aircraft trim adjustment no greater than encountered in normal operation.

8.3.4 Maintenance. - The cryogenic nature of hydrogen fuel will require major changes in the methods used to maintain and repair the aircraft fuel system. These changes are exemplified in the way fuel tank pumps are replaced and in the preparation for repair of fuel system insulation leaks.

A major objective of the design study was to locate all equipment possible external to the fuel tanks so that the time consuming process of entering the tanks for fuel system maintenance could be avoided. This has been accomplished and only the necessary plumbing lines are located in the tank.

Another important objective was to devise a method by which the fuel pumps could be replaced quickly and safely, without requiring that the liquid-hydrogen fuel tank be drained. The design solution to this problem is described in Section 5.3.6. Included are drawings and a description of the physical configuration of the pump mounting, the method of changing the

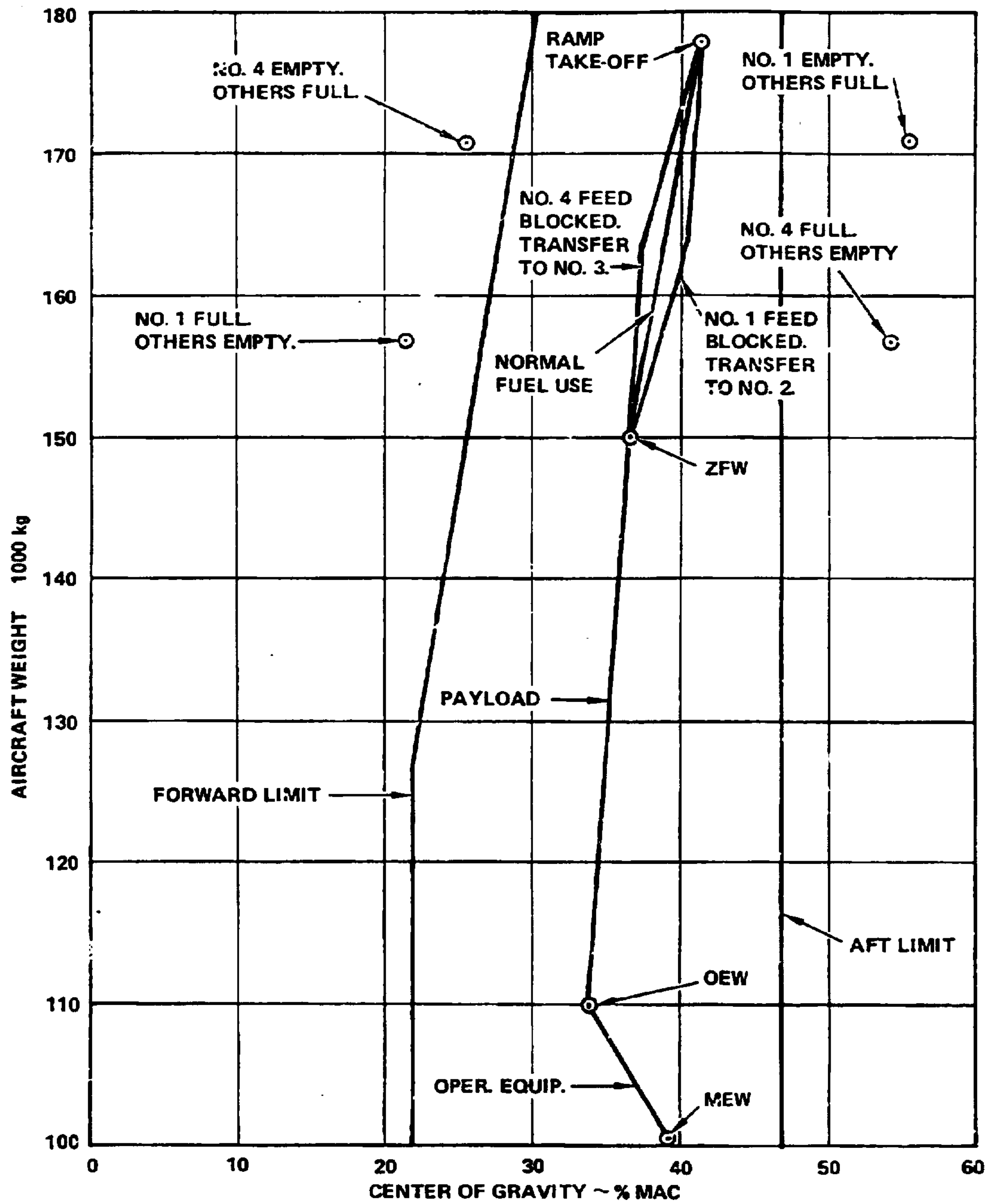

Figure 196. - C.G. travel with blocked feed line.

pump without draining the fuel tank, and a tool designed to accomplish the changing of the pump. Particular consideration was given to ensuring the safety of the personnel involved in the operation and the integrity of the equipment on the airplane.

8.4 Fuel System Malfunction Analysis

Table 84 provides results of an analysis of possible malfunctions which can occur with critical LH_2 fuel system components. The components which were analyzed are used in the engine fuel supply system, the refuel/defuel system, and the pressurization/vent system.

Under each of the system headings the table lists the component, its normal function, possible malfunctions and their cause, and how the existence of the malfunction would be detected. The result of the failure on operation of the system is then described, proper corrective action indicated, and some remarks offered which explain the consequences of the malfunction.

8.5 Reliability Analysis

The following reliability analysis provides an assessment of the probability of loss relative to the function of the two primary critical subsystems of the LH_2 fuel system. The design concept for the two critical functions, fuel pumping and fuel venting, employ redundancy, thus enhancing the functional reliability. In developing the probability expressions, Trans World Airline Boeing 747 statistics for average flight duration of 6.1 hours and an average daily utilization of 12.2 hours were used as the time base for the equations. Thus, in the nominal case, the aircraft is expected to fly two flights per day. Component failure rates which are estimated to be realistic and were assumed to be allowable for an initial evaluation of the systems are listed in Table 85. Where two numbers are listed the number in parenthesis represents the allowable failure rate in the specified mode.

8.5.1 Pumping and distribution system. - The reliability logic employed in the following analysis is conventional using the binomial expansion to evaluate the active/parallel redundant systems. The proposed design concept employs four pumping sources, each source using a three-pump cluster. Each pump cluster has been allocated to a separate tank/engine feed circuit. Successful completion of a prescribed daily flight schedule requires operation of one of the three pumps in each cluster. Crossfeed between pumping sources is provided thus allowing the continuous operation of all engines should a failure of one complete pumping cluster occur during the flight.

TABLE 84. - FUEL SYSTEM MALFUNCTION ANALYSIS

Item No.	System and Component	Function	Malfunction	Cause of Malfunction	Detection of Malfunction	Result of Malfunction	Corrective Action	Remarks
				Engine Feed				
1	Fuel boost pump (3 pumps per tank)	Supplies fuel for: a) engine b) defueling c) jettison	Low flow Low press. or No flow or press.	Mechanical or electrical failure	Low press. light on flt. engrs. panel	Loss of pump	Turn pump off	Loss of 1 pump is not dispatch item. At least one pump should be kept on at all times since engine will not run with all pumps out. Fuel in tank will not be available if 3rd pump fails.
2	Fuel boost pump outlet check valve (1 per pump)	Prevents reverse flow into pump when not running	Fails closed	Mechanical	None	No fuel flow	See remarks	Cannot be detected if at least 2 pumps are running. If valve is in the only pump running flow will stop. Engine can still be supplied from 1 pump. Can be checked on ground by testing each pump for flow and engine pump inlet pressure (engine idling)
			Fails open	Mechanical	None	None		Some reverse flow will occur. Sufficient flow provided for engine.
3	Tank shutoff valve (D.C.) Tanks 1,2,3, and 4	Isolate fuel supply from line when fire handle is pulled. Also controlled from flight engrs. panel (Normally open)	Fails open	Mechanical or electrical failure	Disagreement light goes on if valve is in any position other than selected	None unless emergency exists	None	Pumps should be turned off to stop fuel flow from tank in case line ruptures.
			Fails shut	Mechanical or electrical failure	Disagreement light goes on if valve is in any position other than selected	No flow from tank	Open fuel transfer valve.	Fuel in tank with failed valve can be transferred by pump to any or all tanks by opening the desired refuel valves and made available to the engines. Cross-feed valves must be used to equalize fuel consumption from the remaining tanks.
4	Firewall shutoff valve (D.C.) Engs. 1,2,3 and 4	To shutoff fuel flow to engine when emergency handle is pulled (Normally closed)	Fails open	Mechanical or electrical failure	Disagreement light goes on if valve is in any position other than selected	None unless emergency exists	None	Tank shutoff valve (above) will shutoff flow to engine. Fuel in line will be contained unless line ruptures.
			Fails closed	Mechanical or electrical failure	Disagreement light goes on if valve is in any position other than selected	Loss of engine if valve closes in flight	Shut off engine	Use cross feed to use fuel in tank normally feeding shutdown engine.

TABLE 84. - Continued.

Item No.	System and Component	Function	Malfunction	Cause of Malfunction	Detection of Malfunction	Result of Malfunction	Corrective Action	Remarks
5	Cross feed valves (D.C.) (3 valves)	Permits feeding any any eng. from any tank	Open or closed	Mechanical or electrical failure	Disagreement light goes on if valve is in any position other than selected	See remarks	See remarks	By the proper fuel management and using the intertank transfer capability, all fuel can be made available to all engines in the event of any combination of cross feed valve.
				Refuel/Defuel				
6	Fueling adapter	Provides connection for ground refueling nozzle	Poppet fails closed	Damage or abuse	Nozzle cannot be opened	Aircraft cannot be refueled	Replace	A very unlikely failure. When not in use the poppet is protected by an adapter cap.
			Poppet fails open	Damage or abuse	When nozzle is removed fuel is released. Also visual indication.	Fuel release	Replace	Very unlikely since it is only used on ground. Dual springs are provided for return of poppet in case one fails.
7	Fueling shutoff valve (D.C.)	Shuts off refueling flow. Also allows intertank transfer and level control in flight.	Fails open	Mechanical or electrical failure	Disagreement light goes on when valve is not in position selected.	None	Replace	This valve is prechecked both during and at the end of refueling. Even if valve fails to shut during refueling, tank cannot be overpressurizer since fueling and pressure is 241 kPa (35 psia) and tank can take up to 283 kPa (41 psia) limit load. Fuel overflow is returned to liquefaction facility via vent line. During defuel, open valve will allow fuel from other tanks to enter. This fuel can be removed by pressure transfer after the other tanks have been defueled.
			Fails shut	Mechanical or electrical failure	Disagreement light goes on when valve is not in position selected.	Tank cannot refueled	Replace	Fuel already in tank can be used. In-flight transfer into tank cannot be done however.

TABLE 84. - Continued.

Item No.	System and Component	Function	Malfunction	Cause of Malfunction	Detection of Malfunction	Result of Malfunction	Corrective Action	Remarks
Pressurization/Venting								
8	Tank pressure control valve (2)	a. Primary valve regulates tank pressure to 145 kPa (21 psia)	Fails closed	Mechanical failure	Tank press. rises to 159 kPa (23 psia)	Tank press. rises to 159 kPa (23 psia)	Replace	Tank protected by secondary regulator (b).
			Fails open	Mechanical failure	Loss in tank press.	See remarks	Replace	Fuel will flash in tank until equilibrium temperature corresponding to vent back pressure valve setting is reached. Approximately 9-10% of fuel will be lost. Rest of fuel is usable.
		b. Secondary valve regulates tank to 159 kPa (23 psia) if (a) above fails closed	Fails closed	Mechanical failure	Close override solenoid of (a) above. Tank press. will rise above 159 kPa (23 psia)	None	Replace	If tank pressure rises above 23 psia override solenoid actuated by "push to test" button must be released to prevent overpressure. (See Fig.)
			Fails open	Mechanical failure	Same as item (a) above (all open mode)			
		c. Purge valve permits ground purging of tanks at reduced pressure	Fails closed	Mechanical or electrical failure	Tank press. rises to 145 kPa (21 psia) when purge gas is introduced.	None	Replace	Ground operation only. Tank pressure cannot exceed 21 psia.
			Fails open	Mechanical or electrical failure	Same as item (a) above (fail open mode)			
9	Vent back pressure valve (primary)	Prevents air from entering vent line (Servo operated)	Fails closed	Icing or mechanical failure	Vent line pressure rises to 24.1 kPa (3.5 psig)	Alternate vent is used	Icing will clear. Replace if mechanical.	This is a flight dispatch item. Flight precheck should include using primary vent valve override solenoid to determine if vent line pressure rises to 3.5 psig, indicating alternate vent is operating.
			Fails open	Mechanical failure or foreign object.	Vent line press. falls to zero	See remarks	Replace	If failure occurs in flight, vent scoop airflow should prevent air backflowing into line. On ground tank venting should maintain vent exit pressure higher than ambient. This should be extremely rare due to valve design.

TABLE 84. - Concluded.

Item No.	System and Component	Function	Malfunction	Cause of Malfunction	Detection of Malfunction	Result of Malfunction	Corrective Action	Remarks
10	Vent back pressure valve (alternate)	Prevents air from entering vent. Operates if primary vent fails shut (servo operated)	Fails closed	Mechanical or electrical failure	Press. rises above 24.1 kPa (3.5 psig on precheck	See remarks	Replace	Flight dispatch item. Flight precheck by closing primary vent override solenoid. If pressure rises above 3.5 psig alternate is failed close.
			Fails open	Mechanical or electrical failure	Press. will not rise to 24.1 kPa (3.5 psig or vent fails to close on refuel	See remarks	Replace	See remarks in item 9 (fail open)
11	Vent adapter	a. Provide connection for ground vent nozzle	Fails closed	Damage or abuse	Nozzle can not be opened	Aircraft cannot be refueled	Replace	Unlikely failure. Protected by an adapter cap when not in use.
		b. Closes fail (primary) vent to allow return of vent gases for liquefaction	Fails open	Damage or abuse	When nozzle is removed vent gases are released. Also visual indication.	Vent gas release	Replace	Very unlikely. Used only on ground. Dual springs provided for return of poppet.

TABLE 85. - ALLOWABLE FAILURE RATES FOR LH_2 PUMPING AND VENTING SYSTEM COMPONENTS

Component (Critical Failure Mode)	MTBF (hr)	Failure Rate (λ) Per Flight Hour
1. Pump - Fuel Boost (Failure to operate)	2 500	0.000400
2. Control valve - Vent pressure and regulation.	9 350	0.000107
• Primary regulator - (Failure in closed mode)	50 000	0.000020 (0.000015)
• Secondary regulator - (Failure in closed mode)	50 000	0.000020 (0.000015)
• Vent valve & motor - (Failure to open)	15 000	0.000067 (0.000033)
• Solenoid by pass valve - (Failed in closed mode)	100 000	0.000010 (0.000001)
• Manual over-ride - press. regulator - (Failure to operate when required)	100 000	0.000010 (0.000010)
3. Vent valve - Primary (Failure in closed mode)	50 000	0.000020 (0.000015)
4. Vent valve - Auxiliary (Failure in closed mode)	50 000	0.000020 (0.000015)

8.5.1.1 P_1 probability of loss: The probability (P_1) of partial loss of the pumping system for the typical 6.1 hour flight is illustrated and expressed as follows:

RELIABILITY SERIES/PARALLEL DIAGRAM FOR P_1

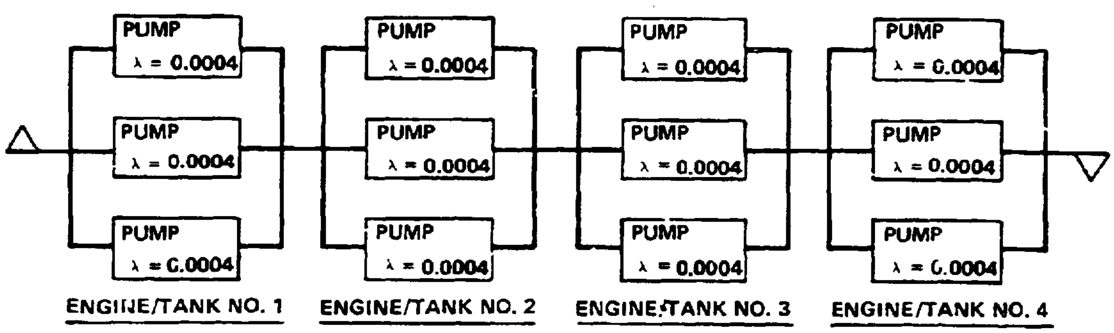

Reliability expression:

$$P_1 = 4 \left[1 - (R^3 + 3R^2Q + 3RQ^2)\right]$$

$$R = e^{-\lambda t}$$

$$Q = 1-R = \text{probability of failure}$$

where

λ = Failure rate/hour = .0004

t = Flight time = 6.1 hours

e = Base of natural logarithms ≈ 2.71828

$$P_1 = 4(1 - 0.999999986) = 5.76 \times 10^{-8}$$

To provide a basis for evaluating whether a given probability of failure is acceptable or not, current practice with commercial aircraft is as follows. In cases where failure of a component or system would result in loss of life or aircraft, P must have a value not greater than 1×10^{-9}. Where failure would result in no hazard to life or aircraft but might require cancellation or diversion of a flight, P is usually required to be not greater than 1×10^{-6} or 1×10^{-7}. Accordingly, the value of 6.4×10^{-7} calculated for this instance is acceptable and the assumed failure rate for boost pumps shown in Table 85 is valid as a design target.

8.5.1.2 P_2 probability of loss: P_2 = Probability of loss of one of the four pump clusters during 2nd flight of the day (6.1 hours), assuming one pump in each of the four pump clusters has already failed.

RELIABILITY SERIES/PARALLEL DIAGRAM FOR P_2

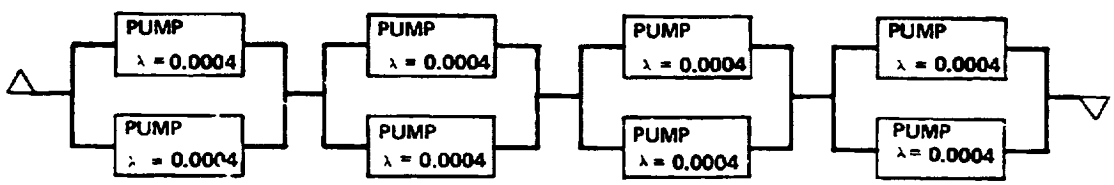

<u>Reliability expression:</u>

$$P_2 = 4(Q^2)$$

$$Q = 1 - R = \text{Probability of Failure}$$

$$R = e^{-\lambda t}$$

where

λ = Failure rate/hour = 0.0004

t = Flight time = 6.1 hours

e = Base of natural log.

$$P_2 = 2.3 \times 10^{-5}$$

This probability of failure is marginal for acceptance as a non-hazardous occurrence. A logical conclusion is that the conventional requirement be adhered to, namely, that an aircraft not be dispatched if more than two pumps are failed.

8.5.1.3 P_3 probability of loss: P_3 = Probability of flight diverting to an alternate landing site due to the loss of one pump cluster which would dictate crossfeed control to the affected engine.

RELIABILITY SERIES/PARALLEL DIAGRAM FOR P_3

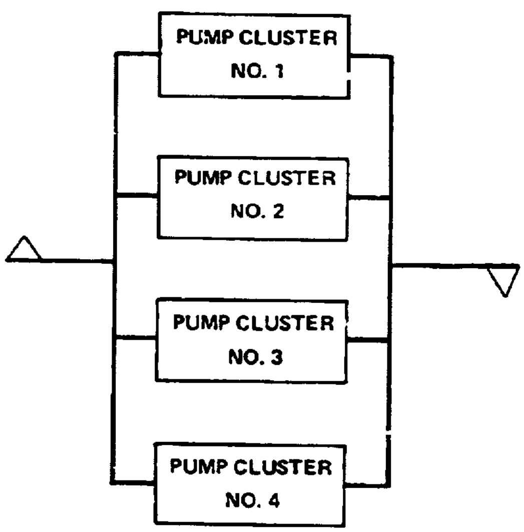

<u>Reliability expression:</u>

$$P_3 = R_1^4 + 4R_1^3Q$$

$$R_1 = \text{Reliability of Pump Cluster} = 1 - Q^3$$

$$Q = 1 - R = \text{Probability of Failure}$$

$$R = e^{-\lambda t}$$

where

λ = Failure rate/hour/pump = 0.0004

t = Flight time = 6.1 hours

e = Base of natural log.

$$P_3 = 5 \times 10^{-16}$$

8.5.2 Fuel venting regulation and control system. - Similar to the pumping distribution system, the reliability logic employed in this system uses the conventional binomial expansion equation to evaluate the probability of failure. The design concept employs redundant control valve logic and redundant vent valve logic. Within the control valve the design uses redundant control for pressure regulating with different regulator pressure settings. This concept provides the flight engineer the capability of monitor/indication of a faulty primary regulator. A manual override function to the pressure control valve is provided thus affording a third level of control for venting. The vent valves are single regulating valves, i.e., the auxiliary valve in a reliability diagram parallel to the primary vent valve. Probability of the loss of the venting system is illustrated and expressed numerically as follows:

P_4 = Probability of the loss of the Venting System during a 6.1 hour flight.

RELIABILITY SERIES/PARALLEL DIAGRAM FOR P_4

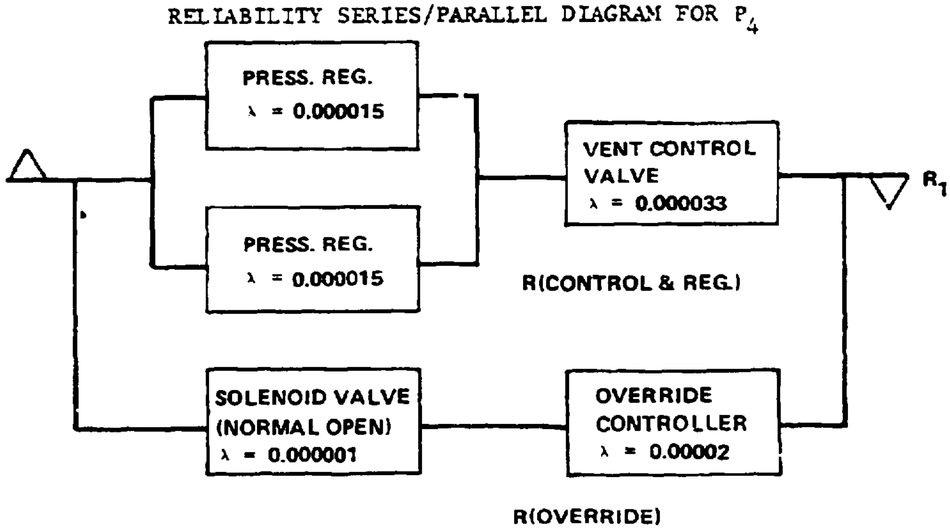

PRESSURE CONTROL AND VENT SYSTEM LOGIC FOR P_4

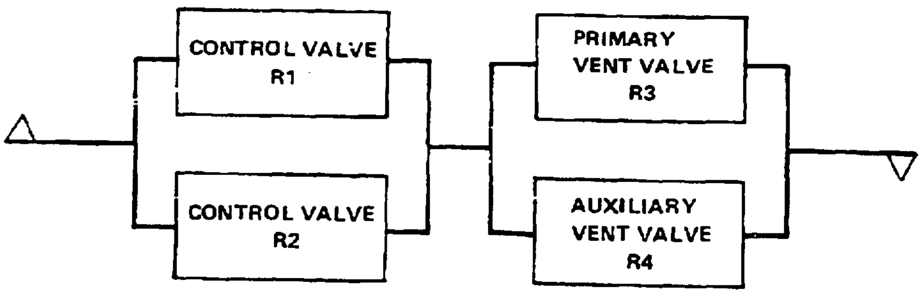

Reliability expression for typical control valve logic:

$$R_1 = R_2$$

$$R_1 = 1 - \left(1 - R_{(\text{control \& reg.})}\right)\left(1 - R_{(\text{override})}\right)$$

$$R = e^{-\lambda t}$$

where

λ = Failure rate for the failure mode defined in Table 85.

t = 6.1 hour flight

e = Base of natural log.

$$R_1 = 1 - (.000033008 \times .000021)$$

$$R_1 = 1 - 6.9(10^{-10})$$

Reliability expression for pressure control and vent system logic:

$$P_4 = \left(6.9(10^{-10})\right)^2 + \left(6.1(10^{-5})\right)^2$$
$$P_4 = 3.6 \times 10^{-9}$$

It is concluded that the LH_2 fuel system arrangements as specified herein will meet operational requirements at least as rigorous as those of current transport aircraft. The only recommendation is that dispatch regulations require that not more than two pumps can be failed.

8.6 Safety and Fire Protection

The usual precautions taken to minimize fire and explosion hazards in hydrocarbon fueled systems, such as separation of combustibles from ignition sources, compartmentization, compartment draining and purging must also be observed in the LH_2 airplane. However, the characteristics of cryogenic hydrogen require unique precautions in all of these areas.

Because of the low spark energy required to ignite gaseous hydrogen, electrical and electrostatic discharge levels which are acceptable in hydrocarbon/air mixtures will have to be reevaluated for acceptability in the presence of hydrogen/air mixtures. On the other hand, the combustible limit of H_2 - Air (4 percent by volume) is considerably higher than that of gasoline-air (1 percent). These effects may require a redefinition of what constitutes an explosion proof component. In this regard, it is probable that flame arrestors, as now conceived, will not be effective for hydrogen/air mixtures.

8.6.1 Compartment purging. - Compartmentation, to localize and minimize the effects of fire as well as to separate sources of potential fuel leaks from areas containing potential ignition sources, will be used extensively. Each compartment can be drained and vented, or protected by fire detecting and extinguishing systems effectively. Because of the low density of gaseous hydrogen, each compartment in which hydrogen can be released must have vent outlets at the top of the compartment as well as at the bottom. Each compartment will incorporate ram scoops for inflight air purging. Those compartments having a high probability of hydrogen leaks under ground static conditions will incorporate an active venting system using fans for forced circulation when a leak is detected. Compartment drainage will be used where the hydrogen leak can be large enough for some of it to accumulate as a liquid. Hydrogen detectors (sniffers) will be placed at vent exits to detect and locate gaseous H_2 leakage. Leakage will be indicated in the flight station.

The extremely low temperature of the stored hydrogen can create an environmental hazard for personnel in and around the airplane. Hence, it is essential that all points of discharge for liquid or gaseous hydrogen be remote to areas normally occupied by people.

8.6.2 Nitrogen inerting. - Both of the preferred fuel containment systems, Nos. 3 and 4, use a N_2 purge system to prevent moisture accumulation and freezing in the flexible open cell foam insulation layer beneath the outer protective cover. This has the added advantage of inerting the space surrounding the fuel tanks in the event of H_2 leakage since the GN_2 purge gas is vented overboard. The system is functionally the same as that described in Section 6.8.

The volume requirements for N_2 are very small and the total system weight is estimated to be 95 kg (210 lb) per aircraft, including the N_2 purge gas. Spaces surrounding the tank ends and lines for these systems will be purged as described above in 8.6.1.

8.6.3 Preparation for repair of insulation leaks. - Insulation leaks do not normally constitute a critical safety item. However, certain precautions must be observed when emptying the fuel system or tanks of liquid hydrogen in preparation for repair of the insulation. The effect of a hydrogen leak will almost always cause condensation and solidification of air by the process of cryopumping in the vicinity of the leak. As the liquid hydrogen is removed from the tank or line where the leak occurs, the system temperature will rise, warmed by the surrounding atmosphere. If this process is too rapid, the rate of air vaporization may be so high that large sections of insulation may be damaged, or even blown off, by the rapidly expanding air. Hence, the rate of heating should be controlled by monitoring the rate of removal of the hydrogen fuel.

8.7 Adjustments Required in FAR or Industry Standards

The use of hydrogen as a fuel for aircraft instead of a hydrocarbon fuel will affect many of the standards currently used in the industry. The standards most directly affected are the Federal Airworthiness Standards for Transport Category Airplanes (FAR Part 25), Airworthiness Standards for Aircraft Engines (FAR Part 33), and the National Fire Protection Association documents for Aircraft Fuel Servicing (NFPA No. 407) and Aircraft Fuel System Maintenance (NFPA No. 410C). In the following paragraphs, affected parts of the standards are listed, as well as the effects that must be considered when liquid hydrogen is used as a fuel.

FAR Part 25

25.801(d) - In ditching operations where structural damage can result in the removal of large sections of fuel tank insulation, a jettison system may be required to preclude excessive tank pressures being developed by the rapid vaporization of liquid hydrogen. Alternatively, a blowout disc of generous proportions should be provided.

25.951 General

(a) ok

(b) and (c) - The effects on engine operation of the introduction of air or water in the fuel does not apply to a hydrogen fueled airplane because contaminants of this type cannot be tolerated in liquid hydrogen fuel tanks.

(b) Revise - "Each fuel system must be designed so as to prevent vapor being introduced to the engine pump, if such should momentarily occur, it shall not result in an engine flameout."

(c) Revise - "Each fuel system must be capable of sustained operation throughout the aircraft operating envelope - including air start - with the liquid fuel in an initially saturated state."

25.953 Fuel system independence - ok

25.954 Fuel system lightning protection - ok

25.955 Fuel flow

(a) ok

(b) ok

(c) Add - "No flameout or interruption of engine thrust shall occur when switching from one tank to another."

25.957 Flow between interconnected tanks - ok

25.959 Unusable fuel supply - ok

25.961 Fuel system hot weather operation.

(a) 1, 2, 3, 4 - ok

(a) 5 - Delete. For hydrogen fueled airplanes, the fuel system must perform satisfactorily with the tank ullage pressure equal to the vapor pressure of the fuel.

(b) Delete last sentence.

25.965(a) (1) and (2) Hydrogen fuel tanks are closed systems in which the pressure is a function of the liquid fuel temperature.

(c) For hydrogen tanks, the fuel temperature during the fuel tank test must be determined by the maximum vapor pressure to be encountered during actual operation.

25.967(b) For hydrogen tanks, spaces adjacent to the tank wall cannot be ventilated because the air would be liquified. Ventilation external to the tank insulation may be advisable but the insulation must be sealed to prevent introduction of air to areas adjacent to the tank wall.

25.969 Fuel tank expansion space - Revise as follows:

Each fuel tank must provide a positive expansion space beyond that required by consideration of the following:

(1) Contraction of the tank from the normal ambient to the cryogenic condition and expansion resulting from pressurization.

(2) Expansion of the fuel when warming from the as-loaded density to that corresponding to a saturated liquid at the tank design pressure

(3) Space occupied by structure, lines and equipment

It must be impossible to fill this total expansion space inadvertently with the airplane in a normal ground attitude.

25.971 Fuel tank sump - delete

25.973 Fuel tank filler connection - delete

25.975 Fuel tank vents and carburetor vapor vents - Revise as follows:

25.975 Fuel tank pressurization and venting

The fuel tank pressurization and venting system shall:

(a) Maintain tank pressures within the design values during all normal and emergency ground and flight conditions.

(b) Prevent overpressurization beyond the limit pressure in the event of any single or probable combination of failures during refueling, ground hold, and all flight conditions.

(c) Prevent air ingestion into the tank and vent lines.

(d) Avoid vent stoppage by dirt or ice formation.

(e) The vent(s) shall discharge in an area clear of the aircraft and potential ignition sources both on the ground and in flight.

25.977 Fuel tank outlet

(a) ok

(b) (c) (d) (e) - delete

25.979 Pressure fueling system

(a) Revise "Each pressure fueling (and vent) connection to ground equipment must have means to prevent the escape of hazardous quantities of liquid or vapor, both upon initial connection and disconnect.

(b) (1) (2), ok

(c) ok

(d) Add - "Means must be provided to prevent excessive pressure rise in the fueling manifold due to vaporization of trapped liquid."

25.981 Fuel tank temperature. Delete

25.991 Fuel pumps

(a) ok

(b) ok

25.993 Fuel system lines and fittings

A paragraph must be added to this section to indicate that no materials which would be adversely affected when exposed to liquid hydrogen can be in the fuel system.

(a) (b) (c) (d) (e) (f) - ok

Add (g) "All lines connected by a means of positive shutoff must be provided with a means of preventing excess pressures due to vaporization of the trapped liquid fuel"

25.994 Fuel system components - ok

25.997 Fuel strainer or filter - delete

25.999 Fuel system drains - delete

25.1001 Fuel jettisoning system - ok

25.1305 Fuel tank pressure indicators must be added at the flight station.

FAR Part 33

3.3.67(a) For a hydrogen fueled engine, operation with water in the fuel is not required.

NFPA

No. 407 Aircraft Fuel Servicing - A section must be added specifying methods of servicing a hydrogen fueled airplane.

No. 410C Aircraft Fuel System Maintenance - A section must be added specifying methods of maintaining a hydrogen fueled airplane.

9. EQUIVALENT JET A-FUELED AIRCRAFT

The characteristics of a conventionally fueled aircraft designed to perform the identical mission using equivalent technology and design requirements as the LH_2-fueled aircraft of Section 8 were developed in order to be able to compare the two on an equitable basis. As noted in the introduction to Section 8, the revised and updated version of ASSET was used to generate the characteristics of the Jet A-fueled aircraft presented herein.

The first requirement was that the characteristics of a Jet A-fueled engine be developed which would have performance and weight based on the same technology as was used to represent the LH_2-fueled engine discussed in Section 4.3. It was then possible to parametrically generate an airplane design using the same guidelines and operational requirements as were used in the LH_2 aircraft design study.

The results of this work are reported in this section, together with a comparison of characteristics and performance of the two aircraft.

9.1 Jet A Engine Definition

The objective of this effort was to provide definition of a Jet A-fueled engine which would be directly comparable in technology to that of the LH_2-fueled design previously discussed. The hydrocarbon fueled engine which was used as a basis for the earlier, equivalent aircraft studies reported in Reference 1, could not be used because of changes made in assessment of component performance and efficiencies which could be available for initial operational capability in 1990-1995, which were incorporated into the LH_2 engine design.

Accordingly, a new design of Jet A engine was developed in which all characteristics matched those of the LH_2 engine developed by AiResearch - Arizona Division; see Section 4.3. Basic component efficiencies and performance were matched and the only changes made were due to differences in properties of the two fuels. The only modifications made to the AiResearch hydrogen fueled engine's thermodynamic cycle in order to develop the Jet A engine thermodynamic cycle were those due to the change in high pressure turbine cooling air temperature. In the hydrogen engine, the turbine cooling air is cooled by the fuel. Since this heat sink is not available for the Jet A engine, the turbine cooling airflow was increased from 3.2 percent to 7 percent. This increase maintains the same level of turbine cooling on both engines but decreases the high pressure turbine efficiency by 0.5 percent.

The aerothermodynamic changes that were required to make a hydrogen fueled engine into a Jet A fueled engine involved modification of the fuel lower heating value to 42.8×10^6 J/kg (18 400 Btu/lb), compared to 119.9×10^6 J/kg (51 590 Btu/lb) for hydrogen, and modification of the thermodynamic properties of the combustion products from the combustor to the nozzle.

The thermodynamic cycle properties listed in Table 86 were used in the gas turbine synthesis computer program, (Reference 39), with the combustion products subroutine supplied for hydrocarbon fuel and air to calculate off-design performance of the Jet A engine. The resulting installed engine performance of the Jet A engine is given in Appendix G.

To have a valid comparison, the Jet A-fueled engine was designed to be physically identical to the AiResearch hydrogen engine with the exception of the fuel system and the heat exchangers. Accordingly, both the physical dimensions and the weight of the Jet A engine are identical with those of the AiResearch hydrogen engine, except for allowances for the fuel system and the heat exchangers. The weight difference amounts to 95 kg (210 lb) for the baseline case. The same scaling relationships are valid for both engines.

TABLE 86. - THERMODYNAMIC DESIGN PARAMETERS

Inlet recovery	0.991
Fan efficiency	0.892
Fan pressure drop $\Delta P/P$	0.015
Compressor efficiency	0.862
Turbine cooling air	7.0%
Combustor efficiency	1.0
High pressure turbine efficiency	0.895
Low pressure turbine efficiency	0.900
Fan nozzle thrust coefficient	0.991
Core nozzle thrust coefficient	0.988
Horsepower extracted	125
Horsepower, accessories	21

9.2 Comparison: LH_2 vs Jet A Equivalent Aircraft

The design of a conventionally fueled transport sized to carry 400 passengers, 10 190 km (5500 n.mi.) at a cruise speed of Mach 0.85 was accomplished using the ASSET computer program. The parametric optimization process was carried out in the same manner as previously described for the LH_2 aircraft.

The characteristics of the resulting Jet A-fueled airplane are listed in Table 87, along with corresponding data on the LH_2 counterpart. The LH_2 airplane data are a repeat of that listed previously in Table 81. They are shown here for convenience in comparing.

The Jet A-fueled design is identical in configuration to the Jet A aircraft reported in Reference 1 except that it is heavier and has a larger wing. The larger wing stems from the more conservative engine component performance postulated for the new engine designs (both LH_2 and Jet A) in the present study, which in turn leads to greater fuel weight because specific fuel consumption is increased. The result is that, although both the previous (Reference 1) and the present Jet A designs were found to be optimum with a wing loading of 610 kg/m^2 (125 lb/ft^2), the greater fuel weight required an increase of 5262 kg (11 600 lb) in gross weight.

The LH_2 engine performance did not suffer as large a decrease, relative to the Reference 1 work, because ways were found to exploit the heat capacity of hydrogen which partially compensated for the effects of the reduction in component efficiencies and performance.

Comparing the aircraft designs shown in Table 87 the LH_2 version is seen to offer quite significant advantages in nearly all parameters. The only parameter in which the Jet A airplane shows an advantage is L/D. This is because its fuselage is smaller in diameter [5.84 m (230 in.) vs 6.63 m (261 in.)] and also shorter [60.05 m (197 ft) vs 65.72 m (215.64 ft)] relative to the LH_2 aircraft. In addition, the Jet A design has a larger wing. The combination of the large wing with a smaller fuselage, compared with the small wing and a larger fuselage on the LH_2 design leads to the ten percent advantage in L/D for the Jet A airplane.

However, this advantage is completely nullified by the almost 300 percent disadvantage the Jet A design suffers in cruise SFC. This leads to the tremendous difference in fuel weights between the two designs and accounts for the advantage the LH_2 aircraft enjoys in price, DOC, and energy utilization.

The direct operating costs shown in Table 82 were calculated on the basis of the respective fuel prices shown at the bottom of the table. Figure 197 shows the effect variation in fuel price would have on DOC for both aircraft. The baseline prices of \$4.74 per GJ (\$5/10^6 Btu) for Jet A and \$5.69 per GJ (\$6/10^6 Btu) for LH_2 were specified to represent reasonable costs assuming both fuels are manufactured from coal and water. As a point of reference, U.S. domestic air carriers today (November, 1977) are paying an average of about 10.6¢/ℓ (40¢/gal) for Jet A produced from petroleum. The direct operating

TABLE 87. – COMPARISON: LH_2 vs JET A SUBSONIC TRANSPORT AIRCRAFT

(400 Passengers; 10 190 km (5 500 m.mi.); Mach 0.85)

		LH_2	Jet A	Ratio (Jet A/LH_2)
Gross Wt.	kg (lb)	168 829 (372 200)	232 056 (511 600)	1.37
Total Fuel Wt.	kg (lb)	25 608 (56 460)	84 777 (186 900)	3.14
Block Fuel Wt.	kg (lb)	21 621 (47 670)	72 365 (159 540)	3.35
Operating Empty Wt.	kg (lb)	103 305 (227 750)	107 363 (23[illegible] 7[illegible]0)	1.04
Aspect Ratio	–	[illegible]	9	
Wing Area	m^2 (ft^2)	296.8 (3195)	380.3 (4093)	1.[illegible]
Sweep	rad (deg)	.524 (30)	.524 (30)	
Span	m (ft)	51.7 (169.6)	58.5 (191.9)	1.13
Fuselage Length	m (ft)	65.7 (215.6)	60.0 (197)	.914
L/D - Cruise	–	17.4	19.1	1.10
SFC - Cruise	$\frac{kg}{hr}$/daN $\left(\frac{lb}{hr}/ lb\right)$	0.206 (0.202)	.615 (.603)	2.99
Initial Cruise Alt.	m (ft)	11 580 (38 000)	11 580 (38 000)	
Wing Loading	kg/m^2 (lb/ft^2)	568.8 (116.5)	610.2 (125)	1.07
Thrust/Weight	N/kg (–)	3.20 (.326)	3.19 (.325)	.997
No. Engines		4	4	
Thrust Per Engine (SLS, uninstalled)	N (lb)	135 000 (30 350)	184 900 (41 567)	1.37
FAR T.O. Distance	m (ft)	2440 (8000)	2431 (7980)	
FAR Ldg. Distance	m (ft)	1768 (5800)	1584 (5200)	
2nd Seg Climb Grad. (Eng Out)		.0300	.0305	
Approach Speed	m/s (KEAS)	71.2 (138.4)	65.5 (127.4)	
Weight Fractions	percent			
Fuel	–	15.17	36.53	
Payload	–	23.64	17.20	
Structure	–	32.39	26.32	
Propulsion (Includes Tanks & Fuel Systems)	–	9.07	5.37	
Price	$\$10^6$	43.39	44.53	1.03
DOC[a]	$\frac{c}{seat\ km}\left(\frac{c}{seat\ n.mi}\right)$	0.869 (1.609)	0.907 (1.679)	1.04
Energy Utilization	$\frac{kJ}{seat\ km}\left(\frac{Btu}{seat\ n.mi}\right)$	636 (1118)	759 (1334)	1.19

(a) DOC based on LH_2 cost = \$5.69 per GJ (\$6/10^6 Btu = 31c/lb)

Jet A cost = \$4.74 per GJ (\$5/10^6 Btu = 62.2c/gal)

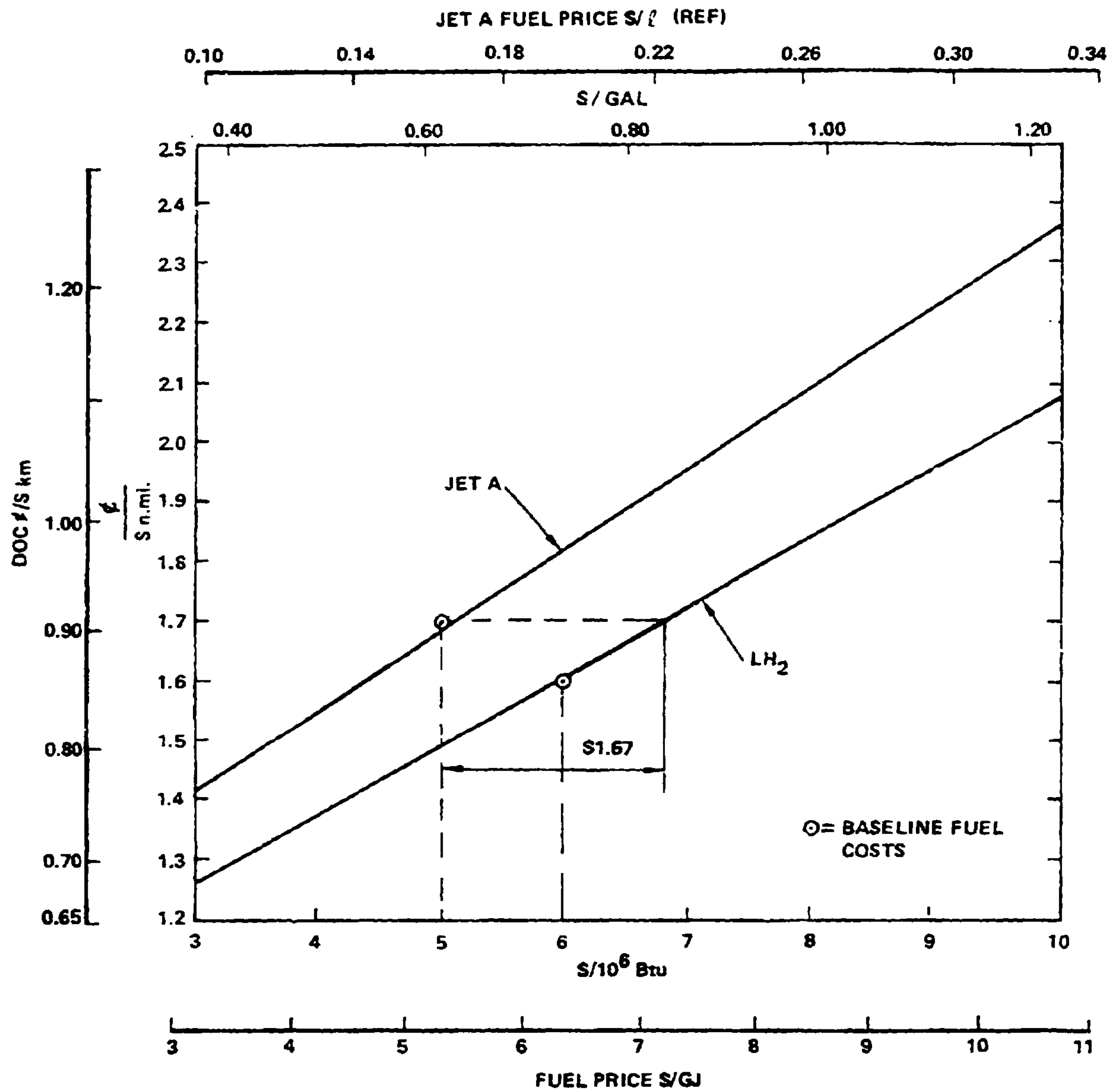

Figure 197. - Sensitivity of DOC to fuel price for both LH_2 and Jet A aircraft.

costs calculated for the LH_2 airplane include consideration of the increment due to fuel losses from boiloff.

Two things are significant to note regarding Figure 197. One is the spread of \$1.67 per 10^6 Btu measured from the baseline price of Jet A to a value which can be paid for LH_2 and still provide the operator with equal DOC. The other is the divergence of the two lines, indicating that as fuel prices continue to climb, the advantage for LH_2 will steadily increase.

9.3 Off-Design Payload Capability

In comparing LH_2 and Jet A - fueled aircraft it is important to recognize that the difference in the properties of the fuels leads to differences in their containment systems and that this, in turn, leads to widely differing capabilities in off-design payload/range operation. Within limits, conventionally fueled transports can readily interchange fuel weight for payload to achieve extended ranges. On the other hand, hydrogen-fueled aircraft are volume limited insofar as fuel capacity is concerned. Therefore, the only increase in range capability which can be obtained with LH_2 fueled aircraft derives from the reduction in weight if the number of passengers or pounds of cargo is limited. Fuel weight cannot be increased beyond that carried for the design mission without major modification of the aircraft fuselage structure.

Figure 198 illustrates the situation. The design mission of the aircraft in the subject study was to carry 400 passengers 10 190 km (5500 n.mi.) (point 1). By limiting the passenger load to only 250, i.e., reducing payload from 39 916 kg (88 000 lb) to 24 948 kg (55 000 lb), and by carrying an equivalent 14 969 kg (33 000 lb) increase in fuel weight, the range capability of the Jet A airplane is increased to 12 501 km (6750 n.mi.) (point 2). There is adequate volume in the wing box and center section to accommodate that much more Jet A fuel. On the other hand, if the LH_2 airplane payload is reduced to 24 948 kg (55 000 lb), its maximum range is increased to only 10 618 km (5733 n.mi.) since its fuel capacity cannot be increased. (point 3).

A parametric investigation was made to determine what size LH_2 airplane would provide the extended range capability of the Jet A design with 250 passengers, and yet would also be capable of carrying 400 passengers at shorter ranges. The result is shown on Figure 198 as point 4. With the full complement of 400 passengers, the resized LH_2 airplane will have a range capability of 11 982 km (6470 n.mi.).

The table on the figure provides a summary of some of the characteristics of the aircraft involved. It may be observed that the energy use rate of the LH_2 fueled airplane is always less than that of the Jet A version for comparable missions.

This issue may be summarized by pointing out that due to the difference in fuel containment provisions it is not feasible for LH_2-fueled and Jet A-fueled aircraft to have exactly the same payload/range trade-off capability. For the general size of aircraft studied herein, a LH_2-fueled design can provide a larger envelope of useful payload-range capability and still perform any specified mission within the envelope using less energy than a corresponding Jet A-fueled version.

POINT DESIGNATION		JET A ①	JET A ②	LH_2 ①	LH_2 ③	LH_2 ④	LH_2 ②
PASSENGERS		400	250	400	250	400	250
RANGE	km (n.mi)	10190 (5500)	12500 (6750)	10190 (5500)	10620 (5733)	11980 (6470)	12500 (6750)
TOGW	kg (lb)	232 060 (511 600)	232 060 (511 600)	168 830 (372 200)	154 090 (339 700)	180 810 (398 610)	166 060 (366 100)
BLOCK FUEL	kg (lb)	72 370 (159 540)	86 190 (190 020)	21 620 (47 670)	21 620 (47 670)	26 590 (58 610)	26 590 (58 610)
OEW	kg (lb)	102 379 (236 700)	107 370 (236 700)	103 310 (227 750)	103 310 (227 750)	108 340 (238 840)	108 340 (238 840)
ENERGY USE RATE	$\frac{kj}{PAX\ km}$ $\frac{Btu}{PAX\ n.mi}$	759 (1334)	1179 (2073)	636 (1118)	976 (1716)	665 (1168)	1020 (1792)

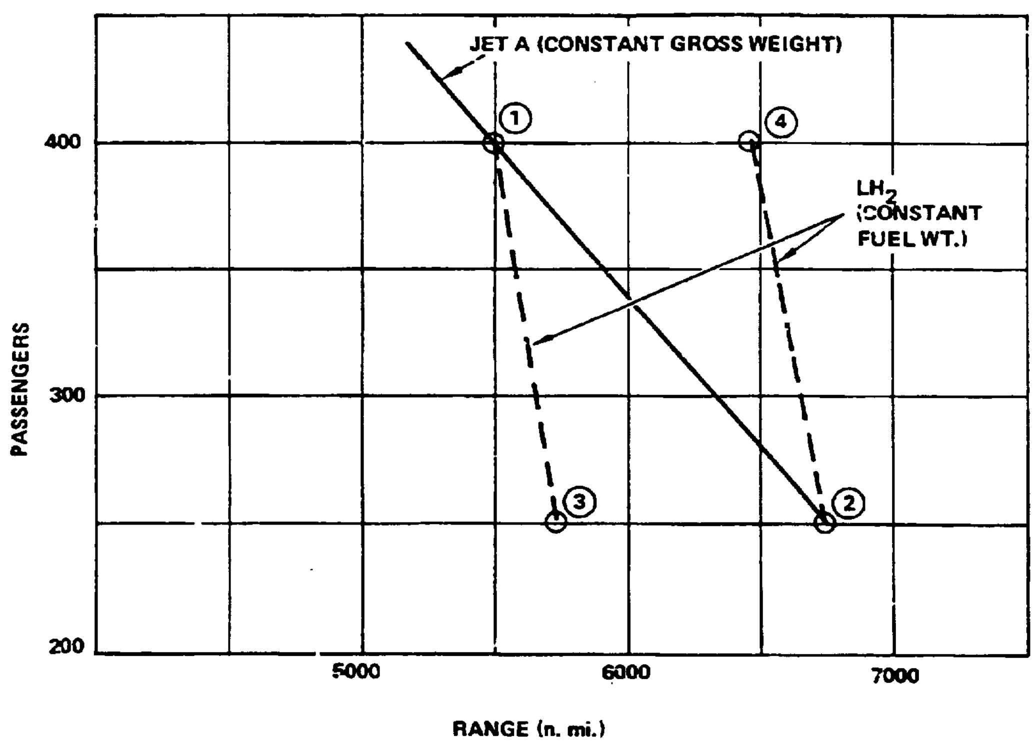

Figure 198. - Off-design payload range capability.

10. TECHNOLOGY DEVELOPMENT

Throughout this report, at the end of most major sections, research and technology development items pertinent to the subject are listed. Each of these items is considered significant and necessary for the ultimate development of LH_2-fueled aircraft. In this section a development program is presented which is the result of consideration and evaluation of these individual items. The items are listed in order of perceived priority, 1 through 5, to indicate recommended scheduling. The priority rating is not intended to designate relative significance or importance.

10.1 First Priority

Item 1) Large Model Tank Fabrication and Test. - Design, fabricate, and test a sizeable model of an aircraft tank, large enough that minimum gage considerations will not seriously distort the heat transfer properties of the structural attachments and the insulation system. A half scale (approximately 10 ft dia) model of either of the subject aircraft tanks is suggested to provide valid experimental data at a reasonable program cost.

Such a tank would serve a number of useful functions:

A. Focus design attention on detail problems which tend to be overlooked or glossed-over in conceptual studies, e.g.,

- specific fabrication methods
- attachment of appendages
- structural support provisions
- inspection and repair provisions.

B. Provide experience in fabricating, maintaining, and operating a sizeable flightweight tank insulated to meet aircraft requirements.

C. Permit experimental determination of the heat transfer mechanism in a large, horizontally inclined, insulated tank containing LH_2. Nusselt Number, tank wall temperatures, vapor volume temperatures, and the temperature and quantity of the GH_2 vented from the tank can all be determined as functions of the following conditions within the tanks, and for various liquid levels:

- stratified (liquid and vapor)
- turbulent (liquid and/or vapor)
- simulated aircraft motions.

D. Investigate aircraft tank filling procedures. Experimentally determine the preferred design of plumbing system and operational procedure which will permit refueling of aircraft tanks within specified time limits.

E. Test various quantity sensor devices to determine which provides most reliable data for an aircraft tank application. Conduct tests with tank in motion to simulate aircraft ride quality with resultant agitation of liquid surface.

F. In conjunction with Items 4 and 7 (following), conduct flow tests of a representation of an engine fuel supply and control system to determine:

- system chill-down time
- transient response characteristics
- delivery conditions of the LH_2 at the engine-end of the feed system
- other characteristics as described under Items 4 and 7.

These flow tests could be performed with the entire feed system functioning except that the output from the engine-mounted pump would be valved to simulate engine consumption vs throttle setting. Flow delivery from the feed system could be captured in a ground storage tank for return and reuse in the experimental equipment.

Item 2.) Pump Development. - Design and development of LH_2 pumps for the aircraft application is recognized as a major requirement. The following characteristics must be provided by both the boost pumps and the high pressure, engine-mounted pumps:

- Long life
- Reliable
- Maintainable
- Efficient over a wide range of flow rates and pressures
- Qualify as line replaceable units.

The proposed effort would include design, fabrication, and experimental development to achieve these objectives.

An initial step would be preliminary design of pumps for both applications in sufficient depth to establish the bearing requirements. Design, fabrication, and feasibility testing of bearing systems would then be carried out to demonstrate that these requirements can be met. The bearing feasibility tests would be conducted in a bearing test rig. It is necessary that both the boost pump and the high pressure engine pump be designed, built, and tested because of the difference in their design requirements and their potential bearing designs.

Item 3.) Systems Analysis of Ways to Initiate LH_2 Fuel Service in Airline Operations. - Analyze airline route structures, traffic densities, and aircraft usage throughout the United States as projected for the 1990-2000 time period. In addition, include consideration of connecting international routes, with special attention to routes to those countries most likely to require early relief from use of hydrocarbon fuel.

A. Determine feasible ways to initiate use of LH_2 fuel in commercial transport aircraft, for example,

- by airline
- by city-pair, e.g., L.A to Washington
- by region, e.g., West Coast

B. Project the fuel changeover from U.S. domestic airlines to international carriers.

C. Establish a feasible schedule for installation of LH_2 facilities at airports and determine costs and fuel requirements vs years.

D. Define principal problems, costs, and possible methods of funding.

E. Determine a logic for initiation of hydrogen in society, i.e., should the air transport industry be the first to convert, rather than other possible candidates, e.g., utilities, industry, etc.

10.2 Second Priority

Item 4.) Engine Fuel Supply System Experiments. - Design, fabricate, and test a complete engine fuel supply system including boost pumps, valves, and line. Duplicate a feed line to an outboard engine with equivalent turns, joints, and length to represent the aircraft installation. Mount on tank (Item No. 1) per aircraft installation. Experimentally determine:

- operational characteristics
  - o chill-down time
  - o flow response transients
  - o temperature rise vs flow rate

- vent requirements vs time after simulated engine shutdown
- requirements to maintain insulation properties
- structural support requirments.

Two types of fuel lines are viable candidates. One uses a vacuum annulus between concentric tubes to provide the insulation. The other also uses concentric tubes but has closed cell foam in the annulus. Experimental work is required on both types of designs to determine a preference on the basis of

- fabricability
- maintenance
- operational characteristics
- susceptibility to mechanical damage.

Item 5.) Advanced Engine Design Study. - The engine conceptual design study conducted in the present program was a very abbreviated effort. It was not intended to be an investigation which would provide final answers to all questions about LH_2 engine design. Rather, it served as a guide, primarily in determining the potential of several possible ways to use the heat capacity of hydrogen to good advantage. Accordingly, it is proposed that a comprehensive design study be made which would involve investigation of more of the design potential of LH_2-fueled turbofan engines on both a broader and a more in-depth basis. The objectives would be as follows:

- Establish design and performance characteristics of an advanced design, quiet, cleanburning LH_2-fueled engine to match requirements of a selected airplane design. Provide size, weight, cycle characteristics, performance, and cost estimates.
- Establish requirements for major components, e.g., high pressure pump, heat exchangers, combustor design, noise suppression devices, engine control system, compressor, fan, turbines, and cooling system.
- Provide input for Item 8.

Item 6.) Aircraft Vent System Design and Test. - The vent which must be provided on an aircraft fueled with LH_2 presents problems which are unique.

- The vent must be capable of releasing cryogenic gaseous hydrogen at any time the pressure in the aircraft fuel tanks exceeds a set upper limit. The release can be into cold moist air which can cause the vent valve to freeze when venting stops. Methods must be devised to avoid the consequences of this happening.

- The vented gas can catch fire. Surrounding aircraft structure must be protected so as to be invulnerable to this occurrence.

- The vent must be provided with the capability of preventing external flame from propagating upstream into the vent system tubes leading to the fuel tanks. Conventional flame suppressors used on hydrocarbon-fueled aircraft will not be effective with hydrogen vapor fires because the very high flame speed and short quenching distance of hydrogen appears to make the system mechanically infeasible.

- The vent exit must be protected from the effects of lightning strikes.

The proposed technology development would involve design and fabrication of a vent system mounted in representative aircraft structures, and tests conducted under typical exposure conditions.

10.3 Third Priority

Item 7.) Engine Fuel Control System Testing. - This item is contingent upon Items 1, 2, 4, and 8A having been successfully completed and the hardware being available for additional flow testing with LH_2. The objective would be to determine transient response characteristics of the entire fuel supply system (to one engine) including the control network. The program would consist of both an analytical and an experimental effort. An analysis and an analog simulation of the engine fuel delivery and control system would be made to determine performance capability, including the effect of transients. The experimental effort would involve fabrication of a representative system and testing to simulate the following operations and verify the analysis:

- start

- shutdown

- control representing flow variation to satisfy design flight conditions.

Use of the 270 Vdc system to control boost pump output with brushless dc motor drives, a high temperature sensor in the engine, and microelectronics in an advanced design of fuel control system will make this development item particularly desirable because of the great flexibility offered by the system.

Item 8.) Engine Technology Development. - The results from the advanced engine design study, Item No. 5, will provide the basis for this task. It involves design, fabrication, and test of components of an advanced design of LH_2-fueled engine, including:

- Heat exchanger
- Combustor
- Cooled turbine vanes and blades

The objective is to develop component technology required to build a liquid hydrogen-fueled engine incorporating features to capitalize on advantages available with the fuel.

Task 8A) <u>Heat Exchanger Development</u>

Design and develop heat exchangers as required by the engine concept, e.g., to cool engine oil, compressor bleed air for cabin air conditioning and turbine cooling, and to heat the fuel with the core engine exhaust. Experimental testing is required to demonstrate:

- anti-icing protection
- heat exchanger effectiveness
- transient fuel flow response characteristics
- compliance with design requirements

Task 8B) <u>Combustor Experiments</u>

Very little experimental development work has been performed on combustors for aircraft gas turbines where the components were designed to use hydrogen as the fuel. Work performed at NASA-Lewis starting in the late 1950's used fuel injectors and combustor cans taken from existing hydrocarbon-fueled engines, modified only as required. The work proposed here involves design of injection systems and combustor configurations specifically for hydrogen fuel, and experimental determination of the temperature profile and NO_x concentrations as functions of various design parameters. The objectives would be to determine:

- a preferred geometry and design of injectors and combustor for hydrogen/air
- the practical limits of NO_x generation at the design combustion temperature
- the variation of NO_x as a function of design combustion temperature
- temperature profile characteristics as a function of injector design and combustor configuration.

Task 8C) Cooled Turbine Vanes and Blades

The present study showed the desirability of cooling the turbine cooling air to reduce the bleed air requirement and to gain HP turbine efficiency. An existing engine could be used as a test article to develop a satisfactory design of hp turbine stage utilizing refrigerated air as a coolant. The testing could be done in conjunction with the appropriate heat exchanger developed in Task (A). Experiments would show:

- the effectiveness of blade and vane cooling as a function of air quantity and temperature for various designs.
- the effect of cooling air flow rate on turbine efficiency.

Item 9.) Materials Development. -

Activity:

Conduct literature searches, obtain manufacturer's data, and perform laboratory experiments.

Objectives:

A. Determine materials preferred for use as

- Cryogenic insulation for fuel tank
- Impermeable barrier to ei. - GH_2 or air
- Tank bladder/structural mater.
- Structural connection between cryoge... tank and ambient temperature aircraft structure
- Cryogenic fuel line/bellows/support structure
- Sealing surfaces for valves

B. Begin determination of effects of long-term exposure to hydrogen of selected structural and component materials.

Item 10.) Hazard Studies and Tests. - Use of LH_2 poses different problems related to safety, compared to conventional aircraft procedures and requirements. The following tasks are suggested to explore those differences and to develop appropriate preventive and combative measures for the hazards which exist with LH_2. This item is considered especially important because of the widespread misapprehension which exists regarding safety of hydrogen. It is felt that studies and demonstrations such as are proposed will provide a basis for dispelling and quieting these fears which are largely based on lack of knowledge.

Task 10A.) Study of Relative Hazards of LH_2 vs Jet A Fuel in Commercial Aircraft

Activity:

Study representative designs of a selected size of commercial transport aircraft: one fueled with LH_2, the other with conventional Jet A. Analyze the designs for probable failure modes, both in-flight and on the ground. Where appropriate, supplement the study with analysis of accident reports.

Objectives:

A. By analysis of probabilities of various kinds of accidents, both in-flight and on the ground, estimate probable failure modes and results which can be expected with both fuel systems.

B. Provide input for Item 10C.

Task 10B.) Hazard Posed by Fire: LH_2 vs Jet A Fuel

Activity:

Expose instrumented fuselage sections of surplus transport aircraft to fire from equal-energy quantities of LH_2 and Jet A fuel.

Objective:

Determine effect of fire from burning fuel adjacent to passenger compartment and compare relative hazards to crew and passengers.

Task 10C.) Safety in Nonfatal Crashes

Activity:

Simulate nonfatal crashes with surplus aircraft components containing fuel in typical tank structures. Perform duplicate tests with surplus aircraft having fuel tanks designed for LH_2 and for Jet A.

Objective:

Determine effect of simulated crash using each fuel system and compare relative hazard to crew and passengers.

10.4 Fourth Priority

Item 11.) Aircraft Fuel System Test. - Before an LH_2-fueled aircraft is committed to flight test a replica or model of its fuel system should be tested on the ground. With equipment from all the foregoing tests, the major portion of the aircraft fuel system will be available for this purpose. Equipment from Items 1, 4, 6, 7, and 8, respectively, will provide the following:

- A half scale model of one tank of the fuel containment system with vapor return and fueling adapters
- Engine fuel supply system
- Aircraft vent system
- Engine fuel control system
- Heat exchangers

This will leave just the following items to be obtained in order to conduct meaningful tests of a replica of a complete aircraft fuel system:

- Parts of the fueling/defuel system
- Parts of the vent and pressurization system
- Leak detection system.

With the entire aircraft fuel system assembled, tests could be conducted which would permit accomplishing the following objectives:

- Determine operational characteristics of an integrated design of an aircraft fuel system.
- Provide a basis for writing design specifications for LH_2 fuel systems and components suitable for aircraft service.
- Determine procedures for performing inspection and repair of LH_2 system components.
- Determine effect of repeated flight cycles and fueling/defueling cycles on tank structure, insulation system, and fuel feed system.

10.5 Fifth Priority

Item 12.) Flight Demonstration Program. - Following the ground tests of the LH_2 fuel system, the next logical step would be a flight demonstration program. This would involve building a complete fuel system for an existing airplane and flying the airplane using the LH_2 fuel system in a routine, operational manner for a significant length of time, e.g., a year or more.

Selection of the airplane should be given very careful consideration. The aircraft needs to be big enough to contain at least one LH_2 tank in the fuselage, with sufficient volume to provide for a range of at least 4630 km (2500 n.mi.). This would permit the converted aircraft to be used operationally during the test period, thus imposing a need to meet schedules and offering a chance to show whether the LH_2 fuel system can be competitive in terms of maintenance, reliability, and operational requirements. On the other hand, the selected aircraft should not be too big because of cost aspects.

The objectives of a flight demonstration program would be:

- Learn how to handle LH_2 as an aircraft fuel in an operational manner.
- Determine the practicability of the cryogenic fuel system in terms of inspection, maintenance, durability, and performance.
- Provide a basis for writing design and operational specifications for hydrogen-related equipment and procedures.
- Establish confidence that hydrogen can be used safely in airline-type operations.

APPENDIX A

PRELIMINARY MISSION FUEL FLOW SCHEDULE

For use during the early stages of the study it was necessary to establish a representative fuel flow schedule for the design mission. The following data were derived using the ASSET computer program and the characteristics of the 400 passenger, 10186 km, (5 500 n. mi.) range, M 0.85 LH_2-fueled aircraft from Reference 1. These data served as a basis for initial sizing of pumps, lines, valves, etc., until the characteristics of the LH_2 engine discussed in Section 4, herein, were determined and the aircraft resized, Section 8.

TABLE 88. - INITIAL DESIGN MISSION FUEL FLOW SCHEDULE

(LH_2, M 0.85, 400 PAX, 10 190 km (5500 n.mi.)

CL 1317-1

ASSET RUN DATED 9-14-76

Segment	Initial Altitude m (ft)	Initial Mach	Incremental			Segment			Total		
			Fuel kg (lb)	Time (min)	Avg. $\dot{w}$ kg/hr (lb/hr)	Fuel kg (lb)	Time (min)	Avg. SFC $\frac{kg}{hr}$/daN $\left(\frac{lb}{hr}/lb\right)$	Fuel kg (lb)	Time (min)	Distance km (n.mi)
Taxi	0 (0)	0	-	-	303 (669)	70.8 (156)	14.0	0.119 (0.117)	70.8 (156)	14.0	0 (0)
Takeoff	0 (0)	0	-	-	4899 (10 800)	81.6 (180)	1.0	0.096 (0.094)	152.4 (336)	15.0	0 (0)
Climb	0 (0)	0.378	-	-	4541 (10 012)	264.9 (584)	3.5	0.155 (0.152)	417.3 (920)	18.5	30 (16)
	305 (1000)	0.385	25.9 (57)	0.31	5004 (11 032)						
	610 (2000)	0.392	26.3 (58)	0.32	4933 (10 875)						
	914 (3000)	0.399	25.9 (57)	0.32	4848 (10 688)						
	1219 (4000)	0.407	26.3 (58)	0.33	4783 (10 545)						
	1524 (5000)	0.414	25.9 (57)	0.34	4563 (10 059)						
	1829 (6000)	0.422	26.3 (58)	0.35	4510 (9943)						
	2134 (7000)	0.430	26.8 (59)	0.35	4588 (10 114)						
	2438 (8000)	0.438	26.8 (59)	0.37	4339 (9566)						
	2743 (9000)	0.447	27.2 (60)	0.39	4187 (9231)						
	3048 (10 000)	0.456	27.7 (61)	0.40	4150 (9150						
Accelerate	3048 (10 000)	0.456	-	-	4082 (9000)	95.3 (210)	1.4	0.176 (0.173)	512.6 (1130)	19.8	44 (24)
	3048 (10 000)	0.476	8.1 (18)	0.12	4082 (9000)						
	3048 (10 050)	0.496	9.1 (20)	0.13	4137 (9120)						
	3048 (10 000)	0.516	9.1 (20)	0.13	4154 (9158)						

TABLE 88. Continued.

Segment	Initial Altitude m (ft)	Initial Mach	Incremental Fuel kg (lb)	Incremental Time (min)	Incremental Avg $\dot{w}$ kg/hr (lb/hr)	Segment Fuel kg (lb)	Segment Time (min)	Segment Avg. SFC $\frac{kg}{hr}$/daN $\left(\frac{lb}{hr}/lb\right)$	Total Fuel kg (lb)	Total (min)	Total Distance km (n.mi.)
Accelerate (Cont'd)	3048 (10 000)	0.536	9.5 (21)	0.14	4134 (9115)						
	3048 (10 000)	0.556	10.0 (22)	0.14	4165 (9182)						
	3048 (10 000)	0.576	10.9 (24)	0.15	4200 (9259)						
	3048 (10 000)	0.596	11.3 (25)	0.16	4208 (9278)						
	3048 (10 000)	0.616	12.7 (28)	0.18	4213 (9287)						
	3048 (10 000)	0.636	13.2 (29)	0.18	4236 (9338)						
	3048 (10 000)	0.638	1.4 (3)	0.02	4233 (9333)						
	3048 (10 000)	0.638	-	-	2922 (6441)	2171.8 (4788)	44.6	0.204 (0.200)	2684.4 (5916)	64.5	719 (388)
	3353 (11 000)	0.651	38.6 (85)	0.54	4284 (9444)						
	3658 (12 000)	0.663	39.5 (87)	0.56	4228 (9321)						
	3962 (13 000)	0.677	41.3 (91)	0.60	4128 (9100)						
	4267 (14 000)	0.690	42.6 (94)	0.63	4061 (8952)						
	4572 (15 000)	0.705	45.4 (100)	0.68	4002 (8824)						
	4877 (16 000)	0.719	47.2 (104)	0.72	3931 (8667)						
	5182 (17 000)	0.734	48.5 (107)	0.76	3831 (8447)						
	5486 (18 000)	0.749	50.8 (112)	0.81	3763 (8296)						
	5791 (19 000)	0.764	54.4 (120)	0.89	3670 (8090)						

TABLE 88. Continued.

Segment	Initial Altitude m (ft)	Initial Mach	Incremental Fuel kg (lb)	Incremental Time (min)	Incremental Avg. $\dot{w}$ kg/hr (lb/hr)	Segment Fuel kg (lb)	Segment Time (min)	Segment Avg. SFC $\frac{kg}{hr}$/daN $\left(\frac{lb}{hr}/lb\right)$	Total Fuel kg (lb)	Total Time (min)	Total Distance km (n.mi.)
Climb (Cont'd.)	6096 (20 000)	0.780	57.2 (126)	0.95	3610 (7958)						
	6401 (21 000)	0.797	62.6 (138)	1.06	3543 (7811)						
	6706 (22 000)	0.814	68.9 (152)	1.19	3476 (7664)						
	7010 (23 000)	0.832	81.2 (179)	1.43	3406 (7510)						
	7315 (24 000)	0.849	103.4 (228)	1.86	3336 (7355)						
	7620 (25 000)	0.850	83.5 (184)	1.54	3252 (7169)						
	7925 (26 000)	0.850	83.5 (184)	1.58	3169 (6987)						
	8230 (27 000)	0.850	84.4 (186)	1.65	3068 (6764)						
	8534 (28 000)	0.850	86.6 (191)	1.74	2987 (6586)						
	8839 (29 000)	0.850	88.9 (196)	1.87	2883 (6357)						
	9144 (30 000)	0.850	92.1 (203)	1.97	2805 (6183)						
	9449 (31 000)	0.850	99.8 (220)	2.21	2709 (5973)						
	9754 (32 000)	0.850	113.9 (251)	2.62	2607 (5748)						
	10 058 (33 000)	0.850	138.8 (306)	3.34	2493 (5497)						
	10 363 (34 000)	0.850	189.1 (417)	4.75	2389 (5267)						
	10 668 (35 000)	0.850	329.8 (727)	8.70	2274 (5014)						

TABLE 88. Continued.

Segment	Initial Altitude m (ft)	Initial Mach	Incremental Fuel kg (lb)	Incremental Time (min)	Incremental Avg $\dot{w}$ kg/hr (lb/hr)	Segment Fuel kg (lb)	Segment Time (min)	Segment Avg. SFC $\frac{kg}{hr}$/daN $\left(\frac{lb}{hr}/lb\right)$	Total Fuel kg (lb)	Total Time (min)	Total Distance km (n.mi.)
Cruise	10 668 (35 000) to 11 582 (38 000)	0.850	-	-	2038 (4492)	20 931.0 (46 145)	616.4	0.203 (0.199)	23 615.4 (52 063)	680.8	9997 (5398)
Descent	10 668 (35 000)	0.850	-	-	594 (1310)	70.3 (155)	7.1	-1.687(-1.654)	23 685.7 (52 218)	687.9	10 101 (5454)
	10 363 (34 000)	0.850	1.4 (3)	0.26	314 (692)						
	10 058 (33 000)	0.850	1.8 (4)	0.26	419 (923)						
	9754 (32 000)	0.850	1.8 (4)	0.25	435 (960)						
	9449 (31 000)	0.850	1.4 (3)	0.24	340 (750)						
	9144 (30 000)	0.850	1.8 (4)	0.23	473 (1043)						
	8839 (29 000)	0.850	1.4 (3)	0.23	355 (783)						
	8534 (28 000)	0.850	1.8 (4)	0.22	495 (1091)						
	8230 (27 000)	0.850	1.8 (4)	0.21	518 (1143)						
	7925 (26 000)	0.850	1.4 (3)	0.21	389 (857)						
	7620 (25 000)	0.850	1.8 (4)	0.20	544 (1200)						
	7315 (24 000)	0.849	1.8 (4)	0.19	573 (1263)						
	7010 (23 000)	0.832	2.7 (6)	0.30	544 (1200)						
	6706 (22 000)	0.314	2.7 (6)	0.31	527 (1161)						
	6401 (21 000)	0.797	3.2 (7)	0.31	615 (1355)						

TABLE 88. Continued.

Segment	Initial Altitude m (ft)	Initial Mach	Incremental Fuel kg (lb)	Incremental Time (min)	Incremental Avg $\dot{w}$ kg/hr (lb/hr)	Segment Fuel kg (lb)	Segment Time (min)	Segment Avg. SFC $\frac{kg}{hr}$/daN $\left(\frac{lb}{hr}/lb\right)$	Total Fuel kg (lb)	Total Time (min)	Total Distance km (n.mi.)
Descent (Cont'd)	6096 (20 000)	0.780	3.2 (7)	0.32	595 (1312)						
	5791 (19 000)	0.754	3.2 (7)	0.32	595 (1312)						
	5486 (18 000)	0.749	3.6 (8)	0.33	660 (1455)						
	5182 (17 000)	0.734	3.6 (8)	0.32	680 (1500)						
	4877 (16 000)	0.719	3.6 (8)	0.33	660 (1455)						
	4572 (15 000)	0.705	4.1 (9)	0.34	720 (1588)						
	4267 (14 000)	0.677	4.1 (9)	0.34	720 (1588)						
	3962 (13 000)	0.677	4.1 (9)	0.34	720 (1588)						
	3658 (12 000)	0.663	4.5 (10)	0.35	777 (1714)						
	3353 (11 000)	0.651	4.5 (10)	0.36	756 (1667)						
	3048 (10 000)	0.638	5.0 (11)	0.36	831 (1833)						
Decelerate	3048 (10 000)	0.638	-	-	800 (1763)	21.3 (47)	1.6	-	23 707.0 (52 265)	689.5	10 117 (5463)
	3048 (10 000)	0.618	1.8 (4)	0.14	777 (1714)						
	3048 (10 000)	0.598	2.3 (5)	0.14	972 (2143)						
	3048 (10 000)	0.578	1.8 (4)	0.16	680 (1500)						
	3048 (10 000)	0.558	2.3 (5)	0.16	850 (1875)						
	3048 (10 000)	0.538	2.3 (5)	0.17	801 (1765)						

TABLE 88. Continued.

Segment	Initial Altitude m (ft)	Initial Mach	Incremental Fuel kg (lb)	Incremental Time (min)	Incremental Avg $\dot{w}$ kg/hr (lb/hr)	Segment Fuel kg (lb)	Segment Time (min)	Segment Avg. SFC $\frac{kg}{hr}$/daN $\left(\frac{lb}{hr}/lb\right)$	Total Fuel kg (lb)	Total Time (min)	Total Distance km (n.mi.)
Decelerate (Cont'd)	3048 (10 000)	0.518	2.7 (6)	0.19	860 (1895)						
	3048 (10 000)	0.498	2.7 (6)	0.19	860 (1895)						
	3048 (10 000)	0.478	2.3 (5)	0.20	680 (1500)						
	3048 (10 000)	0.458	3.2 (7)	0.21	907 (2000)						
	3048 (10 000)	0.456	0	0.02	-						
Descent	3048 (10 000)	0.456	-	-	958 (2111)	132.4 (292)	8.3	-	23839.5 (52 557)	698.8	10 190 (5500)
	2743 (9000)	0.447	10.0 (22)	0.75	798 (1760						
	2438 (8000)	0.438	10.9 (24)	0.76	860 (1895)						
	2134 (7000)	0.430	10.9 (24)	0.78	837 (1846)						
	1829 (6000)	0.422	12.2 (27)	0.80	919 (2025)						
	1524 (5000)	0.414	12.7 (28)	0.82	929 (2049)						
	1219 (4000)	0.407	13.2 (29)	0.84	939 (2071)						
	914 (3000)	0.399	14.5 (32)	0.86	1013 (2233)						
	610 (2000)	0.392	15.0 (33)	0.89	1009 (2225)						
	305 (1000)	0.385	15.9 (35)	0.91	1047 (2308)						
	0 (0)	0.378	17.2 (38)	0.93	1112 (2452)						
Loiter	457 (1500)	0.286	-	-	1324 (2920)	132.4 (292)	6	-	23 971.9 (52 849)	703.9	10 190 (5500)

C-4

TABLE 88. Concluded.

Segment	Initial Altitude m (ft)	Initial Mach	Incremental			Segment			Total		
			Fuel kg (lb)	Time (min)	Avg $\dot{w}$ kg/hr (lb/hr)	Fuel kg (lb)	Time (min)	Avg. SFC $\frac{kg}{hr}$/daN $\left(\frac{lb}{hr}/lb\right)$	Fuel kg (lb)	Time (min)	Distance km (n.mi.)
Cruise	11 582 (38 000)	0.85			1904 (4198)	2221.7 (4898)	70.0	0.203 (0.199)	26 193.6 (57 747)	70	0 (0)
Climb	0 (0)	0.378			4607 (10 157)	215.0 (474)	2.8	0.155 (0.152)	26 408.6 (58 221)	72.8	24 (13)
Accelerate	3048 (10 000)	0.456			4028 (8880)	33.6 (74)	0.5	0.168 (0.165)	26 442.2 (58 295)	73.3	28 (15)
Climb	3048 (10 000)	0.547			3295 (7265)	554.7 (1223)	10.1	0.186 (0.182)	26 996.9 (59 518)	83.4	154 (83)
Cruise	9144 (30 000)	0.695			1647 (3630)	107.0 (236)	3.9	0.189 (0.185)	27 104.0 (59 754)	87.3	204 (110)
Descent	9144 (30 000)	0.700			611 (1346)	83.5 (184)	8.2	-	27 187.4 (59 938)	95.5	304 (164)
Decelerate	3048 (10 000)	0.547			786 (1733)	11.8 (26)	0.9	-	27 199.2 (59 964)	96.4	313 (169)
Descent	3048 (10 000)	0.456			927 (2043)	106.6 (235)	6.9	-	27 305.8 (60 199)	103.3	370 (200)
Loiter	457 (1500)	0.284			1292 (2848)	645.9 (1424)	30.0	0.151 (0.148)	27 951.7 (61 623)	133.3	370 (200)

APPENDIX B

DESIGN CONCEPTS OF SELECTED LH_2 FUEL SYSTEM COMPONENTS

Five fuel system components having critical operational requirements or technically challenging design requirements were selected for conceptual design study. The components studied were:

- Fuel level control shutoff valve
- Ground fueling quick disconnect
- Vapor recovery quick disconnect
- Absolute tank pressure relief and vent valve
- Absolute tank pressure regulator.

B1.1 Component Requirements

Operational and performance requirements were established for each selected component based upon the preliminary fuel system analysis. These requirements were used as the starting point for the component conceptual designs and, in some instances, iteration of the requirements was performed to assure or improve development feasibility.

In addition, some general design requirements were established which applied to all components. These requirements had to do with materials compatibility with GH_2 and LH_2, materials corrosion resistance, avoidance of dissimilar metals in contact, accessibility of the component for installation and adjustment and, in some cases, means for indicating satisfactory functioning or failure. These general requirements were also considered in the analysis and selection of the individual component design concepts.

B1.1.1 Fuel level control shutoff valve. - The fuel level control shutoff valve was an electric motor operated valve, having the purpose of admitting and stopping the flow of fuel to a LH_2 fuel tank. In addition, it had the special requirement for a pressure relief valve set at 1.25 times the maximum stabilized blocked fueling line pressure to provide for thermal pressure relief of the fueling line after valve closure.

Significant parameters of the selected design were:

Rated flow	4.99 kg/sec (11.0 lb/sec)
Pressure drop	23.2 kPa (3.36 psid)
Operating pressure range	241 to 193 kPa (35 to 28 psia)
Operating temperature range	20.6°K to 328°K (37°R to 590°R)
Duct diameter	7.37 cm (2.90 in.)
Weight	4.94 kg (10.90 lb)
Estimated MTBF	15 000 hr

A schematic diagram, and description of the valve design and operation are presented in Figure 199.

For this valve and the following selected components to be discussed, the conceptual design, and estimates of performance, weight, and MTBF were based upon experience with similarly designed equipment.

Also, for this valve and the following selected components to be discussed, the nonrecurring design and development costs, and the production costs in the quantity of 350 ship sets plus 20 percent spares were estimated, and the results used as an input to the ASSET evaluation of aircraft costs.

B1.1.2 Ground fueling quick disconnect. - The ground fueling quick disconnect was a manually operated, aircraft fueling quick disconnect and shutoff valve assembly, intended for use in the aircraft LH_2 fueling operation. The unit consisted of an airborne adapter mounted in the aircraft at the fueling interface, and a ground hose adapter mounted at the end of the ground fueling line. Each unit included an internal valve which was normally seated, preventing flow thru the valve, and which was automatically unseated when the two mating units were joined and secured to each other.

It was a design requirement that no hazard to personnel or equipment occur if ice formed on the units prior to, during, or after the fueling operation, and that the presence of ice on either mating unit not interfere with the mating process. In addition, it was required that the design of the mating units not permit ingestion of ice, water, or other contaminants into the system during the filling process.

It was required that the adapter in the aircraft be easily replaceable and designed to break away without damage to the aircraft if the supply truck pulled away from the aircraft without disconnecting the supply hose, and that the part of the adapter remaining in the aircraft automatically close in the event of a break, to preclude the loss of hydrogen from the aircraft.

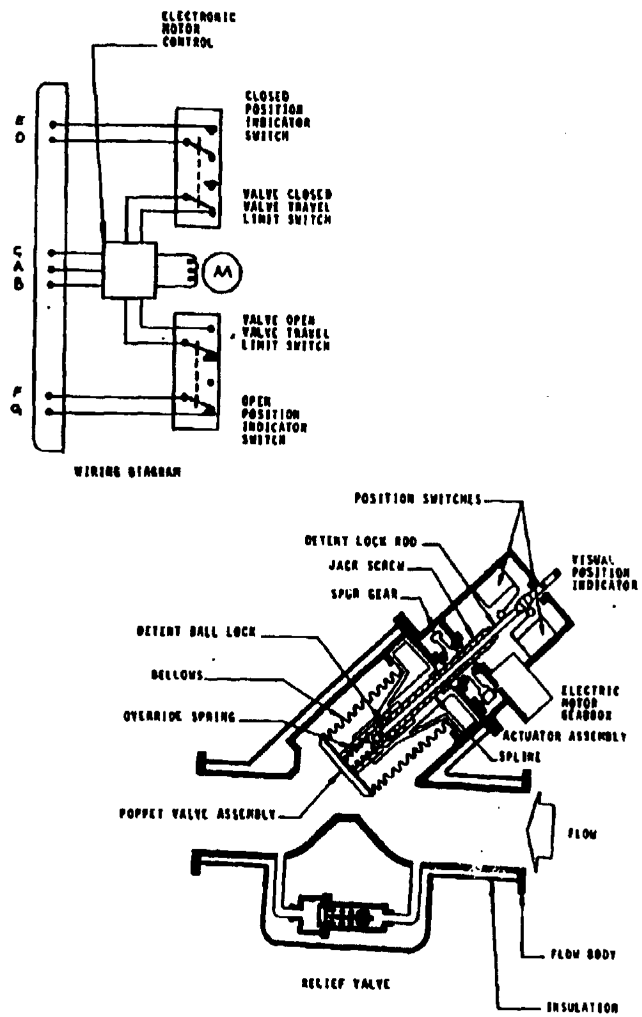

OF POOR QUALITY

Description:

This is an electric motor operated poppet-type shutoff valve designed for cryogenic operation.

The valve has an insulated flow body to reduce heat transfer to the cryogenic flow media. The flow body has an integral bellows-sealed poppet assembly which eliminates the need for any sliding seals.

The valve is operated by a reversible brushless electric motor driven actuator assembly. The actuator assembly is replaceable without opening the cryogenic line. After removing the detent lock rod, the balls are free to de-couple from the poppet assembly, allowing complete removal of the jack screw and actuator assembly. The detent lock rod has a tapered end to allow re-coupling of the jack screw rod when re-installing a new actuator assembly.

All electrical components are located outside of the flow media area.

Operation:

With the motor appropriately energized, the motor torque is transmitted to the spur gear which is threaded to the jack screw. The jack screw is splined to the flow body and coupled to the poppet assembly through the detent ball lock. As the spur gear rotates, the jack screw moves the poppet assembly to the full open or full closed position, as desired.

An override spring is incorporated in the poppet assembly to limit the valve sealing force.

A visual position indicator is provided to indicate poppet position. Open and closed position switches are incorporated to limit the valve travel and to provide a remote indication when the valve is in the open or closed position.

A pressure relief valve is provided to prevent excessive pressure build-up due to thermal expansion of the flow media when the valve is in the closed position.

Electrical Operation:

Energize Pins C & A to close the valve.
Energize Pins C & B to open the valve.
Continuity between Pins E & D valve closed.
Continuity between Pins F & G valve open.

Figure 199. - Liquid hydrogen fuel level control shutoff valve.

It was a design requirement that the quick disconnect be suitable for manual handling, installation, and control, by personnel wearing the necessary protective gloves and clothing, and that the required manual force of installation and actuation not exceed 22.2 daN (50 lb).

From the safety viewpoint, it was required that the ground fueling adapter be designed to preclude inadvertent mating with the vapor recovery nozzle. It was further required that complete electrical contact be established between the two adapters before they were connected, and that the contact resistance not exceed 10 ohms.

Significant parameters of the selected design were:

Rated flow	19.96 kg/sec (44.0 lb/sec)
Pressure drop	49.3 kPa (7.15 psid)
Operating pressure	110.3 kPa (16.0 psia)
Duct diameter	12.40 cm (4.88 in)
Weight	
Airborne adapter	2.90 kg (6.40 lb)
Ground adapter	6.45 kg (14.21 lb)

A schematic diagram, and description of the quick disconnect design and operation are presented in Figure 200.

B1.1.3 Vapor recovery quick disconnect. - The vapor recovery quick disconnect was a manually operated quick disconnect and shutoff valve assembly, intended for use in GH_2 vapor recovery during the aircraft fueling operation. The unit consisted of an airborne adapter mounted in the aircraft at the fueling interface, and a ground hose adapter mounted at the end of the ground vapor recovery line. Each unit included an internal valve which was normally seated, preventing flow thru the valve, and which was automatically unseated when the two mating units were joined and secured to each other.

It was a design requirement that no hazard to personnel or equipment occur if ice formed on the units prior to, during, or after the fueling operation, and that the presence of ice on either mating unit not interfere with the mating process. In addition, it was required that the design of the mating units not permit ingestion of ice, water, or other contaminants into the system during the filling process.

It was required that the adapter in the aircraft be easily replaceable and designed to break away without damage to the aircraft if the supply truck pulled away from the aircraft without disconnecting the supply hose, and that the part of the adapter remaining in the aircraft automatically

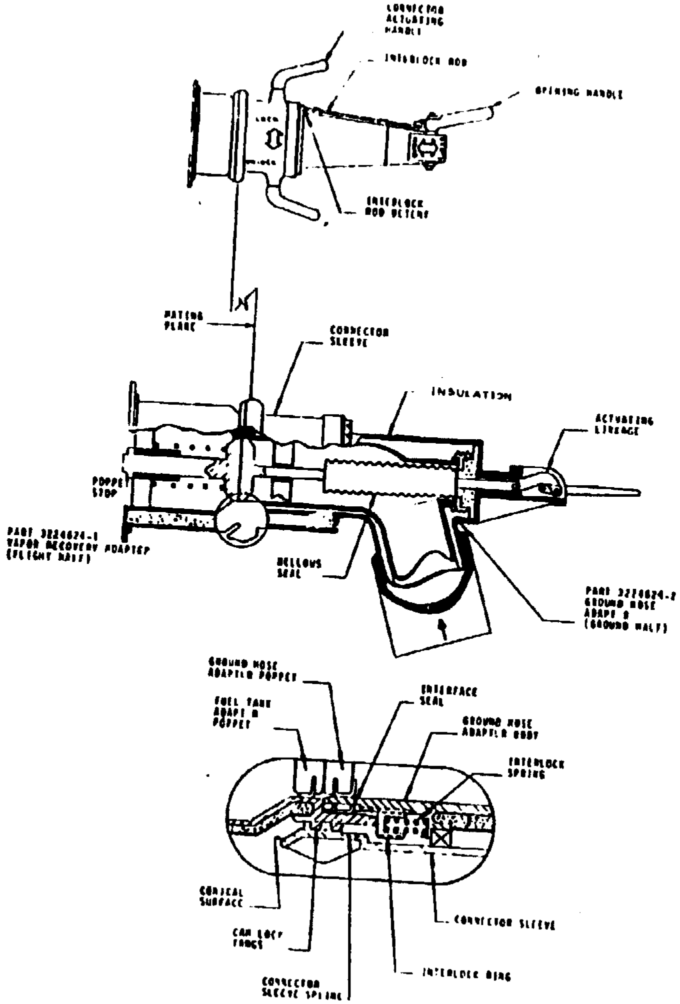

Description

This unit is a manually operated, vapor recovery, quick disconnect shutoff valve, designed for cryogenic service. The unit consists of an airborne vapor recovery adapter and a ground hose adapter

Both components are insulated to minimize the heat transfer to the flow media. The evacuated double wall bellows seals in the ground hose adapter also contributes to isolate the ambient temperature from the flow media and in addition eliminates the requirement for a sliding shaft seal

The unit is shown in the closed position, with the ground hose adapter fully mated to the airborne fuel tank vapor adapter. Dust caps are provided for use when the two elements are disconnected. [illegible] are such that any airborne fuel tank vapor recovery adapter can be mated to any ground hose adapter. The vapor recovery disconnect components cannot be interchanged with the aircraft fueling quick disconnect components shown in schematic P 1221522.

The design of the unit provides a minimum duct volume between the two halves to eliminate the need to purge the connection prior to opening the valve.

Operation:

To connect the two adapters, the ground hose adapter is manually positioned to the fuel tank vapor recovery adapter. The conical surface on the connector sleeve guides the two halves together so that the cam lock lugs are aligned and the interlock ring displaced unlocking the connector sleeve from the ground hose adapter body. With the interlock ring in the position shown, the connector sleeve can be rotated in the direction shown. This action advances the cam lock lugs which fully mates the two halves, placing the poppets face to face and seating the interface seal.

When the connector sleeve is rotated to the fully locked position, the interlock rod detent aligns with the interlock rod.

To open the unit, the opening handle is rotated in the direction shown which advances the interlock rod into the detent and through the actuating linkage, displacing the two poppets to the full open position.

To disconnect the unit, the opening handle is first rotated back to the closed position, which closes both poppets (as shown) and withdraws the interlock rod from the detent on the connector sleeve. The connector sleeve can then be rotated to the unlocked position to decouple the unit. As the two halves are separated, the interlock ring is spring loaded back into the connector sleeve spline preventing rotation of the connector sleeve.

The interlock ring prevents inadvertent rotation of the connector sleeve and subsequent opening of the ground hose adapter (by opening handle rotation) when not properly mated to the fuel tank vapor recovery adapter. The interlock rod prevents accidental de-coupling of the unit when the valve is in the open position.

Figure 200. - Ground fueling quick disconnect.

close in the event of a break, to preclude the loss of hydrogen from the aircraft.

It was a design requirement that the quick disconnect be suitable for manual handling, installation, and control, by personnel wearing the necessary protective gloves and clothing, and that the required manual force of installation and actuation not exceed 22.2 daN (50 lb).

From the safety viewpoint, it was required that the ground vapor recovery adapter be designed to preclude inadvertent mating with the LH_2 fueling nozzle. It was further required that complete electrical contact be established between the two adapters before they were connected, and that the contact resistance not exceed 10 ohms.

Significant parameters of the selected design were:

Rated flow	0.39 kg/sec (0.87 lb/sec)
Pressure drop	3.31 kPa (0.48 psid)
Operating pressure	110.3 kPa (16.0 psia)
Duct diameter	9.86 cm (3.88 in)
Weight	
Airborne adapter	2.32 kg (5.11 lb)
Ground adapter	5.15 kg (11.36 lb)

A schematic diagram, and description of the quick disconnect design and operation are presented in Figure 201.

B1.1.4 Absolute tank pressure relief and vent valve: The absolute tank pressure relief and vent valve was an assembly consisting of two tank pressure relief valves and an electric motor driven shutoff valve. One tank pressure relief valve was designated the primary relief valve and was designed to maintain an absolute tank pressure of 141.3 kPa (20.5 psia) and the other tank pressure relief valve was designated the secondary relief valve and was designed to maintain an absolute tank pressure of 155.1 kPa (22.5 psia). In the event of failure of the primary valve, the secondary valve would maintain tank pressure at the value slightly higher than normal, thus revealing the fact of the primary valve malfunction. The electric motor shutoff valve was required for use as a purge gas vent valve when initially filling the system.

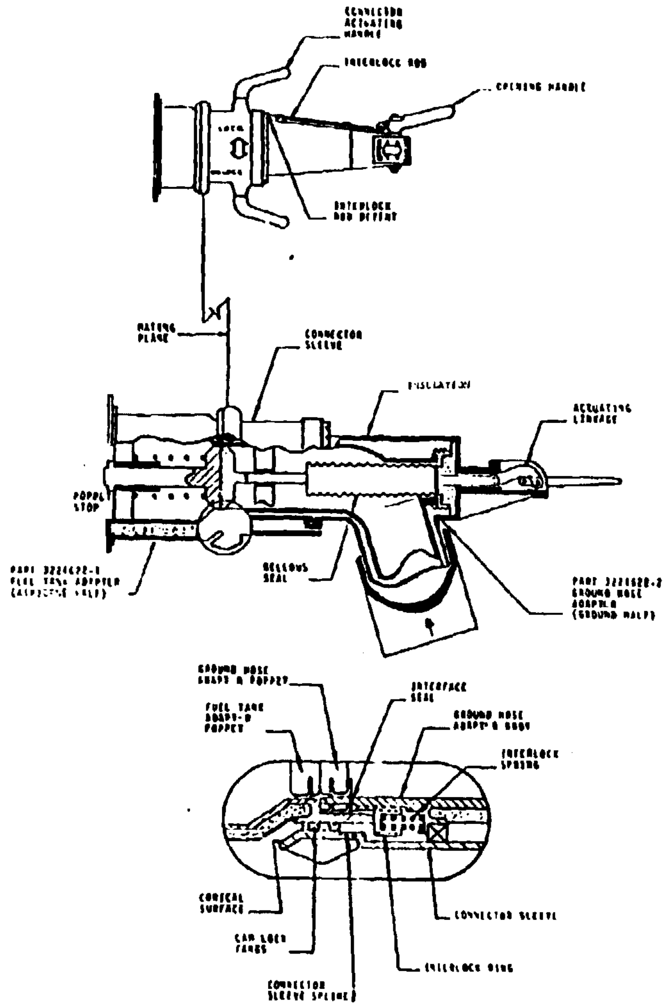

Figure 201. - Vapor recovery quick disconnect

Description:

This unit is a manually operated, aircraft fueling, quick disconnect shutoff valve, designed for cryogenic service. The unit consists of an airborne fuel tank adapter and a ground hose adapter.

Both components are insulated to minimize the heat transfer to the flow media. The evacuated double wall bellows seals in the ground hose adapter also contributes to isolate the ambient temperature from the flow media and in addition eliminates the requirement for a sliding shaft seal.

The unit is shown in the closed position, with ground hose adapter fully mated to the airborne fuel tank adapter. Dust caps are provided for use when the two elements are disconnected. Unit tolerances are such that any airborne fuel tank adapter can be mated to any ground hose adapter. The fueling quick disconnect components cannot be interchanged with the vapor recovery quick disconnect components shown in schematic # 3224624.

The design of the unit provides a minimum duct volume between the two halves to eliminate the need to purge the connection prior to opening the valve.

Operation:

To connect the two adapters, the ground hose adapter is manually positioned to the fuel tank adapter. The conical surface on the connector sleeve guides the two halves together so that the cam lock tangs are aligned and the interlock ring is displaced unlocking the connector sleeve from the ground hose adapter body. With the interlock ring in the position shown, the connector sleeve can be rotated in the direction shown. This action advances the cam lock tangs which fully mates the two halves, placing the poppets face to face and seating the interface seal.

When the connector sleeve is rotated to the fully locked position, the interlock rod detent aligns with the interlock rod.

To open the unit, the opening handle is rotated in the direction shown which advances the interlock rod into the detent and through the actuating linkage, displacing the two poppets to the full open position.

To disconnect the unit, the opening handle is first rotated back to the closed position which closes both poppets (as shown) and withdraws the detent on the connector sleeve interlock rod from the detent of the connector sleeve. The connector sleeve can then be rotated to the unlocked position to decouple the unit. As the two halves are separated, the interlock ring is spring loaded back into the connector sleeve spline preventing rotation of the connector sleeve.

The interlock ring prevents inadvertent rotation of the connector sleeve and subsequent opening of the ground hose adapter (by opening handle rotation) when not properly mated to the fuel tank adapter. The interlock rod prevents accidental decoupling of the unit when the valve is in the open position.

Significant parameters of the selected design were:

	Primary Pressure Relief Valve	Secondary Pressure Relief Valve
Rated flow	0.02 kg/sec (0.05 lb/sec)	0.02 kg/sec (0.05 lb/sec)
Relief pressure	141.3 kPa (20.5 psia)	155.1 kPa (22.5 psia)
Pressure drop	0.025 kPa (0.1 in. H_2O)	0.025 kPa (0.1 in H_2O)
Duct diameter	9.86 cm (3.88 in.)	9.86 cm (3.88 in.)
Weight for complete valve assembly	7.03 kg (15.5 lb)	

Estimated MTBF

Primary pressure relief valve	50 000 hr
Secondard pressure relief valve	50 000 hr
Vent valve	15 000 hr

A schematic diagram, and description of the valve design and operation are presented in Figure 202.

Referring to the schematic drawings for the pressure relief valves, the operation may be understood as follows: Vapor from the tank bleeds thru the poppet orifice into the reference pressure chamber and incurs a pressure drop thru the orifice. The pilot valve and partially evacuated bellows bleed vapor from the reference pressure chamber as required to maintain the chamber absolute pressure at a preselected value. The resulting chamber pressure is determined by the design of the pilot valve and partially evacuated bellows, and by the position setting of the adjustment screw. The value of chamber absolute pressure is selected to be such that the resulting pressure force on the main poppet, plus the force of the poppet actuation bellows, is just equal to the desired tank pressure times the main poppet area. If the tank pressure slightly exceeds the desired value, the main poppet will open to a modulated position, thus venting vapor from the tank and thereby limiting further increase in tank pressure.

B1.1.5 Absolute tank pressure regulator. - The absolute tank pressure regulator was required to sense the LH_2 tank absolute pressure, and supply LH_2 as required to a vaporizing heat exchanger (boiler) to generate vapor for

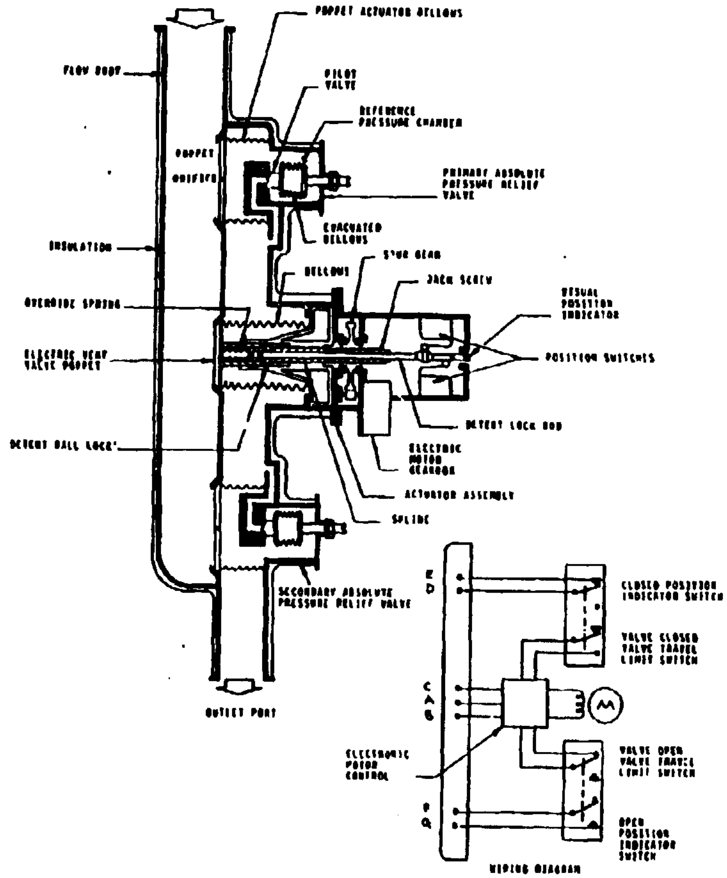

Description:

This unit is composed of a primary and secondary absolute pressure relief valve and an electric motor driven poppet type shutoff valve.

The unit functions to automatically maintain a fixed maximum absolute pressure in an aircraft cryogenic fuel system. The secondary absolute pressure regulator is calibrated above that of the primary to provide back up operation and greater flow capacity in the event of unusual upstream pressure transients. The remotely controlled electrically driven poppet valve can be actuated to bypass both absolute pressure relief valves to provide full venting of the fuel system.

The valve housing is insulated to reduce the heat transfer to the cryogenic flow media. All dynamic seals employ metal bellows to eliminate the need for any sliding seals.

The electric shutoff valve is operated by a reversible brushless electric motor driven actuator assembly. The actuator assembly is replaceable without opening the line. After removing the detent lock rod, the balls are free to decouple from the poppet assembly, allowing complete removal of the jack screw and actuator assembly. The detent lock rod has a tapered end to allow recoupling of the jack screw when reinstalling a new actuator assembly.

All electrical components are located outside of the flow media area.

<u>Pressure Relief Valve Operation</u>:

The primary absolute pressure relief valve poppet is held closed by the preload force in the poppet actuator bellows. When inlet pressure is applied, the orifice admits pressure to the reference pressure chamber and to the evacuated bellows. The evacuated bellows is calibrated so that when the inlet pressure is below the desired actuation point of the primary absolute pressure relief valve, the pilot valve is closed. This results in fluid pressure equalization across the poppet thus keeping the valve closed. As the inlet pressure increases to the desired actuation pressure, the evacuated bellows compresses slightly which moves the pilot valve to vent the reference pressure chamber to the outlet port. The resulting pressure differential across the orifice allows the inlet pressure force to overcome the poppet actuator bellows load to open the poppet and allow inlet pressure to vent to the outlet port. The evacuated bellows will respond to increases or decreases in upstream pressure, sensed through the orifice, to modulate the reference pressure chamber and thus the position of the primary relief valve poppet to maintain a fixed maximum upstream absolute pressure.

The secondary absolute pressure relief valve operates identically to the primary device. The evacuated bellows preload of the secondary system is greater than that of the primary device so as to increase the inlet pressure setting at which the device operates. In this way, the secondary valve provides a backup of the primary relief valve in case the primary pressure relief valve malfunctions or cannot accommodate the necessary flow.

<u>Shutoff Valve Operation</u>:

With the motor appropriately energized, the motor torque is transmitted to the spur gear which is threaded to the jack screw. The jack screw is splined to the flow body and coupled to the poppet assembly through the detent ball lock. As the spur gear rotates, the jack screw moves the poppet assembly to the full open or full closed position as desired.

An override spring is incorporated in the poppet assembly to limit the valve seating force.

A visual position indicator is provided to indicate poppet position. Open and closed position switches are incorporated to limit valve travel and to provide remote position indication.

<u>Electrical Operation</u>:

Energize Pins C & A to close the valve.
Energize Pins C & B to open the valve.
Continuity between Pins E & D valve closed.
Continuity between Pins F & G valve open.

Figure 202. - Absolute tank pressure regulator (relief valve and vent valve).

tank pressurization, if normal tank boil-off was not sufficient to maintain tank pressure at the primary relief valve absolute pressure level.

Significant parameters of the selected design were:

	Liquid Side	Gas Side
Rated flow	0.02 kg/sec (0.050 lb/sec)	0.02 kg/sec (0.050 lb/sec)
Pressure drop	1.77 kPa (0.256 psid)	77.33 kPa (11.22 psid)
Operating pressure	272.3 kPa (39.5 psia)	262.0 kPa (38.0 psia)
Duct diameter	0.960 cm (0.378 in.)	0.960 cm (0.378 in.)
Weight	2.33 kg (5.13 lb)	
Estimated MTBF	40 000 hr	

A schematic diagram, and description of the valve design and operation, are presented in Figure 203.

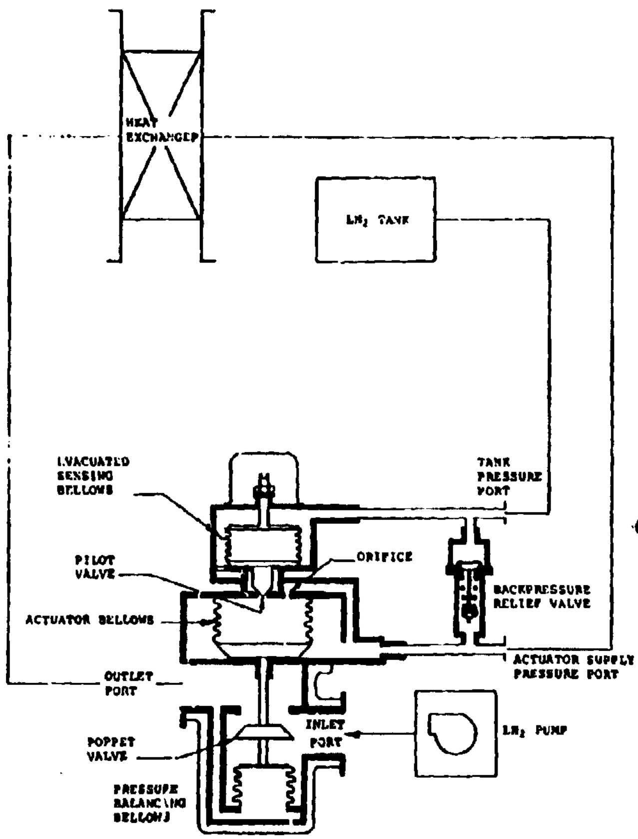

Description:

This unit is a poppet type absolute pressure regulator valve designed for cryogenic service. The valve regulates the pressure in a remotely located liquid hydrogen (LH_2) tank by controlling the amount of fluid passing through the unit. The flow passes through the unit twice, once in the form of liquid and the second time in the form of gas.

Operation:

The liquid hydrogen is routed from the inlet port through the normally open poppet valve to the outlet port. The outlet port is directed to a heat exchanger where the liquid is gasified. The gaseous hydrogen is directed back to the unit to the actuator supply pressure port to a normally closed backpressure relief valve, to the external side of the actuator bellows, through an orifice to the internal side of the actuator bellows, and to a normally closed pilot valve.

As the pressure to the actuator supply pressure port continues to rise, the backpressure relief valve opens and bleeds off flow to the tank pressure port. The backpressure relief valve maintains the pressure at a predetermined value above the tank pressure port. Since the tank pressure port is connected to the LH_2 tank it also provides a means of sensing the LH_2 tank pressure to the evacuated sensing bellows.

As the LH_2 tank pressure rises to calibrated setting of the evacuated sensing bellows, the evacuated sensing bellows moves to open the pilot valve which bleeds off the internal pressure of the actuator bellows. The flow into the actuator bellows is restricted by an orifice which creates a pressure differential across the actuator bellows, causing the poppet valve to modulate towards the closed position. This reduces the liquid H_2 flow through the heat exchanger, and reduces the pressure to the actuator supply pressure port. In turn, this action reduces the flow into the LH_2 tank, to limit the tank pressure to the desired absolute value.

The poppet is inlet pressure balanced by a bellows of identical area of the poppet valve and is exposed to the same differential pressure as the poppet but with a force reaction in the opposite direction. The exterior of the unit is insulated to limit the heat transfer into the flow media.

Figure 203. - Absolute tank pressure regulator.

APPENDIX C

CONCEPT SCREENING ANALYSIS THERMAL MODEL DEVELOPMENT

The LH_2 airplane tank screening model was developed considering an elemental length of a horizontal cylinder filled with LH_2. Both the liquid and vapor volumes can be expected to stratify, with rather high wall temperatures possible opposite the ullage volume. Temperature distribution of the tank wall is needed to determine the heat leak into the tank through the insulation system, and also for structural analysis of the tank. Only two temperatures are fixed in this problem, the liquid surface temperature T_S, which corresponds to the vent pressure, and the ambient temperature T_A surrounding the tank. A complicating feature is the need to consider the variable thermal properties of the tank wall insulation system, and the liquid and vapor phases under the ranges of temperature expected for these components.

Solution for the temperature distribution of the tank wall (Figure C-1) as a function of the heat transfer coefficients to the wall is obtained with an analysis similar to Jakob [41]. Figure 204 assumes that the liquid vapor interface is at $X = 0$, with the liquid at $X < 0$ and the vapor at $X > 0$ along the tank wall. As the temperature distribution solutions of the tank wall will be similar for the regions opposite the liquid and vapor, we solve for the temperature distribution opposite the vapor, where $X \geq 0$. For a steady state energy balance on the differential element dx; of unit width:

$$k\bar{t} \frac{d^2 T}{dx^2} = \left(h_I + h_V\right)\left(T - T_{\infty V}\right) \tag{C1}$$

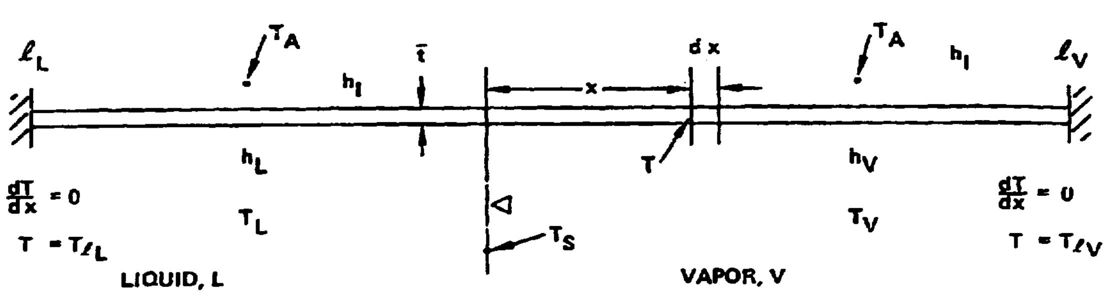

Figure 204. - Tank wall model.

where

$$T_{\infty V} = \frac{h_I\ T_A + h_V\ T_V}{(h_I + h_V)} = \text{the wall temp that would occur if } X \rightarrow \infty.$$

Based upon Carslaw and Jaeger [42] solutions for constant thermal conductivity can be converted to variable conductivity solutions by making use of thermal conductivity integrals, providing the boundary conditions are specified only as temperature or the temperature slope. Starting with a constant thermal property solution of equation (C1), which can be rearranged as:

$$\frac{d^2\ T}{dx^2} = \frac{(h_I + h_V)}{k\bar{t}}\ (T - T_{\infty V}) \tag{C2}$$

Letting

$$m_V = \sqrt{\frac{(h_I + h_V)}{k\bar{t}}}\ , \quad \text{so that}$$

$$\frac{d^2\ T}{dx^2} = m_V^{\ 2}\ (T - T_{\infty V}) \tag{C3}$$

The solution to this differential equation is:

$$T = T_{\infty V} + M_V\ e^{-m_V X} + N_V\ e^{+m_V X}$$

The integration constants M_V and N_V are evaluated from two boundary conditions. The slope is $dT/dx = 0$ at $x = \ell_V$, but neither the magnitude or slope of the temperature is known at $x = 0$. Applying this one boundary condition to the equation (C3) yields:

$$\frac{dT}{dx} = -\ m_V\ m_V\ e^{-m_V X} + m_V\ N_V\ e^{+m_V X} \tag{C4}$$

$$\left.\frac{dT}{dx}\right]_{X=\ell_V} = m_V \left(- M_V \, e^{-m_V \ell_V} + N_V \, e^{+m_V \ell_V} \right) = 0$$

$$N_V = M_V \frac{e^{-m_V \ell_V}}{e^{+m_V \ell_V}} = M_V \, e^{-2m_V \ell_V} \tag{C5}$$

Substituting for N_V, the solution then becomes

$$T = T_{\infty V} + M_V \left(e^{-m_V X} + e^{+m_V (X - 2\ell_V)} \right), \quad \text{for} \quad x \geq 0. \tag{C6}$$

The solution for the region opposite the liquid, where $x \leq 0$, is found from a similar differential equation, which yields:

$$T = T_{\infty L} + M_L \, e^{-m_L X} + N_L \, e^{+m_L X}$$

where

$$T_{\infty L} = \frac{h_I \, T_A + h_L \, T_L}{(h_I + h_L)}$$

$$m_L = \sqrt{\frac{(h_I + h_L)}{k\bar{t}}}$$

One integration constant, M_L, can be solved based upon the boundary condition that $dT/dx = 0$ at $x = -\ell_L$.

$$\frac{dT}{dx} = - m_L \, M_L \, e^{-m_L X} + m_L \, N_L \, e^{+m_L X} \tag{C7}$$

$$\left.\frac{dT}{dx}\right]_{X=-\ell_L} = m_L \left(- M_L\, e^{-m_L(-\ell_L)} + N_L\, e^{+m_L\,(-\ell_L)} \right) = 0$$

$$M_L = N_L \cdot \frac{e^{-m_L \ell_L}}{e^{+m_L \ell_L}} = N_L \cdot e^{-2m_L \ell_L} \qquad \text{(C8)}$$

Substituting for M_L, the solution opposite the liquid becomes:

$$T = T_{\infty L} + N_L \left(e^{-m_L (X+2\ell_L)} + e^{+m_L X} \right), \qquad \text{for } x \le 0. \qquad \text{(C9)}$$

Equations (C6) and (C9) contain 2 unknowns, N_L and M_V, which can be found from the condition at $x = 0$, where T and the slope of T must be equal for both of these solutions. Setting the temperature $T_{x \ge 0} = T_{x \le 0}$ at $x = 0$, then

$$T_{\infty V} + M_V \left(1 + e^{-2m_V \ell_V}\right) = T_{\infty L} + N_L \left(e^{-2m_L \ell_L} + 1\right) \qquad \text{(C10)}$$

Setting the slopes $\left(dT/dx\right)_{x\ge 0} = \left(dT/dx\right)_{x \le 0}$ at $x = 0$ yields:

$$- m_V M_V + m_V M_V\, e^{-2m_V \ell_V} = - m_L N_L\, e^{-2m_L \ell_L} + m_L N_L \qquad \text{(C11)}$$

Solving equation (C11) for N_L, and then substituting N_L into equation (C10) yields:

$$M_V = \frac{T_{\infty V} - T_{\infty L}}{\left[\frac{m_V}{m_L} \cdot \frac{\left(e^{-2m_V \ell_V} - 1\right)}{\left(1 - e^{-2m_L \ell_L}\right)} \cdot \left(1 + e^{-2m_L \ell_L}\right) - \left(1 + e^{-2m_V \ell_V}\right) \right]} \qquad \text{(C12)}$$

The expression for N_L yields the other constant, which is positive:

$$N_L = \frac{\dfrac{m_V}{m_L} \cdot \dfrac{\left(e^{-2m_V \ell_V} - 1\right)}{\left(1 - e^{-2m_L \ell_L}\right)} \cdot (T_{\infty V} - T_{\infty L})}{\left[\dfrac{m_V}{m_L} \cdot \dfrac{\left(e^{-2m_V \ell_V} - 1\right.}{\left(1 - e^{-2m_L \ell_L}\right.} \cdot \left(1 + e^{-2m_L \ell_L}\right) - \left(1 + e^{-2m_V \ell_V}\right)\right]} \tag{C13}$$

Hence, the complete solution, using the above values of M_V and N_L is:

$$T = T_{\infty L} + N_L \quad e^{-m_L (X+2\ell_L)} + e^{+m_L X} \quad , \text{ for } x \le 0. \tag{C14}$$

$$T = T_{\infty V} + M_V \quad e^{-m_V X} + e^{m_V (X-2\ell_V)} \quad , \text{ for } x \ge 0. \tag{C15}$$

where

$$m_L = \sqrt{\frac{h_I + h_L}{kt}}$$

$$m_V = \sqrt{\frac{h_I + h_V}{kt}}$$

The tank wall temperature solution for the case of variable conductivity in the wall, insulation, and fluids is determined by assuming all of the thermal conductivities are proportional to temperature. The thermal conductivity integral then will have the form

$$\int_0^T kdT = \int_0^T k'TdT = \frac{k'}{2} \cdot T^2$$

where k' = slope of thermal conductivity curve.

From Reference (42) the variable properties solution may be obtained from the constant k solution by replacing the temperature by the thermal conducitivity integral. The original steady state differential equation expressed in terms of variable conductivity is

$$\bar{t} \frac{d}{dx} \left(k \frac{dT}{dx}\right) = q''_I + q''_V ,$$

for the wall opposite the vapor phase.

Since $$k = k'T$$

and

$$U = \int_0^T kdT = \int_0^T k'TdT = k' \int_0^T TdT = \frac{k'}{2} \cdot T^2$$

$$\frac{dU}{dT} = \frac{k'}{2} \cdot 2T \frac{dT}{dx} = k'T \frac{dT}{dx} = k \frac{dT}{dx}$$

$$\frac{d^2U}{dx^2} = \frac{d}{dx} \left(\frac{dU}{dx}\right) = \frac{d}{dx} k \left(\frac{dT}{dx}\right)$$

Hence, the differential equation can be expressed by:

$$\bar{t} \cdot \frac{d^2U}{dx^2} = q''_I + q''_V \qquad \text{(C16)}$$

For the case of variable conductivities in the insulation and vapor

$$q''_I = \frac{1}{t_I}\left[\int_o^T k_I dT - \int_o^{T_A} k_I dT\right] = \frac{k'_T}{D_{hV}}\left(T^2 - T_A^{\,2}\right)$$

$$q''_V = \frac{N_{uV}}{D_{hV}}\left[\int_o^T k_V dT - \int_o^{T_V} k_V dT\right] = \frac{N_{uV} k'_V}{D_{hV}}\left(T^2 - T_V^{\,2}\right)$$

Hence, the differential equation becomes

$$\bar{t} \cdot \frac{d^2U}{dx^2} = \frac{k'_I}{2t_I}\left(T^2 - T_A^{\,2}\right) + \frac{N_{uV}\ k'_V}{2\ D_{hV}}\left(T^2 - T_V^{\,2}\right) \qquad \text{(C17)}$$

Since U is defined in terms of the wall conductivity k, then the above differential equation can be put into the form:

$$\bar{t} \cdot \frac{d^2U}{dx^2} = \frac{k'_I}{t_I k'}\left(\frac{k'}{2}\ T^2 - \frac{k'}{2}\ T_A^{\,2}\right) + \frac{Nu_V k'_V}{D_{h_V}\ k'}\left(\frac{k'}{2}\ T^2 - \frac{k'}{2}\ T_V^{2}\right) \qquad \text{(C18)}$$

$$\bar{t} \cdot \frac{d^2U}{dx^2} = \frac{k'_I}{t_I k'}\left(U - U_A\right) + \frac{Nu_V k'_V}{D_{h_V}\ k'}\left(U - U_V\right).$$

since

$$U_i = \frac{k'}{2}\ T_i^{\,2}$$

From the above equation, solve for the value of U at $x \to \infty$, when $d^2U/dx^2 = 0$. Defining that value of the wall conductivity integral as u_{∞_V}, then:

$$U_{\infty_V} = \frac{\frac{k'_I}{t_I} U_A + \frac{Nu_V k'_V}{D_{h_V}} U_V}{\frac{k'_I}{t_I} + \frac{Nu_V k'_V}{D_{h_V}}}$$

Substitution of U_{∞_V} into the differential equation then yields:

$$\frac{d^2U}{dx^2} = \frac{1}{k't}\left(\frac{k'_I}{t_I} + \frac{Nu_V k'_V}{D_{h_V}}\right)\left(U - U_\infty\right) = m^2_V \left(U - U_{\infty_V}\right) \quad \text{(C19)}$$

This equation for variable conductivity has exactly the same form as the constant k differential equation at equation (C3), with U substituted for T. The total solution for the wall temperature opposite the liquid and vapor regions can then be taken from the total constant k solutions completed with the new definitions of m_V and m_L which yields

$$M_V = \frac{\left(U_{\infty V} - U_{\infty L}\right)}{\left[\frac{m_V}{m_L} \cdot \frac{\left(e^{-2m_V \ell_V} - 1\right)}{\left(1 - e^{-2m_L \ell_L}\right)} \cdot \left(1 + e^{-2m_L \ell_L}\right) - \left(1 + E^{-2m_V \ell_V}\right)\right]} \quad \text{(C20)}$$

$$N_L = \frac{\frac{m_V}{m_L} \cdot \frac{\left(e^{-2m_V \ell_V} - 1\right)}{\left(1 - e^{-2m_L L}\right)} \cdot \left(U_{\infty_V} - U_{\infty_L}\right)}{\left[\frac{m_V}{m_L} \cdot \frac{\left(e^{-2m_V \ell_V} - 1\right)}{\left(1 - e^{-2m_L \ell_L}\right)} \cdot \left(1 + e^{-2m_L L}\right) - \left(1 + e^{-2m_V \ell_V}\right)\right]} \quad \text{(C21)}$$

$$U = \frac{k'}{2} \cdot T^2, \quad T^2 = \frac{2U}{k'} \quad \text{and} \quad T = \sqrt{\frac{2U}{A'}}$$

These solutions are then used to compute the heat transfer into the fluid. Assuming that there is no gross vapor motion in the ullage space, $R_a < 10\ 000$, vapor conduction will be the principal mode of heat transfer to a mean vapor temperature, T_V, with the vapor heat transfer coefficient, k_v, defined by a constant Nusselt number, Nu_v, and hydraulic diameter, D_{kv}, of the ullage volume. For steady state heat transfer and venting, not considering LH_2 withdrawal from the tank, the liquid boiloff rate is equal to the heat transfer directly occurring to the liquid phase. The vapor will be formed at temperature, T_S, and then be heated by the dry tank ullage and finally vented from the top of the tank. This vent temperature, T_{V_O}, will be a function of the boiloff rate, heat transfer from the ullage surfaces and vent pressures.

Initially, assume the mean vapor temperature is equal to the average temperature of the walls and liquid surface base of the ullage vapor volume. An iterative solution can then be performed to set the initial assumed T_v equal to the final computed mean T_v based upon the computed wall temperature variation.

The liquid heat transfer coefficient, h_L, is computed based upon free convection along a vertical plate of the same height L as the liquid depth in the tank. Using the Vliet and Liu 43 correlation for constant heat flux, which closely simulates the heat flux into the liquid, the average liquid Nusselt Number is given by the following relations:

$$Nu_L = \frac{h_L L}{k_L} = 0.25\ (Gr^*_L\ Pr)^{0.24} \qquad R_{a_L} \geq 4.2535 \times 10^{12}$$

$$Nu_L = 0.80\ (Gr^*_L\ Pr)^{0.20} \qquad 10^4 \leq R_{a^*_L} \leq 4.2535 \times 10^{12}$$

$$Nu_L = 5.0476 \qquad R_{a^*_L} \leq 10^4$$

where

$$R_{a^*_L}\ L^* = Cr^*_L\ Pr$$

$$Gr^*_L = \frac{g\beta q''\ L^4}{B\nu^2} = \frac{g\beta\rho^2}{B\mu^2} \cdot q''\ L^4 = Z_L \cdot q''\ L^4$$

$$Pr = \frac{ucs}{k}$$

For the ullage vapor, the average conduction Nusselt number, Nu_v, is a constant based upon hydraulic diameter D_{k_v} of the volume, $Nu_v = h_v D_{kv}/k_v = 4.386$.

Having defined temperature distributions and the heat transfer coefficients an energy balance can now be performed to calculate the mass of liquid evaporated and the sensible heat in the vapor.

APPENDIX D

"THERM" PROGRAM

A modification of the basic THERM program is used for the fuel tank analysis program. This program is structured to allow the maximum flexibility in describing energy transport phenomena in a cryogenic storage tank. Calculations during the energy balance can be performed in any of 24 dummy subroutines that are called automatically at various points in the basic integration algorithms. This permits modification or updating of any aspect of the model by simply replacing the appropriate dummy routines with subroutines containing the desired operations. The fluid stratification problem, liquid-ullage coupling through mass and energy exchanges associated with evaporation, bulk boiling and condensation, the geometrical calculations required in the node definition and the various Nusselt number correlations needed for characterization of several energy transport mechanisms are all modeled as subroutines that modify and update the basic heat balance calculation.

The program was developed specifically for operation on the UNIVAC 1100 series system. Structurally, it is divided into three major subprograms, THERM, CYCLE, and OUTPUT, and a number of lesser routines.

THERM is the name of the main program as well as the system. It reads in and stores the network description from cards, tape or disk, saves the network data on disks, if necessary, for restart, and calls CYCLE. (The term "restart" in this context refers to the running of two or more cases on the same run. It does not involve taking the job off the machine.) On return from CYCLE, THERM retrieves the original network from disk, reads in network changes from cards, updates the network, and again calls CYCLE. After the last restart, THERM terminates the run.

CYCLE performs the heat balance calculations. It includes two independent iterative procedures: one for converging (i.e., relaxing the network at a specific time to obtain steady-state conditions at that time) and the other for the usual thermal analyzer transient calculations. In order to increase the speed and efficiency of the program, several routines that are called many times, such as the calculation of $\sum(1/R)$ and $\sum(T/R)$ for each node, are written as assembly language subroutines.

OUTPUT is called from CYCLE at prescribed times during transient calculations and after a prescribed number of iterations during converge. It causes the status of the parameters prescribed in the "O" block (see below) to be listed.

Input consists of nine blocks of data, labeled T, C, Q, R, K, D, O, G, and P. The initial temperature, capacitance, and heat input (internal plus external) of each node are input in the "T", "C", and "Q" blocks, respectively. The "R" block contains the values and connections of the resistors, except the radiation resistors. The "K" block contains the values and connections of the radiation resistors (RADK's). Tabular data are input in the "D" block - the data may consist of periodic or non-periodic tables or of groups of unrelated constants. The "O" block specifies the quantities to be listed during each normal output. These may include temperatures in any desired units, capacitances, resistors RADK's, tabular data, problem variables, heat rates, $\sum$ (1/R), and $\sum$ (T/R). Comments describing the output may also be written. The "P" block contains the values of the problem variables such as initial time, final time, print interval, fractions of the minimum RC to be used in computing the time step, etc. The "G" block specifies the portion of the output that is to be plotted. The data for each case are ended by an "M" card (put data for restart on disk), an "S" card (save restart data from preceding case), or an "F" card (final case).

The user has the option of performing calculations during input through 15 ENTRIES and during the heat balance calculations through 24 MODES. These are provided in THERM in the form of dummy routines of the form SUBROUTINE NAME, RETURN, END and are called automatically at various points during input and during the heat balance. The entry B4D, for example, is called just before the first data input in the "D" block' B4HB is called just before CYCLE is called; the MODES similarly provide entry to CYCLE before and after each significant calculation during the heat balance calculations. If the user wants to perform calculations or modify the model at any of these points, he simply replaces the dummy routine with a hand-coded routine containing the desired operations.

Direct access to all of the parameters of the model is provided through THERM's FIND and STORE routines. The function FINDTF(N), for example, produces the current temperature in ^{o}F of node N; FINDD (N,I) produces the value of the I-th location in table N; CALL FINDRH (N,I,J) give the ID's, I and J, of the nodes to which resistor N is connected: FPTIM(N) finds the present time (N is a dummy variable required by the system). Similarly, CALL STORTF (N,V) stores V in absolute units as the temperature of node N; CALL STORD (N,I,V) stores V in the I-th location of table N; CALL STORRH(N, I,J) destroys the previous connections of resistor N and connects it to nodes I and J; CALL SPTIM(V) changes the present time to V. Other routines find and store the values of the other parameters.

All of the data, except the problem variables and the locations and ID's of the data tables, is stored in one variably-dimensioned array. The number of cells needed for a given program are five times the maximum node ID, plus two times the maximum resistor ID, plus two times the maximum RADK ID, plus one cell for each data item, plus, basically, three cells for each quantity specified in the output (this varies as to the specific type of output). The maximum allowable table ID is 300.

The simplest form of plot output presents the transient temperatures of up to eight nodes per plot. Considerably more complex graphic output, including three-dimensional plots, can be achieved by linking THERM with the DISSPLA plot program that is resident on the computer.

APPENDIX E

SAFETY ANALYSIS

The safety analysis was a four step process. First, a preliminary malfunction analysis was performed to determine if any of the systems had failure modes dangerous to life or aircraft. Secondly, requirements for hydrogen detectors were established, third, an assessment of flammability and toxicity was made, and fourth, the ability to inspect barriers and the tank was evaluated.

The screening malfunction analysis used a standardized format as shown in the following tables. For each system, the type of failure was postulated with the normal resulting condition, the effect of the failure on the flight and the aircraft and existing protective measures. Table 89 summarizes the results of the analysis for each concept.

TABLE 89. - POTENTIAL MALFUNCTION SCREENING ANALYSIS.

Concept	Type of Failure	Normal Resulting Condition	Effect on Flight	Effect on Aircraft	Protective Measures
1. GHe Purge	Jacket leakage	Loss of helium	N (unless excessive)		Carry extra helium on board, monitor press decay rate (with He flow off) prior to flight.
		Buckling of jacket, air liquefaction.	A	D	
	Jacket over pressure	Loss of He through relief valve	A	D	Redundant pressure transducers, dual stage regulator, shut off valves relief valve.
	He flow stopped	Possible jacket buckling during aircraft descent	A	D	Might require parallel redundancy in shut off valves or dual operator on single valve.
	GH_2 tank leakage	None if leakage rate is not excessive	N		H_2 vented with He purge, burst disc/relief valve.
	He bottle overpressure during loading	Loss of He through burst disc/relief valve	A		Burst disc/relief valve, conservative margins of safety.
2. Dual GHe/GN_2 Purge	He jacket leakage	Loss of He, increased heat rate, possible N_2 liquefaction, N_2 jacket buckling.	A	D	Carry extra He and LH_2 on board, monitor press decay rate (with He flow off) prior to flight
	N_2 jacket leakage	Loss of N_2, buckling of jacket if N_2 supply runs out.	N (unless excessive) A	D	Carry extra N_2 on board. Monitor press decay rate (with N_2 flow off) prior to flight

N - None
A - Potential Abort
D - Potential Aircraft Damage
L - Potential Aircraft Loss
NA - Not Applicable

TABLE 89. - Continued.

Concept	Type of Failure	Normal Resulting Condition	Effect on Flight	Effect on Aircraft	Protective Measures
3. & 4. External foam	Effect of 350 thermal cycles/yr				
	o Bond line delamination	Possible local loss of insulation, increased heat rates, buildup of cryo-deposits (moisture, air)	A	D	Inspect insulation for frosting, monitor tank boiloff, periodically replace or repair insulation if required
	o Foam breakup	May cause vapor barrier leakage, increased heat rates	A	D	
	o Vapor barrier leakage	Increased heat rates, buildup of cryo-deposits, further damage to vapor barrier as tank warms up each flt.	A	D	
	GH_2 tank leakage into foam	Increased heat rates, possible safety hazard	A	D	Periodically check tank pressure integrity, frosting of foam, tank boiloff, monitor space outside insulation for GH_2
5. Internal Foam	Liquid seal, foam breakup due to thermal cycling 350 times/yr	Increased heat rate, potential LH_2 pump damage	A	D	Screens over tank outlets, monitor tank for frost, monitor tank boiloff
	Tank leakage	Possible safety hazard	A	D	Periodically check tank pressure integrity, monitor space outside tank for GH_2

N - None
A - Potential Abort
D - Potential Aircraft Damage
L - Potential Aircraft Loss
NA - Not Applicable

TABLE 89. - Continued.

Concept	Type of Failure	Normal Resulting Condition	Effect on Flight	Effect on Aircraft	Protective Measures
6. Internal/ External Foam System	Internal foam breakup	Increased heat rate, potential pump damage	A	D	Screens over tank outlets
	Internal bond line delamination	Same as above, potential decrease in LH_2 flow to pumps	A	D	Same as above
	Excernal bond line delamination	Possible local loss of insulation, increased heat rates, buildup of moisture, cryodeposits	A	D	Inspect insulation for frosting, monitor tank boiloff, periodically replace or repair insulation
	External foam breakup	May cause vapor barrier leakage, increased heat rates	A	D	
	External vapor barrier leakage	Cryopump moisture, damage barrier further with each thermal cycle	A	D	
	Tank leakage	Increased heat rates, possible safety hazard	A	D	Periodically check tank pressure integrity, frost formation on insulation, tank boiloff, monitor space outside insulation for GH_2

N - None
A - Potential Abort
D - Potential Aircraft Damage
L - Potential Aircraft Loss
NA - Not Applicable

TABLE 89. - Continued.

Concept	Type of Failure	Normal Resulting Condition	Effect on Flight	Effect on Aircraft	Protective Measures
	He jacket overpressure	Loss of He through relief valve, tank buckling if tank pressure is exceeded	A	L	Redundant pressure transducers, dual stage regulator shutoff valves, relief valve
	N_2 jacket overpressure	Loss of N_2 through relief valve. Buckling of He jacket if He pressure is exceeded	A	D	Same as above
	He flow stopped	Potential inward buckling of He jacket during descent, N_2 cryopumping	A	D	Might require parallel redundancy in shutoff valves or dual operator on single valve
	N_2 flow stopped	Potential inward buckling of N_2 jacket during descent	A	D	Same as above
	GH_2 tank leakage	None if leakage rate is not excessive	N		H_2 vented with He purge burst disc/relief valve
	He or N_2 bottle overpressure during loading	Loss of gas through burst disc/relief valve	A		Burst disc/relief valve, conservative margins of safety

N - None
A - Potential Abort
D - Potential Aircraft Damage
L - Potential Aircraft Loss
NA - Not Applicable

TABLE 89. - Continued.

Concept	Type of Failure	Normal Resulting Condition	Effect on		Protective Measures
			Flight	Aircraft	
7. PPO	Tank leakage	Possible safety hazard	A	D	Periodically check tank integrity, monitor space outside tank for GH_2
	Foam breakup	Increased heat rates, possible LH_2 pump damage	A		Inspect tank for frosting, monitor tank boiloff, screens over tank outlets
8. Honeycomb/ Perforated Face Sheet	Delamination of face sheet	Sharp rise in heat rate, possible reduction in LH_2 flow to engines, air liquefaction on outside of tank.	A	D	Screens over tank outlets, check tank for frost, monitor boiloff
	Debonding of honeycomb	Minimal effect if localized	N		Screens over tank outlets, check tank for frost, monitor boiloff
	Tank leakage	Possible safety hazard	A	D	Periodically check tank integrity, monitor space outside tank for GH_2
9. Hard Shell Vacuum	Shell leakage	No effect if pressure does not exceed 10^{-5} Torr. Heat rate increases above 10^{-5} Torr	N ($< 10^{-5}$ Torr) A ($> 10^{-5}$ Torr)		Active pumping system, cryopumping at LH_2 surface of 1003.4 ℓ/sec/m^2 (10 800 ℓ/sec/ft^2)

N - None
A - Potential Abort
D - Potential Aircraft Damage
L - Potential Aircraft Loss
NA - Not Applicable

TABLE 89. - Continued.

Concept	Type of Failure	Normal Resulting Condition	Effect on Flight	Effect on Aircraft	Protective Measures
	Tank leakage	No effect if pressure does not exceed 10^{-5} Torr. Heat rate increases up to conductivity of GH_2 at that pressure if 10^{-5} Torr is exceeded, possible air liquefaction on jacket exterior.	N (< A (>	10^{-5} Torr) 10^{-5} Torr)	Active pumping system, relief valve, vent in tail
	Turbomolecular pump shutdown	Pressure in insulation may rise slowly as will heat rate	A		Cryopumping at LH_2 surface of 1003.4 ℓ/sec/m^2 (10 800 ℓ/sec/ft^2), redundant components, getters if required, relief valve
	Blower pump shutdown	No effect if no leakage occurs	N		Same as above
10. External Microspheres, Flexible Vacuum Jacket	Air leakage	No effect if pressure does not exceed .1 Torr. Heat rate increases above .1 Torr pressure	N (< 0.1 Torr) A (> 0.1 Torr)		Active pumps, cryopumping at LH_2 surface of 1003.4 ℓ/sec/m^2 (10 800 ℓ/sec/ft^2)

N - None
A - Potential Abort
D - Potential Aircraft Damage
L - Potential Aircraft Loss
NA - Not Applicable

TABLE 89. - Continued.

Concept	Type of Failure	Normal Resulting Condition	Effect on Flight	Effect on Aircraft	Protective Measures
	Tank leakage	No effect if pressure does not exceed 0.1 Torr. Heat rate increases up to 1/3 conductivity of GH_2 at that pressure if 0.1 Torr is exceeded. Over expansion of jacket if insulation pressure exceeds ambient pressure	N (< 0.1 Torr) A (> 0.1 Torr)	D	Active pumps, insulation relief valves, vent in tail
	Blower shutdown	Slow rise in insulation pressure may occur accompanied by heat rate increase above 0.1 Torr pressure.	A		Cryopumping at LH_2 tank surface of 1003.4 ℓ/sec/m^2 (10 800 ℓ/sec/ft^2), relief valves, redundant components
11. Internal Microspheres, Invar Liner, Evacuated	Liner leakage	No effect if pressure does not exceed 0.1 Torr, heat rate increases up to 1/3 conductivity of GH_2 at that pressure if 0.1 Torr is exceeded. Liner reversal if insulation pressure exceeds tank pressure	N (< 0.1 Torr) A (> 0.1 Torr)	D	Monitor insulation pressure, presence of GH_2 in insulation active pumps, tank pressurization system, insulation relief valves Insulation prevents LH_2 from striking the warm tank wall and vaporizing, exceeding the tank pressure.

N - None
A - Potential Abort
D - Potential Aircraft Damage
L - Potential Aircraft Loss
NA - Not Applicable

TABLE 89. - Continued.

Concept	Type of Failure	Normal Resulting Condition	Effect on Flight	Effect on Aircraft	Protective Measures
	Tank leakage	None if pressure does not exceed .1 Torr. Increased heat rate if pressure exceeds 0.1 Torr	N (< 0.1 Torr) A (> 0.1 Torr)		Active pumps, tank cryopumps at LH_2 temp, 1003.4 ℓ/sec/m^2 (10 800 ℓ/sec/ft^2)
	Blower shutdown	Slow rise in insulation pressure may occur accompanied by heat rate increase above 0.1 Torr pressure.	A		Cryopumping at LH_2 tank surface of 1003.4 ℓ/sec/m^2 (10 800 ℓ/sec/ft^2), relief valves, redundant components
12. Internal SiO_2 Insulation, Invar Liner, Evacuated	Liner leakage	No effect if pressure does not exceed 0.1 Torr. Heat rate increases up to ~ conductivity of GH_2 at that pressure if 0.1 Torr is exceeded. Liner reversal if insulation pressure exceeds tank pressure.	N (< 0.1 Torr) A (> 0.1 Torr)	D	Monitor insulation pressure, presence of GH_2 in insulation, active pumps, tank pressurization system, insulation relief valves. Insulation prevents LH_2 from striking the warm tank wall and vaporizing, exceeding the tank pressure.
	Tank leakage	None if pressure does not exceed 0.1 Torr. Increased heat rate if pressure exceeds 0.1 Torr	N (< 0.1 Torr) A (> 0.1 Torr)		Active pumps, tank cryopumps at LH_2 temp 1003.4 ℓ/sec/m2 (10 800 ℓ/sec/ft^2)

N - None
A - Potential Abort
D - Potential Aircraft Damage
L - Potential Aircraft Loss
NA - Not Applicable

TABLE 89. - Continued.

Concept	Type of Failure	Normal Resulting Condition	Effect on Flight	Effect on Aircraft	Protective Measures
	Blower shutdown	Slow rise in insulation pressure may occur accompanied by heat rate increase above 0.1 Torr pressure.	A		Cryopumping at LH_2 tank surface of 1003.4 ℓ/sec/m^2 (10 800 ℓ/sec/ft^2), relief valves, redundant components
13. Self Evacuating Shingles	Vapor barrier leakage	Increased heat rates, buildup of cryo-deposits, potential further damage to vapor barrier as tank drains (and cryo-deposits vaporize) each flight	A	D	Inspect insulation for frost, monitor tank boiloff, periodically repair vapor barrier if required
	Tank leakage	Potential safety hazard, increased heat rates	A	D	Periodically check tank pressure integrity, frosting of vapor barrier, tank boiloff, monitor space outside insulation for GH_2
14. Self Evacuating Honeycomb/Foam	External vapor barrier leakage	Cryopumping of moisture, increased heat rate	A	D	Inspect insulation for frost, monitor tank boiloff, periodically repair vapor barrier if required

N - None
A - Potential Abort
D - Potential Aircraft Damage
L - Potential Aircraft Loss
NA - Not Applicable

TABLE 89. - Continued.

Concept	Type of Failure	Normal Resulting Condition	Effect on Flight	Effect on Aircraft	Protective Measures
	Honeycomb vapor barrier leakage	Local cryopumping of gas from foam into the honeycomb, increased leakage of vapor barrier probable after thermal cycling	N (unless extensive)		
	GH_2 tank leakage	Increased heat rate, possible safety hazard	A	D	Periodically check tank pressure integrity, inspect insulation for frost, monitor tank boiloff, space outside insulation for GH_2
15. Self Evacuating Honeycomb/ GN_2 Fiberglass	External vapor barrier leakage	Loss of nitrogen	N (unless excessive)		Carry extra nitrogen onboard. Monitor press decay rate prior to flight
		Buckling of Jacket if N_2 supply is exhausted, air liquefaction.	A	D	
	Honeycomb vapor barrier leakage	Local cryopumping of nitrogen into honeycomb, increased heat rate, potential rupture of honeycomb barrier upon tank warm-up.	A	D	

N - None
A - Potential Abort
D - Potential Aircraft Damage
L - Potential Aircraft Loss
NA - Not Applicable

TABLE 89. - Concluded.

Concept	Type of Failure	Normal Resulting Condition	Effect on		Protective Measures
			Flight	Aircraft	
	GH_2 tank leakage	Increased heat rate, possible rupture of honeycomb vapor barrier.	A	D	Periodically check tank pressure integrity, inspect insulation for frost, monitor tank boiloff, nitrogen purge gas for hydrogen

N - None
A - Potential Abort
D - Potential Aircraft Damage
L - Potential Aircraft Loss
NA - Not Applicable

APPENDIX F

INSULATION CONCEPT PRODUCIBILITY AND OPERATIONAL ANALYSIS

Three tables are included in this appendix. Table 90 is an examination of how each of the insulation concepts might be fabricated, inspected, and serviced, and a discussion of areas that may require development. Table 91 is a check list of features of each of the insulation concepts showing the frequency with which inspections, and maintenance or operational activity, are required. Table 92 shows factors which influence the life expectancy of each of the insulation concepts and includes a ranking of the concepts on this basis.

TABLE 90. - PRELIMINARY PRODUCIBILITY ANALYSIS.

Concept	Fab & Assembly	Inspection	Servicing & Maintenance	Areas that May Require Development
1. He Purge	Fab and install fiberglass batting panels and purge jacket standoffs on tank, fab fiberglass/resin purge jacket on mandrel in two parts, leak check, assemble over the insulation. Assemble plumbing, controls, leak check.	Dimensional check, pressure decay leak check, functional check including loading LH_2, temperature measurements and boiloff measurement.	Load helium each flight and perform pressure decay check; periodically service plumbing components, hydrogen detectors, pressure monitoring and control system. Bond repair patches if required.	Purge jacket to tank standoffs to allow differential movement during tank fill.
2. He/N_2 Double Purge	Fab and install fiberglass batting panels and purge jacket standoffs on tank, fab two fiberglass/resin purge jackets on mandrels in two parts, leak check, install first jacket, leak check, install fiberglass batting panels, install second purge jacket with standoffs, leak check, assemble plumbing, controls, leak check.	Same as above for both He and N_2.	Same as above for both He and N_2.	Purge jacket to tank and purge jacket to purge jacket standoffs to allow differential movement during tank fill.
3. & 4. External Closed Cell Foam	Prime tank exterior with adhesive spray on foam in multiple phases, machine, spray on sealer and adhesive, lay on MAAMP and bond.	Visual inspection and dimensional check, LH_2 boiloff test with temperature measurements.	Examine insulation for frosting, monitor boiloff and temperatures in service, repair or replace insulation as required, service external hydrogen detectors.	No direct way to check integrity of seal coat other than by temperature measurements and frost formation. Frost and other cryopumped gases can build up in insulation. Life cycle testing required.
5. Internal Polyurethane Foam, Liquid Seal	Prime tank interior, fab and trim 3-D foam blocks, bond, install fiberglass/resin.	Same as above.	Same as above.	Insulation this thick has not not been installed in tanks before.

TABLE 90. - Continued.

Concept	Fab & Assembly	Inspection	Servicing & Maintenance	Areas that May Require Development
6. Internal PPO Foam/External Polyurethane Foam	Prime tank interior, fab and trim foam blocks, bond. Prime tank exterior, spray on foam, machine, spray on sealer.	Same as above.	Same as above.	PPO in the thicknesses required is not currently available. No direct way to check integrity of seal coat other than by frost formation and temperature measurements. Life cycle testing required.
7. & 8. Internal PPO Foam	See comments on System 6 regarding PPO foam			
Internal Honeycomb Gas Barrier Layer	Prime tank interior, blow fiberglass batting into honeycomb, bond perforated barrier to honeycomb panels, bond panels to tank, bond seal strips.	Visual inspection and dimensional check, LH_2 boil-off test and temperatures.	Examine tank for frosting in service, monitor boiloff and temperatures in service. Service hydrogen detectors.	This thickness of honeycomb will require a special order; blowing fiberglass batting into the honeycomb cells may require development. Life cycle testing may be required.
9. Rigid Vacuum Shell with Fiberglass Batting	Form, trim, weld outer face sheets. Leak check. Bond honeycomb to outer face sheets. Bond perforated inner face sheets. Fab, install insulation panels. Install vacuum jacket, weld final closure. Leak check. Pumpdown.	Visual inspection and dimensional check, pump down to 10^{-5} torr, pressure decay test.	Monitor vacuum pressure and hydrogen detectors, service pumping and pressure measuring system. Service hydrogen detectors.	Life cycle testing of jacket to insure structural and pressure integrity. Development of high vacuum pumping system and controls suitable for use in aircraft.
10. Microspheres with Flexibles External Jacket	Stretch form stainless steel gores, trim, resistance seam weld together, leak check, form wedges, bond spring standoffs to tank, install jacket, weld final closure, leak check, fill with microspheres, evacuate to $< .1$ Torr.	Visual, dimensional check, pressure check, pressure decay test, functional check of blowers and pressure monitoring equipment.	Monitor vacuum pressure and hydrogen detectors, service blowers and pressure measuring system.	Forming wedges after gores have been welded, final closure joint, leak-checking jacket. Demonstration of pumping system and controls suitable for aircraft use.

TABLE 90. - Continued.

Concept	Fab & Assembly	Inspection	Servicing & Maintenance	Areas that May Require Development
11. Microspheres with Internal Invar Liner	Stretch form Invar gores, trim, weld, leak check on mandrel, install spring assemblies and layer of PPO foam, install liner into tank cone section supported on mandrel, [illegible] ings with [illegible] adhesive, re- [illegible] rel, install [illegible] k with Invar [illegible] installed, [illegible] liner, weld tank, leak check, fill with microspheres, evacuate to <.1 torr.	Same as above.	Same as above.	Installation of liner into the tank and final closure welds. Demonstration of pumping system and controls suitable for aircraft use.
12. Silica Insulation with Internal Invar Liner	Fab, trim insulation blocks, bond to tank interior. Fab, install liner as described for system 8b (minus PPO foam). Evacuate.	Visual, dimensional check, pressure check, pressure decay test, functional check of blowers and pressure monitoring equipment.	Monitor vacuum pressure and hydrogen detectors, service blowers and pressure measuring equipment.	Installation of liner into the tank and final closure welds. Demonstration of pumping system and controls suitable for aircraft use.
13. Self-evacuating Shingles	Fab, trim, layup foam and radiation shield layers, assemble with buttons, bag, leak check, purge with CO_2, bond to tank, bond sealing strips.	Visual, dimensional check, LH_2 boiloff test, temperature measurements.	Examine insulation for frosting, monitor boiloff and temperatures in service. Service external hydrogen monitors.	It is doubtful this system can be made vacuum leak tight since metal barriers can't be used due to heat leak considerations.

TABLE 90. - Concluded.

Concept	Fab & Assembly	Inspection	Servicing & Maintenance	Areas that May Require Development
14. Self-evacuating Honeycomb/ Foam	Foam vapor barrier, bond to honeycomb panels, prime tank exterior, bond panels, bond seal strips, spray foam, machine, spray sealer.	Visual inspection, dimensional check, LH_2 boiloff test with temperature measurements.	Examine insulation for frosting, monitor boiloff and temperatures in service, repair or replace insulation as required. Service external hydrogen monitors.	No direct way to check integrity of seals other than temperature measurements and frost formation. Repair of honeycomb seal difficult. Life cycle testing required.
15. Self-evacuating Honeycomb/N_2 Purge	Fab and install honeycomb as described for system 14. Fab and install fiberglass batting panels and purge jacket as described for the system 2 nitrogen purge.	Same as above. Run pressure decay leak check on purge jacket.	Same as above. Load N_2 each flight, service plumbing components, pressure monitoring, temperature and control systems. Service external hydrogen monitors.	No direct way to check integrity of honeycomb seal other than temperature measurements and frost formation.

TABLE 91. - EXAMPLE OF INSPECTION, MAINTENANCE AND OPERATIONAL REQUIREMENTS.

	Time Interval[1]			
	Per Flight	Weekly	Monthly	Quarterly
1. He Purge				
o Load Helium	X			
o Visual Check			X	
o Pressure Decay Check	X			
o Plumbing Functional Check		X		
o Hydrogen Leak Detector Check		X		
o Pressure Monitoring and Control System Check		X		
o Boiloff Measurement	X			
o Complete System Servicing				X
o Weigh Aircraft			X	
2. He/N_2 Double Purge				
o Load He and N_2	X			
o Visual Check			X	
o Pressure Decay Check	X			
o Plumbing Functional Check		X		
o Hydrogen Leak Detector Check		X		
o Pressure Monitoring and Control System Check		X		
o Boiloff Measurement	X			
o Complete System Servicing				X
o Weigh Aircraft			X	

[1] These intervals would probably increase as experience is gained with system.

TABLE 91. - Continued.

	Time Interval[1]			
	Per Flight	Weekly	Monthly	Quarterly
3. & 4. External Closed Cell Foam				
o Visual Check for Frost		X		
o Weigh Aircraft		X		
o Boiloff Measurement	X			
o Temp. Measurement	X			
o Service Hydrogen Detectors		X		
o Service Sensors				
5. Internal Polyurethane Foam, Liquid Seal				
o Visual Check for Frost		X		
o Weigh Aircraft			X	
o Boiloff Measurement	X			
o Temp. Measurement	X			
o Service Hydrogen Detectors		X		
o Examine Foam, Service Sensors				X

[1] These intervals would probably increase as experience is gained with system.

TABLE 91. - Continued.

	Time Interval[1]			
	Per Flight	Weekly	Monthly	Quarterly
6. Internal PPO Foam/External Polyurethane Foam				
o Visual Check for Frost		X		
o Weigh Aircraft		X		
o Boiloff Measurement	X			
o Temp. Measurement	X			
o Service Hydrogen Detectors		X		
o Examine Internal Foam, Service Sensors				X
7. Internal PPO Foam	Same as System 5			
8. Internal Honeycomb Gas Barrier Layer	Same as System 5			
9. Rigid Vacuum Shell with Fiberglass Batting				
o Visual Check			X	
o Vacuum Decay Check	X			
o Vacuum Monitoring and Control System Check		X		
o Pump Servicing				X
o Weigh Aircraft			X	

[1] These intervals would probably increase as experience is gained with system.

TABLE 91. - Continued.

	Time Interval[1]			
	Per Flight	Weekly	Monthly	Quarterly
10. Microspheres with External Flexible Jacket				
o Visual Check			X	
o Vacuum Decay Check	X			
o Vacuum Monitoring and Control System Check		X		
o Pump Servicing				X
o Weigh Aircraft			X	
11. Microspheres with Internal Invar Liner	See System 10	for other items.		
o Examine Liner				X
12. Silica Insulation with Internal Invar Liner	See System 10	for other items.		
o Examine Liner				X
13. Self-Evacuating Shingles				
o Visual Check for Frost		X		
o Weigh Aircraft		X		
o Boiloff Measurement	X			
o Temp. Measurement	X			

[1] These intervals would probably increase as experience is gained with system.

TABLE 91. - Concluded.

	Time Interval[1]			
	Per Flight	Weekly	Monthly	Quarterly
13. Continued				
o Service Hydrogen Detectors		X		
o Service Sensors				
14. Self-Evacuating Honeycomb Foam	Same as System 3			
15. Self-Evacuating Honeycomb/N_2 Purge	Same as System 1			

[1] These intervals would probably increase as experience is gained with system.

TABLE 92. - FACTORS INFLUENCING THE CANDIDATE INSULATION SYSTEM'S LIFE EXPECTANCY

Rank-ing	System No.	Vapor Barrier					Insulation				No. of LH_2 Thermal Cycle Tests Which Have Been Conducted to Date on Similar Systems
		Type	Max. Barrier Temp Change $^oC(^oF)$	ΔP k Pa (psi)	Flex Desir-able ?	Designed to Flex	Type	Press. Loaded	Max. Bond Line Temp Change $^oC(^oF)$	Structural Integrity	
1*	1	Epoxy/ Glass/ Teflon	82.2 (180)	14(2)	No	No	Fiber-glass Batt	No	N.A.	Excellent	100
1	2	He Epoxy/ Glass Teflon	198.9 (390)	14(2)	No	No	"	No	N.A.	Excellent	1
		N_2 Epoxy/ Glass Teflon	82.2 (180)	14(2)	No	No	"	No	N.A.	Excellent	
3	3&4	Poly-urethane Seal Coat	82.2 (180)	103(15)	Yes	No	Closed Cell Poly-urethane Foam	Yes	276.7 (530)	Fair	6
2	3&4	MAAMF	82.2 (180)	103(15)	Yes	No	"	Yes	276.7 (530)	Fair	--
2	5	Glass/ Poly-urethane Seal	276.7 (530)	138(20)	Yes	No	Align Fiber Rein-forced Foam	Yes (Ini-tially)	82.2 (180)	Good	135
3	6	Poly-urethane Seal Coat	82.2 (180)	-14(~2)	Yes	No	Closed Cell Poly-urethane Foam	Yes	198.9 (390)	Fair	--
		None	--	--	--	--	Open Cell PPO Foam	No	198.9 (390)	Excellent	100

*Longest Life Systems

TABLE 92. - Conti...ed.

Ranking	System No.	Vapor Barrier: Type	Vapor Barrier: Max. Barrier Temp Change °C(°F)	Vapor Barrier: ΔP k Pa (psi)	Vapor Barrier: Flex Desirable ?	Vapor Barrier: Designed to Flex	Insulation: Type	Insulation: Press. Loaded	Insulation: Max. Bond Line Temp Change °C(°F)	Insulation: Structural Integrity	No. of LH_2 Thermal Cycle Tests Which Have Been Conducted to Date on Similar Systems
1	7	None	--	--	--	--	Open Cell PPO Foam	No	82.2 (180)	Excellent	100
1	8	Perforated Mylar	276.7 (530)	0	Yes	No	Mylar Honeycomb	No	82.2 (180)	Excellent	?
2	9	Aluminum	82.2 (180)	103 (15)	No	No	Fiberglass Batt & Radiation Shields	No	N.A.	Excellent	29
1	10	Stainless Steel	82.2 (180)	103 (15)	Yes	Yes	Glass Microspheres	Yes	N.A.	Excellent	Test program started Jan. 1977
1	11	Invar	276.7 (530)	138 (20)	No	No	Glass Microspheres	Yes	N.A.	Excellent	--
1	12	Invar	276.7 (530)	138 (20)	No	No	Rigidized Silica Fiber	Yes	82.2 (180)	Excellent	--
3	13	Mylar	82.2 (180)	103 (15)	Yes	Partially	Foam/Radiation Shield Layers	Yes	276.7 (530)	Foam layers Questionable	4 (Panels leaked)

*Longest Life Systems

TABLE 92. - Concluded.

Rank-ing	System No.	Vapor Barrier					Insulation				No. of LH_2 Thermal Cycle Tests Which Have Been Conducted to Date on Similar Systems
		Type	Max. Barrier Temp Change $^oC(^oF)$	ΔP k Pa (psi)	Flex Desir-able ?	Designed to Flex	Type	Press. Loaded	Max. Bond Line Temp Change $^oC(^oF)$	Structural Integrity	
2	14	MAAMF Film	198.9 (390)	90(13)	Yes	No	Mylar Honeycomb	Yes	276.7 (530)	Excellent	14 (Leaked)
		Polyure-thane Seal Coat	82.2 (180)	14(2)	Yes	No	Closed Cell Poly-urethane Foam	Yes	198.9 (390)	Fair	--
2	15	MAAMF Film	198.9 (390)	117 (17)	Yes	No	Mylar Honeycomb	Yes	276.7 (530)	Excellent	14 (Leaked)
		Polyure-thane Seal Coat	82.2 (180)	14(2)	No	No	Fiber-glass Batt	No	N.A.	Excellent	--

*Longest Life Systems

APPENDIX G

INSTALLED ENGINE PERFORMANCE CHARTS

Figure 205 through 210 — LH_2 Engine

Figure 211 through 214 — Jet A Engine

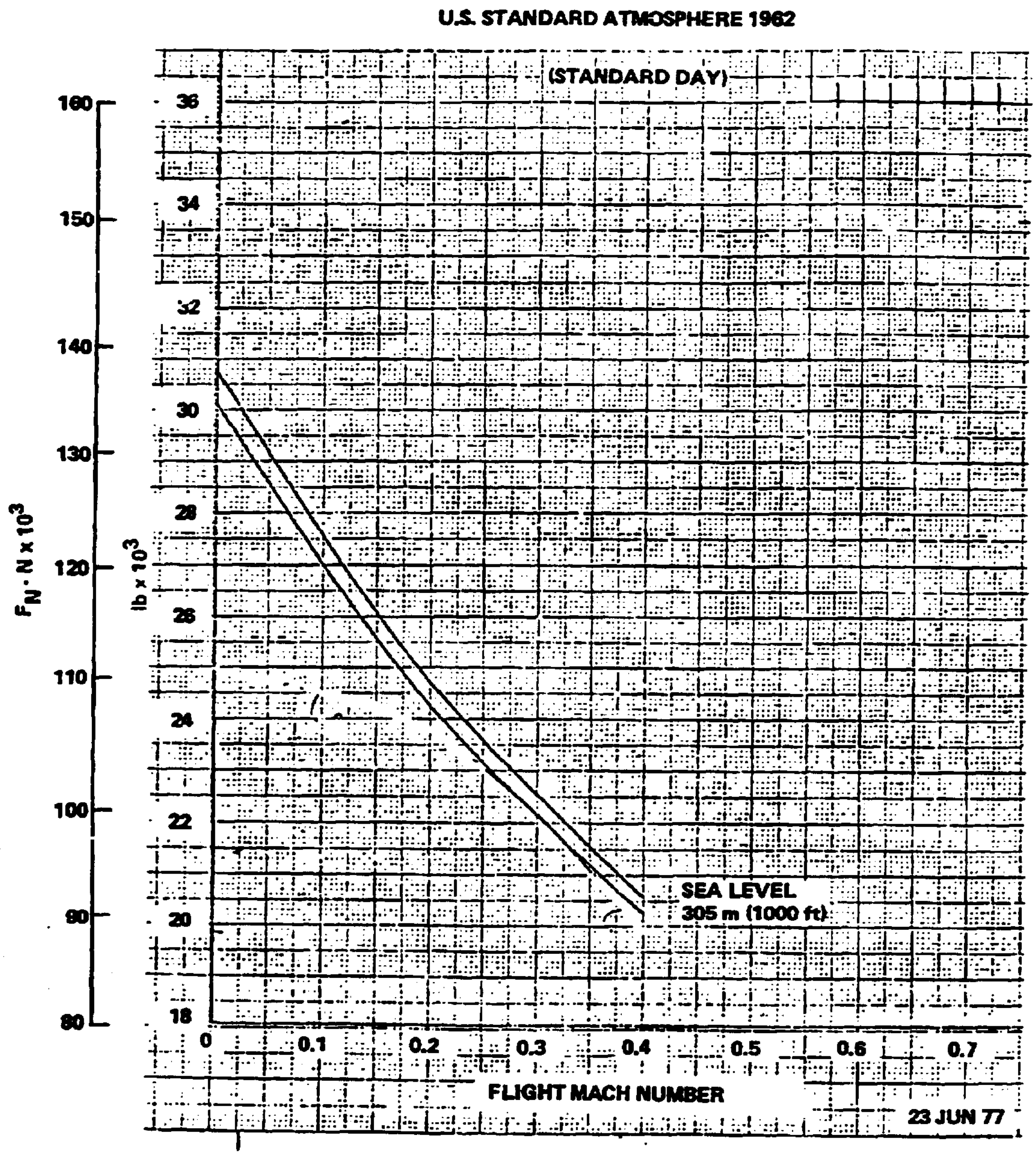

Figure 205. - AiResearch LH_2 engine takeoff power - thrust

ORIGINAL PAGE IS
OF POOR QUALITY

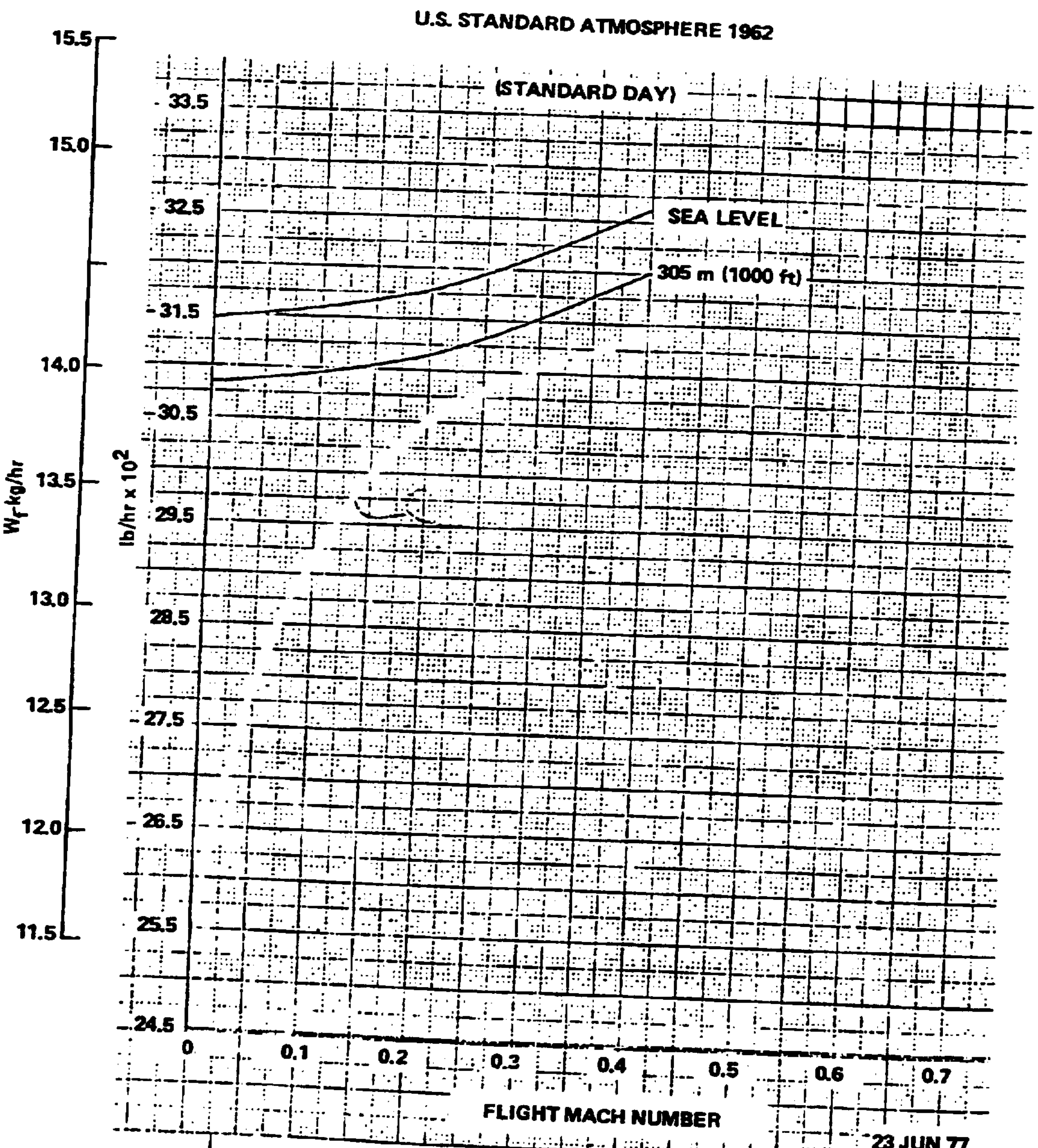

Figure 206. - AiResearch LH_2 engine takeoff power - fuel flow

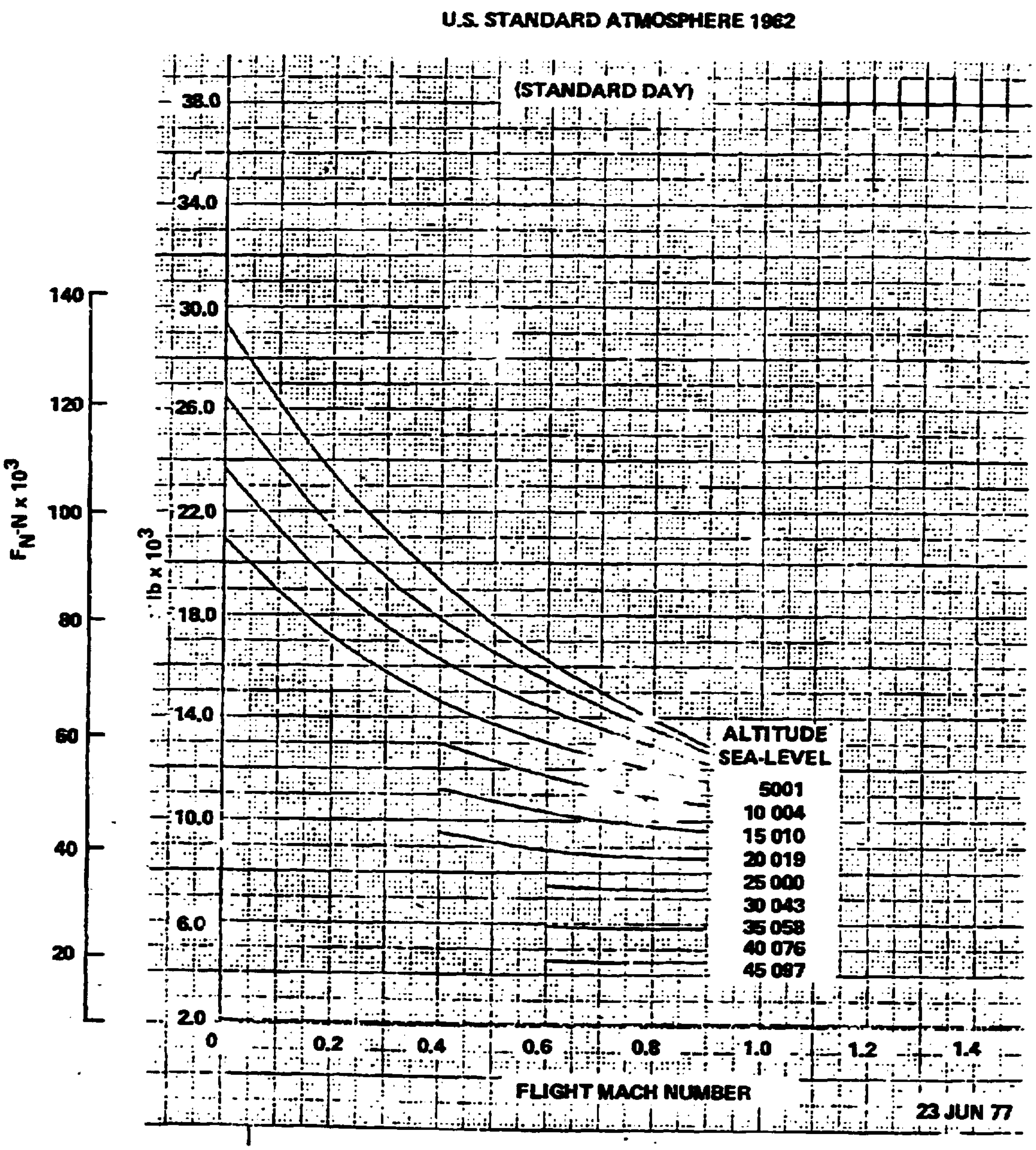

Figure 207. - AiResearch LH_2 engine maximum climb - thrust

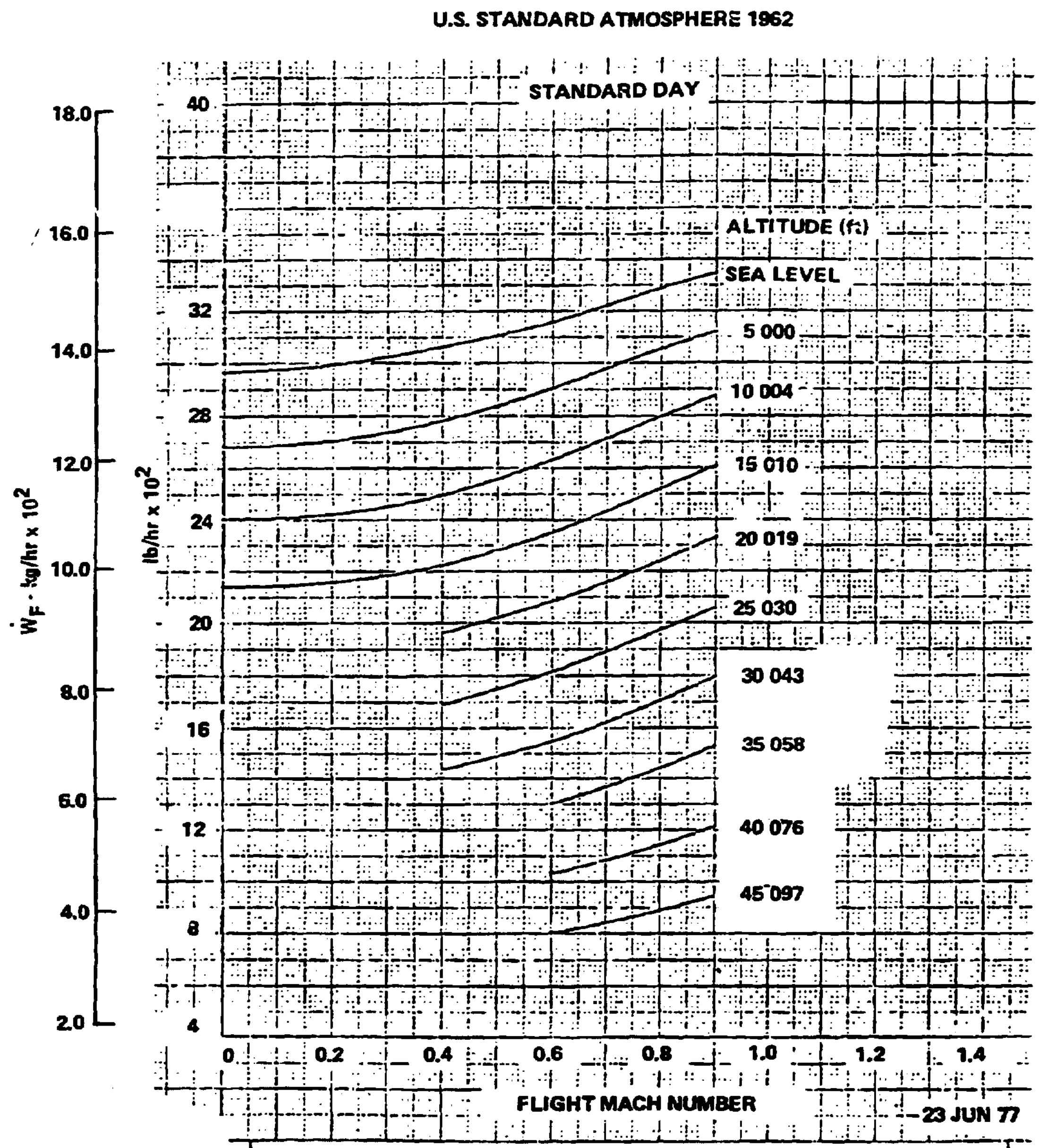

Figure 208. - AiResearch LH_2 engine maximum climb - fuel flow

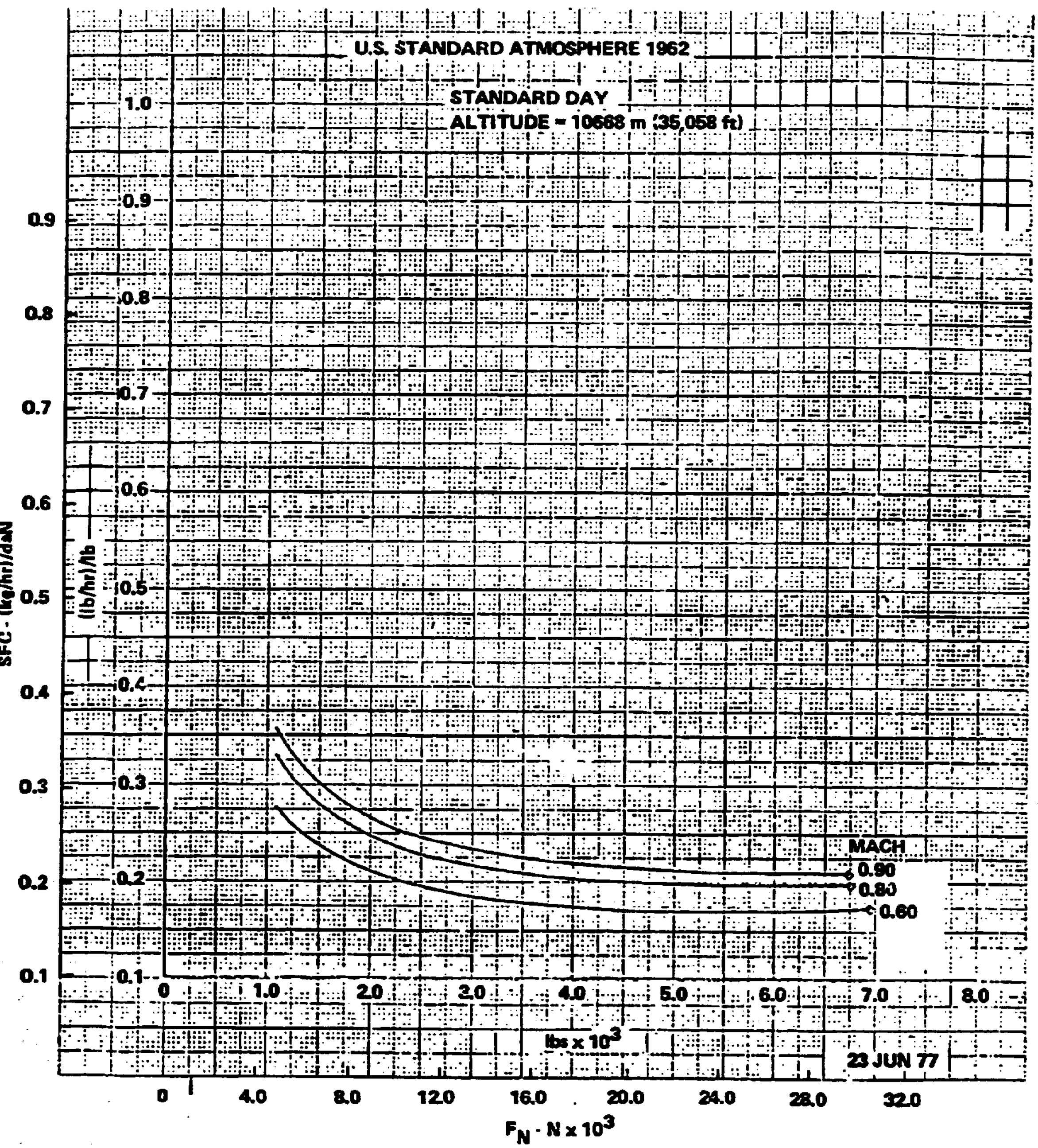

Figure 209. - AiResearch LH_2 engine part power - cruise

ORIGINAL PAGE IS
OF POOR QUALITY

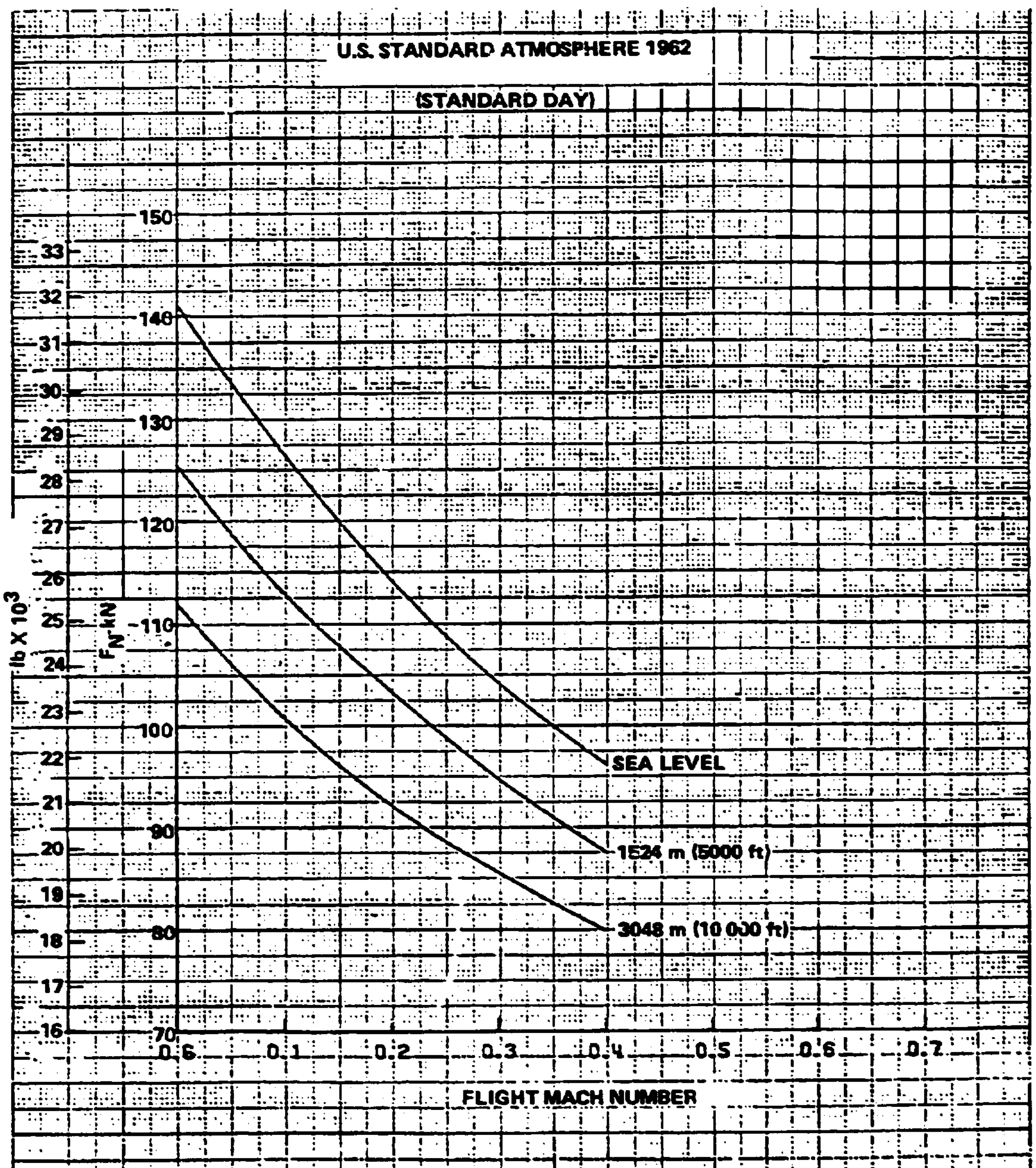

Figure 210. - Jet A engine takeoff power - thrust

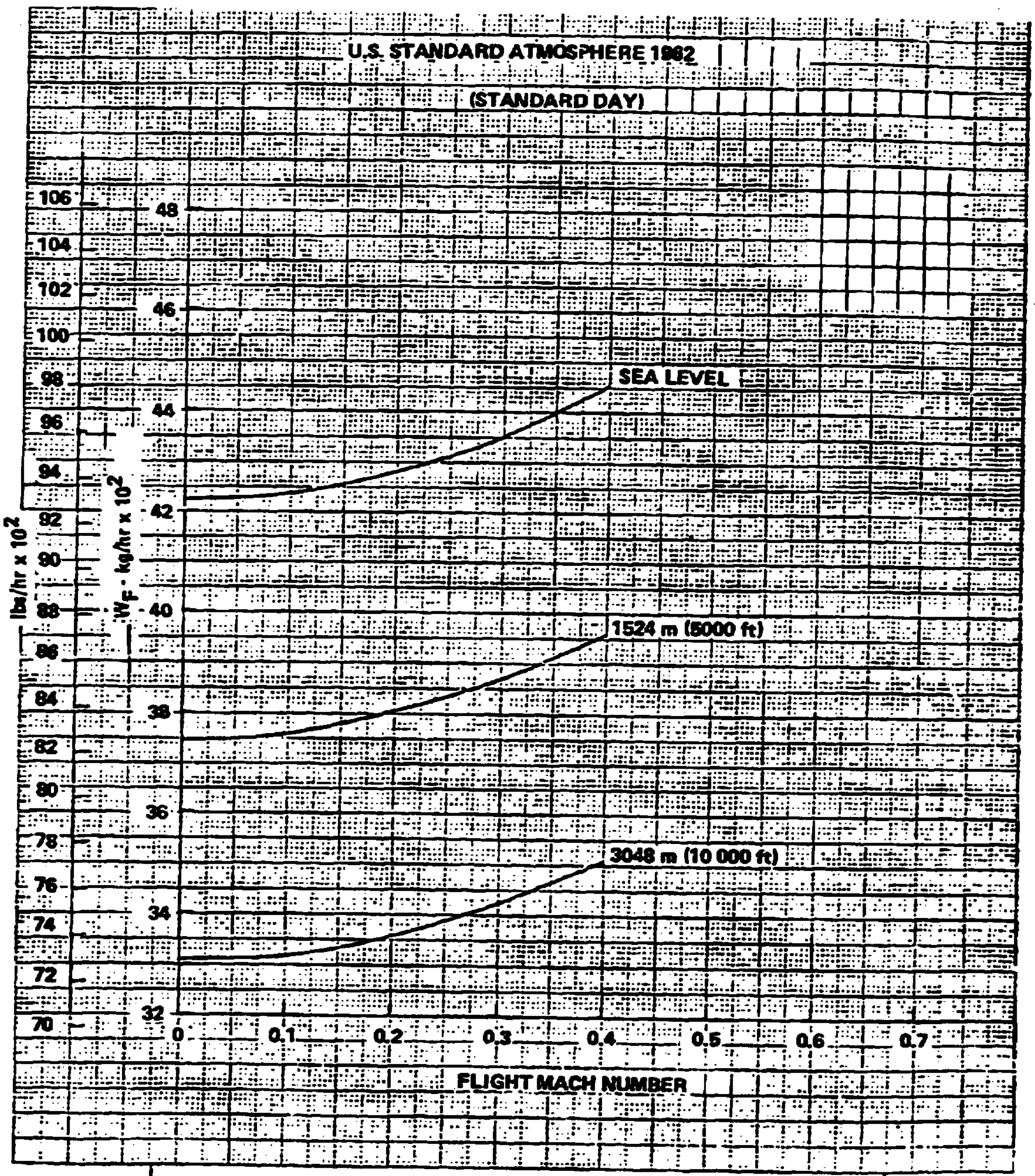

Figure 211. – Jet A engine takeoff power – fuel flow

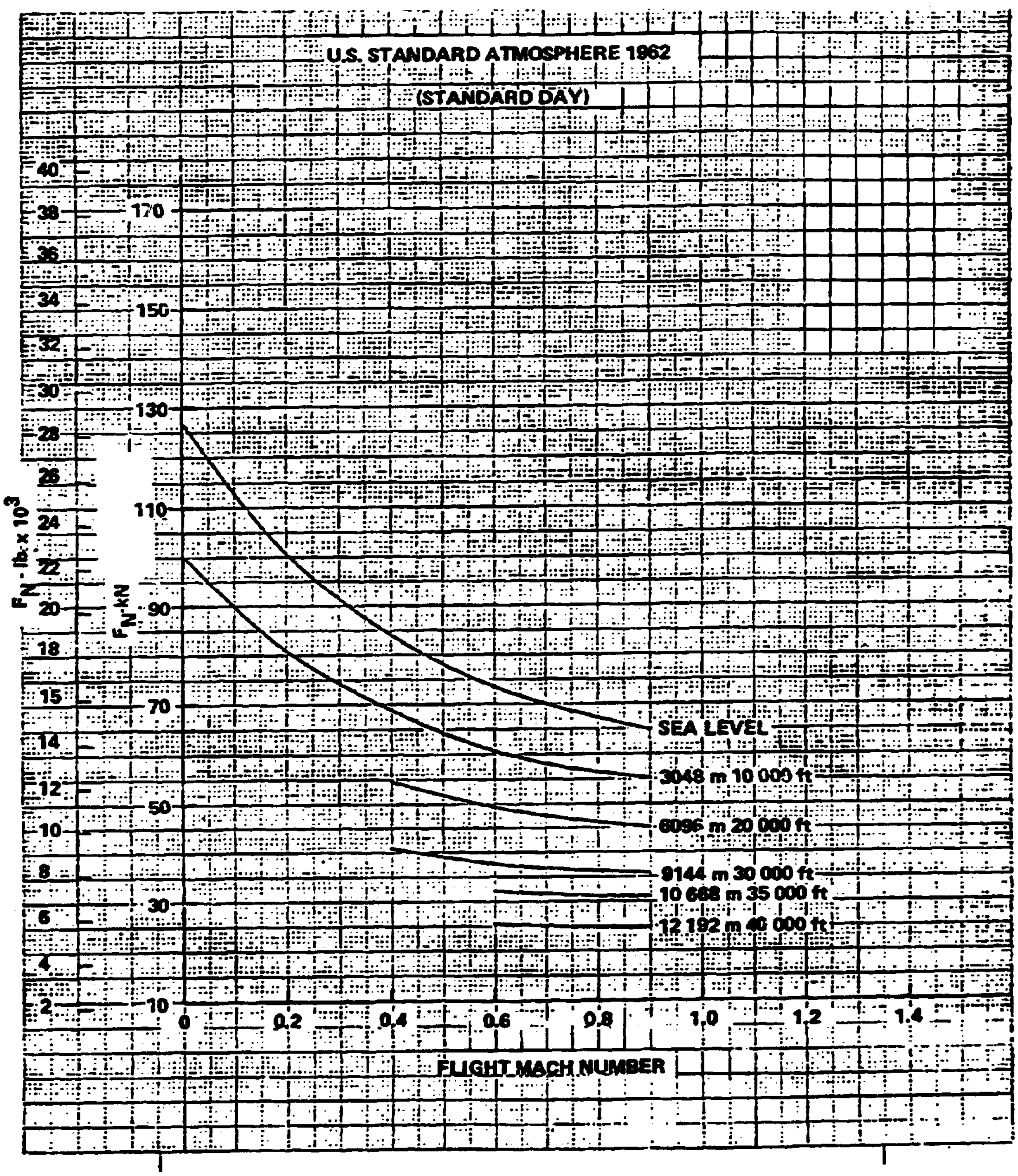

Figure 212. - Jet A engine maximum climb - thrust

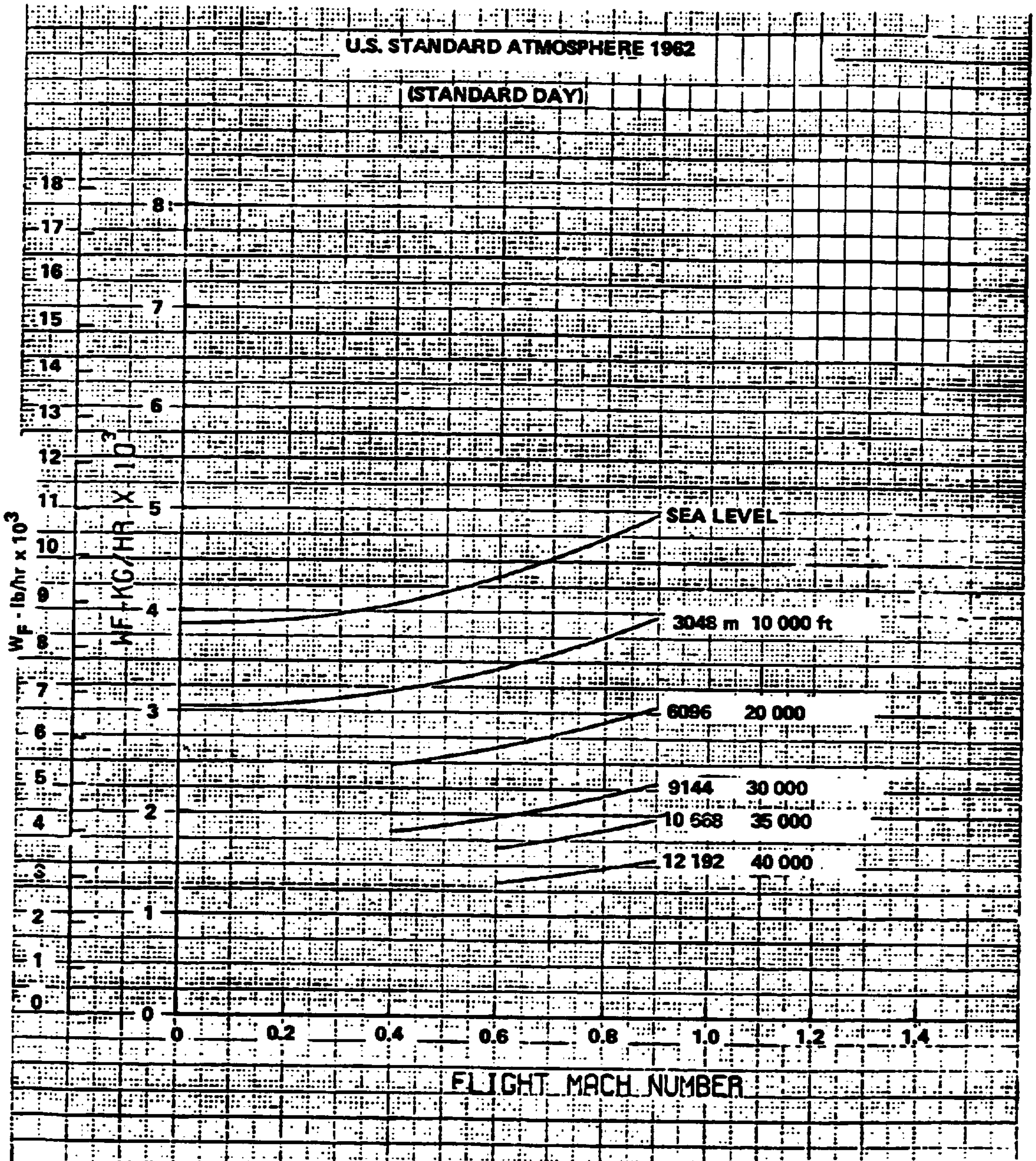

Figure 213. - Jet A engine maximum climb - fuel flow.

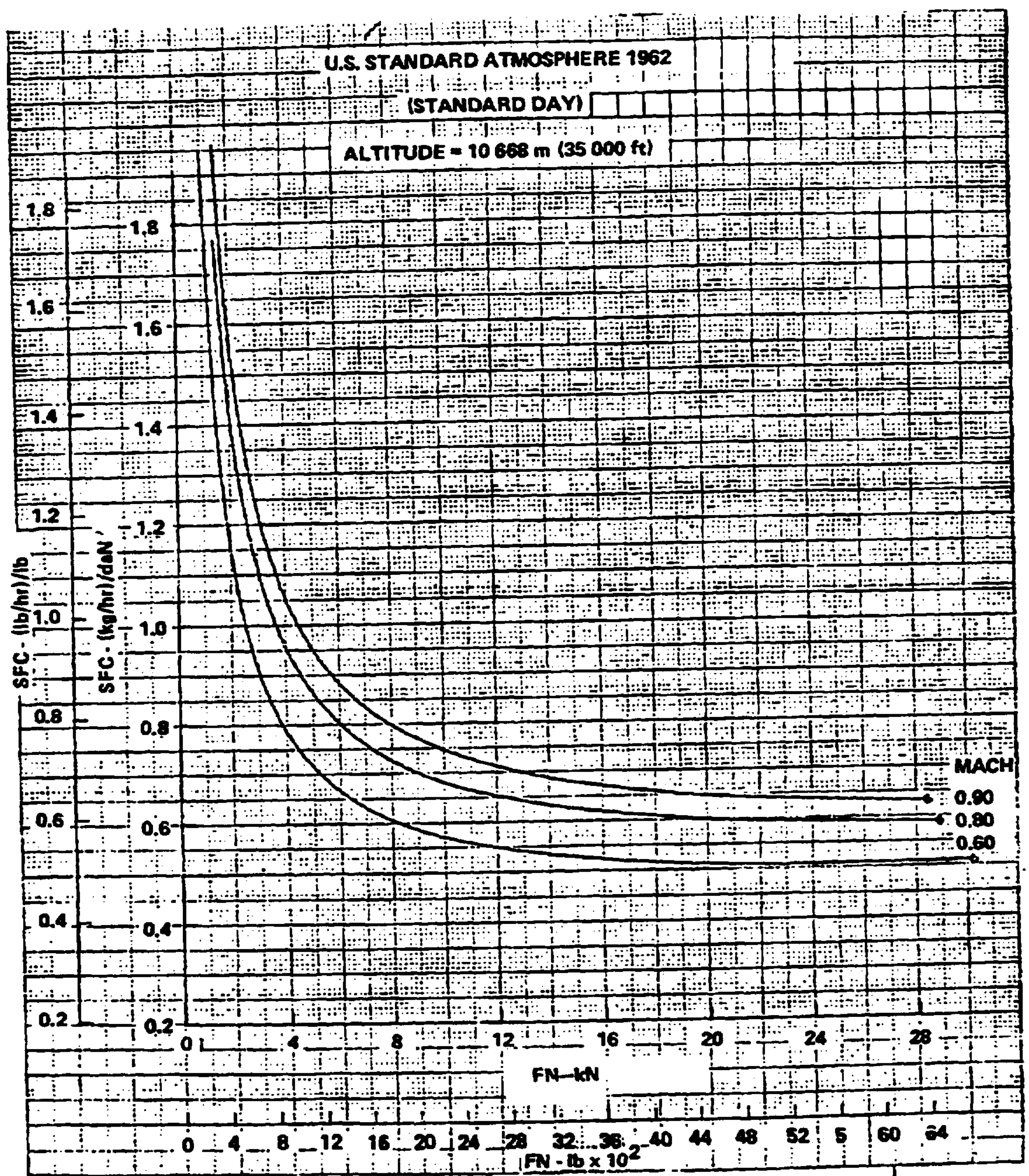

Figure 214. - Jet A engine part power - cruise.